nature genetics

ARTICLES

https://doi.org/10.1038/s41588-022-01058-3

Check for updates

Multi-ancestry genetic study of type 2 diabetes highlights the power of diverse populations for discovery and translation

We assembled an ancestrally diverse collection of genome-wide association studies (GWAS) of type 2 diabetes (T2D) in 180,834 affected individuals and 1,159,055 controls (48.9% non-European descent) through the Diabetes Meta-Analysis of Trans-Ethnic association studies (DIAMANTE) Consortium. Multi-ancestry GWAS meta-analysis identified 237 loci attaining stringent genome-wide significance ($P < 5 \times 10^{-9}$), which were delineated to 338 distinct association signals. Fine-mapping of these signals was enhanced by the increased sample size and expanded population diversity of the multi-ancestry meta-analysis, which localized 54.4% of T2D associations to a single variant with >50% posterior probability. This improved fine-mapping enabled systematic assessment of candidate causal genes and molecular mechanisms through which T2D associations are mediated, laying the foundations for functional investigations. Multi-ancestry genetic risk scores enhanced transferability of T2D prediction across diverse populations. Our study provides a step toward more effective clinical translation of T2D GWAS to improve global health for all, irrespective of genetic background.

The global prevalence of T2D has quadrupled over the last 30 years[1], affecting approximately 392 million individuals in 2015 (ref. [2]). Despite this worldwide impact, the largest T2D GWAS have predominantly featured populations of European ancestry[3–6], compromising prospects for clinical translation. Failure to detect causal variants that contribute to disease risk outside European ancestry populations limits progress toward a full understanding of disease biology and constrains opportunities for development of therapeutics[7]. Implementation of personalized approaches to disease management depends on accurate prediction of individual risk, irrespective of ancestry. However, genetic risk scores (GRS) derived from European ancestry GWAS provide unreliable prediction when deployed in other population groups, in part reflecting differences in effect sizes, allele frequencies and patterns of linkage disequilibrium (LD)[8].

To address the impact of this population bias, recent T2D GWAS have included individuals of non-European ancestry[9–11]. The DIAMANTE Consortium was established to assemble T2D GWAS across diverse ancestry groups. Analyses of the European and East Asian ancestry components of the DIAMANTE study have previously been reported[6,10]. Here, we describe the results of our multi-ancestry meta-analysis, which expands on these published components to a total of 180,834 individuals with T2D and 1,159,055 controls, with 20.5% of the effective sample size ascertained from African, Hispanic and South Asian ancestry groups. With these data, we demonstrate the value of analyses conducted on diverse populations to understand how T2D-associated variants impact downstream molecular and biological processes underlying the disease and advance clinical translation of GWAS findings for all, irrespective of genetic background.

Results

Study overview. We accumulated association summary statistics from 122 GWAS for 180,834 individuals with T2D and 1,159,055 controls (effective sample size, 492,191) across five ancestry groups (Supplementary Tables 1–3). We use the term 'ancestry group' to refer to individuals with similar genetic background: European ancestry (51.1% of the total effective sample size); East Asian ancestry (28.4%); South Asian ancestry (8.3%); African ancestry, including recently admixed African American populations (6.6%); and Hispanic individuals with recent admixture of American, African and European ancestry (5.6%). Each ancestry-specific GWAS was imputed to reference panels from the 1000 Genomes Project[12,13], the Haplotype Reference Consortium[14] or population-specific whole-genome sequence data. Subsequent association analyses were adjusted for population structure and relatedness (Supplementary Table 4). We considered 19,829,461 biallelic autosomal single-nucleotide variants (SNVs) that overlapped reference panels with minor allele frequency >0.5% in at least one of the five ancestry groups (Extended Data Fig. 1 and Methods).

Robust discovery of multi-ancestry T2D associations. We aggregated association summary statistics via multi-ancestry meta-regression, implemented in MR-MEGA[15], which models allelic effect heterogeneity correlated with genetic ancestry. We included three axes of genetic variation as covariates that separated genome-wide associations from the five major ancestry groups (Extended Data Fig. 2 and Methods). We identified 277 loci associated with T2D at the conventional genome-wide significance threshold of $P < 5 \times 10^{-8}$ (Extended Data Fig. 3 and Supplementary Table 5). By accounting for ancestry-correlated allelic effect heterogeneity in the multi-ancestry meta-regression, we observed lower genomic control inflation ($\lambda_{GC} = 1.05$) than when using either fixed- or random-effects meta-analysis ($\lambda_{GC} = 1.25$ under both models) and stronger signals of association at lead SNVs at most loci (Extended Data Fig. 4). Of the 277 loci, 11 have not previously been reported in recently published T2D GWAS meta-analyses[6,10,11] that account for 78.6% of the total effective sample size of this multi-ancestry meta-regression (Extended Data Fig. 3 and Supplementary Note). Of the 100 and 193 loci attaining genome-wide significance ($P < 5 \times 10^{-8}$) in East Asian and European ancestry-specific meta-analyses, respectively, lead SNVs at 94 (94.0%) and 164 (85.0%) demonstrated stronger evidence for association (smaller P values) in the multi-ancestry meta-regression (Extended Data Fig. 5 and Supplementary Note). These results demonstrate the power of multi-ancestry meta-analyses for locus discovery afforded by

A full list of author and affiliations appears at the end of the paper.

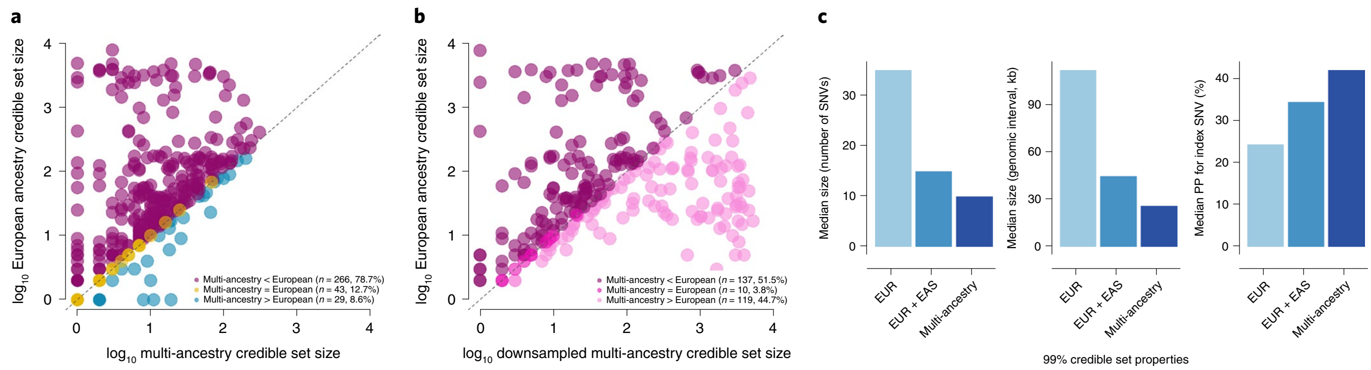

Fig. 1 | Comparison of fine-mapping resolution for distinct association signals for T2D obtained from ancestry-specific meta-analysis and multi-ancestry meta-regression. a, Each point corresponds to a distinct association signal, plotted according to the $\log_{10}$ credible set size in the multi-ancestry meta-regression on the x axis and the $\log_{10}$ credible set size in the European ancestry meta-analysis on the y axis. The 266 (78.7%) signals above the dashed $y=x$ line were more precisely fine-mapped in the multi-ancestry meta-regression. **b**, We 'downsampled' the multi-ancestry meta-regression to the effective sample size of the European ancestry-specific meta-analysis. Each point corresponds to one of the 266 signals that were more precisely fine-mapped in the multi-ancestry meta-regression. The 137 (51.5%) signals above the dashed $y=x$ line were more precisely fine-mapped in the 'downsampled' multi-ancestry meta-regression than in the equivalently sized European ancestry-specific meta-analysis. **c**, Properties of 99% credible sets of variants driving each distinct association signal in European (EUR) ancestry-specific meta-analysis, combined East Asian (EAS) and European ancestry meta-analysis and multi-ancestry meta-regression. The inclusion of the most under-represented ancestry groups (African, Hispanic and South Asian) in the multi-ancestry meta-regression reduced the median size of 99% credible sets and increased the median posterior probability (PP) ascribed to index SNVs.

increased sample size but also emphasize the importance of complementary ancestry-specific GWAS for identification of associations that are not shared across diverse populations.

The conventional genome-wide significance threshold does not allow for different patterns of LD across diverse populations in multi-ancestry meta-analysis. We therefore derived a multi-ancestry genome-wide significance threshold of $P<5\times10^{-9}$ by estimating the effective number of independent SNVs across the five ancestry groups using haplotypes from the 1000 Genomes Project reference panel[13] (Methods). Of the 277 loci reported in this multi-ancestry meta-regression, 237 attained the more stringent significance threshold, which we considered for downstream analyses. Through approximate conditional analyses, conducted using ancestry-matched LD reference panels for each GWAS, we partitioned associations at the 237 loci into 338 distinct signals that were each represented by an index SNV at the same multi-ancestry genome-wide significance threshold (Methods, Supplementary Tables 6–8 and Supplementary Note). Allelic effect estimates for distinct association signals from approximate conditional analyses undertaken in admixed ancestry groups were robust to the choice of reference panel (Supplementary Note).

Allelic effect heterogeneity across ancestry groups. Allelic effect heterogeneity between ancestry groups can occur for several reasons, including differences in LD with causal variants or interactions with environment or polygenic background across diverse populations. An advantage of the multi-ancestry meta-regression model is that heterogeneity can be partitioned into two components. The first captures heterogeneity that is correlated with genetic ancestry (that is, it can be explained by the three axes of genetic variation). The second reflects residual heterogeneity due to differences in geographical location (for example, different environmental exposures) and study design (for example, different phenotype definition, case–control ascertainment or covariate adjustments between GWAS). We observed 136 (40.2%) distinct T2D associations with nominal evidence ($P_{\mathrm{HET}}<0.05$) of ancestry-correlated heterogeneity compared to 16.9 expected by chance (binomial test $P<2.2\times10^{-16}$). By contrast, there was nominal evidence of residual heterogeneity at only 27 (8.0%) T2D-association signals (binomial test $P=0.0037$), suggesting that differences in allelic effect size between GWAS are more likely due to factors related to genetic ancestry than to geography and/or study design (Supplementary Note).

Population diversity improves fine-mapping resolution. We sought to quantify the improvement in fine-mapping resolution offered by increased sample size and population diversity in the multi-ancestry meta-regression. For each of the 338 distinct signals, we first derived multi-ancestry and European ancestry-specific credible sets of variants that account for 99% of the posterior probability (π) of driving the T2D association under a uniform prior model of causality (Methods). Multi-ancestry meta-regression substantially reduced the median 99% credible set size from 35 variants (spanning 112 kb) to ten variants (spanning 26 kb) and increased the median posterior probability ascribed to the index SNV from 24.3% to 42.0%. The 99% credible sets for 266 (78.7%) distinct T2D associations were smaller in the multi-ancestry meta-regression than in the European ancestry-specific meta-analysis, while a further 26 (7.7%) signals were resolved to a single SNV in both (Fig. 1, Supplementary Table 9 and Supplementary Note). Causal variant localization was also more precise in the multi-ancestry meta-regression than in a meta-analysis of GWAS of European and East Asian ancestry, which together account for 79.5% of the total effective sample size, highlighting the important contribution of the most under-represented ancestry groups (African, Hispanic and South Asian) to fine-mapping resolution (Fig. 1 and Supplementary Note).

We next attempted to understand the relative contributions of population diversity and sample size to these improvements in fine-mapping resolution at the 266 distinct T2D associations that were more precisely localized after the multi-ancestry meta-regression. We downsampled studies contributing to the multi-ancestry meta-regression to approximate the effective sample size of the European ancestry-specific meta-analysis, while maintaining the distribution of population diversity (Methods and Supplementary Table 10). The associations were better resolved in the downsampled multi-ancestry meta-regression at 137 signals (51.5%), compared with 119 signals (44.7%) in the European ancestry-specific meta-analysis (Fig. 1 and Supplementary Table 11). These results highlight the value of diverse populations for causal variant localization in multi-ancestry meta-analysis, emphasizing the importance of increased sample size and differences in LD structure and

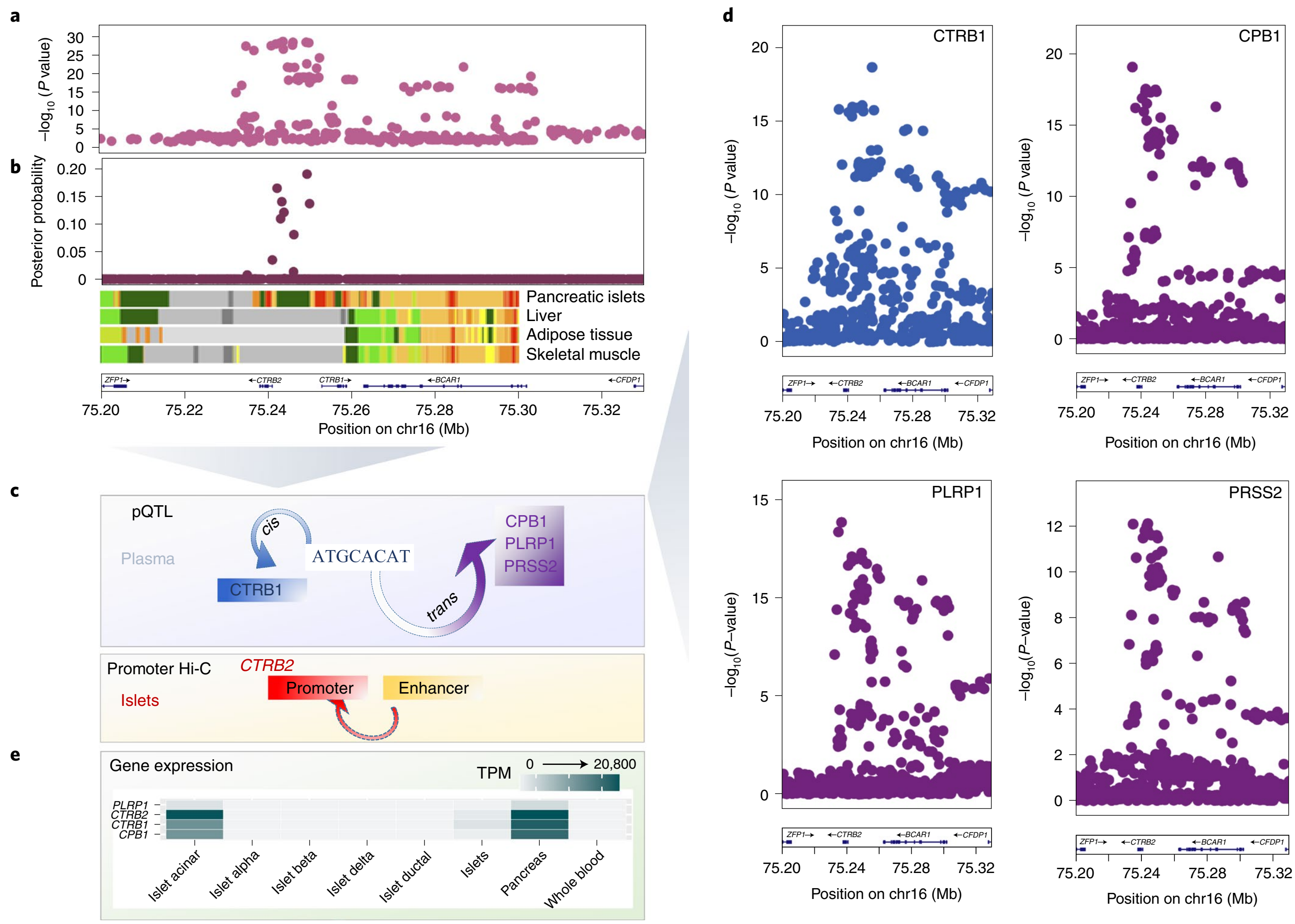

Fig. 2 | T2D-association signal at the *BCAR1* locus colocalizes with multiple circulating plasma pQTL. a, Signal plot for T2D association from multi-ancestry meta-regression of 180,834 affected individuals and 1,159,055 controls of diverse ancestry. Each point represents an SNV, plotted with its *P* value (on a $\log_{10}$ scale) as a function of genomic position (National Center for Biotechnology Information (NCBI) build 37). Gene annotations were taken from the University of California Santa Cruz genome browser. Recombination rates were estimated from the Phase II HapMap. Chr, chromosome. **b**, Fine-mapping of T2D-association signals from multi-ancestry meta-regression. Each point represents an SNV plotted with its posterior probability of driving T2D association as a function of genomic position (NCBI build 37). Chromatin states are presented for four diabetes-relevant tissues: active transcription start sites (TSS) (red), flanking active TSS (orange–red), strong transcription (green), weak transcription (dark green), genic enhancers (green–yellow), active enhancers (orange), weak enhancers (yellow), bivalent or poised TSS (Indian red), flanking bivalent TSS or enhancer (dark salmon), repressed polycomb (silver), weak repressed polycomb (gainsboro) and quiescent or low (white). **c**, Schematic presentation of the single *cis* and multiple *trans* effects mediated by the *BCAR1* locus on plasma proteins and the islet chromatin loop between islet enhancer and promoter elements near *CTRB2*. **d**, Signal plots for four circulating plasma proteins that colocalize with the T2D association in 3,301 European ancestry participants from the INTERVAL study. Each point represents an SNV, plotted with its *P* value (on a $\log_{10}$ scale) as a function of genomic position (NCBI build 37). **e**, Expression of genes (TPM, transcripts per million) encoding colocalized proteins in islets, the pancreas and whole blood.

allele-frequency distribution between ancestry groups that has also been reported for other complex human traits[16].

Multi-ancestry fine-mapping to single-variant resolution. Previous T2D GWAS have demonstrated improved localization of causal variants through integration of fine-mapping data with genomic annotation[6,17]. By mapping SNVs to three categories of functional and regulatory annotation, with an emphasis on diabetes-relevant tissues[18], we observed significant joint enrichment ($P < 0.00023$, Bonferroni correction for 220 annotations) for T2D associations mapping to protein-coding exons, transcription factor binding sites for NKX2.2, FOXA2, EZH and PDX1, and four chromatin states in pancreatic islets that mark active enhancers, active promoters and transcribed regions (Methods, Extended Data Fig. 6 and Supplementary Table 12). We used the enriched annotations to derive a prior model for causality and redefined 99% credible sets of variants for each distinct signal (Methods and Supplementary Table 13). Annotation-informed fine-mapping reduced the size of the 99% credible set, compared to the uniform prior, at 144 (42.6%) distinct association signals (Extended Data Fig. 7) and decreased the median from ten variants (spanning 26 kb) to eight variants (spanning 23 kb). For 184 (54.4%) signals, a single SNV accounted for >50% of the posterior probability of the T2D association (Supplementary Table 14). At 124 (36.7%) signals, >80% of the posterior probability could be attributed to a single SNV.

Missense variants implicate candidate causal genes. After annotation-informed multi-ancestry fine-mapping, 19 of the 184 SNVs accounting for >50% of the posterior probability of the T2D association were missense variants (Supplementary Table 15). Two of

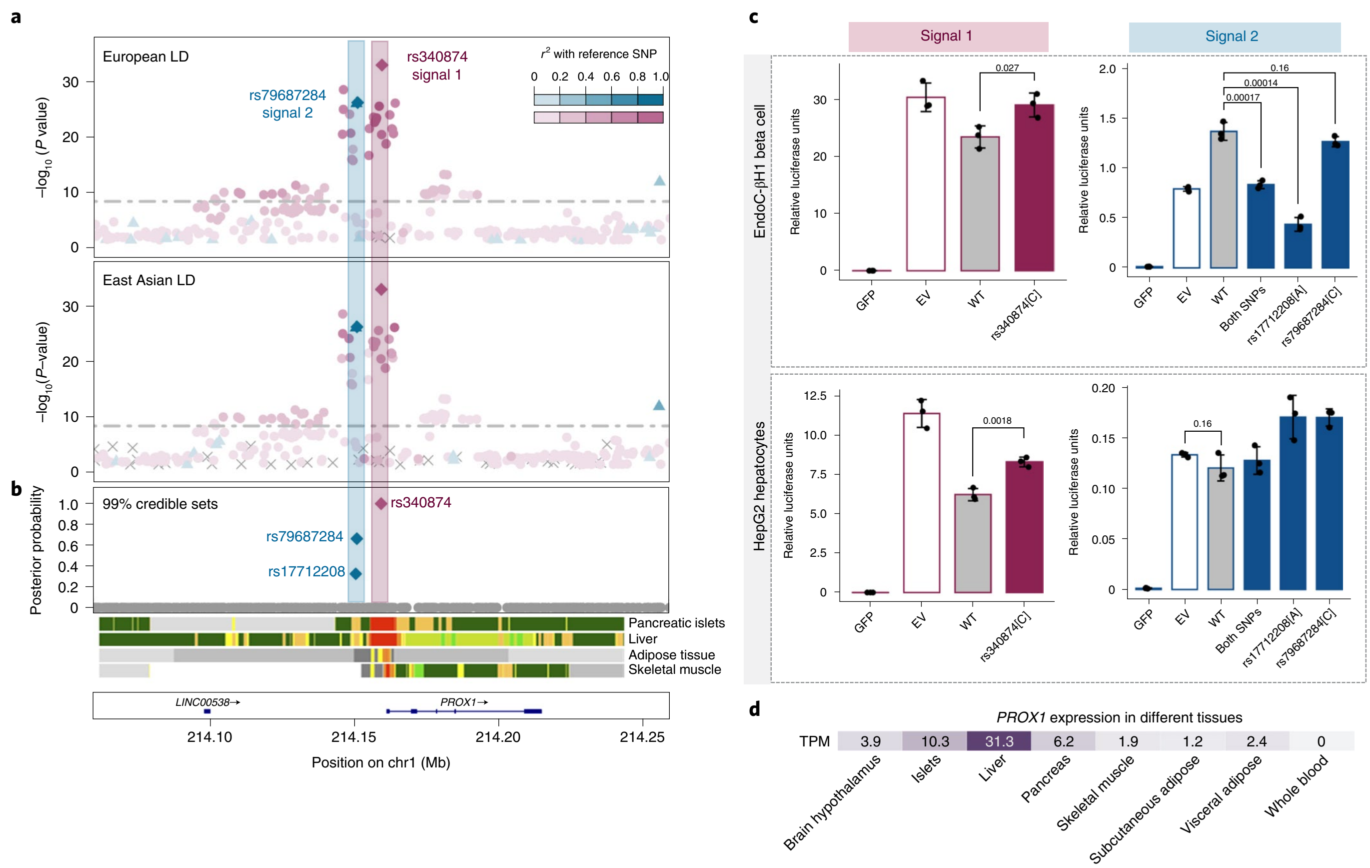

Fig. 3 | Defining causal molecular mechanisms at the *PROX1* locus. a, Signal plot for two distinct T2D associations from multi-ancestry meta-regression of 180,834 affected individuals and 1,159,055 controls of diverse ancestry. Each point represents an SNV, plotted with its *P* value (on a $-\log_{10}$ scale) as a function of genomic position (NCBI build 37). Index SNVs are represented by blue and purple diamonds. All other SNVs are colored according to the LD with the index SNVs in European and East Asian ancestry populations. Gene annotations were taken from the University of California Santa Cruz genome browser. **b**, Fine-mapping of T2D-association signals from multi-ancestry meta-regression. Each point represents an SNV plotted with its posterior probability of driving each distinct T2D association as a function of genomic position (NCBI build 37). The 99% credible sets for the two signals are highlighted by purple and blue diamonds. Chromatin states are presented for four diabetes-relevant tissues: active TSS (red), flanking active TSS (orange-red), strong transcription (green), weak transcription (dark green), genic enhancers (green–yellow), active enhancers (orange), weak enhancers (yellow), bivalent or poised TSS (Indian red), flanking bivalent TSS or enhancer (dark salmon), repressed polycomb (silver), weak repressed polycomb (gainsboro), quiescent or low (white). **c**, Transcriptional activity of the 99 credible set variants at the two T2D-association signals in human HepG2 hepatocytes and EndoC-βH1 beta cell models obtained from in vitro reporter assays. Biological replicates, $n=3$; technical replicates, $n=3$. WT, wild type (non-risk allele or haplotype); GFP, green fluorescent protein (negative control); EV, empty vector (baseline). Heights of bars represent means. Error bars represent s.e.m. Differences in luciferase activity between groups were tested using two-tailed two-sample *t*-tests, for which $P<0.05$ was considered statistically significant. **d**, Expression of *PROX1* across a range of diabetes-relevant tissues.

these implicate new candidate causal genes for the disease: *MYO5C* p.Glu1075Lys (rs3825801, $P=3.8\times10^{-11}$, $\pi=69.2\%$) at the *MYO5C* locus and *ACVR1C* p.Ile482Val (rs7594480, $P=4.0\times10^{-12}$, $\pi=95.2\%$) at the *CYTIP* locus. *ACVR1C* encodes ALK7, a transforming growth factor β receptor, overexpression of which induces growth inhibition and apoptosis of pancreatic beta cells[19]; *ACVR1C* p.Ile482Val has been previously associated with body fat distribution[20]. The multi-ancestry meta-regression also highlighted examples of previously reported associations that were better resolved by fine-mapping across diverse populations, including *SLC16A11*, *KCNJ11–ABCC8* and *ZFAND3–KCNK16–GLP1R* (Supplementary Note).

Multi-omics integration highlights candidate effector genes. We next sought to take advantage of the improved fine-mapping resolution offered by the multi-ancestry meta-regression to extend insights into candidate effector genes, tissue specificity and mechanisms through which regulatory variants at noncoding T2D-association signals impact disease risk. We integrated annotation-informed fine-mapping data with molecular quantitative trait loci (QTL) in *cis* for (1) circulating plasma proteins (pQTL)[21] and (2) gene expression (eQTL) in diverse tissues, including pancreatic islets, subcutaneous and visceral adipose tissue, liver, skeletal muscle and hypothalamus[22,23] (Methods). Bayesian colocalization[24] of each pair of distinct T2D associations and molecular QTL identified 97 candidate effector genes at 72 signals with posterior probability $\pi_{\mathrm{COLOC}}>80\%$ (Supplementary Tables 16 and 17). The colocalizations reinforced evidence supporting several genes previously implicated in T2D through detailed experimental studies, including *ADCY5*, *STARD10*, *IRS1*, *KLF14*, *SIX3* and *TCF7L2* (refs. [25–29]). A single candidate effector gene was implicated at 49 T2D-association signals, of which ten colocalized with eQTL across multiple tissues: *CEP68*, *ITGB6*, *RBM6*, *PCGF3*, *JAZF1*, *ANK1*, *ABO*, *ARHGAP19*, *PLEKHA1* and *AP3S2*. By contrast, we observed that *cis* eQTL at 44 signals were specific to one tissue (24 to pancreatic islets, 11 to subcutaneous adipose tissue, five to skeletal muscle, two to visceral adipose tissue and one each to liver and hypothalamus),

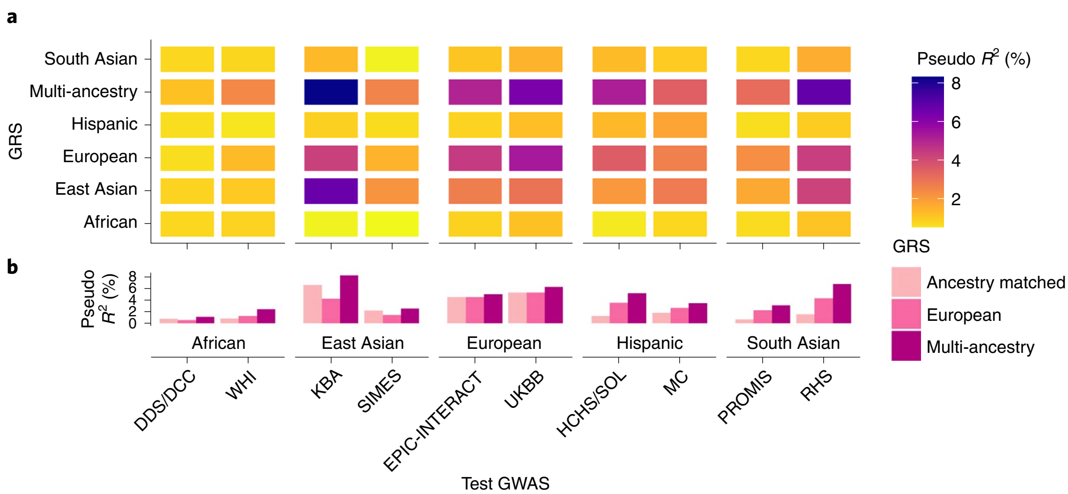

Fig. 4 | Transferability of multi-ancestry and ancestry-specific GRS into GWAS across diverse population groups. Each GRS was constructed using lead SNVs attaining genome-wide significance ($P<5\times10^{-9}$ for multi-ancestry GRS and $P<5\times10^{-8}$ for ancestry-specific GRS). For the multi-ancestry GRS, population-specific allelic effects on T2D were estimated from the meta-regression to generate different GRS weights for each test GWAS. Test GWAS acronyms are defined in Supplementary Table 1. For each ancestry-specific GRS, weights were generated from allelic effect estimates obtained from the fixed-effects meta-analysis. **a**, The trait variance explained (pseudo R^2) by each GRS was assessed in two test GWAS from each ancestry group. **b**, The multi-ancestry GRS out-performed ancestry-specific GRS into all test GWAS, reflecting the shared genetic contribution to T2D across diverse populations, despite differing allele frequencies and LD patterns.

emphasizing the importance of conducting colocalization analyses across multiple tissues. Genome-wide promoter-focused chromatin confirmation capture data (pcHi-C) from pancreatic islets, subcutaneous adipose tissue and liver (equivalent data are not available from hypothalamus or visceral adipose tissue)[30–32] provided complementary support for several candidate effector genes (Supplementary Table 18 and Supplementary Note). These results demonstrate how the increased fine-mapping resolution afforded by our multi-ancestry meta-analysis can be integrated with diverse molecular data resources to reveal putative mechanisms underlying T2D susceptibility.

At the *BCAR1* locus, multi-ancestry fine-mapping resolved the T2D-association signal to a 99% credible set of nine variants. These variants overlap a chromatin-accessible single-nucleus assay for transposase-accessible chromatin using sequencing (snATAC-seq) peak in human pancreatic acinar cells[33] and an enhancer element in human pancreatic islets that interacts with an active promoter upstream of *CTRB2* (encoding the pancreatic exocrine enzyme chymotrypsin B2)[31]. The observations in bulk pancreatic islets are likely to have arisen due to exocrine (acinar cell) contamination, as single-cell data do not support the expression of *CTRB2* in endocrine cells (Fig. 2). The T2D-association signal also colocalized with a *cis* pQTL for circulating plasma levels of chymotrypsin B1 (CTRB1; $\pi_{\mathrm{COLOC}}=98.6\%$). Interestingly, by extending our colocalization analyses at this locus to *trans* pQTL, we found that variants driving the T2D-association signal also regulate levels of three other pancreatic secretory enzymes produced by acinar cells and involved in the digestion of ingested fats and proteins: carboxypeptidase B1 (CPB1; $\pi_{\mathrm{COLOC}}=98.8\%$), pancreatic lipase-related protein 1 (PLRP1; $\pi_{\mathrm{COLOC}}=97.6\%$) and serine protease 2 (PRSS2; $\pi_{\mathrm{COLOC}}=98.3\%$). These observations are consistent with an effect of T2D-associated variants at this locus on gene and protein expression in the exocrine pancreas, with consequences for pancreatic endocrine function. This is in line with a recent study[34] reporting rare mutations in the gene encoding another protein produced by the exocrine pancreas, chymotrypsin-like elastase family member 2A, which were found to influence levels of digestive enzymes and glucagon (secreted from alpha cells in pancreatic islets). In sum, these complementary findings add to a growing body of evidence linking defects in the exocrine pancreas and T2D pathogenesis[35,36].

At the *PROX1* locus, multi-ancestry fine-mapping localized the two distinct association signals to only three variants (Fig. 3 and Extended Data Fig. 8). The index SNV at the first signal (rs340874, $P=1.1\times10^{-18}$, $\pi>99.9\%$) overlaps the *PROX1* promoter in both human liver and pancreatic islets[18,29]. At the second signal, the two credible set variants map to the same enhancer active in islets and liver (rs79687284, $P=6.9\times10^{-19}$, $\pi=66.7\%$; rs17712208, $P=1.4\times10^{-18}$, $\pi=33.3\%$). Recent studies have demonstrated that the T2D-risk allele at rs17712208 (but not rs79687284) results in significant repression of enhancer activity in mouse MIN6 (ref. [33]) and human EndoC-βH1 beta cell models[37]. Furthermore, this enhancer interacts with the *PROX1* promoter in islets[31] but not in liver[32]. Motivated by these observations, we sought to determine whether these distinct signals impact T2D risk (via *PROX1*) in a tissue-specific manner by assessing transcriptional activity of the credible set variants (rs340874, rs79687284 and rs17712208) in human HepG2 hepatocyte and EndoC-βH1 beta cell models using in vitro reporter assays (Methods and Fig. 3). At the first signal, we demonstrated significant differences in luciferase activity between alleles at rs340874 in both hepatocytes (33% increase for risk allele, $P=0.0018$) and beta cells (24% increase for risk allele, $P=0.027$). However, at the second signal, a significant difference in luciferase activity between alleles was observed only for rs17712208 in islets (68% decrease for risk allele, $P=0.00014$). Interestingly, there was evidence that the risk allele at rs79687284 could attenuate the effect, as the combined effect of both risk alleles in the credible set was less severe. In HepG2 cells, both risk alleles increased transcription relative to wild type, although the difference for each variant alone or combined was not statistically significant. In sum, these results suggest that likely causal variants at these distinct association signals exert their impact on T2D through the same effector gene, *PROX1*, but act in different tissue-specific manners.

Transferability of T2D GRS across diverse populations. GRS derived from European ancestry GWAS have limited transferability

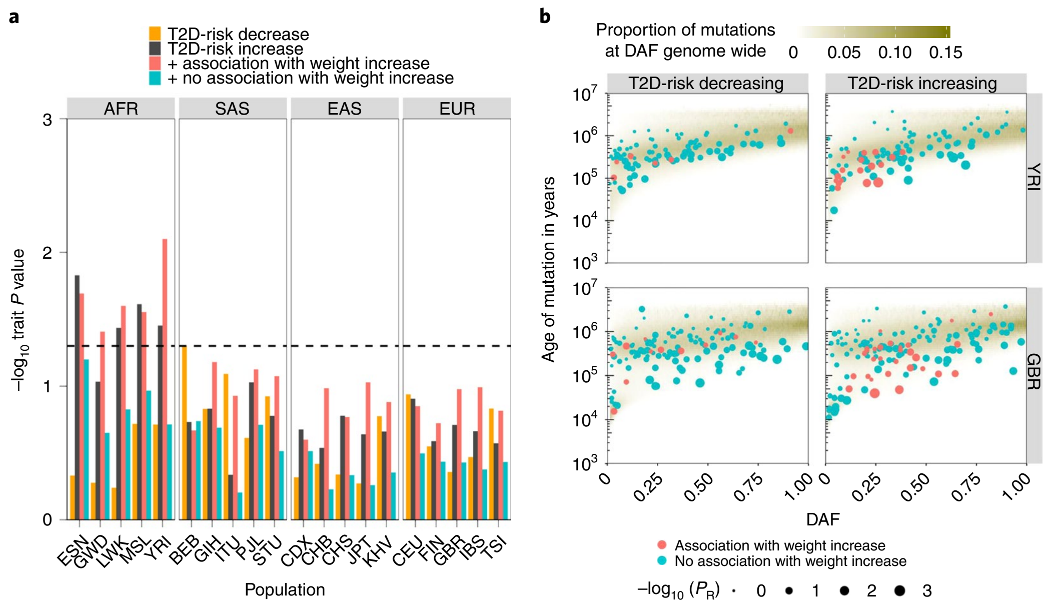

Fig. 5 | Positive selection acting on T2D index SNVs. a, Evidence of selection from Relate. Increased T2D risk is restricted to African (AFR) ancestry populations and is explained by those SNVs that are associated with increased weight. No evidence of selection was observed in South Asian (SAS) ancestry populations, East Asian (EAS) ancestry populations or European (EUR) ancestry populations. **b**, T2D-risk alleles that are associated with increased weight are particularly young for their derived allele frequency (DAF). P_R, P value for selection evidence. Population abbreviations (sample sizes): ESN (98), Esan in Nigeria; GWD (112), Gambian in Western Divisions of the Gambia; LWK (98), Luhya in Webuye, Kenya; MSL (84), Mende in Sierra Leone; YRI (107), Yoruba in Ibadan, Nigeria; BEB (85), Bengali in Bangladesh; GIH (102), Gujarati Indian from Houston, Texas; ITU (101), Indian Telegu from the UK; PJL (95), Punjabi from Lahore, Pakistan; STU (101), Sri Lankan Tamil from the UK; CDX (92), Chinese Dai in Xishuangbanna, China; CHB (102), Han Chinese in Beijing, China; CHS (104), Southern Han Chinese; JPT (103), Japanese in Tokyo, Japan; KHV (98), Kinh in Ho Chi Min City, Vietnam; CEU (98), Utah residents with northern and western European ancestry; FIN (98), Finnish in Finland; GBR (90), British in England and Scotland; IBS (106), Iberian population in Spain; TSI (106), Toscani in Italy.

into other population groups in part because of ancestry-correlated differences in the frequency and effect of risk alleles[38]. We took advantage of the population diversity in the DIAMANTE study to compare the prediction performance of multi-ancestry and ancestry-specific T2D GRS constructed using lead SNVs at loci attaining genome-wide significance. We selected two studies per ancestry group as test GWAS into which the prediction performance of the GRS was assessed using trait variance explained (pseudo R^2) and odds ratio (OR) per risk score unit. We repeated the multi-ancestry meta-regression and ancestry-specific meta-analyses after excluding the test GWAS and defined lead SNVs at loci attaining genome-wide significance ($P<5\times10^{-9}$ for multi-ancestry GRS and $P<5\times10^{-8}$ for ancestry-specific GRS). For each ancestry-specific GRS, we used allelic effect estimates for each lead SNV as weights, irrespective of the population in which the test GWAS was undertaken. However, for the multi-ancestry GRS, we derived weights for each lead SNV that were specific to each test GWAS population by allowing for ancestry-correlated heterogeneity in allelic effects (Methods).

As expected, ancestry-specific GRS performed best in test GWAS from their respective ancestry group (Fig. 4 and Supplementary Table 19). However, for the ancestry groups with the smallest effective sample size (African, Hispanic and South Asian), the predictive power of the ancestry-specific GRS was weak (pseudo $R^2<1\%$) because the number of lead SNVs attaining genome-wide significance was small. For test GWAS from these under-represented ancestry groups, the European ancestry-specific GRS out-performed the ancestry-matched GRS because (1) more lead SNVs attained genome-wide significance in the European ancestry meta-analysis; and (2) the T2D-association signals represented by these lead SNVs are mostly shared across ancestry groups despite differing allele frequencies and LD patterns. Notwithstanding these observations, the greatest predictive power for test GWAS from all ancestry groups was achieved by the multi-ancestry GRS weighted with population-specific allelic effect estimates.

We then tested the power of the multi-ancestry GRS to predict T2D status in 129,230 individuals of Finnish ancestry from FinnGen, a population-based biobank from Finland (Methods). Because FinnGen was not part of the DIAMANTE study, we used association summary statistics from the complete meta-regression to derive Finnish-specific allelic effect estimates to use as weights in the multi-ancestry GRS (Extended Data Fig. 9 and Supplementary Table 20). Individuals in the top decile of the GRS were at 5.3-fold increased risk of T2D compared to those in the bottom decile. Inclusion of the multi-ancestry GRS with Finnish-specific weights to a predictive model including age, sex and body mass index (BMI) increased the area under the receiver operating characteristic curve (AUROC) from 81.8% to 83.5%. We note that modest increases in AUROC attributable to the GRS over lifestyle and/or clinical factors in cross-sectional studies can mask impactful improvements in clinical performance, particularly among those individuals at the extremes of the GRS distribution who may have especially high lifetime disease risk and/or be prone to earlier disease onset[39]. In FinnGen, age impacted the power of a predictive model including the T2D GRS, sex and BMI: the AUROC decreased from 86.9% in individuals under 50 years old to 73.1% in those over 80 years old (Supplementary Table 21). Each unit of the weighted GRS was associated with earlier age of T2D diagnosis by 1.24 years ($P=7.1\times10^{-57}$), indicating that those with a higher genetic burden are more likely to be affected earlier in life.

Positive selection of T2D-risk alleles. Previous investigations[40] have concluded that historical positive selection has not had the major impact on T2D envisaged by the thrifty genotype hypothesis[41].

We sought to re-evaluate the evidence for positive selection of T2D-risk alleles across our expanded collection of distinct multi-ancestry association signals. We fitted demographic histories to haplotypes for each population in the 1000 Genomes Project reference panel[13] using Relate[42]. We quantified the evidence for selection for each T2D index SNV by assessing the extent to which the mutation has more descendants than other lineages that were present when it arose (Methods). This approach is well powered to detect positive selection acting on polygenic traits over a period of a few thousand to a few tens of thousands of years. We detected evidence of selection ($P < 0.05$) in four of the five African ancestry populations in the 1000 Genomes Project reference panel (but not other ancestry groups) toward increased T2D risk (Fig. 5). Given that T2D itself is likely to have been an advantageous phenotype only via pleiotropic variants acting through beneficial traits, we tested for association of index SNVs at distinct T2D signals with phenotypes available in the UK Biobank[43] (Methods and Extended Data Fig. 10). We found that T2D-risk alleles that were also associated with increased weight (and other obesity-related traits) generally displayed more recent origin when compared to the genome-wide mutation age distribution at the same derived allele frequency ($P < 0.05$ in all African ancestry populations), consistent with positive selection (Extended Data Fig. 10). Excluding these weight-related SNVs removed the selection signature observed in African ancestry populations. These observations are consistent with positive selection of T2D-risk alleles that has been driven by the promotion of energy storage and use appropriate to the local environment[44]. Outside Africa, our analysis yields no evidence for selection of T2D-risk alleles. This suggests the absence of a selective advantage outside Africa or, alternatively, that the selective advantage is old and now masked in the relatively more strongly bottlenecked groups outside Africa. Further work is needed to characterize the specific pathways responsible for this adaptation and its finer-scale geographic impact.

Discussion

In consideration of the global burden of T2D, the DIAMANTE Consortium assembled the most ancestrally diverse collection of GWAS of the disease to date. We implemented a powerful meta-regression approach[15] to enable aggregation of GWAS summary statistics across diverse populations that allows for heterogeneity in allelic effects on disease risk that is correlated with ancestry. By representing the ancestry of each study as multidimensional and continuous axes of genetic variation, the meta-regression model is not restricted to broad continental ancestry categories and can allow for finer-scale differences between GWAS within ancestry groups[45]. Our study demonstrated the advantages of applying this approach to ancestrally diverse GWAS in DIAMANTE with regard to (1) discovery of association signals that are shared across populations through increased sample size and by reducing the genomic control inflation due to residual stratification, (2) defining the extent of heterogeneity in allelic effects at distinct association signals, (3) allowing for LD-driven heterogeneity to enable fine-mapping of causal variants and (4) deriving population-specific weights that substantially improve the transferability of multi-ancestry GRS over ancestry-specific GRS. Our analyses considered SNVs present in the 1000 Genomes Project[13] and Haplotype Reference Consortium[14] reference panels used for imputation, which potentially excludes low-frequency population-specific variants, but provides a uniform 'backbone' of variants for fine-mapping association signals that are shared across multiple population groups. The contribution of population-specific variants that do not overlap reference panels is more fully assessed in complementary ancestry-specific meta-analyses, such as those in European and East Asian components of DIAMANTE[6,10]. Further development of fine-mapping methods is required to localize such population-specific causal variants in multi-ancestry meta-analysis[46].

Our study has extended knowledge of T2D genetics over previous efforts that include GWAS that have contributed to our multi-ancestry meta-analysis[6,10,11], demonstrating the opportunities to deliver new biological insights and identify new target genes and mechanisms through which genetic variation impacts on disease risk. Annotation-informed multi-ancestry fine-mapping resolved 54.4% of distinct T2D-association signals to a single variant with >50% posterior probability. Through integration of these fine-mapping data with molecular QTL resources, we identified a total of 117 candidate causal genes at T2D loci, of which 40 were not reported in complementary analyses undertaken in previous efforts (Supplementary Note). Formal Bayesian colocalization analyses across diverse tissues highlighted complex cell type-specific mechanisms through which regulatory variants at noncoding T2D-association signals impact disease risk, exemplified by the *BCAR1* and *PROX1* loci, and lay the foundations for future functional investigations. Our study demonstrates the advantages of a GRS derived from multi-ancestry meta-regression for T2D prediction across five major ancestry groups. Finally, we built on our expanded collection of distinct multi-ancestry association signals to demonstrate evidence of positive selection of T2D-risk alleles in African populations that may have been driven by the promotion of energy storage and use through adaptation to the local environment.

Multi-ancestry meta-analysis maximizes power to detect association signals that are shared across ancestry groups. However, by modeling heterogeneity in allelic effects across ancestries, our meta-regression approach can also allow for association signals that are driven by ancestry-specific causal variants, although power will be limited by the sample size available in that ancestry group. Ancestry-specific variants tend to have lower frequency, with the result that discovery of T2D associations that are unique to African, Hispanic or South Asian ancestry groups in our study will have been limited to those with relatively large effects. To address this limitation, it remains essential that the human genetics research community continues to bolster GWAS collections in under-represented populations that often suffer the greatest burden of disease and to further expand diversity in imputation reference panels, as exemplified by the Trans-Omics for Precision Medicine (TOPMed) Program[47]. Increasing diversity in genetic research will ultimately provide a more comprehensive and refined view of the genetic contribution to complex human traits, powering understanding of the molecular and biological processes underlying common diseases, and offering the most promising opportunities for clinical translation of GWAS findings to improve global public health.

Online content

Any methods, additional references, Nature Research reporting summaries, source data, extended data, supplementary information, acknowledgements, peer review information; details of author contributions and competing interests; and statements of data and code availability are available at https://doi.org/10.1038/s41588-022-01058-3.

Received: 1 March 2021; Accepted: 23 March 2022;
Published online: 12 May 2022

References

1. NCD Risk Factor Collaboration. Worldwide trends in diabetes since 1980: a pooled analysis of 751 population-based studies with 4.4 million participants. *Lancet* **387**, 1513–1530 (2016).
2. GBD 2015 Disease and Injury Incidence and Prevalence Collaborators. Global, regional, and national incidence, prevalence, and years lived with disability for 310 diseases and injuries, 1990–2015: a systematic analysis for the Global Burden of Disease Study 2015. *Lancet* **388**, 1545–1602 (2016).
3. Voight, B. F. et al. Twelve type 2 diabetes susceptibility loci identified through large-scale association analysis. *Nat. Genet.* **42**, 579–589 (2010).
4. Morris, A. P. et al. Large-scale association analysis provides insights into the genetic architecture and pathophysiology of type 2 diabetes. *Nat. Genet.* **44**, 981–990 (2012).

5. Scott, R. A. et al. An expanded genome-wide association study of type 2 diabetes in Europeans. *Diabetes* **66**, 2888–2902 (2017).
6. Mahajan, A. et al. Fine-mapping type 2 diabetes loci to single-variant resolution using high-density imputation and islet-specific epigenome maps. *Nat. Genet.* **50**, 1505–1513 (2018).
7. Moltke, I. et al. A common Greenlandic *TBC1D4* variant confers muscle insulin resistance and type 2 diabetes. *Nature* **512**, 190–193 (2014).
8. Martin, A. R. et al. Human demographic history impacts genetic risk prediction across diverse populations. *Am. J. Hum. Genet.* **100**, 635–649 (2017).
9. Suzuki, K. et al. Identification of 28 new susceptibility loci for type 2 diabetes in the Japanese population. *Nat. Genet.* **51**, 379–386 (2019).
10. Spracklen, C. N. et al. Identification of type 2 diabetes loci in 433,540 East Asian individuals. *Nature* **582**, 240–245 (2020).
11. Vujkovic, M. et al. Discovery of 318 new risk loci for type 2 diabetes and related vascular outcomes among 1.4 million participants in a multi-ancestry meta-analysis. *Nat. Genet.* **52**, 680–691 (2020).
12. The 1000 Genomes Project Consortium. An integrated map of genetic variation from 1,092 human genomes. *Nature* **491**, 56–65 (2012).
13. The 1000 Genomes Project Consortium. A global reference for human genetic variation. *Nature* **526**, 68–74 (2015).
14. McCarthy, S. et al. A reference panel of 64,976 haplotypes for genotype imputation. *Nat. Genet.* **48**, 1279–1283 (2016).
15. Mägi, R. et al. Trans-ethnic meta-regression of genome-wide association studies accounting for ancestry increases power for discovery and improves fine-mapping resolution. *Hum. Mol. Genet.* **26**, 3639–3650 (2017).
16. Chen, M.-H. et al. Trans-ethnic and ancestry-specific blood-cell genetics in 746,667 individuals from 5 global populations. *Cell* **182**, 1198–1213 (2020).
17. Mahajan, A. et al. Refining the accuracy of validated target identification through coding variant fine-mapping in type 2 diabetes. *Nat. Genet.* **50**, 559–571 (2018).
18. Varshney, A. et al. Genetic regulatory signatures underlying islet gene expression and type 2 diabetes. *Proc. Natl Acad. Sci. USA* **114**, 2301–2306 (2017).
19. Zhao, F. et al. Nodal induces apoptosis through activation of the ALK7 signaling pathway in pancreatic INS-1 β-cells. *Am. J. Physiol. Endocrinol. Metab.* **303**, E132–E143 (2012).
20. Emdin, C. A. et al. DNA sequence variation in *ACVR1C* encoding the activin receptor-like kinase 7 influences body fat distribution and protects against type 2 diabetes. *Diabetes* **68**, 226–234 (2019).
21. Sun, B. B. et al. Genomic atlas of the human plasma proteome. *Nature* **558**, 73–79 (2018).
22. GTEx Consortium. Genetic effects on gene expression across human tissues. *Nature* **550**, 204–213 (2017).
23. Vinuela, A. et al. Genetic variant effects on gene expression in human pancreatic islets and their implications for T2D. *Nat. Commun.* **11**, 4912 (2020).
24. Giambartolomei, C. et al. Bayesian test for colocalization between pairs of genetic association studies using summary statistics. *PLoS Genet.* **10**, e1004383 (2014).
25. van de Bunt, M. et al. Transcript expression data from human islets links regulatory signals from genome-wide association studies for type 2 diabetes and glycemic traits to their downstream effectors. *PLoS Genet.* **11**, e1005694 (2015).
26. Roman, T. S. et al. A type 2 diabetes-associated functional regulatory variant in a pancreatic islet enhancer at the *ADCY5* locus. *Diabetes* **66**, 2521–2530 (2017).
27. Carrat, G. R. et al. Decreased *STARD10* expression is associated with defective insulin secretion in humans and mice. *Am. J. Hum. Genet.* **100**, 238–256 (2017).
28. Small, K. S. et al. Regulatory variants at *KLF14* influence type 2 diabetes risk via a female-specific effect on adipocyte size and body composition. *Nat. Genet.* **50**, 572–580 (2018).
29. Thurner, M. et al. Integration of human pancreatic islet genomic data refines regulatory mechanisms at type 2 diabetes susceptibility loci. *eLife* **7**, e31977 (2018).
30. Pan, D. Z. et al. Integration of human adipocyte chromosomal interactions with adipose gene expression prioritizes obesity-related genes from GWAS. *Nat. Commun.* **9**, 1512 (2018).
31. Miguel-Escalada, I. et al. Human pancreatic islet three-dimensional chromatin architecture provides insights into the genetics of type 2 diabetes. *Nat. Genet.* **51**, 1137–1148 (2019).
32. Chesi, A. et al. Genome-scale Capture C promoter interactions implicate effector genes at GWAS loci for bone mineral density. *Nat. Commun.* **10**, 1260 (2019).
33. Chiou, J. et al. Single-cell chromatin accessibility reveals pancreatic islet cell type- and state-specific regulatory programs of diabetes risk. *Nat. Genet.* **53**, 455–466 (2021).
34. Esteghamat, F. et al. *CELA2A* mutations predispose to early-onset atherosclerosis and metabolic syndrome and affect plasma insulin and platelet activation. *Nat. Genet.* **51**, 1233–1243 (2019).
35. Ng, N. H. J. et al. Tissue-specific alteration of metabolic pathways influences glycemic regulation. Preprint at *bioRxiv* https://doi.org/10.1101/790618 (2019).
36. Gloyn, A. L. Exocrine or endocrine? A circulating pancreatic elastase that regulates glucose homeostasis. *Nat. Metab.* **1**, 853–855 (2019).
37. Wesolowska-Andersen, A. et al. Deep learning models predict regulatory variants in pancreatic islets and refine type 2 diabetes association signals. *eLife* **9**, e51503 (2020).
38. Martin, A. R. et al. Clinical use of current polygenic risk scores may exacerbate health disparities. *Nat. Genet.* **51**, 584–591 (2019).
39. Mars, N. et al. Polygenic and clinical risk scores and their impact on age at onset and prediction of cardiometabolic diseases and common cancers. *Nat. Med.* **26**, 549–557 (2020).
40. Ayub, Q. et al. Revisiting the thrifty gene hypothesis via 65 loci associated with susceptibility to type 2 diabetes. *Am. J. Hum. Genet.* **94**, 176–185 (2014).
41. Neel, J. V. Diabetes mellitus: a "thrifty" genotype rendered detrimental by "progress"?. *Am. J. Hum. Genet.* **14**, 353–362 (1962).
42. Speidel, L., Forest, M., Shi, S. & Myers, S. R. A method for genome-wide genealogy estimation for thousands of samples. *Nat. Genet.* **51**, 1321–1329 (2019).
43. Bycroft, C. et al. The UK Biobank resource with deep phenotyping and genomic data. *Nature* **562**, 203–209 (2018).
44. Chen, R. et al. Type 2 diabetes risk alleles demonstrate extreme directional differentiation among human populations, compared to other diseases. *PLoS Genet.* **8**, e1002621 (2012).
45. Lewis, A. C. F. et al. Getting genetic ancestry right for science and society. *Science* **376**, 250–252 (2022).
46. Kanai, M. et al. Insights from complex trait fine-mapping across diverse populations. Preprint at *medRxiv* https://doi.org/10.1101/2021.09.03.21262975 (2021).
47. Taliun, D. et al. Sequencing of 53,831 diverse genomes from the NHLBI TOPMed Program. *Nature* **590**, 290–299 (2021).

Anubha Mahajan[1,2,277] ✉, Cassandra N. Spracklen[3,4,291], Weihua Zhang[5,6,291], Maggie C. Y. Ng[7,8,9,291], Lauren E. Petty[7,291], Hidetoshi Kitajima[2,10,11,12,291], Grace Z. Yu[1,2,291], Sina Rüeger[13,291], Leo Speidel[14,15,291], Young Jin Kim[16], Momoko Horikoshi[17], Josep M. Mercader[18,19,20], Daniel Taliun[21], Sanghoon Moon[16,2], Soo-Heon Kwak[22,2], Neil R. Robertson[1,2], Nigel W. Rayner[1,2,23,24], Marie Loh[5,25,26], Bong-Jo Kim[16], Joshua Chiou[27,278], Irene Miguel-Escalada[28,29], Pietro della Briotta Parolo[13], Kuang Lin[30], Fiona Bragg[30,31], Michael H. Preuss[32], Fumihiko Takeuchi[33], Jana Nano[34], Xiuqing Guo[35], Amel Lamri[36,37], Masahiro Nakatochi[38], Robert A. Scott[39], Jung-Jin Lee[40], Alicia Huerta-Chagoya[41,279], Mariaelisa Graff[42], Jin-Fang Chai[43], Esteban J. Parra[44], Jie Yao[35], Lawrence F. Bielak[45], Yasuharu Tabara[46], Yang Hai[35], Valgerdur Steinthorsdottir[47], James P. Cook[48], Mart Kals[49],

Niels Grarup[50], Ellen M. Schmidt[21], Ian Pan[51], Tamar Sofer[52,53,54], Matthias Wuttke[55], Chloe Sarnowski[56,280], Christian Gieger[57,58,59], Darryl Nousome[60], Stella Trompet[61,62], Jirong Long[63], Meng Sun[2], Lin Tong[64], Wei-Min Chen[65], Meraj Ahmad[66], Raymond Noordam[62], Victor J. Y. Lim[43], Claudia H. T. Tam[67,68], Yoonjung Yoonie Joo[69,70,281], Chien-Hsiun Chen[71], Laura M. Raffield[3], Cécile Lecoeur[72,73], Bram Peter Prins[23], Aude Nicolas[74], Lisa R. Yanek[75], Guanjie Chen[76], Richard A. Jensen[77], Salman Tajuddin[78], Edmond K. Kabagambe[63,282], Ping An[79], Anny H. Xiang[80], Hyeok Sun Choi[81], Brian E. Cade[20,53], Jingyi Tan[35], Jack Flanagan[17,48], Fernando Abaitua[2,283], Linda S. Adair[82], Adebowale Adeyemo[76,2], Carlos A. Aguilar-Salinas[83], Masato Akiyama[84,85], Sonia S. Anand[36,37,86], Alain Bertoni[87], Zheng Bian[88], Jette Bork-Jensen[50], Ivan Brandslund[89,90], Jennifer A. Brody[77], Chad M. Brummett[91], Thomas A. Buchanan[92], Mickaël Canouil[72,73], Juliana C. N. Chan[67,68,93,94], Li-Ching Chang[71], Miao-Li Chee[95], Ji Chen[96,284], Shyh-Huei Chen[97], Yuan-Tsong Chen[71], Zhengming Chen[30,31], Lee-Ming Chuang[98,99], Mary Cushman[100], Swapan K. Das[101], H. Janaka de Silva[102], George Dedoussis[103], Latchezar Dimitrov[8], Ayo P. Doumatey[76], Shufa Du[82,104], Qing Duan[3], Kai-Uwe Eckardt[105,106], Leslie S. Emery[107], Daniel S. Evans[108], Michele K. Evans[78], Krista Fischer[49], James S. Floyd[77], Ian Ford[109], Myriam Fornage[110], Oscar H. Franco[34], Timothy M. Frayling[111], Barry I. Freedman[112], Christian Fuchsberger[21,113], Pauline Genter[114], Hertzel C. Gerstein[36,37,86], Vilmantas Giedraitis[115], Clicerio González-Villalpando[116], Maria Elena González-Villalpando[116], Mark O. Goodarzi[117], Penny Gordon-Larsen[82,104], David Gorkin[118], Myron Gross[119], Yu Guo[88], Sophie Hackinger[23], Sohee Han[16], Andrew T. Hattersley[120], Christian Herder[57,121,122], Annie-Green Howard[104,123], Willa Hsueh[124], Mengna Huang[51,125], Wei Huang[126], Yi-Jen Hung[127,128], Mi Yeong Hwang[16], Chii-Min Hwu[129,130], Sahoko Ichihara[131], Mohammad Arfan Ikram[34], Martin Ingelsson[115], Md Tariqul Islam[132], Masato Isono[33], Hye-Mi Jang[16], Farzana Jasmine[64], Guozhi Jiang[67,68], Jost B. Jonas[133], Marit E. Jørgensen[134,135], Torben Jørgensen[136,137,138], Yoichiro Kamatani[84,139], Fouad R. Kandeel[140], Anuradhani Kasturiratne[141], Tomohiro Katsuya[142,143], Varinderpal Kaur[19], Takahisa Kawaguchi[46], Jacob M. Keaton[8,63,285], Abel N. Kho[144,145], Chiea-Chuen Khor[146], Muhammad G. Kibriya[64], Duk-Hwan Kim[147], Katsuhiko Kohara[148,286], Jennifer Kriebel[57,58,59], Florian Kronenberg[149], Johanna Kuusisto[150], Kristi Läll[49,151], Leslie A. Lange[152], Myung-Shik Lee[153,154], Nanette R. Lee[155], Aaron Leong[19,156,157], Liming Li[158], Yun Li[3], Ruifang Li-Gao[159], Symen Ligthart[34], Cecilia M. Lindgren[2,160,161], Allan Linneberg[136,162], Ching-Ti Liu[56], Jianjun Liu[146,163], Adam E. Locke[164,165,287], Tin Louie[107], Jian'an Luan[39], Andrea O. Luk[67,68], Xi Luo[166], Jun Lv[158], Valeriya Lyssenko[167,168], Vasiliki Mamakou[169], K. Radha Mani[66,292], Thomas Meitinger[170,171,172], Andres Metspalu[49], Andrew D. Morris[173], Girish N. Nadkarni[32,174,175], Jerry L. Nadler[176], Michael A. Nalls[74,177,178], Uma Nayak[65], Suraj S. Nongmaithem[66], Ioanna Ntalla[179], Yukinori Okada[180,181,182], Lorena Orozco[183], Sanjay R. Patel[184], Mark A. Pereira[185], Annette Peters[57,58,172], Fraser J. Pirie[186], Bianca Porneala[157], Gauri Prasad[187,188], Sebastian Preissl[118], Laura J. Rasmussen-Torvik[189], Alexander P. Reiner[190], Michael Roden[57,121,122], Rebecca Rohde[42], Kathryn Roll[35], Charumathi Sabanayagam[95,191,192], Maike Sander[193,194,195], Kevin Sandow[35], Naveed Sattar[196], Sebastian Schönherr[149], Claudia Schurmann[32,174,197], Mohammad Shahriar[64,288], Jinxiu Shi[126], Dong Mun Shin[16], Daniel Shriner[76], Jennifer A. Smith[45,198], Wing Yee So[67,93,2], Alena Stančáková[150], Adrienne M. Stilp[107], Konstantin Strauch[2,199,200,201], Ken Suzuki[17,84,180,202], Atsushi Takahashi[84,203], Kent D. Taylor[35], Barbara Thorand[57,58], Gudmar Thorleifsson[47], Unnur Thorsteinsdottir[47,204], Brian Tomlinson[67,205], Jason M. Torres[2,289], Fuu-Jen Tsai[206], Jaakko Tuomilehto[207,208,209,210], Teresa Tusie-Luna[211,212], Miriam S. Udler[18,19,156], Adan Valladares-Salgado[213], Rob M. van Dam[43,163], Jan B. van Klinken[214,215,216], Rohit Varma[217], Marijana Vujkovic[218], Niels Wacher-Rodarte[219], Eleanor Wheeler[39], Eric A. Whitsel[42,220], Ananda R. Wickremasinghe[141], Ko Willems van Dijk[214,215,221], Daniel R. Witte[222,223], Chittaranjan S. Yajnik[224], Ken Yamamoto[225], Toshimasa Yamauchi[202], Loïc Yengo[226], Kyungheon Yoon[16], Canqing Yu[158], Jian-Min Yuan[227,228], Salim Yusuf[36,37,86], Liang Zhang[95], Wei Zheng[63], FinnGen*, eMERGE Consortium*, Leslie J. Raffel[229], Michiya Igase[230], Eli Ipp[114], Susan Redline[20,53,231], Yoon Shin Cho[81], Lars Lind[232], Michael A. Province[79], Craig L. Hanis[233], Patricia A. Peyser[45], Erik Ingelsson[234,235], Alan B. Zonderman[78], Bruce M. Psaty[77,236,237], Ya-Xing Wang[238], Charles N. Rotimi[76], Diane M. Becker[75], Fumihiko Matsuda[46], Yongmei Liu[87,239], Eleftheria Zeggini[23,24,240], Mitsuhiro Yokota[241], Stephen S. Rich[242], Charles Kooperberg[190], James S. Pankow[185], James C. Engert[243,244], Yii-Der Ida Chen[35], Philippe Froguel[72,73,245], James G. Wilson[246], Wayne H. H. Sheu[128,130,247], Sharon L. R. Kardia[45], Jer-Yuarn Wu[71], M. Geoffrey Hayes[69,248,249], Ronald C. W. Ma[67,68,93,94], Tien-Yin Wong[95,191,192], Leif Groop[13,167], Dennis O. Mook-Kanamori[159], Giriraj R. Chandak[66], Francis S. Collins[250], Dwaipayan Bharadwaj[187,251], Guillaume Paré[37,252], Michèle M. Sale[65,293], Habibul Ahsan[64], Ayesha A. Motala[186], Xiao-Ou Shu[63], Kyong-Soo Park[22,253,254], J. Wouter Jukema[61,255], Miguel Cruz[213], Roberta McKean-Cowdin[60], Harald Grallert[57,58,59], Ching-Yu Cheng[95,191,192], Erwin P. Bottinger[32,174,197], Abbas Dehghan[5,34,256], E-Shyong Tai[43,163,257], Josée Dupuis[56], Norihiro Kato[33], Markku Laakso[150], Anna Köttgen[55], Woon-Puay Koh[258,259], Colin N. A. Palmer[260], Simin Liu[51,125,261], Goncalo Abecasis[21], Jaspal S. Kooner[6,256,262,263], Ruth J. F. Loos[32,50,264], Kari E. North[42], Christopher A. Haiman[60], Jose C. Florez[18,19,156], Danish Saleheen[40,265,266], Torben Hansen[50], Oluf Pedersen[50], Reedik Mägi[49], Claudia Langenberg[39,267], Nicholas J. Wareham[39], Shiro Maeda[17,268,269], Takashi Kadowaki[202,290], Juyoung Lee[16], Iona Y. Millwood[30,31], Robin G. Walters[30,31], Kari Stefansson[47,204], Simon R. Myers[2,270], Jorge Ferrer[28,29,271], Kyle J. Gaulton[193,194], James B. Meigs[18,156,157], Karen L. Mohlke[3], Anna L. Gloyn[1,2,272,273,294], Donald W. Bowden[8,9,274,294], Jennifer E. Below[7,294], John C. Chambers[5,6,25,256,262,294], Xueling Sim[43,294], Michael Boehnke[21,294], Jerome I. Rotter[35,294], Mark I. McCarthy[1,2,272,277,294] ✉ and Andrew P. Morris[2,48,49,275,276,294] ✉

[1]Oxford Centre for Diabetes, Endocrinology and Metabolism, Radcliffe Department of Medicine, University of Oxford, Oxford, UK. [2]Wellcome Centre for Human Genetics, Nuffield Department of Medicine, University of Oxford, Oxford, UK. [3]Department of Genetics, University of North Carolina at Chapel Hill, Chapel Hill, NC, USA. [4]Department of Epidemiology and Biostatistics, University of Massachusetts Amherst, Amherst, MA, USA. [5]Department of Epidemiology and Biostatistics, Imperial College London, London, UK. [6]Department of Cardiology, Ealing Hospital, London North West Healthcare NHS Trust, London, UK. [7]Vanderbilt Genetics Institute, Division of Genetic Medicine, Vanderbilt University Medical Center, Nashville, TN, USA. [8]Center for Genomics and Personalized Medicine Research, Wake Forest School of Medicine, Winston-Salem, NC, USA. [9]Department of Biochemistry, Wake Forest School of Medicine, Winston-Salem, NC, USA. [10]The Advanced Research Center for Innovations in Next-Generation Medicine (INGEM), Tohoku University, Sendai, Japan. [11]Department of Integrative Genomics, Tohoku Medical Megabank Organization, Tohoku University, Sendai, Japan. [12]Cancer Center, Tohoku University Hospital, Tohoku University, Sendai, Japan. [13]Institute for Molecular Medicine Finland (FIMM), University of Helsinki, Helsinki, Finland. [14]Genetics Institute, University College London, London, UK. [15]Francis Crick Institute, London, UK. [16]Division of Genome Science, Department of Precision Medicine, National Institute of Health, Cheongju-si, Republic of Korea. [17]Laboratory for Genomics of Diabetes and Metabolism, RIKEN Center for Integrative Medical Sciences, Yokohama, Japan. [18]Programs in Metabolism and Medical & Population Genetics, Broad Institute of Harvard and MIT, Cambridge, MA, USA. [19]Diabetes Unit and Center for Genomic Medicine, Massachusetts General Hospital, Boston, MA, USA. [20]Harvard Medical School, Boston, MA, USA. [21]Department of Biostatistics and Center for Statistical Genetics, University of Michigan, Ann Arbor, MI, USA. [22]Department of Internal Medicine, Seoul National University Hospital, Seoul, South Korea. [23]Department of Human Genetics, Wellcome Sanger Institute, Hinxton, UK. [24]Institute of Translational Genomics, Helmholtz Zentrum München, German Research Center for Environmental Health, Neuherberg, Germany. [25]Lee Kong Chian School of Medicine, Nanyang Technological University, Singapore, Singapore. [26]Translational Laboratory in Genetic Medicine (TLGM), Agency for Science, Technology and Research (A*STAR) and National University of Singapore (NUS), Singapore, Singapore. [27]Biomedical Sciences Graduate Studies Program, University of California San Diego, La Jolla, CA, USA. [28]Regulatory Genomics and Diabetes, Centre for Genomic Regulation, the Barcelona Institute of Science and Technology, Barcelona, Spain. [29]Centro de Investigación Biomédica en Red Diabetes y Enfermedades Metabólicas asociadas (CIBERDEM), Madrid, Spain. [30]Nuffield Department of Population Health, University of Oxford, Oxford, UK. [31]Medical Research Council Population Health Research Unit, University of Oxford, Oxford, UK. [32]The Charles Bronfman Institute for Personalized Medicine, Icahn School of Medicine at Mount Sinai, New York, NY, USA. [33]Department of Gene Diagnostics and Therapeutics, Research Institute, National Center for Global Health and Medicine, Tokyo, Japan. [34]Department of Epidemiology, Erasmus University Medical Center, Rotterdam, the Netherlands. [35]The Institute for Translational Genomics and Population

Sciences, Department of Pediatrics, the Lundquist Institute for Biomedical Innovation (formerly Los Angeles Biomedical Research Institute) at Harbor–UCLA Medical Center, Torrance, CA, USA. [36]Department of Medicine, McMaster University, Hamilton, Ontario, Canada. [37]Population Health Research Institute, Hamilton Health Sciences and McMaster University, Hamilton, Ontario, Canada. [38]Public Health Informatics Unit, Department of Integrated Health Sciences, Nagoya University Graduate School of Medicine, Nagoya, Japan. [39]MRC Epidemiology Unit, Institute of Metabolic Science, University of Cambridge, Cambridge, UK. [40]Division of Translational Medicine and Human Genetics, University of Pennsylvania, Philadelphia, PA, USA. [41]Consejo Nacional de Ciencia y Tecnología (CONACYT), Instituto Nacional de Ciencias Médicas y Nutrición Salvador Zubirán, Mexico City, Mexico. [42]Department of Epidemiology, Gillings School of Global Public Health, University of North Carolina at Chapel Hill, Chapel Hill, NC, USA. [43]Saw Swee Hock School of Public Health, National University of Singapore and National University Health System, Singapore, Singapore. [44]Department of Anthropology, University of Toronto at Mississauga, Mississauga, Ontario, Canada. [45]Department of Epidemiology, School of Public Health, University of Michigan, Ann Arbor, MI, USA. [46]Center for Genomic Medicine, Kyoto University Graduate School of Medicine, Kyoto, Japan. [47]deCODE Genetics, Amgen Inc., Reykjavik, Iceland. [48]Department of Health Data Science, University of Liverpool, Liverpool, UK. [49]Estonian Genome Centre, Institute of Genomics, University of Tartu, Tartu, Estonia. [50]Novo Nordisk Foundation Center for Basic Metabolic Research, Faculty of Health and Medical Sciences, University of Copenhagen, Copenhagen, Denmark. [51]Department of Epidemiology, Brown University School of Public Health, Providence, RI, USA. [52]Department of Biostatistics, Harvard University, Boston, MA, USA. [53]Division of Sleep and Circadian Disorders, Brigham and Women's Hospital, Boston, MA, USA. [54]Department of Medicine, Harvard University, Boston, MA, USA. [55]Institute of Genetic Epidemiology, Department of Data Driven Medicine, Faculty of Medicine and Medical Center, University of Freiburg, Freiburg, Germany. [56]Department of Biostatistics, Boston University School of Public Health, Boston, MA, USA. [57]German Center for Diabetes Research (DZD), Neuherberg, Germany. [58]Institute of Epidemiology, Helmholtz Zentrum München, German Research Center for Environmental Health, Neuherberg, Germany. [59]Research Unit of Molecular Epidemiology, Helmholtz Zentrum München, German Research Center for Environmental Health, Neuherberg, Germany. [60]Department of Population and Public Health Sciences, Keck School of Medicine of USC, Los Angeles, CA, USA. [61]Department of Cardiology, Leiden University Medical Center, Leiden, the Netherlands. [62]Section of Gerontology and Geriatrics, Department of Internal Medicine, Leiden University Medical Center, Leiden, the Netherlands. [63]Division of Epidemiology, Department of Medicine, Institute for Medicine and Public Health, Vanderbilt Genetics Institute, Vanderbilt University Medical Center, Nashville, TN, USA. [64]Institute for Population and Precision Health, the University of Chicago, Chicago, IL, USA. [65]Department of Public Health Sciences and Center for Public Health Genomics, University of Virginia School of Medicine, Charlottesville, VA, USA. [66]Genomic Research on Complex Diseases (GRC-Group), CSIR–Centre for Cellular and Molecular Biology (CSIR-CCMB), Hyderabad, India. [67]Department of Medicine and Therapeutics, the Chinese University of Hong Kong, Hong Kong, China. [68]Chinese University of Hong Kong–Shanghai Jiao Tong University Joint Research Centre in Diabetes Genomics and Precision Medicine, the Chinese University of Hong Kong, Hong Kong, China. [69]Division of Endocrinology, Metabolism, and Molecular Medicine, Department of Medicine, Northwestern University Feinberg School of Medicine, Chicago, IL, USA. [70]Department of Health and Biomedical Informatics, Northwestern University Feinberg School of Medicine, Chicago, IL, USA. [71]Institute of Biomedical Sciences, Academia Sinica, Taipei, Taiwan. [72]Inserm U1283, CNRS UMR 8199, European Genomic Institute for Diabetes, Institut Pasteur de Lille, Lille, France. [73]University of Lille, Lille University Hospital, Lille, France. [74]Laboratory of Neurogenetics, National Institute on Aging, National Institutes of Health, Bethesda, MD, USA. [75]Department of Medicine, Johns Hopkins University School of Medicine, Baltimore, MD, USA. [76]Center for Research on Genomics and Global Health, National Human Genome Research Institute, National Institutes of Health, Bethesda, MD, USA. [77]Cardiovascular Health Research Unit, Department of Medicine, University of Washington, Seattle, WA, USA. [78]Laboratory of Epidemiology and Population Sciences, National Institute on Aging, National Institutes of Health, Baltimore, MD, USA. [79]Division of Statistical Genomics, Washington University School of Medicine, St Louis, MO, USA. [80]Department of Research and Evaluation, Division of Biostatistics Research, Kaiser Permanente of Southern California, Pasadena, CA, USA. [81]Department of Biomedical Science, Hallym University, Chuncheon, South Korea. [82]Department of Nutrition, Gillings School of Global Public Health, University of North Carolina at Chapel Hill, Chapel Hill, NC, USA. [83]Unidad de Investigación en Enfermedades Metabólicas and Departamento de Endocrinología y Metabolismo, Instituto Nacional de Ciencias Médicas y Nutrición Salvador Zubirán, Mexico City, Mexico. [84]Laboratory for Statistical and Translational Genetics, RIKEN Center for Integrative Medical Sciences, Yokohama, Japan. [85]Department of Ocular Pathology and Imaging Science, Graduate School of Medical Sciences, Kyushu University, Fukuoka, Japan. [86]Department of Health Research Methods, Evidence, and Impact, McMaster University, Hamilton, Ontario, Canada. [87]Department of Epidemiology and Prevention, Division of Public Health Sciences, Wake Forest School of Medicine, Winston-Salem, NC, USA. [88]Chinese Academy of Medical Sciences, Beijing, China. [89]Institute of Regional Health Research, University of Southern Denmark, Odense, Denmark. [90]Department of Clinical Biochemistry, Vejle Hospital, Vejle, Denmark. [91]Department of Anesthesiology, University of Michigan Medical School, Ann Arbor, MI, USA. [92]Department of Medicine, Division of Endocrinology and Diabetes, Keck School of Medicine of USC, Los Angeles, CA, USA. [93]Hong Kong Institute of Diabetes and Obesity, the Chinese University of Hong Kong, Hong Kong, China. [94]Li Ka Shing Institute of Health Sciences, the Chinese University of Hong Kong, Hong Kong, China. [95]Singapore Eye Research Institute, Singapore National Eye Centre, Singapore, Singapore. [96]Wellcome Sanger Institute, Hinxton, UK. [97]Department of Biostatistics and Data Science, Wake Forest School of Medicine, Winston-Salem, NC, USA. [98]Division of Endocrinology and Metabolism, Department of Internal Medicine, National Taiwan University Hospital, Taipei, Taiwan. [99]Institute of Epidemiology and Preventive Medicine, National Taiwan University, Taipei, Taiwan. [100]Department of Medicine, University of Vermont, Colchester, VT, USA. [101]Section on Endocrinology and Metabolism, Department of Internal Medicine, Wake Forest School of Medicine, Winston-Salem, NC, USA. [102]Department of Medicine, Faculty of Medicine, University of Kelaniya, Ragama, Sri Lanka. [103]Department of Nutrition and Dietetics, Harokopio University of Athens, Athens, Greece. [104]Carolina Population Center, University of North Carolina at Chapel Hill, Chapel Hill, NC, USA. [105]Department of Nephrology and Medical Intensive Care Medicine, Charité Universitätsmedizin Berlin, Berlin, Germany. [106]Department of Nephrology and Hypertension, Friedrich-Alexander-Universität Erlangen-Nürnberg, Erlangen, Germany. [107]Department of Biostatistics, University of Washington, Seattle, WA, USA. [108]California Pacific Medical Center Research Institute, San Francisco, CA, USA. [109]Robertson Centre for Biostatistics, University of Glasgow, Glasgow, UK. [110]Institute of Molecular Medicine, University of Texas Health Science Center at Houston, Houston, TX, USA. [111]Genetics of Complex Traits, University of Exeter Medical School, University of Exeter, Exeter, UK. [112]Department of Internal Medicine, Wake Forest School of Medicine, Winston-Salem, NC, USA. [113]Institute for Biomedicine, Eurac Research, Affiliated Institute of the University of Lübeck, Bolzano, Italy. [114]Department of Medicine, Division of Endocrinology and Metabolism, Lundquist Research Institute at Harbor–UCLA Medical Center, Torrance, CA, USA. [115]Department of Public Health and Caring Sciences, Uppsala University, Uppsala, Sweden. [116]Centro de Estudios en Diabetes, Unidad de Investigacion en Diabetes y Riesgo Cardiovascular, Centro de Investigacion en Salud Poblacional, Instituto Nacional de Salud Publica, Mexico City, Mexico. [117]Department of Medicine, Division of Endocrinology, Diabetes and Metabolism, Cedars-Sinai Medical Center, Los Angeles, CA, USA. [118]Center for Epigenomics, University of California San Diego, La Jolla, CA, USA. [119]Department of Laboratory Medicine and Pathology, University of Minnesota, Minneapolis, MN, USA. [120]University of Exeter Medical School, University of Exeter, Exeter, UK. [121]Institute for Clinical Diabetology, German Diabetes Center, Leibniz Center for Diabetes Research at Heinrich Heine University Düsseldorf, Düsseldorf, Germany. [122]Department of Endocrinology and Diabetology, Medical Faculty and University Hospital Düsseldorf, Heinrich Heine University Düsseldorf, Düsseldorf, Germany. [123]Department of Biostatistics, Gillings School of Global Public Health, University of North Carolina at Chapel Hill, Chapel Hill, NC, USA. [124]Department of Internal Medicine, Diabetes and Metabolism Research Center, the Ohio State University Wexner Medical Center, Columbus, OH, USA. [125]Center for Global Cardiometabolic Health, Brown University, Providence, RI, USA. [126]Shanghai-MOST Key Laboratory of Health and Disease Genomics, Chinese National Human Genome Center at Shanghai (CHGC) and Shanghai

Institute for Biomedical and Pharmaceutical Technologies (SIBPT), Shanghai, China. [127]Division of Endocrine and Metabolism, Tri-Service General Hospital Songshan Branch, Taipei, Taiwan. [128]School of Medicine, National Defense Medical Center, Taipei, Taiwan. [129]Section of Endocrinology and Metabolism, Department of Medicine, Taipei Veterans General Hospital, Taipei, Taiwan. [130]School of Medicine, National Yang Ming Chiao Tung University, Taipei, Taiwan. [131]Department of Environmental and Preventive Medicine, Jichi Medical University School of Medicine, Shimotsuke, Japan. [132]University of Chicago Research Bangladesh, Dhaka, Bangladesh. [133]Institute of Molecular and Clinical Ophthalmology Basel, Basel, Switzerland. [134]Steno Diabetes Center Copenhagen, Gentofte, Denmark. [135]National Institute of Public Health, Southern Denmark University, Copenhagen, Denmark. [136]Center for Clinical Research and Prevention, Bispebjerg and Frederiksberg Hospital, Frederiksberg, Denmark. [137]Faculty of Health and Medical Sciences, University of Copenhagen, Copenhagen, Denmark. [138]Faculty of Medicine, Aalborg University, Aalborg, Denmark. [139]Laboratory of Complex Trait Genomics, Department of Computational Biology and Medical Sciences, Graduate School of Frontier Sciences, the University of Tokyo, Tokyo, Japan. [140]Department of Clinical Diabetes, Endocrinology & Metabolism, Department of Translational Research and Cellular Therapeutics, City of Hope, Duarte, CA, USA. [141]Department of Public Health, Faculty of Medicine, University of Kelaniya, Ragama, Sri Lanka. [142]Department of Clinical Gene Therapy, Osaka University Graduate School of Medicine, Osaka, Japan. [143]Department of Geriatric and General Medicine, Graduate School of Medicine, Osaka University, Osaka, Japan. [144]Division of General Internal Medicine and Geriatrics, Department of Medicine, Northwestern University Feinberg School of Medicine, Chicago, IL, USA. [145]Center for Health Information Partnerships, Institute for Public Health and Medicine, Northwestern University Feinberg School of Medicine, Chicago, IL, USA. [146]Genome Institute of Singapore, Agency for Science, Technology and Research, Singapore, Singapore. [147]Department of Molecular Cell Biology, Sungkyunkwan University School of Medicine, Suwon, South Korea. [148]Department of Regional Resource Management, Ehime University Faculty of Collaborative Regional Innovation, Ehime, Japan. [149]Institute of Genetic Epidemiology, Department of Genetics and Pharmacology, Medical University of Innsbruck, Innsbruck, Austria. [150]Institute of Clinical Medicine, Internal Medicine, University of Eastern Finland and Kuopio University Hospital, Kuopio, Finland. [151]Institute of Mathematics and Statistics, University of Tartu, Tartu, Estonia. [152]Department of Medicine, University of Colorado Denver, Anschutz Medical Campus, Aurora, CO, USA. [153]Severance Biomedical Science Institute and Department of Internal Medicine, Yonsei University College of Medicine, Seoul, South Korea. [154]Department of Medicine, Samsung Medical Center, Sungkyunkwan University School of Medicine, Seoul, South Korea. [155]USC—Office of Population Studies Foundation, Inc., University of San Carlos, Cebu City, Philippines. [156]Department of Medicine, Harvard Medical School, Boston, MA, USA. [157]Division of General Internal Medicine, Massachusetts General Hospital, Boston, MA, USA. [158]Department of Epidemiology and Biostatistics, Peking University Health Science Centre, Peking University, Beijing, China. [159]Department of Clinical Epidemiology, Leiden University Medical Center, Leiden, the Netherlands. [160]Program in Medical & Population Genetics, Broad Institute, Cambridge, MA, USA. [161]Big Data Institute, Li Ka Shing Centre for Health Information and Discovery, University of Oxford, Oxford, UK. [162]Department of Clinical Medicine, Faculty of Health and Medical Sciences, University of Copenhagen, Copenhagen, Denmark. [163]Department of Medicine, Yong Loo Lin School of Medicine, National University of Singapore and National University Health System, Singapore, Singapore. [164]McDonnell Genome Institute, Washington University School of Medicine, St Louis, MO, USA. [165]Department of Medicine, Division of Genomics and Bioinformatics, Washington University School of Medicine, St Louis, MO, USA. [166]Department of Biostatistics and Data Science, University of Texas Health Science Center at Houston, Houston, TX, USA. [167]Department of Clinical Sciences, Diabetes and Endocrinology, Lund University Diabetes Centre, Malmö, Sweden. [168]Department of Clinical Science, Center for Diabetes Research, University of Bergen, Bergen, Norway. [169]Dromokaiteio Psychiatric Hospital, National and Kapodistrian University of Athens, Athens, Greece. [170]Institute of Human Genetics, Helmholtz Zentrum München, German Research Center for Environmental Health, Neuherberg, Germany. [171]Institute of Human Genetics, Technical University of Munich, Munich, Germany. [172]German Centre for Cardiovascular Research (DZHK), Partner Site Munich Heart Alliance, Munich, Germany. [173]The Usher Institute to the Population Health Sciences and Informatics, University of Edinburgh, Edinburgh, UK. [174]Digital Health Center, Digital Engineering Faculty of Hasso Plattner Institue and University Potsdam, Potsdam, Germany. [175]The Division of Data Driven and Digital Medicine (D3M), Department of Medicine, Icahn School of Medicine at Mount Sinai, New York, NY, USA. [176]Department of Medicine and Pharmacology, New York Medical College, Valhalla, NY, USA. [177]Data Tecnica International LLC, Glen Echo, MD, USA. [178]Center for Alzheimer's and Related Dementias, National Institutes of Health, Baltimore, MD, USA. [179]William Harvey Research Institute, Barts and the London School of Medicine and Dentistry, Queen Mary University of London, London, UK. [180]Department of Statistical Genetics, Osaka University Graduate School of Medicine, Osaka, Japan. [181]Laboratory of Statistical Immunology, Immunology Frontier Research Center (WPI-IFReC), Osaka University, Osaka, Japan. [182]Laboratory for Systems Genetics, RIKEN Center for Integrative Medical Sciences, Yokohama, Japan. [183]Instituto Nacional de Medicina Genómica, Mexico City, Mexico. [184]Division of Pulmonary, Allergy, and Critical Care Medicine, Department of Medicine, University of Pittsburgh, Pittsburgh, PA, USA. [185]Division of Epidemiology and Community Health, School of Public Health, University of Minnesota, Minneapolis, MN, USA. [186]Department of Diabetes and Endocrinology, Nelson R. Mandela School of Medicine, College of Health Sciences, University of KwaZulu-Natal, Durban, South Africa. [187]Academy of Scientific and Innovative Research, CSIR—Human Resource Development Centre Campus, Ghaziabad, India. [188]Genomics and Molecular Medicine Unit, CSIR—Institute of Genomics and Integrative Biology, New Delhi, India. [189]Department of Preventive Medicine, Northwestern University Feinberg School of Medicine, Chicago, IL, USA. [190]Fred Hutchinson Cancer Research Center, Seattle, WA, USA. [191]Ophthalmology and Visual Sciences Academic Clinical Program (Eye ACP), Duke–NUS Medical School, Singapore, Singapore. [192]Department of Ophthalmology, Yong Loo Lin School of Medicine, National University of Singapore and National University Health System, Singapore, Singapore. [193]Department of Pediatrics, Pediatric Diabetes Research Center, University of California San Diego, La Jolla, CA, USA. [194]Institute for Genomic Medicine, University of California San Diego, La Jolla, CA, USA. [195]Department of Cellular and Molecular Medicine, University of California San Diego, La Jolla, CA, USA. [196]Institute of Cardiovascular and Medical Sciences, University of Glasgow, Glasgow, UK. [197]Hasso Plattner Institute for Digital Health at Mount Sinai, Icahn School of Medicine at Mount Sinai, New York, NY, USA. [198]Survey Research Center, Institute for Social Research, University of Michigan, Ann Arbor, MI, USA. [199]Institute of Genetic Epidemiology, Helmholtz Zentrum München, German Research Center for Environmental Health, Neuherberg, Germany. [200]Chair of Genetic Epidemiology, IBE, Faculty of Medicine, LMU Munich, Munich, Germany. [201]Institute of Medical Biostatistics, Epidemiology and Informatics (IMBEI), University Medical Center, Johannes Gutenberg University, Mainz, Germany. [202]Department of Diabetes and Metabolic Diseases, Graduate School of Medicine, the University of Tokyo, Tokyo, Japan. [203]Department of Genomic Medicine, National Cerebral and Cardiovascular Center, Osaka, Japan. [204]Faculty of Medicine, University of Reykjavik, Reykjavik, Iceland. [205]Faculty of Medicine, Macau University of Science and Technology, Macau, China. [206]Department of Medical Genetics and Medical Research, China Medical University Hospital, Taichung, Taiwan. [207]Department of Health, Finnish Institute for Health and Welfare, Helsinki, Finland. [208]National School of Public Health, Madrid, Spain. [209]Department of Neuroscience and Preventive Medicine, Danube University Krems, Krems, Austria. [210]Diabetes Research Group, King Abdulaziz University, Jeddah, Saudi Arabia. [211]Unidad de Biología Molecular y Medicina Genómica, Instituto Nacional de Ciencias Médicas y Nutrición Salvador Zubirán, Mexico City, Mexico. [212]Departamento de Medicina Genómica y Toxiología, Ambiental Instituto de Investigaciones Biomédicas, UNAM, Mexico City, Mexico. [213]Unidad de Investigacion Medica en Bioquimica, Hospital de Especialidades, Centro Medico Nacional Siglo XXI, IMSS, Mexico City, Mexico. [214]Einthoven Laboratory for Experimental Vascular Medicine, Leiden University Medical Center, Leiden, the Netherlands. [215]Department of Human Genetics, Leiden University Medical Center, Leiden, the Netherlands. [216]Department of Clinical Chemistry, Laboratory of Genetic Metabolic Disease, Amsterdam University Medical Center, Amsterdam, the Netherlands. [217]Southern California Eye Institute, CHA Hollywood Presbyterian Medical Center, Los Angeles, CA, USA. [218]Department of Medicine, University of Pennsylvania Perelman School of Medicine, Philadelphia, PA, USA. [219]Unidad de Investigación Médica en Epidemiologia Clinica, Hospital de Especialidades, Centro Medico Nacional Siglo XXI, IMSS, Mexico City, Mexico. [220]Department of Medicine, School of

Medicine, University of North Carolina at Chapel Hill, Chapel Hill, NC, USA. [221]Department of Internal Medicine, Division of Endocrinology, Leiden University Medical Center, Leiden, the Netherlands. [222]Department of Public Health, Aarhus University, Aarhus, Denmark. [223]Danish Diabetes Academy, Odense, Denmark. [224]Diabetology Research Centre, King Edward Memorial Hospital and Research Centre, Pune, India. [225]Department of Medical Biochemistry, Kurume University School of Medicine, Kurume, Japan. [226]Institute for Molecular Bioscience, University of Queensland, Brisbane, Queensland, Australia. [227]Division of Cancer Control and Population Sciences, UPMC Hillman Cancer Center, University of Pittsburgh, Pittsburgh, PA, USA. [228]Department of Epidemiology, Graduate School of Public Health, University of Pittsburgh, Pittsburgh, PA, USA. [229]Department of Pediatrics, Division of Genetic and Genomic Medicine, UCI Irvine School of Medicine, Irvine, CA, USA. [230]Department of Anti-Aging Medicine, Ehime University Graduate School of Medicine, Ehime, Japan. [231]Division of Pulmonary, Critical Care, and Sleep Medicine, Beth Israel Deaconess Medical Center, Boston, MA, USA. [232]Department of Medical Sciences, Uppsala University, Uppsala, Sweden. [233]Human Genetics Center, University of Texas Health Science Center at Houston, Houston, TX, USA. [234]Department of Medicine, Division of Cardiovascular Medicine, Stanford University School of Medicine, Stanford, CA, USA. [235]Department of Medical Sciences, Molecular Epidemiology and Science for Life Laboratory, Uppsala University, Uppsala, Sweden. [236]Department of Epidemiology, University of Washington, Seattle, WA, USA. [237]Department of Health Services, University of Washington, Seattle, WA, USA. [238]Beijing Institute of Ophthalmology, Ophthalmology and Visual Sciences Key Laboratory, Beijing Tongren Hospital, Capital Medical University, Beijing, China. [239]Department of Medicine, Division of Cardiology, Duke University School of Medicine, Durham, NC, USA. [240]Technical University of Munich (TUM) and Klinikum Rechts der Isar, TUM School of Medicine, Munich, Germany. [241]Kurume University School of Medicine, Kurume, Japan. [242]Center for Public Health Genomics, University of Virginia School of Medicine, Charlottesville, VA, USA. [243]Department of Medicine, McGill University, Montreal, Quebec, Canada. [244]Department of Human Genetics, McGill University, Montreal, Quebec, Canada. [245]Department of Genomics of Common Disease, School of Public Health, Imperial College London, London, UK. [246]Department of Physiology and Biophysics, University of Mississippi Medical Center, Jackson, MS, USA. [247]Division of Endocrinology and Metabolism, Department of Medicine, Taichung Veterans General Hospital, Taichung, Taiwan. [248]Center for Genetic Medicine, Northwestern University Feinberg School of Medicine, Chicago, IL, USA. [249]Department of Anthropology, Northwestern University, Evanston, IL, USA. [250]Center for Precision Health Research, National Human Genome Research Institute, National Institutes of Health, Bethesda, MD, USA. [251]Systems Genomics Laboratory, School of Biotechnology, Jawaharlal Nehru University, New Delhi, India. [252]Department of Pathology and Molecular Medicine, McMaster University, Hamilton, Ontario, Canada. [253]Department of Internal Medicine, Seoul National University College of Medicine, Seoul, South Korea. [254]Department of Molecular Medicine and Biopharmaceutical Sciences, Graduate School of Convergence Science and Technology, Seoul National University, Seoul, South Korea. [255]Netherlands Heart Institute, Utrecht, the Netherlands. [256]MRC-PHE Centre for Environment and Health, Imperial College London, London, UK. [257]Duke–NUS Medical School, Singapore, Singapore. [258]Singapore Institute for Clinical Sciences, Agency for Science Technology and Research (A*STAR), Singapore, Singapore. [259]Healthy Longevity Translational Research Programme, Yong Loo Lin School of Medicine, National University of Singapore, Singapore, Singapore. [260]Pat Macpherson Centre for Pharmacogenetics and Pharmacogenomics, University of Dundee, Dundee, UK. [261]Department of Medicine, Brown University Alpert School of Medicine, Providence, RI, USA. [262]Imperial College Healthcare NHS Trust, Imperial College London, London, UK. [263]National Heart and Lung Institute, Imperial College London, London, UK. [264]The Mindich Child Health and Development Institute, Ichan School of Medicine at Mount Sinai, New York, NY, USA. [265]Department of Biostatistics and Epidemiology, University of Pennsylvania, Philadelphia, PA, USA. [266]Center for Non-Communicable Diseases, Karachi, Pakistan. [267]Computational Medicine, Berlin Institute of Health at Charité Universitätsmedizin, Berlin, Germany. [268]Department of Advanced Genomic and Laboratory Medicine, Graduate School of Medicine, University of the Ryukyus, Okinawa, Japan. [269]Division of Clinical Laboratory and Blood Transfusion, University of the Ryukyus Hospital, Okinawa, Japan. [270]Department of Statistics, University of Oxford, Oxford, UK. [271]Section of Genetics and Genomics, Department of Metabolism, Digestion and Reproduction, Imperial College London, London, UK. [272]Oxford NIHR Biomedical Research Centre, Churchill Hospital, Oxford University Hospitals NHS Foundation Trust, Oxford, UK. [273]Division of Endocrinology, Department of Pediatrics, Stanford School of Medicine, Stanford University, Stanford, CA, USA. [274]Center for Diabetes Research, Wake Forest School of Medicine, Winston-Salem, NC, USA. [275]Centre for Genetics and Genomics Versus Arthritis, Centre for Musculoskeletal Research, Division of Musculoskeletal and Dermatological Sciences, University of Manchester, Manchester, UK. [276]NIHR Manchester Biomedical Research Centre, Manchester University NHS Foundation Trust, Manchester, UK. [277]Present address: Genentech, South San Francisco, CA, USA. [278]Present address: Internal Medicine Research Unit, Pfizer Worldwide Research, Cambridge, MA, USA. [279]Present address: Departamento de Medicina Genómica y Toxicologí, a AmbientalInstituto de Investigaciones Biomédicas, UNAM, Ciudad de Mexico, Mexico, Mexico. [280]Present address: Department of Epidemiology, Human Genetics, and Environmental Sciences, the University of Texas Health Science Center at Houston, School of Public Health, Houston, TX, USA. [281]Present address: Institute of Data Science, Korea University, Seoul, South Korea. [282]Present address: Division of Academics, Ochsner Health, New Orleans, LA, USA. [283]Present address: Vertex Pharmaceuticals Ltd, Oxford, UK. [284]Present address: Exeter Centre of Excellence in Diabetes (ExCEeD), Exeter Medical School, University of Exeter, Exeter, UK. [285]Present address: Center for Precision Health Research, National Human Genome Research Institute, National Institutes of Health, Bethesda, MD, USA. [286]Present address: Ibusuki Kozenkai Hospital, Ibusuki, Japan. [287]Present address: Regeneron Genetics Center, Tarrytown, NY, USA. [288]Present address: Institute for Population and Precision Health (IPPH), Biological Sciences Division, the University of Chicago, Chicago, IL, USA. [289]Present address: Clinical Trial Service Unit and Epidemiological Studies Unit, Nuffield Department of Population Health, University of Oxford, Oxford, UK. [290]Present address: Toranomon Hospital, Tokyo, Japan. [291]These authors contributed equally: Cassandra N. Spracklen, Weihua Zhang, Maggie C. Y. Ng, Lauren E. Petty, Hidetoshi Kitajima, Grace Z. Yu, Sina Rüeger, Leo Speidel. [292]Deceased: K. Radha Mani. [293]Deceased: Michèle M. Sale. [294]These authors jointly supervised this work: Anna L. Gloyn, Donald W. Bowden, Jennifer E. Below, John C. Chambers, Xueling Sim, Michael Boehnke, Jerome I. Rotter, Mark I. McCarthy, Andrew P. Morris. *Lists of authors and their affiliations appear at the end of the paper.
✉e-mail: mahajan.anubha@gene.com; mccarthy.mark@gene.com; andrew.morris-5@manchester.ac.uk

FinnGen

Sina Rüeger[14] and Pietro della Briotta Parolo[14]

A full list of members and their affiliations appears in the Supplementary Information.

eMERGE Consortium

Yoonjung Yoonie Joo[68,69], Abel N. Kho[144,145] and M. Geoffrey Hayes[68,247,248]

A full list of members and their affiliations appears in the Supplementary Information.

Methods

Ethics statement. All human research was approved by the relevant Institutional Review Boards and conducted according to the Declaration of Helsinki. All participants provided written informed consent. Study-level ethical statements are provided in the Supplementary Note.

Study-level analyses. Individuals were assayed with a range of GWAS genotyping arrays, with sample and SNV quality control undertaken within each study (Supplementary Tables 2 and 4). Most GWAS were undertaken with individuals from one ancestry group (Supplementary Table 1), where population outliers were excluded using self-reported and genetic ancestry. For the remaining multi-ancestry GWAS (Supplementary Table 1), individuals were first assigned to an ancestry group using both self-reported and genetic ancestry, and analyses were then undertaken separately within each ancestry group. For each ancestry-specific GWAS, samples were pre-phased and imputed up to reference panels from the 1000 Genomes Project (phase 1, March 2012 release; phase 3, October 2014 release)[12,13], the Haplotype Reference Consortium[14] or population-specific whole-genome sequencing[48–50] (Supplementary Table 4). SNVs with poor imputation quality and/or minor allele count <5 were excluded from downstream association analyses (Supplementary Table 4). Association with T2D was evaluated in a regression framework under an additive model in the dosage of the minor allele, with adjustment for age and sex (when appropriate) and additional study-specific covariates (Supplementary Table 4). Analyses accounted for structure (population stratification and/or familial relationships) by (1) excluding related samples and adjusting for principal components derived from a genetic relatedness matrix as additional covariates in the regression model or (2) incorporating a random effect for the genetic relatedness matrix in a mixed model (Supplementary Table 4). Allelic effects and corresponding standard errors that were estimated from a linear (mixed) model were converted to the log odds scale[51]. Study-level association summary statistics (P values and standard error of allelic log ORs) were corrected for residual structure, not accounted for in the regression analysis, by means of genomic control[52] if the inflation factor was >1 (Supplementary Table 4).

Multi-ancestry meta-analyses. To account for the different reference panels used for imputation, we considered autosomal biallelic SNVs that overlap the 1000 Genomes Project reference panel (phase 3, October 2014 release)[13] and the Haplotype Reference Consortium reference panel[14]. We considered only those SNVs with minor allele frequency >0.5% in haplotypes in at least one of the five ancestry groups (Supplementary Table 22) in the 1000 Genomes Project (phase 3, October 2014 release)[13]. We excluded SNVs that differed in allele frequency by >20% when comparing reference panels in the same subsets of samples.

The most powerful methods for discovery of new loci through multi-ancestry meta-analysis allow for potential allelic effect heterogeneity between ancestry groups that cannot be accommodated in a fixed-effects model[53]. Random-effects meta-analysis allows for 'unstructured' heterogeneity but cannot allow for the expectation that GWAS from the same ancestry group are likely to have more similar allelic effects than those from different ancestry groups. Some of these limitations could be addressed with a two-stage hierarchical model (within and then between ancestry). However, we preferred a meta-regression approach, implemented in MR-MEGA[15], which models allelic effect heterogeneity that is correlated with genetic ancestry by including axes of genetic variation as covariates to capture ancestral diversity between GWAS. We constructed a distance matrix of differences in mean effect allele frequency between each pair of GWAS across a subset of 386,563 SNVs reported in all studies. We implemented multidimensional scaling of the distance matrix to obtain three principal components that defined axes of genetic variation to separate GWAS from the five ancestry groups (Extended Data Fig. 2).

For each SNV, we modeled allelic log ORs across GWAS in a linear regression framework, weighted by the inverse of the variance of the effect estimates, incorporating the three axes of genetic variation as covariates. We tested for (1) association with T2D allowing for allelic effect heterogeneity between GWAS that is correlated with ancestry, (2) heterogeneity in allelic effects on T2D between GWAS that is correlated with ancestry and (3) residual allelic effect heterogeneity between GWAS due to unmeasured confounders. We corrected the meta-regression association P values for inflation due to residual structure between GWAS using genomic control adjustment (allowing for four degrees of freedom): $\lambda_{\mathrm{TA}} = 1.052$. We included SNVs reported in ≥50% of the total effective sample size ($N_{\mathrm{TA}} \geq 246{,}095$) in downstream analyses.

We also aggregated association summary statistics across GWAS via fixed-effects meta-analysis using METAL[54] and random-effects (RE2 model) meta-analysis using METASOFT[55]. Both meta-analyses were based on inverse-variance weighting of allelic log ORs to obtain effect-size estimates. We corrected standard errors for inflation due to residual structure between GWAS by genomic control adjustment: $\lambda_{\mathrm{TA}}^{\mathrm{FE}} = 1.253$ and $\lambda_{\mathrm{TA}}^{\mathrm{RE}} = 1.253$. We assessed evidence for heterogeneity in allelic effects between GWAS by Cochran's Q statistic.

Defining T2D loci. We initially selected lead SNVs attaining genome-wide significant evidence of association ($P < 5 \times 10^{-8}$) in the multi-ancestry meta-regression that were separated by at least 500 kb. Loci were first defined by the flanking genomic interval mapping 500 kb upstream and downstream of lead SNVs. Next, when lead SNVs were separated by less than 1 Mb, the corresponding loci were aggregated as a single locus. The lead SNV for each locus was then selected as the SNV with minimum association P value.

Genome-wide significance threshold. We considered haplotypes from the 1000 Genomes Project reference panel (phase 3, October 2014 release)[13]. We extracted autosomal biallelic SNVs that overlapped between reference panels used in study-level analyses. We estimated the effective number of independent SNVs across ancestry groups using LD pruning in PLINK[56] to be 9,966,662 at $r^2 > 0.5$ (ref. [57]). We therefore chose a multi-ancestry genome-wide significance threshold by Bonferroni correction for the effective number of SNVs as $P < 5 \times 10^{-9}$. Exemplar power calculations are provided in the Supplementary Note.

Dissection of distinct multi-ancestry association signals. We used iterative approximate conditioning, implemented in GCTA[58], making use of forward selection and backward elimination, to identify index SNVs at multi-ancestry genome-wide significance ($P < 5 \times 10^{-9}$). We used haplotypes from the 1000 Genomes Project reference panel (phase 3, October 2014 release)[13] that were specific to each ancestry group (Supplementary Table 22) as a reference for LD between SNVs across loci in the approximate conditional analysis. Details of the iterative approximate conditioning are provided in the Supplementary Note.

Ancestry-specific meta-analyses. We aggregated association summary statistics across GWAS via fixed-effects meta-analysis using METAL[54] based on inverse-variance weighting of allelic log ORs to obtain effect-size estimates. Details are provided in the Supplementary Note.

Fine-mapping resolution. Within each locus, we approximated the Bayes factor[59] Λ_{ij} in favor of T2D association of the jth SNV at the ith distinct association signal using summary statistics from (1) the multi-ancestry meta-regression, (2) the European ancestry-specific meta-analysis and (3) the combined East Asian and European ancestry meta-analysis. For loci with a single association signal, association summary statistics were obtained from unconditional analysis. For loci with multiple distinct association signals, association summary statistics were obtained from approximate conditional analyses. Details of the derivation of approximate Bayes factors are provided in the Supplementary Note. The posterior probability for the jth SNV at the ith distinct signal was then given by $\pi_{ij} \propto \Lambda_{ij}$. We derived a 99% credible set[60] for the ith distinct association signal by (1) ranking all SNVs according to their posterior probability π_{ij} and (2) including ranked SNVs until their cumulative posterior probability attains or exceeds 0.99.

Downsampled multi-ancestry meta-regression. We selected GWAS contributing to the multi-ancestry meta-regression to approximate the effective sample size of the European ancestry-specific meta-analysis and maintain the distribution of effective sample size across ancestry groups (Supplementary Table 10). The selected GWAS are summarized in the Supplementary Note. We conducted a 'downsampled' multi-ancestry meta-regression implemented in MR-MEGA[15] for the selected studies. For each SNV, we modeled allelic log ORs across GWAS in a linear regression framework, weighted by the inverse of the variance of the effect estimates, incorporating the same three axes of genetic variation as covariates (Extended Data Fig. 2). We corrected the meta-regression association P values for inflation due to residual structure between the selected GWAS using genomic control adjustment (allowing for four degrees of freedom): $\lambda_{\mathrm{TA}*} = 1.012$. For each distinct association signal identified in the complete multi-ancestry meta-regression, we derived a 99% credible set[60] using association summary statistics from the downsampled multi-ancestry meta-regression. Details of the fine-mapping procedure are provided in the Supplementary Note.

Enrichment of T2D-association signals in genomic annotations. We mapped each SNV across T2D loci to three categories of functional and regulatory annotations: (1) genic regions, as defined by the GENCODE Project[61], including protein-coding exons, and 3′ and 5′ UTRs as different annotations; (2) chromatin immunoprecipitation followed by sequencing (ChIP–seq) binding sites for 165 transcription factors (161 proteins from the ENCODE Project[62] and four additional factors assayed in primary pancreatic islets[63]); and (3) 13 unique and recurrent chromatin states, including promoter, enhancer, transcribed and repressed regions in four T2D-relevant tissues[18] (pancreatic islets, the liver, adipose tissue and skeletal muscle). This resulted in a total of 220 genomic annotations for downstream enrichment analyses. We used fGWAS[64] to identify a joint model of enriched annotations across distinct T2D-association signals from the multi-ancestry meta-regression. Details are provided in the Supplementary Note.

Annotation-informed fine-mapping. Within each locus, for each distinct signal, we recalibrated the posterior probability of driving the T2D association for each SNV under an annotation-informed prior derived from the joint model of enriched annotations identified by fGWAS. Specifically, for the jth SNV at the ith distinct signal, the posterior probability $\pi_{ij} \propto \gamma_j \Lambda_{ij}$, where Λ_{ij} is the Bayes factor in favor of T2D association. In this expression, the relative annotation-informed prior for the SNV is given by

$$\gamma_j = \exp\left(\sum_k \hat{\beta}_k z_{jk}\right),$$

where the summation is over the enriched annotations, $\hat{\beta}_k$ is the estimated log fold enrichment of the kth annotation from the final joint model, and z_{jk} is an indicator variable taking the value 1 if the jth SNV maps to the kth annotation and 0 otherwise. We derived a 99% credible set[60] for the ith distinct association signal by (1) ranking all SNVs according to their posterior probability π_{ij} and (2) including ranked SNVs until their cumulative posterior probability attains or exceeds 0.99.

Dissection of molecular QTL in diverse tissues. We accessed association summary statistics for molecular QTL in diverse tissues from three published resources: (1) 3,622 circulating plasma proteins in 3,301 healthy blood donors of European ancestry from the INTERVAL study[21] (2) pancreatic islet expression in 420 individuals of European ancestry from the InsPIRE Consortium[23] and (3) multi-tissue expression in 620 donors from the GTEx Project (release version 7)[22], including subcutaneous adipose tissue (328 samples), visceral adipose tissue (273 samples), brain hypothalamus (108 samples), liver (134 samples) and skeletal muscle (421 samples). We defined *cis* molecular QTL as mapping within 1 Mb of the TSS of the gene. Recognizing that molecular QTL may also be driven by multiple causal variants, we dissected signals for each significant *cis* and *trans* pQTL ($P < 1.5 \times 10^{-11}$) and for each significant *cis* eQTL (FDR Q value < 5%) via approximate conditional analyses implemented in GCTA[58]. We used a genotype reference panel of 6,000 unrelated individuals of white British origin, randomly selected from the UK Biobank[43], to model LD between SNVs. We excluded SNVs from the reference panel with poor imputation quality (info < 0.4) and/or significant deviation from Hardy–Weinberg equilibrium ($P < 10^{-6}$). We first identified index SNVs for each distinct molecular QTL signal using the '–cojo-slct' option: $P < 1.5 \times 10^{-11}$ for *cis* and *trans* pQTL and $P < 5 \times 10^{-8}$ for *cis* eQTL. For each molecular QTL with multiple index SNVs, we dissected each distinct signal using GCTA, removing each index SNV, and adjusting for the remainder using the '–cojo-cond' option.

Colocalization of T2D associations and molecular QTL. For each distinct T2D-association signal, we used COLOC version 3.1 (ref. [24]) to assess the evidence for colocalization with (1) each distinct *cis* and *trans* pQTL signal and (2) each distinct *cis* eQTL signal across tissues. COLOC assumes that at most one variant is causal for each distinct T2D association and each distinct molecular QTL, which is reasonable after deconvolution of signals via approximate conditional analyses. Under this assumption, there are five hypotheses: association with neither T2D nor the molecular QTL (H_0); association only with T2D (H_1) or the molecular QTL (H_2); or association with both T2D and the molecular QTL, driven either by two different causal variants (H_3) or by the same causal variant (H_4). We assumed the default prior probabilities of (1) 10^{-4} that a variant is causal only for T2D or only for the molecular QTL and (2) 10^{-6} that a variant is causal for both T2D and the molecular QTL. To take account of our annotation-informed prior model of causality, we then replaced the Bayes factor in favor of T2D association, Λ_{ij}, for the jth SNV at the ith distinct signal by $\pi_{ij}\Psi_i$, where $\Psi_i = \sum_j \Lambda_{ij}$ is the total Bayes factor for the signal. For the molecular QTL, approximate Bayes factors in favor of association for each variant were derived using Wakefield's method[65]. Under this model, COLOC then estimates the posterior probability of colocalization of the T2D association and molecular QTL (that is, hypothesis H_4, denoted as π_{COLOC}).

Plasmid transfection and luciferase reporter assay. We experimentally validated 99% credible set variants for distinct T2D-association signals at the *PROX1* locus using a luciferase reporter assay. Briefly, human EndoC-βH1 cells[66] and human liver cells were grown at 50–60% confluence in 24-well plates and were transfected (2×10^5 EndoC-βH1 cells per well and 5×10^4 HepG2 cells per well) with 500 ng of empty pGL3-Promoter vector (Promega) or pGL3-Promoter-PROX_insert with FuGENE HD (Roche Applied Science) using a FuGENE:DNA ratio of 6:1 according to the manufacturer's instructions. Details are provided in the Supplementary Note and at https://www.promega.co.uk/products/luciferase-assays/genetic-reporter-vectors-and-cell-lines/pgl3-luciferase-reporter-vectors/?catNum=E1751. Luciferase activities were measured 48 h after transfection using the Dual-Luciferase Reporter Assay kit (Promega) according to the manufacturer's instructions in half-volume 96-well format on an EnSpire Multimode Plate Reader (PerkinElmer). Firefly luciferase activity was normalized to the Renilla luciferase activity obtained by cotransfection of 10 ng of the pGL4.74[hRluc/TK] Renilla luciferase vector (Promega). All experiments were performed in triplicate on three different passages of each cell type. Differences in luciferase activity between groups were tested using two-tailed two-sample t-tests, and $P < 0.05$ was considered statistically significant.

Transferability of GRS across ancestry groups. We selected two studies per ancestry group as test GWAS, prioritizing those with larger effective sample sizes and greater genetic diversity (Supplementary Note). We repeated the multi-ancestry meta-regression after excluding the ten test GWAS, incorporating the same three axes of genetic variation as covariates to account for ancestry. The association P values from this 'reduced' meta-regression were then corrected for inflation due to residual structure between GWAS by means of genomic control adjustment (allowing for four degrees of freedom): $\lambda_{\mathrm{TA}} = 1.037$. SNVs reported in ≥50% of the total effective sample size of the 'reduced' meta-regression ($N_{\mathrm{TA}} \geq 179{,}074$) were included in downstream analyses. We identified loci attaining genome-wide significant evidence of association ($P < 5 \times 10^{-9}$) in the 'reduced' meta-regression, and the lead SNV for each locus was selected as the variant with the minimum association P value. For each test GWAS, we next estimated population-specific 'predicted' allelic effects for each lead SNV to be used as weights in the GRS. We also repeated each of the ancestry-specific fixed-effects meta-analyses after excluding the ten test GWAS and identified lead SNVs attaining genome-wide significant evidence of association ($P < 5 \times 10^{-8}$). For each test GWAS, we estimated the OR per unit of the population-specific multi-ancestry GRS and each ancestry-specific weighted GRS and the corresponding percentage of T2D variance explained (pseudo R^2). Details are provided in the Supplementary Note.

Predictive power of GRS in FinnGen. Individuals from FinnGen were genotyped with Illumina and Affymetrix arrays and were imputed up to the Finnish population-specific reference panel (SISu version 3). We excluded individuals due to non-Finnish ancestry, relatedness or missing age and/or sex. We derived Finnish-specific 'predicted' allelic effect estimates for each lead SNV from the multi-ancestry meta-regression to be used as weights in calculating the centered GRS for each individual. We excluded lead SNVs from the GRS that were not reported in FinnGen. We excluded individuals with missing T2D status or BMI from subsequent analyses, resulting in a total of 18,111 affected individuals and 111,119 unaffected individuals. We calculated the variance in T2D status explained (pseudo R^2) and the AUROC (calculated with a tenfold cross-validation) for models including BMI and/or GRS. We also conducted age-stratified analyses and tested for association of the GRS with age of T2D diagnosis. Details are provided in the Supplementary Note.

Selection analyses. We used Relate[42] to reconstruct genealogies for haplotypes from the 1000 Genomes Project reference panel (phase 3, October 2014 release)[13] separately for each population after excluding African American and admixed American populations in whom high levels of admixture are likely to confound selection evidence. We then used P values calculated for selection evidence for any variant that segregated in the population and passed quality-control filters[42], which quantify the extent to which the mutation has more descendants than other lineages that were present when it arose. We tested for evidence of selection for index SNVs for distinct T2D-association signals, which were partitioned into two groups, risk and protective, according to the direction of the allelic effect when aligned to the derived allele. We also tested for selection on a range of traits available in the UK Biobank[43] at the subset of index SNVs for which the derived allele increased risk of T2D. Details are provided in the Supplementary Note.

Reporting Summary. Further information on research design is available in the Nature Research Reporting Summary linked to this article.

Data availability

Association summary statistics from the multi-ancestry meta-analysis and annotation-informed fine-mapping are available through the AMP T2D Knowledge Portal (http://www.type2diabetesgenetics.org/) and the DIAGRAM Consortium data download website (http://diagram-consortium.org/downloads.html). Source data are provided with this paper.

References

48. Jónsson, H. et al. Whole genome characterization of sequence diversity of 15,220 Icelanders. *Sci. Data* **4**, 170115 (2017).
49. Mitt, M. et al. Improved imputation accuracy of rare and low-frequency variants using population-specific high-coverage WGS-based imputation reference panel. *Eur. J. Hum. Genet.* **25**, 869–876 (2017).
50. Moon, S. et al. The Korea Biobank Array: design and identification of coding variants associated with blood biochemical traits. *Sci. Rep.* **9**, 1382 (2019).
51. Cook, J. P., Mahajan, A. & Morris, A. P. Guidance for the utility of linear models in meta-analysis of genetic association studies of binary phenotypes. *Eur. J. Hum. Genet.* **25**, 240–245 (2016).
52. Devlin, B. & Roeder, K. Genomic control for association studies. *Biometrics* **55**, 997–1004 (1999).
53. Gurdasani, D., Barroso, I., Zeggini, E. & Sandhu, M. S. Genomics of disease risk in globally diverse populations. *Nat. Rev. Genet.* **20**, 520–535 (2019).
54. Willer, C. J., Li, Y. & Abecasis, G. R. METAL: fast and efficient meta-analysis of genome-wide association scans. *Bioinformatics* **26**, 2190–2191 (2010).
55. Han, B. & Eskin, E. Random-effects model aimed at discovering associations in meta-analysis of genome-wide association studies. *Am. J. Hum. Genet.* **88**, 586–598 (2011).

56. Purcell, S. et al. PLINK: a tool set for whole-genome association and population-based linkage analyses. *Am. J. Hum. Genet.* **81**, 559–575 (2007).
57. Sobota, R. S. et al. Addressing population-specific multiple testing burdens in genetic association studies. *Ann. Hum. Genet.* **79**, 136–147 (2015).
58. Yang, J. et al. Conditional and joint multiple-SNP analysis of GWAS summary statistics identifies additional variants influencing complex traits. *Nat. Genet.* **44**, 369–375 (2012).
59. Kass, R. E. & Raftery, A. E. Bayes factors. *J. Am. Stat. Assoc.* **90**, 773–795 (1995).
60. Maller, J. B. et al. Bayesian refinement of association signals for 14 loci in 3 common diseases. *Nat. Genet.* **44**, 1294–1301 (2012).
61. Harrow, J. et al. GENCODE: the reference human genome annotation for the ENCODE Project. *Genome Res.* **22**, 1760–1774 (2012).
62. ENCODE Project Consortium. An integrated encyclopedia of DNA elements in the human genome. *Nature* **489**, 57–74 (2012).
63. Pasquali, L. et al. Pancreatic islet enhancer clusters enriched in type 2 diabetes risk-associated variants. *Nat. Genet.* **46**, 136–143 (2014).
64. Pickrell, J. Joint analysis of functional genomic data and genome-wide association studies of 18 human traits. *Am. J. Hum. Genet.* **94**, 559–573 (2014).
65. Wakefield, J. A. Bayesian measure of the probability of false discovery in genetic epidemiology studies. *Am. J. Hum. Genet.* **81**, 208–227 (2007).
66. Ravassard, P. et al. A genetically engineered human pancreatic β cell line exhibiting glucose-inducible insulin secretion. *J. Clin. Invest.* **121**, 3589–3597 (2011).

Acknowledgements

A complete list of acknowledgements and funding appears in the Supplementary Note. This research was funded in part by the Wellcome Trust (grant numbers 064890, 072960, 083948, 084723, 085475, 086113, 088158, 090367, 090532, 095101, 098017, 098051, 098381, 098395, 101033, 101630, 104085, 106130, 200186, 200837, 202922, 203141, 206194, 212259, 212284, 212946 and 220457). For the purpose of open access, the authors have applied a CC-BY public copyright licence to any author accepted manuscript version arising from this submission.

Author contributions

DIAMANTE Consortium coordination, A. Mahajan, M.I.M., A.P.M.; manuscript preparation, A. Mahajan, C.N.S., W. Zhang, M.C.Y.N., L.E.P., H.K., G.Z.Y., S. Rüeger, L.S., A.L.G., M.B., J.I.R., M.I.M., A.P.M.; coordination of ancestry-specific GWAS collections, A. Mahajan, C.N.S., W. Zhang, M.C.Y.N., L.E.P., D.W.B., J.E.B., J.C.C., X.S., M.B.; central analysis group, A. Mahajan, C.N.S., W. Zhang, M.C.Y.N., L.E.P., H.K., Y.J.K., M. Horikoshi, J.M.M., D.T., S. Moon, S.-H.K., N.R.R., N.W.R., M. Loh, B.-J.K., J. Flanagan, J.B.M., K.L.M., J.E.B., J.C.C., X.S., M.B., J.I.R., M.I.M., A.P.M.; *PROX1* functional analyses, G.Z.Y., F.A., J.M.T., A.L.G.; GRS analyses in FinnGen, S. Rüeger, P.d.B.P.; selection analyses, L.S., S.R.M.; single-cell chromatin accessibility data, J. Chiou, D.G., S.P., M. Sander, K.J.G.; islet promoter Hi-C data generation, I.M.-E., J. Ferrer; study-level primary analyses, A. Mahajan, C.N.S., W. Zhang, M.C.Y.N., L.E.P., Y.J.K., M. Horikoshi, J.M.M., D.T., S. Moon, S.-H.K., K. Lin, F.B., M.H.P., F.T., J.N., X.G., A. Lamri, M.N., R.A.S., J.-J.L., A.H.-C., M. Graff, J.-F.C., E.J.P., J.Y., L.F.B., Y.T., Y.H., V.S., J.P.C., M.K., N.G., E.M.S., I.P., T.S., M.W., C. Sarnowski, C.G., D.N., S. Trompet, J. Long, M. Sun, L.T., W.-M.C., M. Ahmad, R.N., V.J.Y.L., C.H.T.T., Y.Y.J., C.-H.C., L.M.R., C. Lecoeur, B.P.P., A.N., L.R.Y., G.C., R.A.J., S. Tajuddin, E.K.K., P.A., A.H.X., H.S.C., B.E.C., J. Tan, X.S., A.P.M.; study-level phenotyping, genotyping and additional analyses, L.S.A., A.A., C.A.A.-S., M. Akiyama, S.S.A., A.B., Z.B., J.B.-J., I.B., J.A.B., C.M.B., T.A.B., M. Canouil, J.C.N.C., L.-C.C., M.-L.C., J. Chen, S.-H.C., Y.-T.C., Z.C., L.-M.C., M. Cushman, S.K.D., H.J.d.S., G.D., L.D., A.P.D., S.D., Q.D., K.-U.E., L.S.E., D.S.E., M.K.E., K.F., J.S.F., I.F., M.F., O.H.F., T.M.F., B.I.F., C.F., P.G., H.C.G., V.G., C.G.-V., M.E.G.-V., M.O.G., P.G.-L., M. Gross, Y.G., S. Hackinger, S. Han, A.T.H., C.H., A.-G.H., W. Hsueh, M. Huang, W. Huang, Y.-J.H., M.Y.H., C.-M.H., S.I., M.A.I., M. Ingelsson, M.T.I., M. Isono, H.-M.J., F.J., G.J., J.B.J., M.E.J., T.J., Y.K., F.R.K., A. Kasturiratne, T. Katsuya, V.K., T. Kawaguchi, J.M.K., A.N.K., C.-C.K., M.G.K., K.K., J. Kriebel, F.K., J. Kuusisto, K. Läll, L.A.L., M.-S.L., N.R.L., A. Leong, L. Li, Y. Li, R.L.-G., S. Ligthart, C.M.L., A. Linneberg, C.-T.L., J. Liu, A.E.L., T.L., J. Luan, A.O.L., X.L., J. Lv, V.L., V.M., K.R.M., T.M., A. Metspalu, A.D.M., G.N.N., J.L.N., M.A.N., U.N., S.S.N., I.N., Y.O., L.O., S.R.P., M.A. Pereira, A.P., F.J.P., B.P., G. Prasad, L.J.R.-T., A.P.R., M.R., R.R., K.R., C. Sabanayagam, K. Sandow, N.S., S.S., C. Schurmann, M. Shahriar, J.S., D.M.S., D. Shriner, J.A.S., W.Y.S., A.S., A.M.S., K. Strauch, K. Suzuki, A.T., K.D.T., B. Thorand, G.T., U.T., B. Tomlinson, F.-J.T., J. Tuomilehto, T.T.-L., M.S.U., A.V.-S., R.M.v.D., J.B.v.K., R.V., M.V., N.W.-R., E.W., E.A.W., A.R.W., K.W.v.D., D.R.W., C.S.Y., K. Yamamoto, T.Y., L.Y., K. Yoon, C.Y., J.-M.Y., S.Y., L.Z., W. Zheng; study-level principal investigator, L.J.R., M. Igase, E. Ipp, S. Redline, Y.S.C., L. Lind, M.A. Province, C.L.H., P.A.P., E. Ingelsson, A.B.Z., B.M.P., Y.-X.W., C.N.R., D.M.B., F.M., Y. Liu, E.Z., M.Y., S.S.R., C.K., J.S.P., J.C.E., Y.-D.I.C., P.F., J.G.W., W.H.H.S., S.L.R.K., J.-Y.W., M.G.H., R.C.W.M., T.-Y.W., L.G., D.O.M.-K., G.R.C., F.S.C., D.B., G. Paré, M.M.S., H.A., A.A.M., X.-O.S., K.-S.P., J.W.J., M. Cruz, R.M.-C., H.G., C.-Y.C., E.P.B., A.D., E.-S.T., J.D., N.K., M. Laakso, A. Köttgen, W.-P.K., C.N.A.P., S. Liu, G.A., J.S.K., R.J.F.L., K.E.N., C.A.H., J.C.F., D. Saleheen, T.H., O.P., R.M., C. Langenberg, N.J.W., S. Maeda, T. Kadowaki, J. Lee, I.Y.M., R.G.W., K. Stefansson, J.B.M., K.L.M., D.W.B., J.C.C., M.B., J.I.R., M.I.M., A.P.M.

Competing interests

A. Mahajan is now an employee of Genentech and a holder of Roche stock. R.A.S. is now an employee of GlaxoSmithKline. V.S. is an employee of deCODE Genetics–Amgen. L.S.E. is now an employee of Bristol Myers Squibb. J.S.F. has consulted for Shionogi. T.M.F. has consulted for Sanofi and Boerhinger Ingelheim and received funding from GSK. H.C.G. holds the McMaster–Sanofi Population Health Institute Chair in Diabetes Research and Care; reports research grants from Eli Lilly, AstraZeneca, Merck, Novo Nordisk and Sanofi; reports honoraria for speaking from AstraZeneca, Boehringer Ingelheim, Eli Lilly, Novo Nordisk, DKSH, Zuellig, Roche and Sanofi; and reports consulting fees from Abbott, AstraZeneca, Boehringer Ingelheim, Eli Lilly, Merck, Novo Nordisk, Pfizer, Sanofi, Kowa and Hanmi. M. Ingelsson is a paid consultant for BioArctic. R.L.-G. is a part-time consultant for Metabolon. A.E.L. is now an employee of the Regeneron Genetics Center and holds shares in Regeneron Pharmaceuticals. M.A.N. currently serves on the scientific advisory board for Clover Therapeutics and is an advisor to Neuron23. S.R.P. has received grant funding from Bayer Pharmaceuticals, Philips Respironics and Respicardia. N.S. has consulted for or been on speaker bureaus for Abbott, Amgen, AstraZeneca, Boehringer Ingelheim, Eli Lilly, Hanmi, Novartis, Novo Nordisk, Sanofi and Pfizer and has received grant funding from AstraZeneca, Boehringer Ingelheim, Novartis and Roche Diagnostics. A.M.S. receives funding from Seven Bridges Genomics to develop tools for the NHLBI BioData Catalyst consortium. G.T. is an employee of deCODE Genetics–Amgen. U.T. is an employee of deCODE Genetics–Amgen. E. Ingelsson is now an employee of GlaxoSmithKline. B.M.P. serves on the steering committee of the Yale Open Data Access Project funded by Johnson & Johnson. R.C.W.M. reports research funding from AstraZeneca, Bayer, Novo Nordisk, Pfizer, Tricida and Sanofi and has consulted for or received speakers fees from AstraZeneca, Bayer and Boehringer Ingelheim, all of which have been donated to the Chinese University of Hong Kong to support diabetes research. D.O.M.-K. is a part-time clinical research consultant for Metabolon. S. Liu reports consulting payments and honoraria or promises of the same for scientific presentations or reviews at numerous venues, including but not limited to Barilla, by-Health, Ausa Pharmed, the Fred Hutchinson Cancer Center, Harvard University, the University of Buffalo, Guangdong General Hospital and the Academy of Medical Sciences; is a consulting member for Novo Nordisk; is a member of the data safety and monitoring board for a trial of pulmonary hypertension in patients with diabetes at Massachusetts General Hospital; receives royalties from UpToDate; and receives an honorarium from the American Society for Nutrition for his duties as an associate editor. K. Stefansson is an employee of deCODE Genetics–Amgen. K.J.G. consults for Genentech and holds stock in Vertex Pharmaceuticals. A.L.G.'s spouse is an employee of Genentech and holds stock options in Roche. M.I.M. has served on advisory panels for Pfizer, Novo Nordisk and Zoe Global; has received honoraria from Merck, Pfizer, Novo Nordisk and Eli Lilly and research funding from AbbVie, AstraZeneca, Boehringer Ingelheim, Eli Lilly, Janssen, Merck, Novo Nordisk, Pfizer, Roche, Sanofi Aventis, Servier and Takeda; is now an employee of Genentech and a holder of Roche stock. The remaining authors declare no competing interests. The views expressed in this article are those of the authors and do not necessarily represent those of the NHS, the NIHR or the UK Department of Health; the National Heart, Lung, and Blood Institute, the National Institutes of Health or the US Department of Health and Human Services.

Additional information

Extended data is available for this paper at https://doi.org/10.1038/s41588-022-01058-3.

Supplementary information The online version contains supplementary material available at https://doi.org/10.1038/s41588-022-01058-3.

Correspondence and requests for materials should be addressed to Anubha Mahajan, Mark I. McCarthy or Andrew P. Morris.

Peer review information *Nature Genetics* thanks Constantin Polychronakos and the other, anonymous, reviewer(s) for their contribution to the peer review of this work.

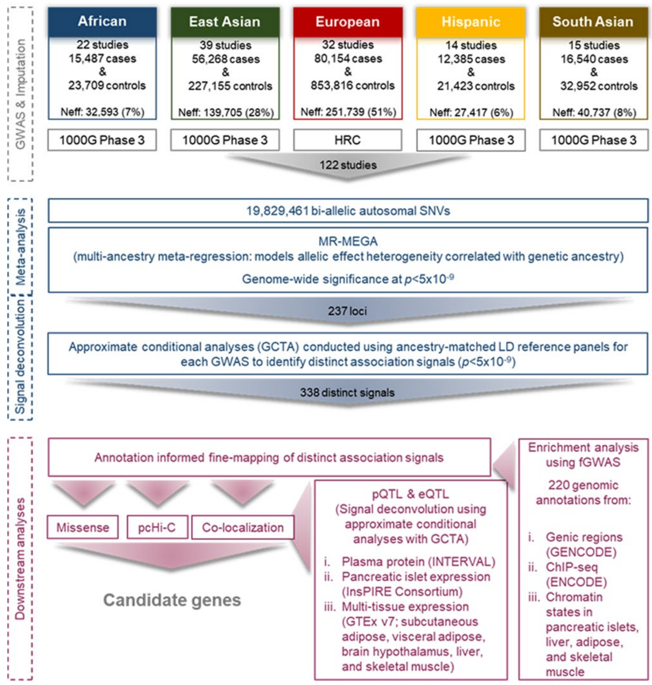

Extended Data Fig. 1 | Study overview. Summary of data resources and downstream analyses to identify candidate causal genes at T2D susceptibility loci.

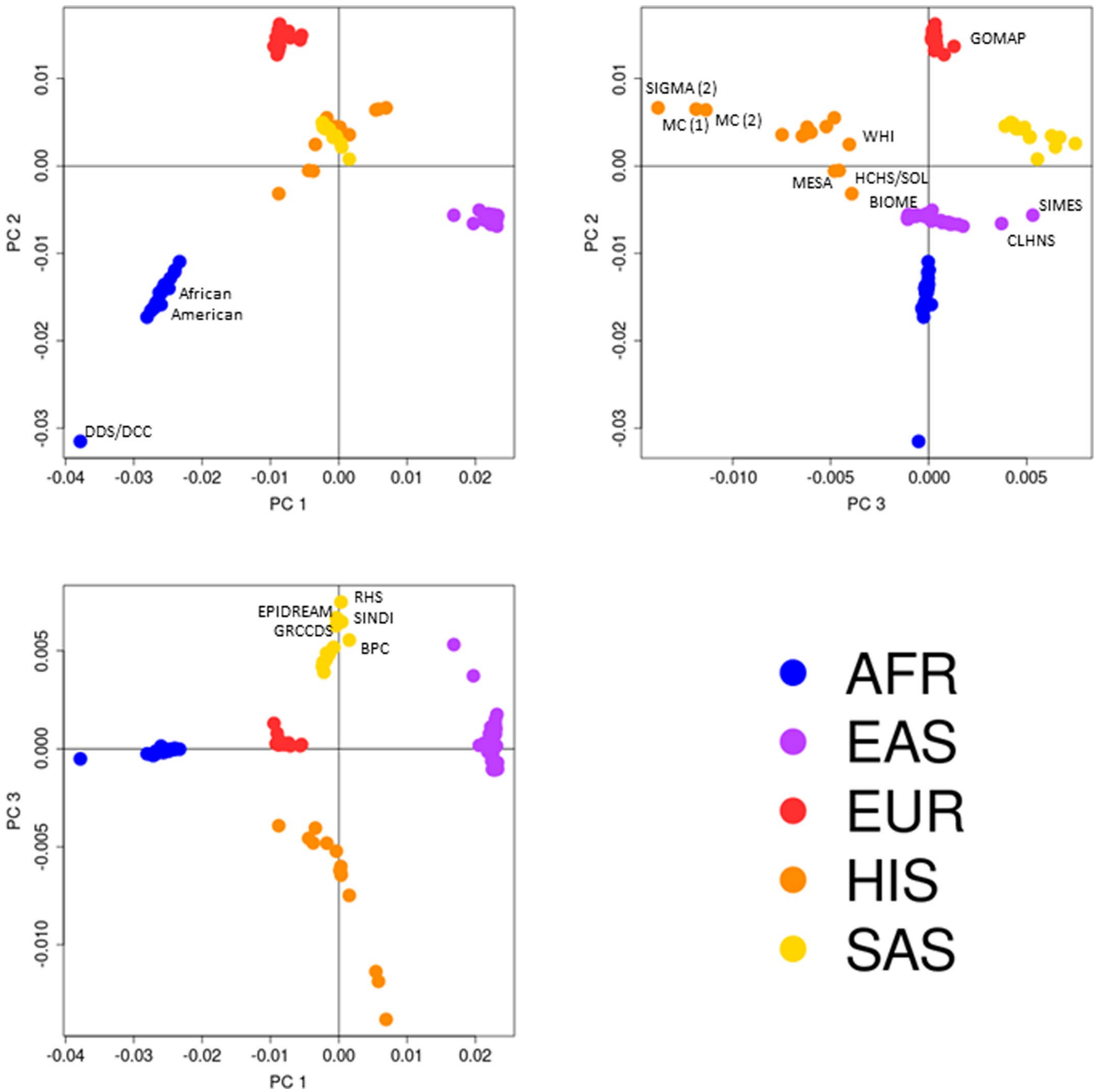

Extended Data Fig. 2 | Axes of genetic variation separating GWAS of T2D across diverse populations. The first three axes of genetic variation (PC 1, PC 2 and PC 3) from multi-dimensional scaling of the Euclidean distance matrix between populations are sufficient to separate five ancestry groups: African (AFR), East Asian (EAS), European (EUR), Hispanic (HIS) and South Asian (SAS). GWAS acronyms are defined in Supplementary Table 1. The second axis of genetic variation (PC 2) separates African American and continental African GWAS. The third axis of genetic variation (PC 3) reveals finer-scale differences between GWAS within ancestry groups: Hispanic studies with a greater proportion of American ancestry (SIGMA (2), MC (1) and MC (2)) or African ancestry (WHI, MESA, HCHS/SOL and BIOME); East Asian studies of Chinese, Japanese and Korean ancestry from those of Malay and Filipino ancestry (SIMES and CLHNS); South Asian studies of Sri Lankan, Bangladeshi and South Indian ancestry (RHS, EPIDREAM, SINDI, GRCCDS and BPC) from those of North Indian and Pakistani ancestry; and Northern European ancestry studies from the study of Greek ancestry from Southern Europe (GOMAP). GWAS were aligned to ancestry groups based on self-report at the study level.

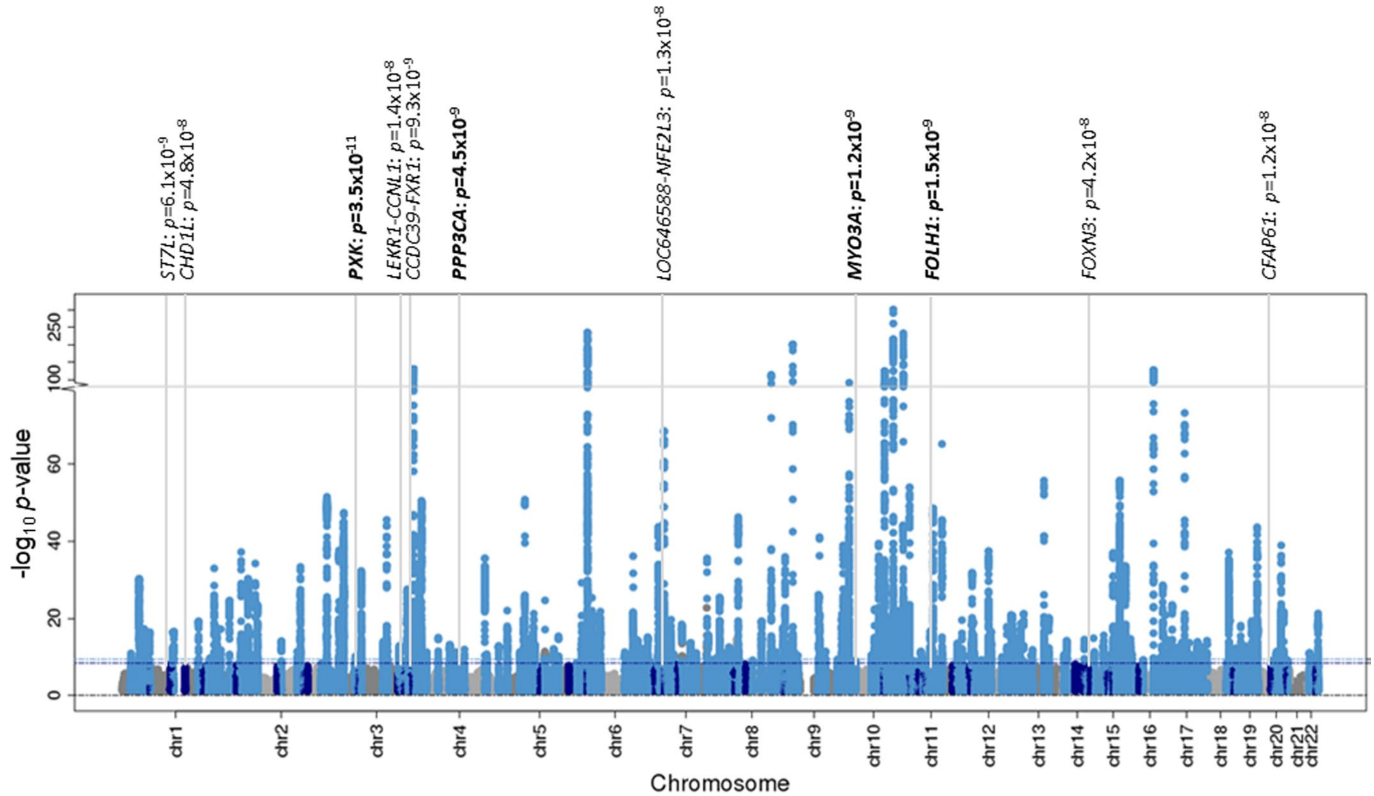

Extended Data Fig. 3 | Manhattan plot of genome-wide T2D association from multi-ancestry meta-regression (MR-MEGA) of up to 180,834 cases and 1,159,055 controls. Each point represents an SNV passing quality control in the multi-ancestry meta-regression, plotted with their association *P*-value (on a $-\log_{10}$ scale, truncated at 300) as a function of genomic position (NCBI build 37). Association signals attaining genome-wide significance are highlighted in pale blue ($P < 5 \times 10^{-9}$) and dark blue ($P < 5 \times 10^{-8}$). The names of novel loci names are highlighted with their association *P*-value from the multi-ancestry meta-regression.

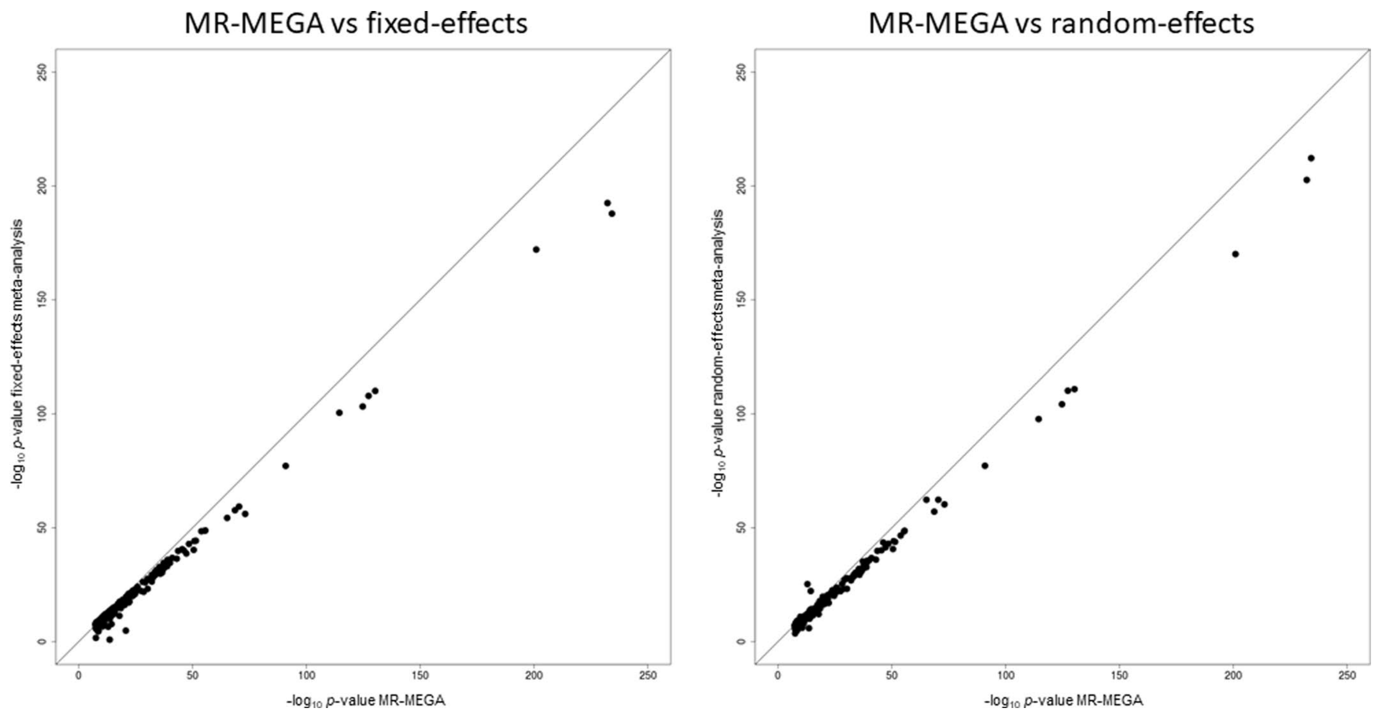

Extended Data Fig. 4 | Comparison of association *P*-values at lead SNVs at T2D loci between multi-ancestry meta-regression (MR-MEGA), fixed-effects meta-analysis and random-effects (RE2) meta-analysis of up to 180,834 cases and 1,159,055 controls. Each point corresponds to an SNV, plotted according to *P*-values (on a -$\log_{10}$ scale) from MR-MEGA on the *x*-axis and fixed- or random-effects meta-analysis on the *y*-axis. SNVs below the $y = x$ line demonstrate stronger association with MR-MEGA. The lead SNV at the *TCF7L2* locus has been removed to improve clarity of presentation.

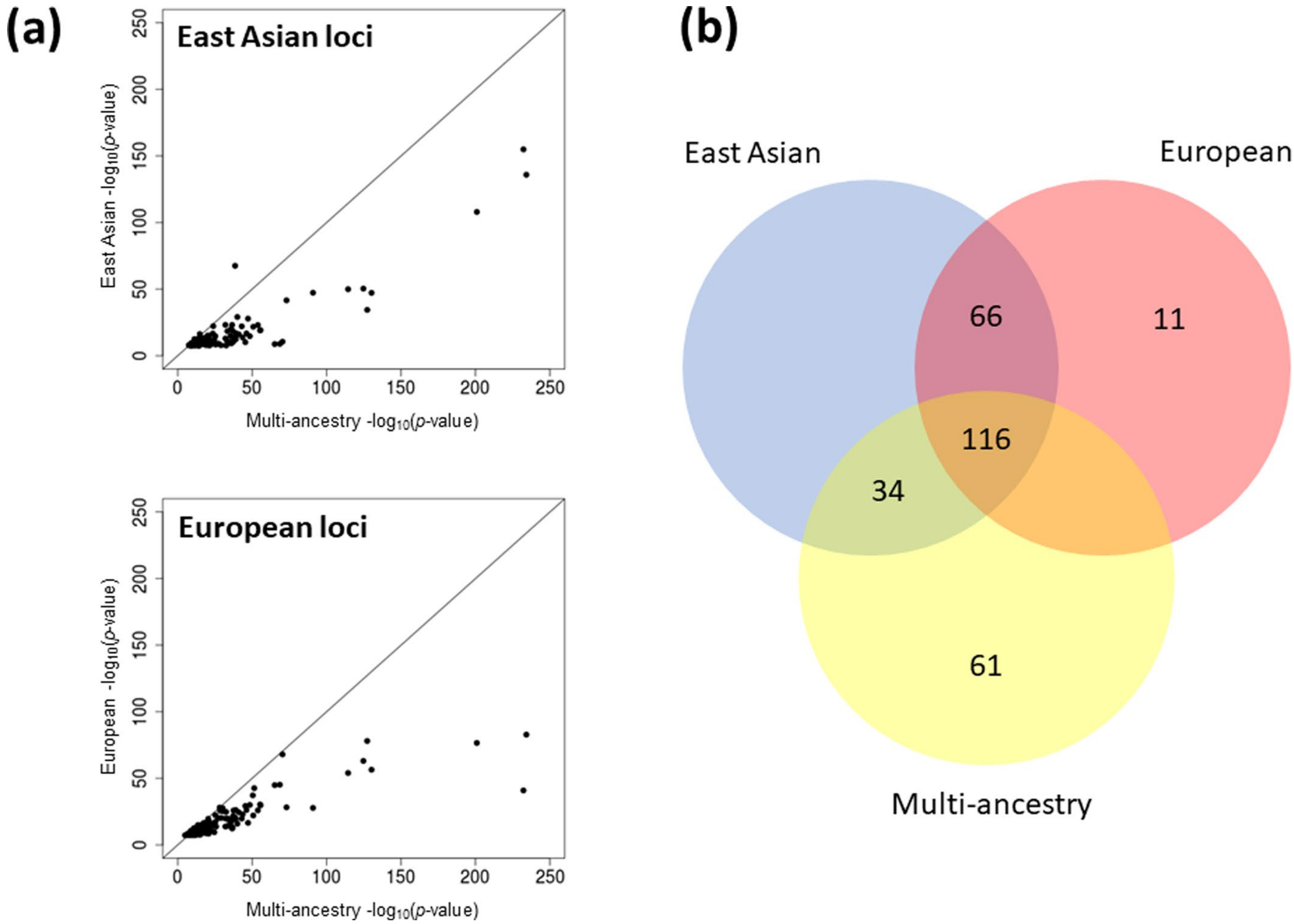

Extended Data Fig. 5 | Comparison of loci identified at genome-wide significance ($P<5\times10^{-8}$) in multi-ancestry meta-regression (180,834 cases and 1,159,055 controls), and East Asian and European ancestry-specific meta-analyses (56,268 cases and 227,155 controls, and 80,154 cases and 853,816 controls, respectively). a, Association *P*-values at loci identified in East Asian and European ancestry-specific meta-analyses. Each point corresponds to a locus, plotted according to the *P*-value (on a $-\log_{10}$ scale) for the lead SNP in the multi-ancestry meta-regression on the *x*-axis and the lead SNP in the ancestry-specific meta-analysis on the *y*-axis. The *TCF7L2* locus has been removed to improve clarity of presentation. Loci plotted below the $y=x$ line show stronger evidence for association in the multi-ancestry meta-regression. **b**, Overlap of loci identified in multi-ancestry meta-regression and ancestry-specific meta-analyses.

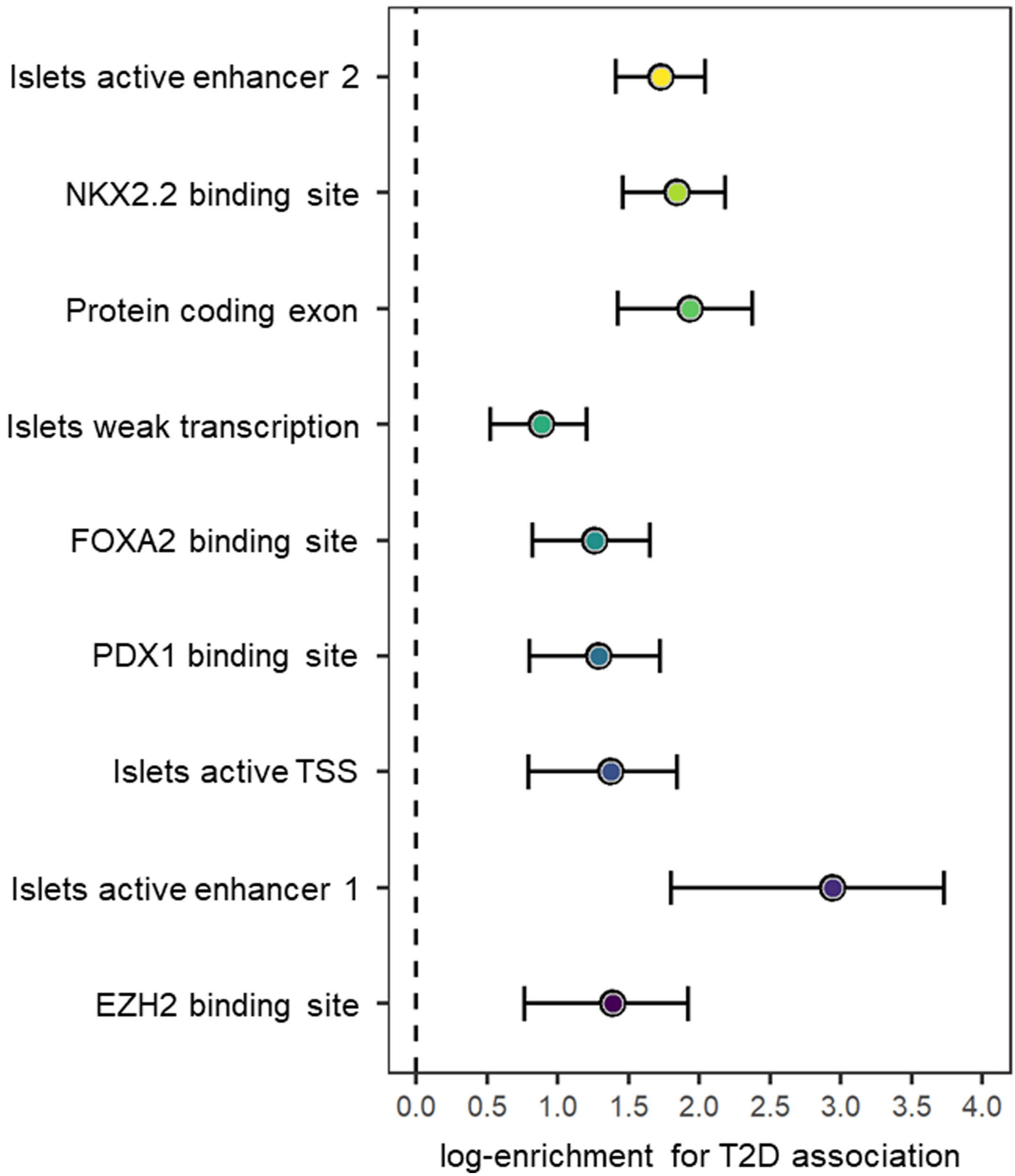

Extended Data Fig. 6 | Summary statistics from joint fGWAS model of enriched functional and regulatory annotations across distinct T2D association signals from multi-ancestry meta-regression (MR-MEGA) of up to 180,834 cases and 1,159,055 controls. Each point corresponds to an annotation, plotted for the log-enrichment for T2D association on the *x*-axis, with bars representing the corresponding 95% confidence interval (CI).

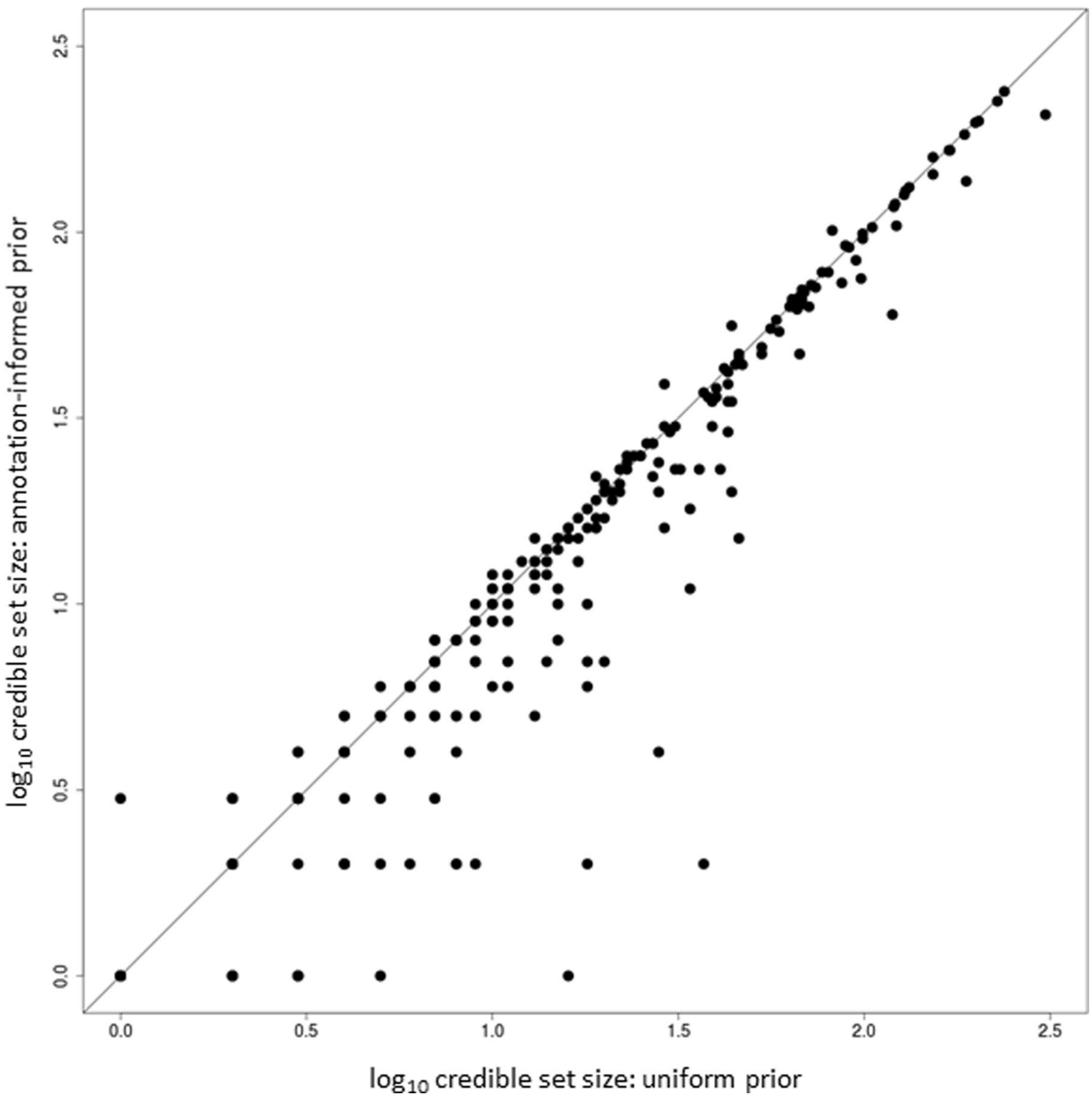

Extended Data Fig. 7 | Comparison of number of SNVs in 99% credible set for distinct association signals for T2D obtained from the multi-ancestry meta-regression of 180,834 cases and 1,159,055 controls under uniform and annotation-informed prior models of causality. Each point corresponds to a distinct association signal, plotted according to the $\log_{10}$ credible set size under the uniform prior on the *x*-axis and the $\log_{10}$ credible set size under the annotation-informed prior on the *y*-axis. The 144 (42.6%) signals below the $y = x$ line were more precisely fine-mapped under the annotation-informed prior.

Signal indexed by rs79687284

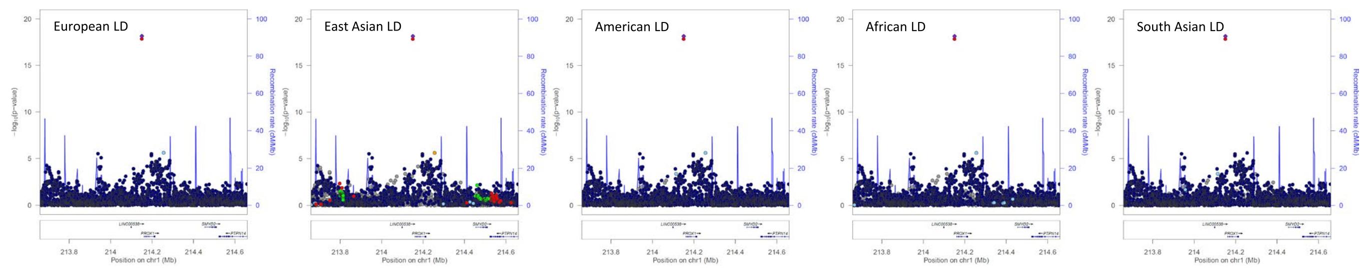

Signal indexed by rs340874

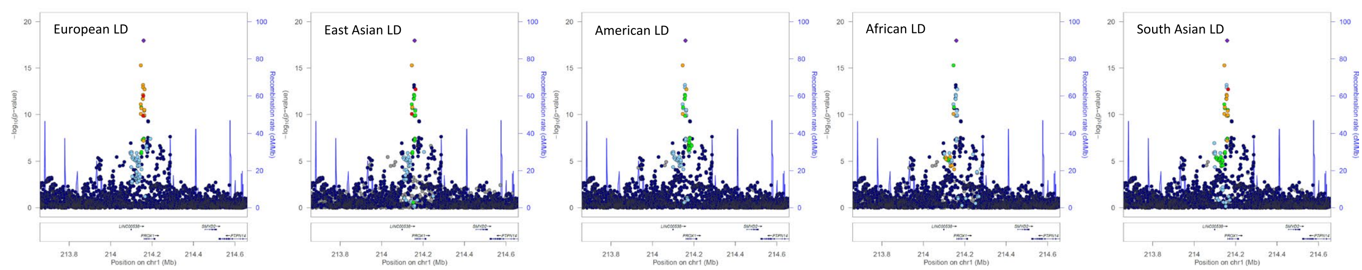

Extended Data Fig. 8 | Differences in LD structure between ancestry groups at the *PROX1* locus for distinct association signals from multi-ancestry meta-regression (MR-MEGA) of up to 180,840 cases and 1,159,185 controls. Each point represents an SNV passing quality control in the multi-ancestry meta-regression (after conditional analysis), plotted with their association *P*-value (on a $\log_{10}$ scale) as a function of genomic position (NCBI build 37). The index SNV is represented by the purple symbol. The color coding of all other SNVs indicates LD with the index variant in the ancestry-matched reference haplotypes from the 1000 Genomes Project panel: red, $r^2 \geq 0.8$; gold, $0.6 \leq r^2 < 0.8$; green, $0.4 \leq r^2 < 0.6$; cyan, $0.2 \leq r^2 < 0.4$; blue, $r^2 < 0.2$; grey, r^2 unknown. Recombination rates are estimated from Phase II HapMap and gene annotations are taken from the University of California Santa Cruz genome browser.

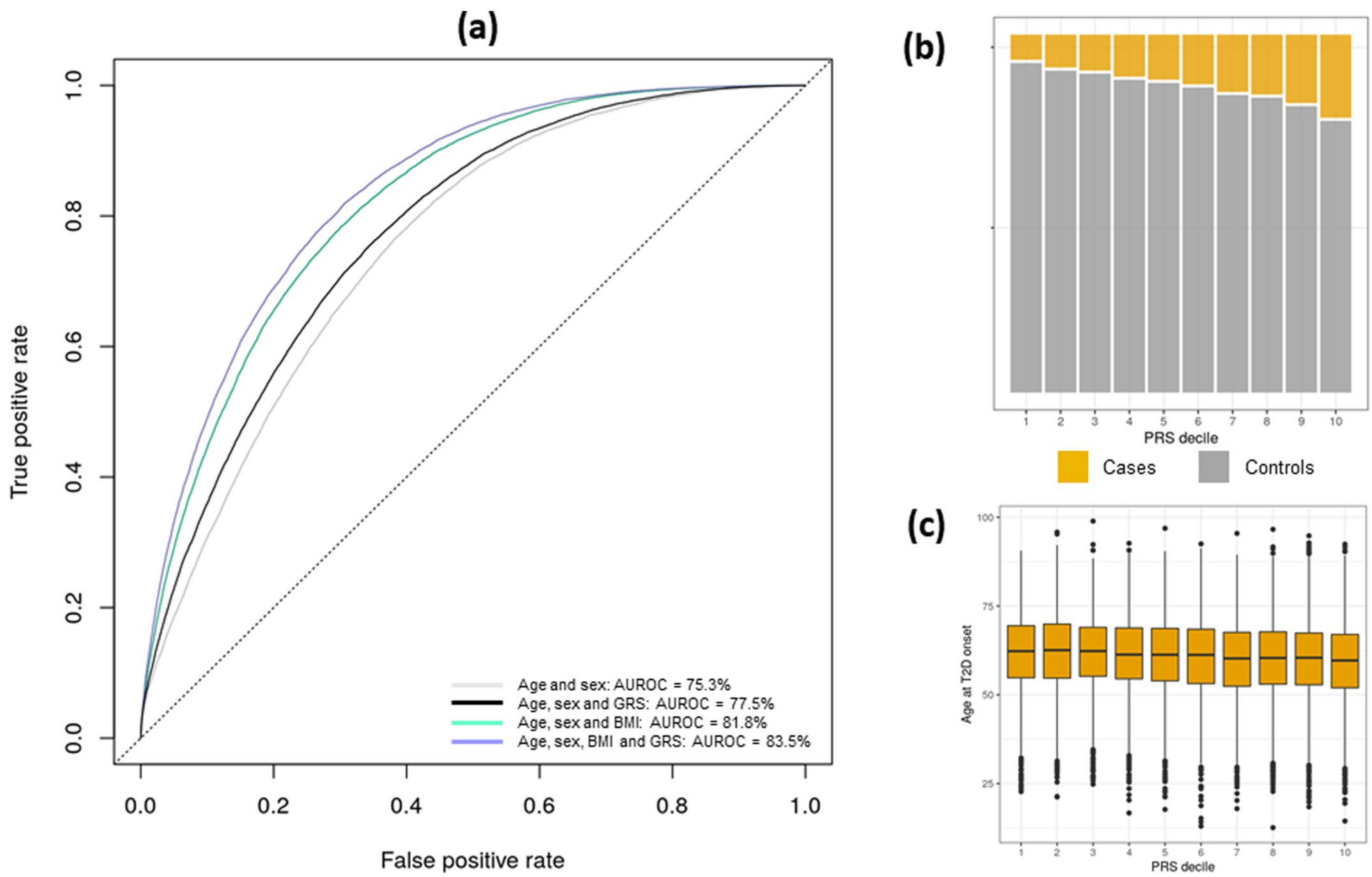

Extended Data Fig. 9 | Power of multi-ancestry GRS to predict T2D status in 129,230 individuals of Finnish ancestry from FinnGen. a, Age under receiver operating characteristic curve (AUROC) after adding BMI and GRS to a baseline model adjusting for age and sex. **b**, Prevalence of T2D across GRS deciles. **c**, Boxplot of the distribution of age at T2D diagnosis across GRS deciles: box defines upper quartile, median and lower quartile, bars define maximum and minimum values within 1.5 x interquartile range of the upper and lower quartiles, other points are outliers.

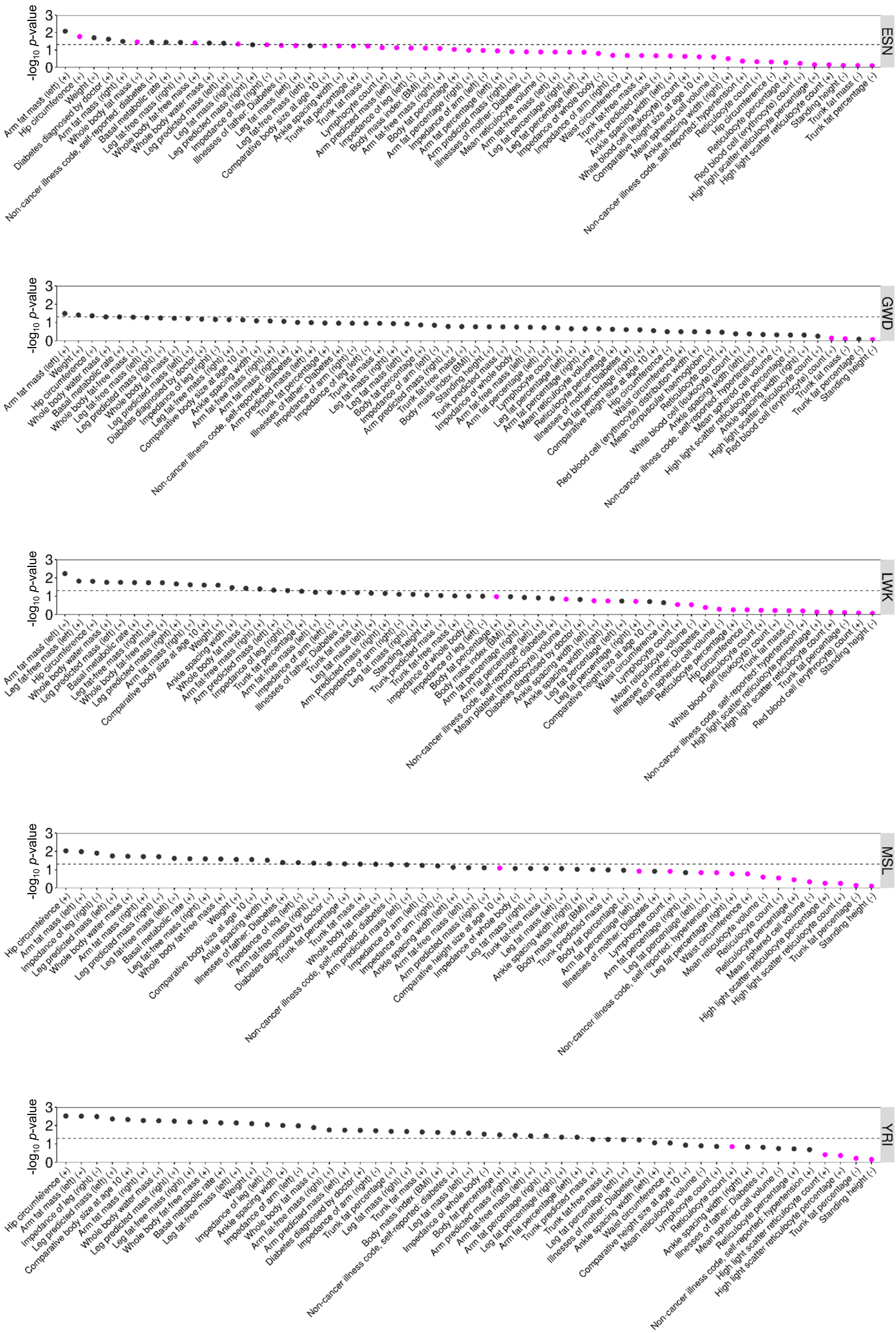

Extended Data Fig. 10 | Evidence for selection from Relate in African ancestry populations of subsets of T2D risk variants (effect aligned to derived allele) that are associated with other traits available in the UK Biobank. Nominal evidence for selection ($P < 0.05$) is indicated by the dashed line. The color of each point indicates the evidence for selection of subsets of T2D risk variants that are not associated with the other trait: $P < 0.05$ (pink) and $P \geq 0.05$ (black). Population abbreviations: ESN, Esan in Nigeria; GWD, Gambian in Western Divisions in the Gambia; LWK, Luhya in Webuye, Kenya; MSL, Mende in Sierra Leone; YRI, Yoruba in Ibadan, Nigeria.

nature research

Corresponding author(s): Andrew Morris

Last updated by author(s): Nov 29, 2021

Reporting Summary

Nature Research wishes to improve the reproducibility of the work that we publish. This form provides structure for consistency and transparency in reporting. For further information on Nature Research policies, see our Editorial Policies and the Editorial Policy Checklist.

Statistics

For all statistical analyses, confirm that the following items are present in the figure legend, table legend, main text, or Methods section.

n/a	Confirmed	
☐	☒	The exact sample size (*n*) for each experimental group/condition, given as a discrete number and unit of measurement
☒	☐	A statement on whether measurements were taken from distinct samples or whether the same sample was measured repeatedly
☐	☒	The statistical test(s) used AND whether they are one- or two-sided *Only common tests should be described solely by name; describe more complex techniques in the Methods section.*
☐	☒	A description of all covariates tested
☐	☒	A description of any assumptions or corrections, such as tests of normality and adjustment for multiple comparisons
☐	☒	A full description of the statistical parameters including central tendency (e.g. means) or other basic estimates (e.g. regression coefficient) AND variation (e.g. standard deviation) or associated estimates of uncertainty (e.g. confidence intervals)
☐	☒	For null hypothesis testing, the test statistic (e.g. *F*, *t*, *r*) with confidence intervals, effect sizes, degrees of freedom and *P* value noted *Give P values as exact values whenever suitable.*
☐	☒	For Bayesian analysis, information on the choice of priors and Markov chain Monte Carlo settings
☒	☐	For hierarchical and complex designs, identification of the appropriate level for tests and full reporting of outcomes
☒	☐	Estimates of effect sizes (e.g. Cohen's *d*, Pearson's *r*), indicating how they were calculated

Our web collection on statistics for biologists contains articles on many of the points above.

Software and code

Policy information about availability of computer code

Data collection	No software was used.
Data analysis	MR-MEGA v0.2, METAL v2011-03-25, METASOFT v2.0.0, PLINK v1.9, GCTA v1.26.0, fGWAS v0.3.6, coloc v3.1, R v3.4.2 (gtx package), Relate v1.0

For manuscripts utilizing custom algorithms or software that are central to the research but not yet described in published literature, software must be made available to editors and reviewers. We strongly encourage code deposition in a community repository (e.g. GitHub). See the Nature Research guidelines for submitting code & software for further information.

Data

Policy information about availability of data

All manuscripts must include a data availability statement. This statement should provide the following information, where applicable:

- Accession codes, unique identifiers, or web links for publicly available datasets
- A list of figures that have associated raw data
- A description of any restrictions on data availability

Association summary statistics from the trans-ancestry meta-analysis and annotation informed fine-mapping will be made available through the AMP-T2D Knowledge Portal (http://www.type2diabetesgenetics.org/) and the DIAGRAM Consortium repository (http://diagram-consortium.org/downloads.html).

Field-specific reporting

Please select the one below that is the best fit for your research. If you are not sure, read the appropriate sections before making your selection.

☒ Life sciences ☐ Behavioural & social sciences ☐ Ecological, evolutionary & environmental sciences

For a reference copy of the document with all sections, see nature.com/documents/nr-reporting-summary-flat.pdf

Life sciences study design

All studies must disclose on these points even when the disclosure is negative.

Sample size

GWAS meta-analysis. We combined the largest sample size of type 2 diabetes cases and (population) controls that was available to the DIAMANTE Consortium. At our trans-ancestry genome-wide significance threshold (p<5x10-9), under an additive genetic model, we had ≥80% power to detect association of SNVs with MAF ≥5% and OR ≥1.045 or MAF ≥0.5% and OR ≥1.145.

Luciferase reporter assays. The sample size was set as n=3; which means the vector transfection was performed three time (using different passage numbers) of each cell type.

Data exclusions

GWAS meta-analysis. Within each contributing study, individuals were excluded on the basis of well-established individual and variant quality control (QC) procedures to remove poor quality genotypes, samples and SNVs. These QC procedures are described in Supplementary Table 3 for each study.

Luciferase reporter assays. There were no data exclusions.

Replication

GWAS meta-analysis. We did not conduct replication since we had already brought together all study data available to us via meta-analysis. All reported association signals were checked to confirm that effects were not driven by false positives in single studies.

Luciferase reporter assays. Assays were performed with three biological replicates by using three different passage numbers of cells of each cell type. Within each assay, three technical replicates were included for each condition.

Randomization

GWAS meta-analysis. Randomization was not performed. Within each study, covariates were adjusted for to account for potential confounding. Covariate adjustments are reported in Supplementary Table 3.

Luciferase reporter assays. Randomization was not performed.

Blinding

GWAS meta-analysis. Group allocation was not relevant to this study, so blinding was not necessary.

Luciferase reporter assays. Blinding was not needed because the construction of each vector was designed before performing the assays.

Reporting for specific materials, systems and methods

We require information from authors about some types of materials, experimental systems and methods used in many studies. Here, indicate whether each material, system or method listed is relevant to your study. If you are not sure if a list item applies to your research, read the appropriate section before selecting a response.

Materials & experimental systems

n/a	Involved in the study
☒	☐ Antibodies
☐	☒ Eukaryotic cell lines
☒	☐ Palaeontology and archaeology
☒	☐ Animals and other organisms
☐	☒ Human research participants
☒	☐ Clinical data
☒	☐ Dual use research of concern

Methods

n/a	Involved in the study
☒	☐ ChIP-seq
☒	☐ Flow cytometry
☒	☐ MRI-based neuroimaging

Eukaryotic cell lines

Policy information about cell lines

Cell line source(s)

Two cell lines were used for the Luciferase reporter assays. The EndoC-BH1 cell line, which is a commerically available genetically engineered from a human Beta cell line (https://www.jci.org/articles/view/58447) purchased from Human Cell Design (https://www.humancelldesign.com/). The HepG2 cell line was generated from human liver tissue and was purchased from ATCC (https://www.atcc.org/products/hb-8065).

Authentication

The EndoC-BH1 cell line was authenticated at a transcriptomic level (European Nucleotide Archive [ENA;] http://

Authentication	www.ebi.ac.uk/ena) under accession number PRJEB15283) and extensively characterized (Hastoy et al Scientific Reports 8, 16994; 2018). The HepG2 cell line (BH-8065) purchased from ATCC was authenticated by ATCC through the accessioning process.
Mycoplasma contamination	Both the EndoC-BH1 and HepG2 cell lines tested negative for mycoplasma contamination.
Commonly misidentified lines (See ICLAC register)	No misidentified cell line was used in the Luciferase reporter assays.

Human research participants

Policy information about studies involving human research participants

Population characteristics	Characteristics are presented for each contributing study in Supplementary Table 2.
Recruitment	Ascertainment of type 2 diabetes cases and controls for each contributing study are presented in Supplementary Table 1.
Ethics oversight	All human research was approved within each contributing study by the relevant institutional review boards and conducted according to the Declaration of Helsinki. All participants provided written informed consent. Ethics statements from each contributing study are provided in the Supplementary Note.

Note that full information on the approval of the study protocol must also be provided in the manuscript.

nature portfolio

https://doi.org/10.1038/s41588-022-01058-3

Supplementary information

Multi-ancestry genetic study of type 2 diabetes highlights the power of diverse populations for discovery and translation

In the format provided by the authors and unedited

Multi-ancestry genetic study of type 2 diabetes highlights the power of diverse populations for discovery and translation

SUPPLEMENTARY INFORMATION

Supplementary Note: Supplementary Text
Supplementary Note: Supplementary Methods
Supplementary Note: Acknowledgements and Funding
Supplementary Note: Contributors to FinnGen
Supplementary Note: Contributors to eMERGE Consortium
Supplementary Note: Ethics Statements
Supplementary Figures
Supplementary Note Tables

Supplementary Text

Summary of loci identified through recent ancestry-specific and multi-ancestry meta-analyses incorporating GWAS from the DIAMANTE Consortium. Three recently published meta-analyses of T2D GWAS together account for 77.8% of the total effective sample size contributing to the DIAMANTE multi-ancestry meta-regression (**Supplementary Figure 1**). First, the European ancestry-specific DIAMANTE study[1], which includes 74,124 T2D cases and 824,006 controls, accounting for 47.0% of the effective sample size of the multi-ancestry meta-regression. The multi-ancestry meta-regression includes an additional 6,030 T2D cases and 29,810 controls from EGCUT, NEO and MGB, which were not part of the European ancestry-specific DIAMANTE study. Second, the East Asian ancestry-specific DIAMANTE study[2], which includes 77,418 T2D cases and 356,122 controls, accounting for 28.4% of the effective sample size of the trans-ethnic meta-regression. The multi-ancestry meta-regression does not include 21,151 T2D cases and 128,967 controls from BBJ that were part of the East Asian ancestry-specific DIAMANTE study. Third, the meta-analysis of GWAS from the Million Veteran Program (MVP), DIAMANTE and other cohorts[3], which includes 228,499 T2D cases and 1,178,783 controls, accounting for 57.1% of the effective sample size of the multi-ancestry meta-regression. GWAS contributing to the multi-ancestry meta-regression account for 45.4% of the effective sample size of the MVP meta-analysis. Both multi-ancestry and ancestry-specific (European, African, Hispanic/Latino and East/South Asian) meta-analyses were undertaken. Making comparisons of the numbers of (novel) loci reported by each of these investigations is not an appropriate evaluation of their relative power because of differences in thresholds of genome-wide significance, corrections for residual population structure after meta-analysis, reference panels used for imputation and SNV filtering criteria (**Supplementary Note Table 1**). Instead, we sought to present an all-inclusive summary of loci reported in studies to which DIAMANTE GWAS have contributed to provide the most comprehensive overview of the genetic contribution to T2D susceptibility to date.

We began by considering loci reported in each of the published ancestry-specific and multi-ancestry meta-analyses incorporating GWAS from the DIAMANTE Consortium (without adjustment for BMI). For each of these efforts, loci were defined as mapping 500kb up- and downstream of a lead SNV attaining genome-wide significance (p<5x10^{-8}). We also considered loci reported in the multi-ancestry meta-regression, which used a more conservative definition (**Methods**) that: (i) considered the flanking genomic interval mapping 500kb up- and downstream of a lead SNV attaining stringent multi-ancestry genome-wide significance (p<5x10^{-9}); and (ii) merged loci where lead SNVs were separated by less than 1Mb. We then aggregated loci across the four studies, ensuring no overlap between adjacent loci (**Supplementary Figure 2**). Taken together, the four studies report 520 non-overlapping loci spanning 624.5Mb, including 405 (77.9%) attaining stringent multi-ancestry genome-wide significance (**Supplementary Note Table 2**). Of the 520 loci, 35 (6.7%) were reported only in ancestry-specific meta-analyses: 21 European ancestry-specific, 12 East Asian ancestry-specific and 2 African ancestry-specific.

Comparison of ancestry-specific meta-analyses and multi-ancestry meta-regression. To gain insight into the power offered by aggregating GWAS from diverse populations, we compared the number of loci identified in multi-ancestry meta-regression with that detected in ancestry-specific meta-analyses. As there are minor differences in the GWAS contributing to the multi-ancestry meta-regression and the previously reported European and East Asian ancestry components of DIAMANTE[1,2], we restricted comparisons to those that contributed to both. Of the 100 and 193 loci attaining genome-wide significance in the East Asian and European ancestry-specific meta-analyses, respectively, lead SNVs at 94 (94.0%) and 164 (85.0%) demonstrated stronger evidence for association (i.e. smaller *p*-value) in the multi-ancestry meta-regression (**Extended Data Figure 4**), in line with differences in sample size. In contrast, eleven (5.7%) of the 193 loci identified in the European ancestry-specific meta-analysis did not attain genome-wide significance in the multi-ancestry meta-regression (**Supplementary Note Table 3**). None of these eleven SNVs demonstrated significant evidence of T2D association in a meta-analysis of non-European ancestry GWAS. Such signals could arise when the lead SNV is in strong linkage disequilibrium (LD) with an ancestry-specific causal variant that has not been interrogated in the multi-ancestry meta-regression, or because of haplotype/epistatic effects across variants with differing allele frequency between ancestry groups. Taken together, these results demonstrate the power of multi-ancestry meta-analyses for locus discovery and replication that is afforded by increased sample size, but also emphasize the importance of complementary ancestry-specific GWAS for optimal identification of associations driven by causal variants that are not shared across diverse populations.

Dissection of distinct T2D association signals. Through approximate conditional analyses, conducted using ancestry-matched LD reference panels for each GWAS, we partitioned associations at the 237 T2D loci into 338 distinct signals that were each represented by an index SNV at the same multi-ancestry genome-wide significance threshold (**Methods, Supplementary Tables 6 and 7**). We observed multiple distinct association signals at 52 (21.9%) loci, of which 50 were represented by between two and five index SNVs. The most complex genetic architecture was observed across a 1Mb region flanking the lead SNV at the *TCF7L2* locus, where the T2D association was delineated to 16 distinct signals **(Supplementary Figure 3**), and a 1.7Mb imprinted region encompassing the previously reported loci *INS-IGF2* and *KCNQ1*, which was delineated into 14 distinct signals (**Supplementary Figure 4**).

Assessment of the impact of reference panel choice on approximate conditional analyses undertaken in admixed ancestry groups. We used haplotypes from the 1000 Genomes Project reference panel (phase 3, October 2014 release)[4] that were specific to each ancestry group (**Supplementary Table 22**) as a reference for LD between SNVs across loci in the approximate conditional analysis. African ancestry GWAS, including admixed African American studies, were matched to African haplotypes, derived from 661 individuals from: African Caribbean in Barbados; African Ancestry in Southwest USA; Esan in Nigeria; Gambian in Western Division, The Gambia; Luhya in Webuye, Kenya; Mende in Sierra Leone; and Yoruba in Ibadan, Nigeria. Hispanic GWAS were matched to American haplotypes, derived from 347 individuals from: Colombian in Medellin, Colombia; Mexican Ancestry in Los Angeles, California; Peruvian in Lima, Peru; and Puerto Rican in Puerto Rico. The 1000 Genomes Project reference panel has the advantage that it includes individuals from diverse populations across each ancestry group, with haplotypes derived from high-quality whole genome sequence data that includes all variants tested in the multi-ancestry meta-analysis. However, the disadvantage of this reference panel is that it includes only of the order of 500 individuals per ancestry group, and approximate conditional analyses may therefore be susceptible to unstable effect size estimates at lower frequency variants.

An alternative approach is to make use of individual-level genotype data from GWAS contributing to the multi-ancestry meta-regression as a reference for LD in approximate conditional analyses. These studies typically include larger numbers of individuals than are available in the 1000 Genomes Project reference panel. However, these GWAS will usually have been imputed, such that many variants present in the reference panel will fail imputation quality control. Furthermore, the approximate conditional analyses implemented in GCTA require that imputed genotypes be converted to hard calls, which can lead to over-confidence in downstream analyses by ignoring imputation uncertainty. A single study may also not be representative of the genetic diversity amongst GWAS from an ancestry group, particularly those with variable levels of admixture.

To gain insight into the robustness of our approximate conditional analyses to the choice of LD reference panel in admixed ancestry groups, we considered subsets of 1,000 African American and 1,000 Hispanic individuals from the Resource for Genetic Epidemiology on Adult Health and Aging (GERA), a large multi-ancestry population-based cohort, created for investigating the genetic and environmental basis of age-related diseases [database of Genotypes and Phenotypes (dbGaP) phs000674.p1]. GERA participants have previously been genotyped using one of four custom arrays, which have been designed to maximise coverage of common and low-frequency variants in non-Hispanic white, East Asian, African American and Hispanic individuals[5,6]. We undertook quality control of these genotype data, removing individuals from known pedigrees and/or with call rate (<97%), and excluding SNVs with call rate (<95%) and extreme deviation from Hardy-Weinberg equilibrium (autosomes only, exact $p<10^{-6}$). We constructed a genetic relationship matrix (GRM) from pair-wise identity by descent metrics estimated from LD pruned ($r^2<0.01$ across individuals) autosomal SNVs shared across the four genotyping arrays, and with MAF ≥1%, after exclusion of those in high-LD and complex regions, and those mapping to established T2D loci. We defined related individuals with pair-wise pi-hat >0.2 and removed those with the lowest call rate from each related set.

We applied multi-dimensional scaling, implemented in PLINK[7], to the GRM to obtain principal components to represent axes of genetic variation that separate the major ancestry groups. Clusters of African American and Hispanic individuals were identified in principal component space, and subsets of 1,000 randomly selected individuals from each cluster for use as a reference for LD in approximate conditional analyses.

For each subset of individuals, we constructed a scaffold for imputation after excluding SNVs with MAF<1%. The scaffold was then pre-phased using SHAPEITv2.5[8], based on estimates of recombination rate from the International HapMap Project[9]. The resulting haplotypes were imputed up to the 1000 Genomes Project reference panel (phase 3, October 2014 release) using minimac4 via the Michigan Imputation Server[10]. SNVs with r^2 ≥0.4 were retained for downstream analyses. African and Hispanic LD reference panels were then obtained by converting imputed genotype dosages to hard calls using PLINKv1.9[11].

For each locus with more than one distinct association signal in the multi-ancestry meta-regression, we used GCTA in each African and Hispanic ancestry GWAS, removing each SNV, in turn, from the conditional set, and adjusting for the remainder, using the "--cojo-cond" option. If any SNV from the conditional set failed imputation quality control in the LD reference panel, the locus was excluded from downstream analyses. We aggregated allelic log-ORs from the approximate conditional analyses across African and Hispanic ancestry

GWAS via fixed-effects meta-analysis using METAL[12] based on inverse-variance weighting. We corrected association *p*-values and standard errors of allelic effects from each ancestry group for residual inflation due to structure between GWAS using the same genomic control adjustments as in the unconditional analyses (**Methods**).

We compared allelic effect estimates (log-OR) and *p*-values (on a $-\log_{10}$ scale) in African and Hispanic ancestry-specific meta-analyses using ancestry-matched LD reference panels from the 1000 Genomes Project and GERA (**Supplementary Figure 5, Supplementary Note Tables 4 and 5**). There was a strong correlation in allelic effect estimates from the different LD reference panels: African ancestry r=0.997; Hispanic ancestry r=0.988. The strength of evidence in favour of association (as measured by the conditional *p*-value) of each index SNV was mostly within one order of magnitude between the LD reference panels. We conclude, therefore, that our approximate conditional analyses undertaken in admixed ancestry groups are robust to the choice of reference panel.

Impact of obesity on multi-ancestry heterogeneity. We were interested to determine whether ancestry-correlated heterogeneous association signals could be explained by an interaction with obesity, given the leftwards shift in the distribution of body mass index (BMI) in individuals of East Asian ancestry. To do this, we considered the 136 association signals with nominal evidence of ancestry-correlated heterogeneity in allelic effects (**Supplementary Note Table 6**). For each index SNV, we modelled allelic log-ORs across GWAS in a linear regression framework, weighted by the inverse of the variance of the effect estimates. For index SNVs at loci with a single distinct association signal, log-ORs and variances were obtained from unconditional analysis. For index SNVs at loci with multiple distinct association signals, log-ORs and variances were obtained from approximate conditional analysis. We excluded GWAS for which BMI was not reported: BIOME (HIS), GERA (AFR), GERA (EUR), GODARTS, KORA and WTCCC. For each GWAS, we included as covariates: (i) mean BMI; and (ii) the three axes of genetic variation representing ancestry. In this modelling framework, we tested for: (i) heterogeneity in allelic effects on T2D between GWAS that is correlated with BMI, after adjusting for ancestry; (ii) heterogeneity in allelic effects on T2D between GWAS that is correlated with ancestry, after adjusting for BMI; and (iii) residual allelic effect heterogeneity between GWAS due to unmeasured confounders.

The strongest evidence for heterogeneity in allelic effects that was correlated with BMI (after accounting for ancestry) was observed for the T2D association signal at the *CDKAL1* locus (rs9348441, $p_{HET}=3.0\times10^{-6}$). At this signal, the effect of the risk allele on T2D was greatest in East Asian ancestry populations, and there was a negative correlation between BMI and log-OR across GWAS (**Supplementary Figure 6**). This relationship is consistent with a model of "favourable adiposity", whereby a subset of BMI-increasing alleles are associated with higher subcutaneous-to-visceral adipose tissue ratio and a paradoxical reduction in insulin levels, protecting against T2D through higher adipose storage capacity[13]. A protective interaction with obesity at this locus is supported by evidence of: (i) stronger association at the index SNV after adjustment for BMI in the European and East Asian ancestry components of DIAMANTE[1,2]; and (ii) significant association of the T2D-risk allele with decreased BMI in European and East Asian ancestry GWAS meta-analyses of obesity in the general population[14,15]. However, confirmation of the impact of obesity on the heterogeneity of allelic effects at the *CDKAL1* locus requires formal testing of SNV x BMI interaction within GWAS across ancestry groups.

Impact of allele frequency, allelic effect size and LD on fine-mapping resolution. Compared to the European ancestry-specific meta-analysis, some of the most dramatic improvements in fine-mapping resolution after multi-ancestry meta-regression included signals where the index SNV was of lower frequency and/or of smaller effect in European ancestry populations. For these signals, including those at *GCC1-PAX4-LEP*, *SGCG*, *RGMA*, *DSTYK-MDM4* and *MYO3A*, the evidence for association was weak in the European ancestry-specific meta-analysis, resulting in large credible sets compared to other ancestry groups. However, we also observed examples of T2D signals with strong associations across all five ancestry groups, for which the credible sets were smaller in the multi-ancestry meta-regression. The most noticeable improvements in fine-mapping resolution were seen at *TMEM154*, *HMGA2*, *GRP-MC4R*, *IGF2BP2*, *SPRY2* and *FTO* (**Supplementary Table 9**). At *FTO*, for example, the 18 variants in the European ancestry-specific 99% credible set were in strong LD with the index SNV (rs55872725) in European ancestry populations (r^2>0.8). However, the 99% credible set after multi-ancestry meta-regression included just six of these variants that were in strong LD with the index SNV in all five ancestry groups (**Supplementary Figure 7**).

Improved fine-mapping of T2D coding variant associations. The multi-ancestry meta-regression highlighted two examples of previously reported T2D coding variant associations that were better resolved by fine-mapping across diverse populations (**Supplementary Figure 8**). A set of five coding variants in *SLC16A11* has been associated with T2D in Hispanic populations[16,17], but causality could not be ascribed because of strong LD between them. However, after multi-ancestry fine-mapping, *SLC16A11* p.Val113Ile (rs117767867, p=6.5x10^{-24}, π=59.8%) emerged as the variant most likely driving this association signal (the other four coding variants together account for just 14.0% of the posterior probability). Similarly, strong LD at the *KCNJ11-ABCC8* locus has frustrated efforts in European ancestry studies to distinguish the impact on T2D of three missense variants: *KCNJ11* p.Val250Ile (rs5215), *KCNJ11* p.Lys23Glu (rs5219) and *ABCC8* p.Ala1369Ser (rs757110). *ABCC8* and *KCNJ11* code for the two elements of the hetero-octameric beta-cell K_{ATP} channel and both represent strong biological candidates. Whilst multi-ancestry fine-mapping cannot equivocally distinguish between *KCNJ11* p.Val250Ile (p=1.3x10^{-54}, π=67.1%) and *KCNJ11* p.Lys23Glu (p=2.6x10^{-54}, π=32.5%), it is less likely that the association signal is mediated via *ABCC8* p.Ala1369Ser (p=1.2x10^{-51}, π=0.1%).

Multi-ancestry fine-mapping provided a more detailed view of the role of missense variants in driving three distinct T2D association signals at the *ZFAND3-KCNK16-GLP1R* locus (**Supplementary Figure 9**). Previous East Asian ancestry GWAS and exome-array meta-analyses[18,19] reported T2D association with *GLP1R* p.Arg131Gln (rs3765467). Whilst this variant is included in the 99% credible set of the signal indexed by rs742762, a non-coding SNV, in the multi-ancestry meta-regression, it has a relatively low posterior probability of association (π=2.0%, compared with π=75.0% for the index SNV). However, we identified a different *GLP1R* missense variant, p.Pro7Leu (rs10305420, p=1.1x10^{-9}, π=94.1%), not in LD with p.Arg131Gln, which seems likely to be causal for the second association signal at the locus. At the third signal, 61.4% of the posterior probability of association could be attributed to three different missense variants: p.Ser21Gly (rs10947804, π=39.2%) in *KCNK17*; and p.Pro254His (rs11756091, π=14.8%) and p.Ala277Glu (rs1535500, π=13.7%) in *KCNK16*. Both genes encode members of the TWIK-related alkaline pH-activated K2P family, TALK-1 and TALK-2, and are expressed in islets with high specificity. The missense variants are in strong LD with each other across ancestry groups, and the T2D-risk haplotype is associated with increased *KCNK17* expression in pancreatic islets[20]. These results highlight the mechanistic complexity at this locus, with evidence that missense variants in *GLP1R*, *KCNK16* and *KCNK17* may each be contributing to T2D susceptibility.

Integration of fine-mapping and chromatin interaction data in diverse tissues. We intersected 99% credible set variants for distinct T2D association signals with genome-wide promoter-focussed chromatin conformation capture data (pcHi-C) from pancreatic islets, subcutaneous adipose and liver (equivalent data are not available in hypothalamus and visceral adipose)[21-23]. Across the three tissues, we observed contacts between credible set variants and putative target gene promoters for 214 (63.3%) of the association signals (**Supplementary Table 18**). The contacts at 119 of these signals were observed in only one tissue: 51 in islets, 45 in liver, and 23 in subcutaneous adipose. Some targets were expected based on their proximity to the index SNV for the T2D association (including *TCF7L2*, *PROX1*, *PTEN*, *DLEU1*, *GLIS3*, *CCND2*, *CMIP* and *BCL2*), but for 143 (66.8%) of the 214 signals, we identified more distant candidate effector genes (including *AQP5* and *AQP6* at the *FAIM2* locus, *P2RX1* at the *ZZEF1* locus, *STX16* at the *GNAS* locus, and *ISL1* at the *ITGA1* locus). Several of these targets provide complementary support for candidate effector genes identified via colocalization with *cis*-eQTLs in the same tissue: *PLEKHA1* in islets and subcutaneous adipose; *ST6GAL1*, *CARD9*, *DNLZ*, *CAMK1D*, *TCF7L2*, *TH*, *DLK1* and *AP3S2* in islets; *DCAF16*, *STEAP2* and *MAN2C1* in subcutaneous adipose; and *CEP68* and *SLC22A3* in liver.

Summary of candidate causal genes at T2D loci identified from functional annotation and colocalization with molecular QTLs. We identified a total of 117 candidate causal genes at T2D loci through integration of multi-ancestry fine-mapping, functional annotation, and molecular QTL data resources (**Supplementary Note Table 7**). First, we identified missense variants accounting for more than 50% posterior probability of driving distinct T2D association signals after annotation-informed fine-mapping. Second, we identified distinct T2D association signals that colocalized with more than 80% posterior probability with: (i) circulating plasma proteins (pQTLs)[24]; or (ii) gene expression (eQTLs) in diabetes-relevant tissues (pancreatic islets, subcutaneous and visceral adipose, liver, skeletal muscle, and hypothalamus)[25,26].

We sought to evaluate the support for these candidate causal genes from complementary analyses undertaken in three recently published meta-analyses of T2D GWAS together account for 77.8% of the total effective sample size contributing to the DIAMANTE multi-ancestry meta-regression. First, the European ancestry-specific DIAMANTE study[1] reported missense variants accounting for more than 50% posterior probability of driving distinct T2D association signals after annotation-informed fine-mapping. Second, the East Asian ancestry-specific DIAMANTE study[2] reported index SNVs for T2D that are in strong LD (r^2>0.8) with significant eQTLs in: (i) pancreas[25] and pancreatic islets[20]; (ii) subcutaneous adipose[25,27]; (iii) skeletal muscle[25]; and (iv) blood[25,28]. Here, we focussed only on those significant eQTLs in diabetes-relevant tissues (pancreas, pancreatic islets, subcutaneous adipose and skeletal muscle). Third, the meta-analysis of GWAS from the Million Veteran Program (MVP), DIAMANTE and other cohorts[3] reported missense variants attaining genome-wide significance at T2D loci. Here, we considered only those missense variants in strong LD (r^2>0.8) with lead SNVs for T2D. The study also reported the results of transcriptome-wide association studies across the diverse range of tissues available in GTEx[25]. Here, we focussed on those genes with significant association (p<1.93x10^{-7}) of T2D with genetically-regulated expression, which also colocalized with more than 80% posterior probability in diabetes-relevant tissues (pancreas, subcutaneous and visceral adipose, liver, skeletal muscle, and hypothalamus).

Of the 117 candidate causal genes identified in the DIAMANTE multi-ancestry study, 40 were not reported in these complementary analyses (**Supplementary Note Table 7**). These include genes previously implicated in T2D through detailed experimental studies (such as *TCF7L2*, *MTNR1B*, *ARAP1*, *STARD10* and *CAMK1D*), but also novel candidates that provide new leads for functional follow-up. These findings highlight the importance of: (i) diverse populations to enable high-resolution fine-mapping of T2D association signals; (ii) gene expression profiling in diabetes-relevant tissues to understand cell-type specific contexts through which association signals are mediated; and (iii) dissection of both T2D associations and molecular QTLs through conditional analysis to allow colocalization at the level of a signal (and not a locus).

1. Mahajan, A. et al. Fine-mapping type 2 diabetes loci to single-variant resolution using high-density imputation and islet-specific epigenome maps. *Nat. Genet.* **50**, 1505-1513 (2018).
2. Spracklen, C. N. et al. Identification of type 2 diabetes loci in 433,540 East Asian individuals. *Nature* **582**, 240-245 (2020).
3. Vujkovic, M. et al. Discovery of 318 new risk loci for type 2 diabetes and related vascular outcomes among 1. 4 million participants in a multi-ancestry meta-analysis. *Nat. Genet.* **52**, 680-691 (2020).
4. The 1000 Genomes Project Consortium. A global reference for human genetic variation. *Nature* **526**, 68-74 (2015).
5. Hoffmann, T.J. et al. Next generation genome-wide association tool: design and coverage of a high-throughput European-optimized SNP array. *Genomics* **98**, 79-89 (2011).
6. Hoffmann, T.J. et al. Design and coverage of high-throughput genotyping arrays optimised for individuals of East Asian, African American, and Latino race/ethnicity using imputation and a novel hybrid SNP selection algorithm. *Genomics* **98**, 422-430 (2011).
7. Purcell, S. et al. PLINK: a tool set for whole-genome association and population-based linkage analyses. *Am. J. Hum. Genet.* **81**, 559-575 (2007).
8. O'Connell, J. et al. A general approach for haplotype phasing across the full spectrum of relatedness. *PLoS Genet.* **10**, e1004234 (2011).
9. The International HapMap 3 Consortium. Integrating common and rare genetic variation in diverse human populations. *Nature* **467**, 52-58 (2010).
10. Das, S., et al. Next-generation genotype imputation service and methods. *Nat. Genet.* **48**, 1284-1287 (2016).
11. Chang, C. C. et al. Second-generation PLINK: rising to the challenge of larger and richer datasets. *GigaScience* **4**, 7 (2015).
12. Willer, C. J., Li, Y. & Abecasis, G. R. METAL: fast and efficient meta-analysis of genome-wide association scans. *Bioinformatics* **26**, 2190-2191 (2010).

13. Yaghootkar, H. et al. Genetic evidence for a link between favorable adiposity and lower risk of type 2 diabetes, hypertension, and heart disease. *Diabetes* **65**, 2448-2460 (2016).
14. Akiyama, M. et al. Genome-wide association study identifies 112 new loci for body mass index in the Japanese population. *Nat. Genet.* **49**, 1458-1467 (2017).
15. Yengo, L. et al. Visscher, Meta-analysis of genome-wide association studies for height and body mass index in ~700000 individuals of European ancestry. *Hum. Mol. Genet.* **27**, 3641-3649 (2018).
16. SIGMA Type 2 Diabetes Consortium. Sequence variants in SLC16A11 are a common risk factor for type 2 diabetes in Mexico. *Nature* **506**, 97-101 (2014).
17. Rusu, V. et al. Type 2 diabetes variants disrupt function of SLC16A11 through two distinct mechanisms. *Cell* **170**, 199-212 (2017).
18. Suzuki, K. et al. Identification of 28 new susceptibility loci for type 2 diabetes in the Japanese population. *Nat. Genet.* **51**, 379-386 (2019).
19. Kwak, S. H. et al. Nonsynonymous variants in PAX4 and GLP1R are associated with type 2 diabetes in an East Asian population. *Diabetes* **67**, 1892-1902 (2018).
20. Varshney, A. et al. Genetic regulatory signatures underlying islet gene expression and type 2 diabetes. *Proc. Natl. Acad. Sci. U. S. A.* **114**, 2301-2306 (2017).
21. Pan, D. Z. et al. Integration of human adipocyte chromosomal interactions with adipose gene expression prioritizes obesity-related genes from GWAS. *Nat. Commun.* **9**, 1512 (2018).
22. Miguel-Escalada, I. et al. Human pancreatic islet three-dimensional chromatin architecture provides insights into the genetics of type 2 diabetes. *Nat. Genet.* **51**, 1137-1148 (2019).
23. Chesi, A. et al. Genome-scale Capture C promoter interactions implicate effector genes at GWAS loci for bone mineral density. *Nat. Commun.* **10**, 1260 (2019).
24. Sun, B. B. et al. Genomic atlas of the human plasma proteome. *Nature* **558**, 73-79 (2018).
25. GTEx Consortium. Genetic effects on gene expression across human tissues. *Nature* **550**, 204-213 (2017).
26. Vinuela, A. et al. Genetic variant effects on gene expression in human pancreatic islets and their implications for T2D. *Nat. Commun.* **11**, 4912 (2020).
27. Civelek, M. et al. Genetic regulation of adipose gene expression and cardio-metabolic traits. Am. J. Hum. Genet. **100**, *428-443* (2017).
28. Vosa, U. et al. Unraveling the polygenic architecture of complex traits using blood eQTL meta-analysis. Preprint at https://www.biorxiv.org/content/10.1101/447367v1 (2018).

Supplementary Methods

Exemplar power calculations. Assuming homogeneous effects on T2D across ancestry groups, we estimated power to detect association with an SNV under an additive model from the non-centrality parameter of a chi-squared distribution with one degree of freedom, given by $N_{\mathrm{eff}}\psi^2 q(1-q)$, where q denotes the mean effect allele frequency across populations and ψ denotes the allelic log-OR, and N_{eff} is the total effective sample size across studies[1]. At our multi-ancestry genome-wide significance threshold, $p<5\text{x}10^{-9}$, under an additive genetic model, we had ≥80% power to detect association of SNVs with MAF ≥5% and OR ≥1.045 or MAF ≥0.5% and OR ≥1.145.

Dissection of distinct multi-ancestry association signals. We used iterative approximate conditioning, implemented in GCTA[2], making use of forward selection and backward elimination, to identify index SNVs at multi-ancestry genome-wide significance ($p<5\text{x}10^{-9}$). We used haplotypes from the 1000 Genomes Project reference panel (phase 3, October 2014 release)[3] that were specific to each ancestry group (**Supplementary Table 22**) as a reference for LD between SNVs across loci in the approximate conditional analysis.

For each locus, we first used GCTA in each ancestry-specific GWAS, using the study-level association summary statistics and ancestry-matched LD reference, implementing a forward selection scheme. At each iteration, we adjusted for the "conditional set" of variants at the locus using the "--cojo-cond" option. In the first iteration, the conditional set included only the lead SNV at the locus. Allelic log-ORs from the approximate conditional analyses across GWAS were modelled in the multi-ancestry meta-regression framework, incorporating the three axes of genetic variation as covariates, and weighted by the inverse of the variance of the effect estimates. The meta-regression association p-values were corrected for inflation due to residual structure between GWAS by using the same genomic control adjustment as in the unconditional analysis (λ_{TA} = 1.052). If no SNVs attained genome-wide significant ($p<5\text{x}10^{-9}$) evidence of residual T2D association in the meta-regression, the iterative approximate conditional analysis for the locus was stopped. Otherwise, the SNV with the strongest residual association signal was added to the conditional set. This process continued, at each iteration adding the SNV with the strongest residual T2D association from the meta-regression to the conditional set, until no remaining SNVs attained genome-wide significance. Note, that at each iteration, GWAS with missing association summary statistics for any variant in the conditional set were excluded from the meta-regression.

For each locus with more than one SNV in the conditional set, we then checked that all variants in the conditional set attained genome-wide significant evidence of association in a joint model after meta-regression. To do this, we used GCTA in each GWAS, but this time using the "--cojo-joint" option, including all SNVs in the conditional set in the joint model. Allelic log-ORs from the approximate conditional analyses across GWAS were modelled in the multi-ancestry meta-regression framework, incorporating the three axes of genetic variation as covariates, and weighted by the inverse of the variance of the effect estimates. The meta-regression association p-values were corrected for inflation due to residual structure between GWAS by using the same genomic control adjustment as in the unconditional analysis (λ_{TA} = 1.052). If any SNV in the conditional set did not attain genome-wide significant evidence of association, the SNV with the least significant p-value was removed (backward elimination). The procedure then iterated between forward selection and backward elimination steps until: (i) no SNVs outside the conditional set attained genome-wide significant evidence of residual association in the meta-regression; and (ii) all SNVs in the conditional set attained genome-wide significant evidence of association in the joint model after meta-regression.

For each locus including more than one SNV in the conditional set, we next dissected each distinct association signal. We again used GCTA in each GWAS, but this time removing each SNV, in turn, from the conditional set, and adjusting for the remainder, using the "--cojo-cond" option. Allelic log-ORs from the approximate conditional analyses across GWAS were modelled in the multi-ancestry meta-regression framework, incorporating the three axes of genetic variation as covariates, and weighted by the inverse of the variance of the effect estimates. The meta-regression association *p*-values were corrected for inflation due to residual structure between GWAS by using the same genomic control adjustment as in the unconditional analysis (λ_{TA} = 1.052). The variant with the strongest residual association was defined as the "index SNV" for the signal. We also aggregated allelic log-ORs from the approximate conditional analyses across GWAS via fixed-effects meta-analysis using METAL[4] based on inverse-variance weighting. Standard errors were corrected for residual inflation due to structure between GWAS using the same genomic control adjustment as in the unconditional analysis (λ_{TA}^{FE} = 1.253).

Ancestry-specific meta-analyses. We aggregated association summary statistics across GWAS from the same ancestry group via fixed-effects meta-analysis using METAL[4] based on inverse-variance weighting of allelic log-OR to obtain effect size estimates. We corrected association *p*-values and standard errors of allelic effects from each ancestry group for residual inflation due to structure between GWAS by genomic control adjustment: African λ_{AFR} = 1.056; East Asian λ_{EAS} = 1.111; European λ_{EUR} = 1.096; Hispanic λ_{HIS} = 1.008; South Asian λ_{SAS} = 0.973 (no correction made). We estimated the mean effect allele frequency across GWAS from each ancestry group, weighted by the effective sample size of the study. We also aggregated association summary statistics across GWAS from non-European ancestry groups via fixed-effects meta-analysis using METAL based on inverse-variance weighting of allelic log-OR to obtain effect size estimates. We corrected association *p*-values and standard errors of allelic effects for residual inflation due to structure between GWAS by genomic control adjustment: λ_{nonEUR} = 1.133. Finally, we aggregated association summary statistics across GWAS from East Asian and European ancestry groups via fixed-effects meta-analysis using METAL based on inverse-variance weighting of allelic log-OR to obtain effect size estimates. We corrected association *p*-values and standard errors of allelic effects for residual inflation due to structure between GWAS by genomic control adjustment: λ_{EASEUR} = 1.147.

For each locus with more than one distinct association signal in the multi-ancestry meta-regression, we used GCTA in each GWAS, removing each SNV, in turn, from the conditional set, and adjusting for the remainder, using the "--cojo-cond" option. We aggregated allelic log-ORs from the approximate conditional analyses across GWAS within the same ancestry group (and combined across East Asian and European ancestry groups) via fixed-effects meta-analysis using METAL based on inverse-variance weighting. We corrected association *p*-values and standard errors of allelic effects from each ancestry group for residual inflation due to structure between GWAS using the same genomic control adjustments as in the unconditional analyses.

Derivation of approximate Bayes' factors in favour of association. For the multi-ancestry meta-regression, we approximated the Bayes' factor for the jth SNV at the ith distinct association signal by

$$\Lambda_{ij} = \exp\left[\frac{D_{ij} - 4\ln K_{ij}}{2}\right],$$

where D_{ij} is the deviance across K_{ij} contributing GWAS[5].

For the European ancestry-specific meta-analysis and combined East Asian and European ancestry meta-analysis, we approximated the Bayes' factor for the jth SNV at the ith distinct association signal by

$$\Lambda_{ij} = \exp\left[\frac{D_{ij} - \ln K_{ij}}{2}\right],$$

where $D_{ij} = b_{ij}^2 / v_{ij}$, and b_{ij} and v_{ij} are the allelic log-OR and corresponding variance, respectively, across K_{ij} contributing GWAS.

Assessment of fine-mapping resolution in "down-sampled" multi-ancestry meta-regression. We selected GWAS contributing to the multi-ancestry meta-regression to approximate the effective sample size of the European ancestry-specific meta-analysis and maintain the distribution of effective sample size across ancestry groups (**Supplementary Table 10**). The selected GWAS were: African ancestry BIOME (AFR 2), CARDIA, CHS, EMERGE, GENOA (AFR), GERA (AFR), REGARDS, WHI (AFR); East Asian ancestry BBJ (1), CAGE-KING (2), CKB-12, CKB-16, CKB-58, CKB-68, CKB-78, CKB-88, KBA (2), SCES (2), SCHS; European ancestry BIOME (EUR), DECODE, DGI, EPIC-INTERACT (2), FHS, FUSION, GCKD, GENOA (EUR), GERA (EUR), GODARTS, GOMAP, KORA, METSIM, MGI, NUGENE, PIVUS, PROSPER, RS (1), UCPH, ULSAM; Hispanic ancestry BIOME (HIS), HCHS/SOL, MACAD, MC (1), MC (2), MESA (HIS); South Asian EPIDREAM, GRCCDS, INDICO, INTERHEART (2), LOLIPOP (1), LOLIPOP (2), LOLIPOP (4), PROMIS (1).

We conducted a "down-sampled" multi-ancestry meta-regression, implemented in the MR-MEGA software[5], for the selected studies. For each SNV, we modelled allelic log-ORs across GWAS in a linear regression framework, weighted by the inverse of the variance of the effect estimates, incorporating the same three axes of genetic variation as covariates (**Extended Data Figure 2**). We corrected the meta-regression association *p*-values for inflation due to residual structure between the selected GWAS using genomic control adjustment (allowing for four degrees of freedom): λ_{TA*} = 1.012.

For each locus with more than one distinct association signal in the complete multi-ancestry meta-regression, we used GCTA in each GWAS, removing each SNV, in turn, from the conditional set, and adjusting for the remainder, using the "--cojo-cond" option (as described above). Allelic log-ORs from the approximate conditional analyses across GWAS were modelled in the multi-ancestry meta-regression framework, incorporating the three axes of genetic variation as covariates, and weighted by the inverse of the variance of the effect estimates. The meta-regression association *p*-values were corrected for inflation due to residual structure between GWAS by using the same genomic control adjustment as in the unconditional analysis (λ_{TA*} = 1.012).

Within each locus, we approximated the Bayes' factor[6], Λ_{ij}, in favour of T2D association of the jth SNV at the ith distinct association signal on the basis of summary statistics from the down-sampled multi-ancestry meta-regression. For loci with a single association signal, the association summary statistics were obtained from unconditional analysis. For loci with multiple distinct association signals, the association summary statistics were obtained from the approximate conditional analyses. The posterior probability for the jth SNV at the ith distinct signal, was then given by $\pi_{ij} \propto \Lambda_{ij}$, where

$$\Lambda_{ij} = \exp\left[\frac{D_{ij} - 4\ln K_{ij}}{2}\right],$$

and D_{ij} is the deviance across K_{ij} contributing GWAS[5]. We derived a 99% credible set[7] for the ith distinct association signal by: (i) ranking all SNVs according to their posterior probability π_{ij}; and (ii) including ranked SNVs until their cumulative posterior probability attains or exceeds 0.99.

Enrichment of distinct T2D association signals in genomic annotations. We tested for enrichment of distinct T2D association signals from the multi-ancestry meta-regression (as measured by the approximate Bayes' factor) that map to genomic annotations using fGWAS[8] with the region-based input format (-fine). We first considered each annotation separately and identified those with significant enrichment (p<0.00023, Bonferroni correction for 220 annotations), which we refer to as the "enriched set". We then used an iterative approach to identify a joint model of enriched annotations. At each iteration, we added the annotation from the enriched set to the joint model that maximised the improvement in the penalised likelihood. We continued until no additional annotations improved the fit of the joint model at nominal significance (p<0.05). We next used the cross-validation likelihood because the significance of parameter estimates from the penalised likelihood cannot be assessed using standard statistical approaches. For the selected joint model, we identified the penalty that maximised the cross-validation likelihood. Finally, we dropped any annotations from the joint model that resulted in a decrease in the cross-validation likelihood.

Transferability of multi-ancestry GRS across ancestry groups. We selected two studies per ancestry group as test GWAS, prioritising those with larger effective sample sizes and greater genetic diversity: DDS/DCC, WHI (AFR), KBA, SIMES, EPIC-INTERACT (2), UKBB, HCHS/SOL, MC, PROMIS and RHS. We repeated the multi-ancestry meta-regression, after excluding the ten test GWAS, incorporating the same three axes of genetic variation as covariates to account for ancestry. The association p-values from this "reduced" meta-regression were then corrected for inflation due to residual structure between GWAS by means of genomic control adjustment (allowing for four degrees of freedom): λ_{TA} = 1.037. SNVs reported in ≥50% of the total effective sample size of the "reduced" meta-regression (N_{TE}≥179,074) were included in downstream analyses. We identified loci attaining genome-wide significant evidence of association (p<5x10^{-9}) in the "reduced" meta-regression, and the lead SNV for each locus was selected as the variant with minimum association p-value.

For each test GWAS, we next estimated population-specific "predicted" allelic effects for each lead SNV to be used as weights in the GRS. For the ith study, we estimated the allelic effect of the jth SNV by

$$\hat{b}_{TAij} = \alpha_{TA0j} + \sum_k \alpha_{TAkj} x_{ki},$$

where x_{ki} is the position of the ith study on the kth axis of genetic variation from the "complete" multi-ancestry meta-regression, and α_{TA0j} and α_{TAkj} denote the intercept and effect of the kth axis of genetic variation for the SNV from the "reduced" multi-ancestry meta-regression. For each test GWAS, we then regressed the observed allelic effect estimates at lead SNVs, weighted by their corresponding variances, on the "predicted" allelic effect estimates, as implemented in grs.summary function[9] of the gtx package in R. We estimated the OR per unit of the weighted GRS and the corresponding percentage of T2D variance explained, measured by pseudo R^2.

Transferability of ancestry-specific GRS across ancestry groups. We selected two studies per ancestry group as test GWAS. We repeated each of the ancestry-specific fixed-effects meta-analyses after excluding the ten test GWAS. We aggregated association summary statistics across GWAS from the same ancestry group via fixed-effects meta-analysis using METAL[4] based on inverse-variance weighting of allelic log-OR to obtain effect size estimates. We corrected association *p*-values for residual inflation due to structure between GWAS by genomic control adjustment: African λ_{AFR} = 1.049; East Asian λ_{EAS} = 1.092; European λ_{EUR} = 1.180; Hispanic λ_{HIS} = 1.004; South Asian λ_{SAS} = 0.974 (no correction made). SNVs reported in ≥50% of the total effective sample size of the "reduced" ancestry-specific meta-analyses were included in downstream analyses: African N_{AFR}≥11,613; East Asian N_{EAS}≥57,129; European N_{EUR}≥85,062; Hispanic N_{HIS}≥9,480; South Asian N_{SAS}≥15,789. We identified loci attaining genome-wide significant evidence of association (p<5x10^{-8}) in each of the "reduced" ancestry-specific meta-analyses, and the lead SNV for each locus was selected as the variant with minimum association *p*-value. For each test GWAS, we then regressed the observed allelic effect estimates at lead SNVs, weighted by their corresponding variances, on the allelic effect estimates from the each of the ancestry-specific meta-analyses, as implemented in grs.summary function[9] of the gtx package in R, and estimated the OR per unit of the weighted GRS and the corresponding percentage of T2D variance explained, measured by pseudo R^2.

Predictive power of GRS in FinnGen. Individuals from FinnGen were genotyped with Illumina and Affymetrix arrays. After quality control, individuals were imputed with Beagle 4[10] up to the Finnish population-specific reference panel (SISu version 3), comprising 3,775 whole genome sequences (www.sisuproject.fi). We excluded individuals due to non-Finnish ancestry, relatedness, or missing age and/or sex. We estimated the positions of FinnGen on the three axes of genetic variation from the multi-ancestry meta-regression as the mean of the two Finnish studies, FUSION and METSIM (**Supplementary Tables 1 and 2**), which we denoted x_1, x_2 and x_3. We derived Finnish-specific "predicted" allelic effect estimates for each lead SNV from the multi-ancestry meta-regression to be used as weights in the GRS. For the jth SNV, the "predicted" effect was given by

$$\hat{b}_{TAj} = \alpha_{TA0j} + \sum_k \alpha_{TAkj} x_k,$$

where α_{TA0j} and α_{TAkj} denote the intercept and effect of the kth axis of genetic variation for the SNV from the multi-ancestry meta-regression.

For each individual, we calculated the centred GRS from the multi-ancestry meta-regression given by

$$GRS_{TAi} = \sum_{j} (G_{ij} - 2q_j)\, \hat{b}_{TAj}$$

for the ith individual. In this expression, q_j denotes the frequency of the effect allele at the jth SNV, and G_{ij} is the effect allele dosage for the ith individual, which we replaced by $2q_j$ if the genotype was missing. We excluded lead SNVs from the GRS that were not reported in FinnGen. T2D status was defined using two variables: T2D-I and T2D-II. T2D-I included individuals with ICD-10 E11 and/or ICD-9 250*A, but excluded individuals with pancreatitis. T2D-II included individuals with ICD-10 E11, T2D complications, or medicine purchases of Anatomical Therapeutic Chemical (ATC) class A10B (blood glucose lowering drugs, excluding insulins). We defined controls as non-diabetic individuals (type 1, type 2, or undefined). We excluded individuals with missing T2D status or BMI from subsequent analyses, resulting in a total of 18,111 affected individuals and 111,119 unaffected individuals.

In a logistic regression framework, we first fitted a "null" model that included age, sex, genotyping batch, and ten axes of genetic variation to account for population structure. We then fitted models that additionally added BMI only, GRS only, and both BMI and GRS. For each model, we calculated the variance in T2D status explained (pseudo R^2) and the AUROC (calculated with a 10-fold cross-validation). We also conducted age-stratified analyses, after excluding age from the "null" model, within five age groups: under 50 years; 50-60 years; 60-70 years; 70-80 years; and over 80 years. We next considered the subset of individuals in the highest and lowest deciles of the GRS, testing for association of T2D status with an indicator variable of high/low decile in a logistic regression framework after adjustment for age, sex, BMI, genotyping batch, and ten axes of genetic variation. Finally, we considered T2D cases only, and tested for association of age of diagnosis of the disease with GRS in a linear regression framework after adjustment for sex, BMI, genotyping batch, and ten axes of genetic variation.

Selection analyses. We tested for evidence of selection for index SNVs for distinct T2D association signals, which were partitioned into two groups, risk and protective, according to the direction of the allelic effect when aligned to the derived allele. For each population, we excluded index SNVs that were not segregating in that population. We also excluded SNVs with T2D association *p*-value >0.5 for the ancestry group to which the population belongs because allelic effect estimates are close to zero and are imprecise. To test for selection, we sampled 20 variants for each index SNV, selected at random from those with the same derived allele frequency for the population in the 1000 Genomes Project reference panel. We conducted a one-sided Wilcoxon rank-sum test of whether the index SNVs have smaller than expected selection *p*-values, derived by Relate[11], when compared to the rest of the genome. We repeated this test 20 times and reported the mean *p*-value across replicates.

We next tested for selection on a range of traits available in the UK Biobank[12] at the subset of index SNVs for which the derived allele increased risk of T2D. We downloaded association summary statistics from http://www.nealelab.is/uk-biobank, which were derived from 361,194 white British individuals using PHESANT[13]. We considered traits for which the number of significantly associated T2D index SNVs (*p*<0.00015, Bonferroni correction for 338 variants) exceeded ten (**Extended Data Figure 10**). For each population, we then evaluated the evidence for selection for the subset of associated index SNVs for the trait, using the same approach as described above. We also conducted a one-side Wilcoxon rank-sum test of whether the subset of index SNVs had younger age, conditional on derived allele frequency, when compared with the rest of the genome.

1. Spencer, C. C., Su, Z., Donnelly, P. & Marchini, J. Designing genome-wide association studies: sample size, power, imputation, and the choice of genotyping chip. *PLoS Genet.* **5**, e1000477 (2009).
2. Yang, J. et al. Conditional and joint multiple-SNP analysis of GWAS summary statistics identifies additional variants influencing complex traits. *Nat. Genet.* **44**, 369-375 (2012).
3. The 1000 Genomes Project Consortium. A global reference for human genetic variation. *Nature* **526**, 68-74 (2015).
4. Willer, C. J., Li, Y. & Abecasis, G. R. METAL: fast and efficient meta-analysis of genome-wide association scans. *Bioinformatics* **26**, 2190-2191 (2010).
5. Mägi, R. et al. Trans-ethnic meta-regression of genome-wide association studies accounting for ancestry increases power for discovery and improves fine-mapping resolution. *Hum. Mol. Genet.* **26**, 3639-3650 (2017).
6. Kass, R. E. & Raftery, A. E. (1995). Bayes factors. *J. Am. Stat. Assoc.* **90**, 773-795 (1995).
7. Maller, J. B. et al. Bayesian refinement of association signals for 14 loci in 3 common diseases. *Nat. Genet.* **44**, 1294-1301 (2012).
8. Pickrell, J. Joint analysis of functional genomic data and genome-wide association studies of 18 human traits. *Am. J. Hum. Genet.* **94**, 559-573 (2014).
9. Dastani, Z. et al. Novel loci for adiponectin levels and their influence on type 2 diabetes and metabolic traits: a multi-ethnic meta-analysis of 45,891 individuals. *PLoS Genet.* **8**, e1002607 (2012).
10. Browning, S. R. & Browning, B. L. Rapid and accurate haplotype phasing and missing data inference for whole genome association studies by use of localized haplotype clustering. *Am. J. Hum. Genet.* **81**, 1084-1097 (2007).
11. Speidel, L., Forest, M., Shi, S. & Myers, S. R. A method for genome-wide genealogy estimation for thousands of samples. *Nat. Genet.* **51**, 1321-1329 (2019).
12. Bycroft, C. et al. The UK Biobank resource with deep phenotyping and genomic data. *Nature* **562**, 203-209 (2018).
13. Millard, L. A. C., Davies, N. M., Gaunt, T. R., Davey Smith, G. & Tilling, K. PHESANT: a tool for performing automated phenome scans in UK Biobank. *Int. J. Epidemiol.* **47**, 29-35 (2018).

Inserted DNA sequences and primers used for functional experimentation at the *PROX1* locus.

Signal 1
Credible set SNP: rs340874 (chr1:206600992, G)

Primers used for amplification:
Primer_F: TTGTGGGCTAAAGTGCAAGC
Primer_R: GGGTGTATTGAGCGGGGAAA

DNA fragment used for constructs: (>hg19_dna range=chr1:214159081-214159431)
CTATGTGCAATTGACACAAAC**TTGTGGGCTAAAGTGCAAGC**CATTTTTTTCGCGTTTGAATCTTTTTCTCTGTCCCTGAC
TCCTTTCTTCCCCCTACTCCCCCCTCCTCCTTCTCTGCTCTCCGCCCTTTTAAATGTCAAACTGAGCAGATGGTTTTAAGGT
GTGGAAAGGTATATAGCCCTTACTCCTACCAGTTTATTTGTGGGCTGGCGCTAACTTATATGTACAAACCAAGATTCTTA
AAGAAAACTAGTAGGACGAAAAATAAGAAAGAAAGTAGCTTTGATCCATTCTCAGATCCCAAG**TTTCCCCGCTCAATAC**
ACCCGCTTACCTCGAAGGGACCCAACCAAT

Signal 2
Credible set SNP 1: rs17712208 (chr1: 214150445, **T**)
Credible set SNP 2: rs79687284 (chr1:214150821, **G**)

Primers used for amplification:
Primer_F: GGACTTCACTGGCAGACACA
Primer_R: TACTCATTCCCTGGCTTTGC

DNA fragment used for constructs: (>hg19_dna range=chr1:214149600-214151600)
GGAAACACTTAAACCACACTGATTATACAGATTTTTCTCATCTAATGGTA TAATATCTATAACTACATGCATCTGGTAAC
ATACTAAATGCTGTCTAGAACAACAAAGCAAAGCAAACCAAAAGCCCACAATTTAAATTAAAAAAAAAAAAAAGATCTA
AGCCCACCTTCGTAAACATGTGCTTCTGTAAGAAGTTAAAAAAAAAAAAAAAAGAAAGAAAAGGAAAAGAAAAAAGAT
CCACCAGAAGTACCAAAATCAAATATTTATTAGTCTTTTAATTTTCTACTTATTTGAAATTCAAAAATAATTTTCATGCTTT
GATAGGAATGTGCGGTTGTTTATCATTTCAAAAGCACTTCTCCTTTTATCACGAATCGAAGAAGAACTAACATTGAGAA
ACAAGGAACCAGAATATTTAGAGATGCTGGGAATAAACTACAAACTAACATGGTCAAGGGAGAGAAAATATGATCCTC
TCAGAAGAATAATGTAACAACAATCAGAGCACATCTGGGATTTGATTCAAACCAACCTGGAACCAGATTGGATCTCCAA
GCTGTTCTGTGTATACACACACACACACACACACACACACACAGACACACACGCTGAGATTTCCAAAAGTGAAATTTCC
AGAAGTTATCCTACAGAGTTAACCCCAGAAA**GGACTTCACTGGCAGACACA**GGCATAACTTTACTCCTTTTGTGATGAC
CCATGAGTGGGGTCTATGGCAGTCTGAATAGATGGGCCTTTCTGTTGAAAGATTCTGCCTAATCCTTCCCACCAAAGCA
GGGTTCTAAAGGTGTCAGCAGGATTTGGCTGACTGGATCGTTAATGGAGCTATGG**T**TAATTATTGACTGATTAGGGATT
TACCTTATCTTTCCGTCAGGAGCTGGCTCAAGACTTAACGGTAAGCAATTTAGAGCCAGGGTGAACCTACACACATGCC
TTTTTCTTCTTTTCCTTTGGGTCACTTTAGCTTGCCCCTCCCCATAATTCACATTCAGGACAGAATGGCCAGTCCTTACAA
GGCGTGGGAGTCCTCAAGAGCACCGAAAATGAGAGGGGCCAGGTCCACGTGACAAGTGTCCAGAGACAGAGGCTTA
GAGAAATGTGCCTTTTGCAAAACAGTGTTTATGTGTAAAGGTTTTCCAGTTAAGTCCCTGGGAGAAAAAAAAAAAAAA
GCACTTGCTTTTTGTCTCTAAAAGGTCTGGTGATGCCC**G**TGGGTGAGAATCCACCCCGCACTCCCCAAGGCCCCTTG**GC**
AAAGCCAGGGAATGAGTACAGGCAGCTCAGGCCCAGCTGCCCCAGATAAGAGGTGGCCCGTGTTAATGCACAGGCTT
CCTCTGCACCTCAGCAGGGCCTTCCTTTTCTAAACAGTCTCCCTTTAATGTTGGCGAATGTTGTTTTTCCATTGACTCAAC
ATCTCGCCTGGTGGTAAGCCAGTGAGGAAAGTTGCAGCGGGGGAGGGGGAAAGTGGGAGAGAGTGATGCCAAAGCA
AAAGAGCGGGACGGTCAGCCAGGTTTCCAAACAAGCTAGACACCTGCTTTGGAAAGACAGTGACCAAGCCTAGACTTC
TGGCTTCCTCTTCACTTTGATCAGCCTTTTGTTCCCTGCGGGTCTGTGATGGGCTCCCTGCCCCTCCCCTCACCACTGCCC
CCTTCACTGGGAGCTACTTCAACTTAGAAACCATCAAAAAATTCATAGCTTTTCTCTATGAATGTAACTGTCTTATCTGAA
GAAAAGGGAAAACAGTTATTGGAATGCATGAAAGAAGAGAAAGGAATTCTAAGGAAGAGAAGATGGAAGGAAAGTA
AGTGAGAAGAGGAAAATTGGAGAGAAAAATAAAGAAAGG
GGAAAAGAGAATAGAGGAATAGAAATTAAAGGCAAAAAGAAAAGAATAAAAGGATAGAACAAAAAATAAAGAAAAG
GGAGGAGGGCAAAGGAGAAGGACGGCAGAAAAGTGAAATCCAAAAAGGGAGCTTTTCTCCCAGAAGCTCAGTTTC

Acknowledgements and Funding

Anti-aging study cohort (AASC) is supported by the Grant-in-Aid for Scientific Research (20018020, 19659163, 20390185, 23659382, 24390084, 23659352, 25293141, 26670313, 17H04123) from the Ministry of Education, Culture, Sports, Science and Technology of Japan, research grant from the Japan Atherosclerosis Prevention Found, National Cardiovascular Research Grants, and Research Promotion Award from Ehime University.

Atherosclerosis Risk in Communities (ARIC) study has been funded in whole or in part with Federal funds from the National Heart, Lung, and Blood Institute, National Institutes of Health, Department of Health and Human Services (contract numbers HHSN268201700001I, HHSN268201700002I, HHSN268201700003I, HHSN268201700004I and HHSN268201700005I), R01HL087641, R01HL059367 and R01HL086694; National Human Genome Research Institute contract U01HG004402; and National Institutes of Health contract HHSN268200625226C. The authors thank the staff and participants of the ARIC study for their important contributions. Infrastructure was partly supported by Grant Number UL1RR025005, a component of the National Institutes of Health and NIH Roadmap for Medical Research.

Biobank Japan (BBJ) acknowledges all the staff, as well as the doctors and staff of the contributing hospitals for their outstanding work on collecting samples and clinical information, and thanks all the patients participating in this project. This research was supported by the Tailor-Made Medical Treatment Program (the BioBank Japan Project) of the Ministry of Education, Culture, Sports, Science, and Technology (MEXT) and the Japan Agency for Medical Research and Development (AMED). This research was also supported by the Advanced Genome Research and Bioinformatics Study to Facilitate Medical Innovation (GRIFIN) in the Platform Program for Promotion of Genome Medicine (P3GM) of AMED (JP18km0405202).

Beijing Eye Study (BES) was supported by National Natural Science Foundation of China (grant 81570835).

BioMe Biobank (BIOME) is supported by The Andrea and Charles Bronfman Philanthropies and in part by funding of the NIH (U01HG007417; R56HG010297; X01HL134588). BIOME thanks all participants in the Mount Sinai Biobank, and also thanks all the recruiters who have assisted and continue to assist in data collection and management. BIOME is grateful for the computational resources and staff expertise provided by Scientific Computing at the Icahn School of Medicine at Mount Sinai.

Bangladesh Population Cohort (BPC) was supported by US National Institute of Environmental Health Sciences Grants P42 ES10349 and P30 ES09089.

Cardiometabolic Genome Epidemiology (CAGE-AMAGASKI and CAKE-GWAS) was supported by grants for the Core Research for Evolutional Science and Technology (CREST) from the Japan Science Technology Agency; KAKENHI (Grant-in-Aid for Scientific Research) from the Ministry of Education, Culture, Sports, Science and Technology of Japan; and the Grant and research budget of National Center for Global Health and Medicine (NCGM).

CAGE-AMAGASKI thanks Drs. Toshio Ogihara, Yukio Yamori, Akihiro Fujioka, Chikanori Makibayashi, Sekiharu Katsuya, Ken Sugimoto, Kei Kamide, and Ryuichi Morishita and the many physicians of the participating hospitals and medical institutions in Amagasaki Medical Association for their assistance in collecting the DNA samples and accompanying clinical information.

Cardiometabolic Genome Epidemiology (CAGE-KING) was supported in part by Grants-in-Aid from MEXT (nos. 24390169, 16H05250, 15K19242, 16H06277) as well as by a grant from the Funding Program for Next-Generation World-Leading Researchers (NEXT Program, no. LS056).

Coronary Artery Risk Development in Young Adults (CARDIA) was conducted and supported by the National Heart, Lung, and Blood Institute (NHLBI) in collaboration with the University of Alabama at Birmingham (HHSN268201800005I & HHSN268201800007I), Northwestern University (HHSN268201800003I), University of Minnesota (HHSN268201800006I), and Kaiser Foundation Research Institute (HHSN268201800004I). CARDIA was also partially supported by the Intramural Research Program of the National Institute on Aging (NIA) and an intra-agency agreement between NIA and NHLBI (AG0005). Genotyping was funded as part of the NHLBI Candidate-gene Association Resource (N01-HC-65226) and the NHGRI Gene Environment Association Studies (GENEVA) (U01-HG004729, U01-HG04424, and U01-HG004446).

Cleveland Family Study (CFS) is supported by grants to Case Western Reserve University (NIH HL 46380, M01RR00080) and Brigham and Women's Hospital (K01-HL135405-01, R01-HL113338-04, R35-HL135818-01, 5-R01-HL046380-15 and 5-KL2-RR024990-05).

China Health and Nutrition Survey (CHNS) was supported by: the National Institute for Nutrition and Health, the Chinese Center for Disease Control and Prevention; the National Institutes of Health (R01AG065357, R01HD30880, R01HL108427 and R01DK104371); the Fogarty International Center of the National Institutes of Health (TW009077); the China-Japan Friendship Hospital, the Beijing Municipal Center for Disease Prevention and Control, the China National Health Commission (formerly the Chinese Ministry of Health); the Chinese National Human Genome Center at Shanghai; and the Carolina Population Center (P2CHD050924), The University of North Carolina at Chapel Hill.

Cardiovascular Health Study (CHS) was supported by NHLBI contracts HHSN268201200036C, HHSN268200800007C, HHSN268201800001C, N01HC55222, N01HC85079, N01HC85080, N01HC85081, N01HC85082, N01HC85083, N01HC85086, 75N92021D00006; and NHLBI grants U01HL080295, R01HL085251, R01HL087652, R01HL105756, R01HL103612, R01HL120393, and R01HL130114 with additional contribution from the National Institute of Neurological Disorders and Stroke (NINDS). Additional support was provided through R01AG023629 from the National Institute on Aging (NIA). A full list of principal CHS investigators and institutions can be found at CHS-NHLBI.org. The provision of genotyping data was supported in part by the National Center for Advancing Translational Sciences, CTSI grant UL1-TR-001881, and the National Institute of Diabetes and Digestive and Kidney Disease Diabetes Research Center (DRC) grant DK063491 to the Southern California Diabetes Endocrinology Research Center. The content is solely the responsibility of the authors and does not necessarily represent the official views of the National Institutes of Health.

China Kadoorie Biobank (CKB) chiefly acknowledges the participants, project staff, and the China National Centre for Disease Control and Prevention (CDC) and its regional offices. China's National Health Insurance provides electronic linkage to all hospital treatment. Funding sources: Baseline survey and first re-survey - Kadoorie Charitable Foundation, Hong Kong; long-term follow-up - UK Wellcome Trust (212946/Z/18/Z, 202922/Z/16/Z, 104085/Z/14/Z, 088158/Z/09/Z), National Natural Science Foundation of China (91843302), and National Key Research and Development Program of China (2016YFC 0900500, 0900501, 0900504, 1303904); DNA extraction and genotyping – GlaxoSmithKline, and the UK Medical Research Council (MC-PC-13049, MC-PC-14135); core funding for the project to the Clinical Trial Service Unit and Epidemiological Studies Unit at Oxford University - British Heart Foundation (CH/1996001/9454), UK MRC (MC-UU-00017/1, MC-UU-12026/2, MC_U137686851), and Cancer Research UK (C16077/A29186, C500/A16896).

Cebu Longitudinal Health and Nutrition Survey (CLHNS) was supported by: US National Institutes of Health grants DK078150, TW005596 and HL085144; pilot funds from RR020649, ES010126, and DK056350; and the Office of Population Studies Foundation.

Diabetic Cohort and Singapore Prospective Study Program (DC/SP2) was supported by the individual research grant and clinician scientist award schemes from the National Medical Research Council (NMRC) and the Biomedical Research Council (BMRC) of Singapore, Ministry of Health, Singapore, National University of Singapore and National University Health System, Singapore.

Durban Diabetes Study and Durban Diabetes Case Control (DDS/DCC) was supported by: the Wellcome Trust (grant number 098051); the African Partnership for Chronic Disease Research (Medical Research Council UK partnership grant number MR/K013491/1); the National Institute for Health Research Cambridge Biomedical Research Centre (UK); Novo-Nordisk (South Africa); Sanofi-Aventis (South Africa); MSD Pharmaceuticals (Pty) Ltd (Southern Africa); Servier Laboratories (South Africa); South African Sugar Association; and the Victor Daitz Foundation.

deCODE genetics (DECODE) thank the participants in the deCODE study, the staff at deCODE genetics core facilities and the staff at the Research Service Center for their contribution to this work.

Diabetes Gene Discovery Group (DGDG) was supported by Genome Canada, Génome Québec, the Canada Foundation for Innovation, the French Government ("Agence Nationale de la Recherche"), the French Region of "Nord Pas De Calais" ("Contrat de Projets État-Région"), and the charities: "Association Française des Diabétiques", "Programme National de Recherche sur le Diabète" and "Association de Langue Française pour l'Etude du Diabète et des Maladies Métaboliques". This study was also supported in part by a grant from the European Union (Integrated Project EuroDia LSHM-CT-2006-518153in the Framework Programme 6 [FP6] of the European Community). This work was supported by grants from the French National Research Agency (ANR-10-LABX-46 [European Genomics Institute for

Diabetes] and ANR-10-EQPX-07-01 [LIGAN-PM]). Case and control recruitment was supported by the Fédération Française des Diabetiques, INSERM, CNAMTS, Centre Hospitalier Universitaire Poitiers, La Fondation de France, and the Endocrinology-Diabetology department of the Corbeil-Essonnes Hospital. C. Petit, J.-P. Riveline, and S. Franc were instrumental in recruitment and S. Brunet, F. Bacot, R. Frechette, V. Catudal, M. Deweirder, F. Allegaert, P. Laflamme, P. Lepage, W. Astle, M. Leboeuf, and S. Leroux provided technical assistance. K. Shazand and N. Foisset provided organizational guidance. The D.E.S.I.R. study, which mostly contributed controls, was supported by CNAMTS, Lilly, Novartis Pharma and Sanofi-Aventis, by INSERM ("Réseaux en Santé Publique, Interactions entre les déterminants de la santé"), by "Association Diabète Risque Vasculaire", "Fédération Française de Cardiologie", "Fondation de France", ALFEDIAM, ONIVINS, Ardix Medical, Bayer Diagnostics, Becton Dickinson, Cardionics, Merck Santé, Novo Nordisk, Pierre Fabre, Roche, Topcon. The D.E.S.I.R. Study Group: INSERM U780: B. Balkau, P. Ducimetière, E. Eschwège; INSERM U367: F. Alhenc-Gelas; CHU D'Angers: Y. Gallois, A. Girault; Bichat Hospital: F. Fumeron, M. Marre; Medical Examination Services: Alençon, Angers, Caen, Chateauroux, Cholet, Le Mans, and Tours; Research Institute for General Medicine: J. Cogneau; General practitioners of the region; Cross-Regional Institute for Health: C. Born, E. Caces, M. Cailleau, J. G. Moreau, F. Rakotozafy, J. Tichet, S. Vol. DGDG thank M. Deweider and F. Allegaert for the DNA bank management and are sincerely indebted to all study participants.

Diabetes Genetics Initiative (DGI) was supported by the Novartis Institute for BioMedical Research with additional support from The Richard and Susan Smith Family Foundation and American Diabetes Association Pinnacle Program Project Award. The Botnia Study (study subject cohort) was financially supported by the Folkhalsan Research Foundation, the Sigrid Juselius Foundation, Nordic Center of Excellence in Disease Genetics, EU (EXGENESIS), The Academy of Finland, University of Helsinki, Finnish Diabetes Research Foundation, Foundation for Life and Health in Finland, Finnish Medical Society, Helsinki University Central Hospital Research Foundation, Perklén Foundation, Ollqvist Foundation, Närpes Health Care Foundation, Municipal Heath Care Center and Hospital in Jakobstad and Health Care Centers in Vasa, Närpes and Korsholm. The work in Malmö, Sweden, was also funded by a Linné grant from the Swedish Research Council (349-2006-237). The contribution of the Botnia and Skara research teams is gratefully acknowledged.

Estonian Genome Center of the University of Tartu (EGCUT) was funded by the Estonian Research Council Grant IUT20-60, IUT24-6, PRG687, and the European Union through the European Regional Development Fund Project No. 2014-2020.4.01.15-0012 GENTRANSMED.

Electronic Medical Records and Genomics Network (EMERGE) was initiated and funded by NHGRI through the following grants: U01HG006828 (Cincinnati Children's Hospital Medical Center/Boston Children's Hospital); U01HG006830 (Children's Hospital of Philadelphia); U01HG006389 (Essentia Institute of Rural Health, Marshfield Clinic Research Foundation and Pennsylvania State University); U01HG006382 (Geisinger Clinic); U01HG006375 (Group Health Cooperative/University of Washington); U01HG006379 (Mayo Clinic); U01HG006380 (Icahn School of Medicine at Mount Sinai); U01HG006388 (Northwestern University); U01HG006378 (Vanderbilt University Medical Center); and U01HG006385 (Vanderbilt University Medical Center serving as the Coordinating Center). The Northwestern University

Enterprise Data Warehouse was funded in part by a grant from the National Center for Research Resources, UL1RR025741. Part of the dataset(s) used for the analyses described were obtained from Vanderbilt University Medical Center's BioVU which is supported by institutional funding and by the Vanderbilt CTSA grant UL1 TR000445 from NCATS/NIH. The eMERGE imputed merged Phase I and Phase II dataset was generated by genotyping centers CIDR (U01HG004438) and the Broad Institute (U01HG004424).

European Prospective Investigation into Cancer and Nutrition (EPIC-INTERACT) project (LSHM-CT-2006-037197) is a European-Community funded project under Framework Programme 6. EPIC-INTERACT thank all EPIC participants and staff for their contribution to the study. EPIC-INTERACT thank Nicola Kerrison (MRC Epidemiology Unit, Cambridge) for managing the data for the InterAct Project and staff from the Laboratory Team, Field Epidemiology Team, and Data Functional Group of the MRC Epidemiology Unit in Cambridge, UK, for carrying out sample preparation, DNA provision and quality control, genotyping, and data-handling work. The funders had no role in study design, data collection and analysis, decision to publish, or preparation of the manuscript. GWAS summary statistics from the EPIC-InterAct study are available to download from the Dryad Digital Repository (https://doi.org/10.5061/dryad.qnk98sfcg).

Epidemiologic Study of the Screenees for Diabetes Reduction Assessment with Ramipril and Rosiglitazone Medication (EPIDREAM) was funded by a grant from the Canadian Institutes of Health Research University Industry competition with partner funding from the GlaxoSmithKline and Sanofi Aventis Global, Sanofi Aventis Canada, Genome Quebec Innovation Centre, Heart and Stroke Foundation of Canada.

Family Heart Study (FAMHS) was supported by NIH grants R01-HL-087700 and R01-HL-088215 from NHLBI, and R01-DK-089256 and R01-DK-075681 from NIDDK.

Framingham Heart Study (FHS) was conducted and supported by the National Heart, Lung and Blood Institute (NHLBI) in collaboration with Boston University (contracts 75N92019D00031, HHSN268201500001I and N01-HC-25195), and its contract with Affymetrix, Inc for genotyping services (contract number N02-HL-6-4278). The analyses reflect intellectual input and resource development from the Framingham Heart Study investigators participating in the SNP Health Association Resource (SHARe) project. FHS was also supported by: NHLBI R01 HL105756, National Institute for Diabetes and Digestive and Kidney Diseases (NIDDK) R01 DK078616, U01 DK078616, NIDDK K24 DK080140 and American Diabetes Association Mentor-Based Postdoctoral Fellowship Award #7-09-MN-32 (to J.B.M.); and NIDDK K24 DK110550 (to J.C.F.).

Finland-United States Investigation of NIDDM Genetics (FUSION) was supported by DK093757, DK072193, DK062370, and ZIA-HG000024.

German Chronic Kidney Disease (GCKD) was funded by the German Ministry of Research and Education (Bundesminsterium für Bildung und Forschung, BMBF) and by the Foundation KfH Stiftung Präventivmedizin. Unregistered grants to support the study were provided by Bayer, Fresenius Medical Care and Amgen. Genotyping was supported by Bayer AG.

Genetic Study of Atherosclerosis Risk (GENESTAR) was supported by NIH grants through the National Heart, Lung, and Blood Institute (HL49762, HL58625, HL59684, HL071025, U01HL72518, and HL087698) and the National Institute of Nursing Research (NR0224103) and by M01-RR000052 to the Johns Hopkins General Clinical Research Center.

Genetic Epidemiology Network of Arteriosclerosis (GENOA) was supported by the National Institutes of Health grant numbers HL054457, HL054464, HL054481, HL087660 and HL119443 from the National Heart, Lung, and Blood Institute. Genotyping was performed at the Mayo Clinic by Stephen Turner, Mariza de Andrade, and Julie Cunningham. GENOA thanks Eric Boerwinkle and Megan Grove from the Human Genetics Center and Institute of Molecular Medicine and Division of Epidemiology, University of Texas Health Science Center, Houston, Texas, USA for their help with genotyping. GENOA also thanks the families that participated in the study.

Resource for Genetic Epidemiology on Adult Heath and Aging (GERA) was supported by a grant (RC2 AG033067; PIs Schaefer and Risch) awarded to the Kaiser Permanente Research Program on Genes, Environment, and Health (RPGEH) and the UCSF Institute for Human Genetics. The RPGEH was supported by grants from the Robert Wood Johnson Foundation, the Wayne and Gladys Valley Foundation, the Ellison Medical Foundation, Kaiser Permanente Northern California, and the Kaiser Permanente National and Northern California Community Benefit Programs.

Genetics of Diabetes and Audit Research in Tayside Scotland (GODARTS) was funded by The Wellcome Trust Study Cohort Functional Genomics Grant (2004-2008, 072960/Z/03/Z) and The Wellcome Trust Scottish Health Informatics Programme (SHIP, 2009-2012, 086113/Z/08/Z).

Genetics of Latinos Diabetic Retinopathy (GOLDR) was supported by grants EY14684 and UL1TR000124.

Genetic Overlap Between Metabolic and Psychiatric Traits and Teens of Attica: Genes and Environment (GOMAP-TEENAGE) was funded by the Wellcome Trust (098051) and was also co-financed by the European Union (European Social Fund - ESF) and Greek national funds through the Operational Program "Education and Lifelong Learning" of the National Strategic Reference Framework (NSRF) - Research Funding Program: Heracleitus II. GOMAP-TEENAGE thanks all study participants and their families, as well as all volunteers for their contribution in this study. GOMAP-TEENAGE is grateful to: Georgia Markou, Laiko General Hospital Diabetes Centre; Maria Emetsidou and Panagiota Fotinopoulou, Hippokratio General Hospital Diabetes Centre; Athina Karabela, Dafni Psychiatric Hospital; Eirini Glezou and Marios Mangioros, Dromokaiteio Psychiatric Hospital; Angela Rentari, Harokopio University of Athens; and Danielle Walker, Wellcome Trust Sanger Institute. GOMAP-TEENAGE thanks the Sample Management and Genotyping Facilities staff at the Wellcome Trust Sanger Institute for sample preparation, quality control and genotyping.

Genomic Research Cohort for CCMB Diabetes Study (GRCCDS) comprises of various cohorts that are supported by: Council of Scientific Industrial Research (CSIR); Ministry of Science and Technology, Govt. of India, India; and Wellcome Trust, London, UK. GRCCDS is grateful to the patients and subjects who voluntarily participated in the study, and thankfully acknowledge other researchers who have supported the study.

Health, Aging and Body Composition Study (HABC) was supported by NIA contracts N01AG62101, N01AG62103, and N01AG62106. The genome-wide association study was funded by NIA grant 1R01AG032098-01A1 to Wake Forest University Health Sciences and genotyping services were provided by the Center for Inherited Disease Research (CIDR). CIDR is fully funded through a federal contract from the National Institutes of Health to The Johns Hopkins University, contract number HHSN268200782096C. This research was supported in part by the Intramural Research Program of the NIH, National Institute on Aging.

Healthy Aging in Neighborhoods of Diversity Across the Life Span Study (HANDLS) was supported by the Intramural Research Program of the NIH, National Institute on Aging (project Z01-AG000513 and human subjects protocol 09 AGN248). Data analyses for HANDLS utilized the high-performance computational resources of the Biowulf Linux cluster at the National Institutes of Health, Bethesda, MD (http://hpc.nih.gov).

Hispanic Community Health Study/Study of Latinos (HCHS/SOL) is a collaborative study supported by contracts from the National Heart, Lung, and Blood Institute (NHLBI) to the University of North Carolina (HHSN268201300001I / N01-HC-65233), University of Miami (HHSN268201300004I / N01-HC-65234), Albert Einstein College of Medicine (HHSN268201300002I / N01-HC-65235), University of Illinois at Chicago (HHSN268201300003I / N01-HC-65236 Northwestern Univ), and San Diego State University (HHSN268201300005I / N01-HC-65237). The following Institutes/Centers/Offices have contributed to the HCHS/SOL through a transfer of funds to the NHLBI: National Institute on Minority Health and Health Disparities, National Institute on Deafness and Other Communication Disorders, National Institute of Dental and Craniofacial Research, National Institute of Diabetes and Digestive and Kidney Diseases, National Institute of Neurological Disorders and Stroke, NIH Institution-Office of Dietary Supplements. The Genetic Analysis Center at the University of Washington was supported by NHLBI and NIDCR contracts (HHSN268201300005C AM03 and MOD03). The authors thank the staff and participants of HCHS/SOL for their important contributions.

Hong Kong Diabetes Registry (HKDR) acknowledge support from the Theme-based Research Scheme from the Research Grants Council of the Hong Kong Special Administrative Region, China (Project no: T12-402/13-N), the Research Grants Council Research Impact Fund (R4012-18), the Hong Kong Foundation for Research and Development in Diabetes, the Vice-Chancellor One-off Discretionary Fund, the Focused Innovations Scheme, the Postdoctoral Fellowship Scheme of the Chinese University of Hong Kong, and the Croucher Foundation Senior Medical Research Fellowship.

Health Professionals' Follow-Up Study (HPFS) and Nurses Health Study (NHS) acknowledge assistance with data cleaning that was provided by the National Center for Biotechnology Information. Support for collection of datasets and samples was provided by the Collaborative Study on the Genetics of Alcoholism (COGA; U10 AA008401), the Collaborative Genetic Study of Nicotine Dependence (COGEND; P01 CA089392), and the Family Study of

Cocaine Dependence (FSCD; R01 DA013423). Funding support for genotyping, which was performed at the Johns Hopkins University Center for Inherited Disease Research, was provided by the NIH GEI (U01HG004438), the National Institute on Alcohol Abuse and Alcoholism, the National Institute on Drug Abuse, and the NIH contract "High throughput genotyping for studying the genetic contributions to human disease" (HHSN268200782096C). The datasets used for the analyses described in this manuscript were obtained from dbGaP at http://www.ncbi.nlm.nih.gov/projects/gap/cgi-bin/study.cgi?study_id=phs000091.v1.p1 through dbGaP accession number phs000091.v1.p.

Mexican American Hypertension and Insulin Resistance (HTNIR) was supported by grant HL0597974.

Howard University Family Study (HUFS) was supported by National Institutes of Health grants S06GM008016-320107 to CNR and S06GM008016-380111 to AA. Participant enrollment was carried out at the Howard University General Clinical Research Center, supported by National Institutes of Health grant 2M01RR010284. Genotyping support was provided by the Coriell Institute for Medical Research. This research was supported by the Intramural Research Program of the Center for Research on Genomics and Global Health (CRGGH). The CRGGH is supported by the National Human Genome Research Institute, the National Institute of Diabetes and Digestive and Kidney Diseases, the Center for Information Technology, and the Office of the Director at the National Institutes of Health (Z01HG200362).

Indian Diabetes Consortium (INDICO) was majorly supported by Council of Scientific and Industrial Research (CSIR), Government of India through CARDIOMED project Grant Number: BSC0122 provided to CSIR-Institute of Genomics and Integrative Biology. INDICO was also partially funded by Department of Science and Technology-PURSE-II (DST/SR/PURSE II/11) given to Jawaharlal Nehru University. INDICO are very much thankful to all the volunteers who have participated in the study.

INTERHEART (INTERHEART) was funded by: the Canadian Institutes of Health Research, the Heart and Stroke Foundation of Ontario, and the International Clinical Epidemiology Network (INCLEN); unrestricted grants from several pharmaceutical companies (with major contributions from AstraZeneca, Novartis, Hoechst Marion Roussel [now Aventis], Knoll Pharmaceuticals [now Abbott], Bristol-Myers Squibb, King Pharma, and Sanofi-Synthelabo); and various national bodies in different countries (see Online Appendix at http://image.thelancet.com/extras/04art8001webappendix2.pdf). Funding sources had no involvement in the study design; in the collection, analysis, and interpretation of data; or the writing of the manuscript.

Jackson Heart Study (JHS) is supported and conducted in collaboration with Jackson State University (HHSN268201800013I), Tougaloo College (HHSN268201800014I), the Mississippi State Department of Health (HHSN268201800015I) and the University of Mississippi Medical Center (HHSN268201800010I, HHSN268201800011I and HHSN268201800012I) contracts from the National Heart, Lung, and Blood Institute (NHLBI) and the National Institute on Minority Health and Health Disparities (NIMHD). The authors also wish to thank the staff and participants of the JHS.

Korean Association Resource (KARE) was supported by grants from Korea Centers for Disease Control and Prevention (4845–301, 4851–302, 4851–307) and intramural grants from the Korea National Institute of Health (2016-NI73001-00, 2019-NG-053-00). KARE was performed with bioresources from National Biobank of Korea, the Centers for Disease Control and Prevention, Republic of Korea.

Korean Biobank Array from the Korean Genome and Epidemiology (KoGES) Consortium (KBA) was supported by grants from Korea Centers for Disease Control and Prevention (4845–301, 4851–302, 4851–307) and intramural grants from the Korea National Institute of Health (2016-NI73001-00, 2019-NG-053-00). KBA was performed with bioresources from National Biobank of Korea, the Centers for Disease Control and Prevention, Republic of Korea. Genotype data were provided by the Collaborative Genome Program for Fostering New Post-Genome Industry (3000-3031b).

Collaborative Health Research in the Region of Augsburg (KORA) research platform was initiated and financed by the Helmholtz Zentrum München – German Research Center for Environmental Health, which is funded by the German Federal Ministry of Education and Research and by the State of Bavaria. Furthermore, KORA research was supported within the Munich Center of Health Sciences (MC Health), Ludwig-Maximilians-Universität, as part of LMUinnovativ and by the German Center for Diabetes Research (DZD).

Los Angeles Latino Eye Study (LALES) acknowledges funding from NEI grant U10EY011753.

London Life Sciences Prospective Population (LOLIPOP) is supported by the National Institute for Health Research (NIHR) Comprehensive Biomedical Research Centre Imperial College Healthcare NHS Trust, the British Heart Foundation (SP/04/002), the Medical Research Council (G0601966, G0700931), the Wellcome Trust (084723/Z/08/Z, 090532 & 098381) the NIHR (RP-PG-0407-10371), the NIHR Official Development Assistance (ODA, award 16/136/68), the European Union FP7 (EpiMigrant, 279143) and H2020 programs (iHealth-T2D, 643774). LOLIPOP acknowledges support of the MRC-PHE Centre for Environment and Health, and the NIHR Health Protection Research Unit on Health Impact of Environmental Hazards. The work was carried out in part at the NIHR/Wellcome Trust Imperial Clinical Research Facility. The views expressed are those of the author(s) and not necessarily those of the Imperial College Healthcare NHS Trust, the NHS, the NIHR or the Department of Health. LOLIPOP thanks the participants and research staff who made the study possible.

Mexican American Study of Coronary Artery Disease (MACAD) was supported by grant HL088457.

Mexico City (MC) was supported, in Mexico, by the Fondo Sectorial de Investigación en Salud y Seguridad Social (SSA/IMSS/ISSSTECONACYT, project 150352), Temas Prioritarios de Salud Instituto Mexicano del Seguro Social (2014-FIS/IMSS/PROT/PRIO/14/34), and the Fundación IMSS. MC thanks Jaime Gómez Zamudio and Araceli Méndez Padrón for technical support. In Canada, computations were performed on the GPC supercomputer at the SciNet HPC Consortium. SciNet is funded by: the Canada Foundation for Innovation under the auspices of Compute Canada; the Government of Ontario; Ontario Research Fund - Research Excellence; and the University of Toronto.

Multi-Ethnic Study of Atherosclerosis (MESA) and the MESA SHARe projects are conducted and supported by the National Heart, Lung, and Blood Institute (NHLBI) in collaboration with MESA investigators. Support for MESA is provided by contracts 75N92020D00001, HHSN268201500003I, N01-HC-95159, 75N92020D00005, N01-HC-95160, 75N92020D00002, N01-HC-95161, 75N92020D00003, N01-HC-95162, 75N92020D00006, N01-HC-95163, 75N92020D00004, N01-HC-95164, 75N92020D00007, N01-HC-95165, N01-HC-95166, N01-HC-95167, N01-HC-95168, N01-HC-95169, UL1-TR-000040, UL1-TR-001079, and UL1-TR-001420. Also supported by the National Center for Advancing Translational Sciences, CTSI grant UL1TR001881, and the National Institute of Diabetes and Digestive and Kidney Disease Diabetes Research Center (DRC) grant DK063491 to the Southern California Diabetes Endocrinology Research Center. Funding for SHARe genotyping was provided by NHLBI Contract N02-HL-64278. Genotyping was performed at Affymetrix (Santa Clara, California, USA) and the Broad Institute of Harvard and MIT (Boston, Massachusetts, USA) using the Affymetrix Genome-Wide Human SNP Array 6.0.

Metabolic Syndrome in Men (METSIM) was supported by the Academy of Finland (contract 124243), the Finnish Heart Foundation, the Finnish Diabetes Foundation, Tekes (contract 1510/31/06), and the Commission of the European Community (HEALTH-F2-2007 201681), and the US National Institutes of Health grants DK093757, DK072193, DK062370, and ZIA-HG000024.

Mass General Brigham Biobank (MGB) acknowledges the Partners HealthCare System for support of the MGB biobank and MGB patients for providing samples, genomic data, and health information data, as well as research support by NIDDK K24 DK110550 (to J.C.F.), K24 DK080140 (to J.B.M.) and NIDDK K23DK114551 (to M.S.U).

Michigan Genomics Initiative (MGI) was supported by NIH research grants HL117626 and HG007022. MGI was supported by internal research funds from the University of Michigan School of Public Health, the University of Michigan Medical School, and the University of Michigan President's Office. MGI are especially grateful to the generosity of all research participants.

Nagahama Study (NAGAHAMA) was supported by a university grant, The Center of Innovation Program, The Global University Project, and a Grant-in-Aid for Scientific Research (25293141, 26670313, 26293198, 17H04182, 17H04126, 17H04123, 18K18450) from the Ministry of Education, Culture, Sports, Science and Technology of Japan, the Practical Research Project for Rare/Intractable Diseases (ek0109070, ek0109070, ek0109196, ek0109348), the Comprehensive Research on Aging and Health Science Research Grants for Dementia R&D (dk0207006, dk0207027), the Program for an Integrated Database of Clinical and Genomic Information (kk0205008), the Practical Research Project for Life-style-related Diseases including Cardiovascular Diseases and Diabetes Mellitus (ek0210066, ek0210096, ek0210116), and the Research Program for Health Behavior Modification by Utilizing IoT (le0110005) from Japan Agency for Medical Research and Development (AMED); Takeda

Medical Research Foundation, and Mitsubishi Foundation, Daiwa Securities Health Foundation, and Sumitomo Foundation.

Netherlands Epidemiology of Obesity (NEO) thanks all individuals who participated in the study, all participating general practitioners for inviting eligible participants and all research nurses for collection of the data. NEO thank the study group, Pat van Beelen, Petra Noordijk and Ingeborg de Jonge for the coordination, lab and data management of the study. Genotyping was supported by the Centre National de Génotypage (Paris, France), headed by Jean-Francois Deleuze. NEO is supported by the participating Departments, the Division and the Board of Directors of the Leiden University Medical Center, and by the Leiden University, Research Profile Area Vascular and Regenerative Medicine.

NIDDM-Atherosclerosis Study Hispanic Cohorts (NIDDM) was supported by grant HL055798.

Northewestern University Genetics (NUGENE) was funded by the Northwestern University's Center for Genetic Medicine, Northwestern University, and Northwestern Memorial Hospital. Samples and data used in this study were provided by the NUgene Project (www.nugene.org). Assistance with phenotype harmonization was provided by the eMERGE Coordinating Center (Grant number U01HG04603). This study was funded through the NIH, NHGRI eMERGE Network (U01HG004609). Funding support for genotyping, which was performed at The Broad Institute, was provided by the NIH (U01HG004424). Assistance with phenotype harmonization and genotype data cleaning was provided by the eMERGE Administrative Coordinating Center (U01HG004603) and the National Center for Biotechnology Information (NCBI). The datasets used for the analyses described in this manuscript were obtained from dbGaP at http://www.ncbi.nlm.nih.gov/gap through dbGaP accession number phs000237.v1.p1.

Prospective Investigation of the Vasculature in Uppsala Seniors (PIVUS) was supported by Wellcome Trust Grants (WT098017, WT064890, WT090532), Uppsala University, Uppsala University Hospital, the Swedish Research Council and the Swedish Heart-Lung Foundation.

Pakistan Risk of Myocardial Infarction Study (PROMIS) was funded by the Wellcome Trust, UK, and Pfizer (genotyping) and was supported through funds available to investigators at the Center for Non-Communicable Diseases, Pakistan, and the University of Cambridge, UK (fieldwork). Biomarker assays in PROMIS have been funded through grants awarded by the National Institutes of Health (RC2HL101834 and RC1TW008485) and the Fogarty International (RC1TW008485).

Prospective Study of Pravastatin in the Elderly at Risk (PROSPER) was supported by an investigator-initiated grant obtained from Bristol-Myers Squibb. Prof. J.W.J. is an Established Clinical Investigator of the Netherlands Heart Foundation (grant 2001 D 032). Support for genotyping was provided by the seventh framework program of the European commission (grant 223004) and by the Netherlands Genomics Initiative (Netherlands Consortium for Healthy Aging grant 050-060-810).

Sea Islands Genetic Network Reasons for Geographic and Racial Differences in Stroke (REGARDS) is supported by cooperative agreement U01 NS041588 co-funded by the National Institute of Neurological Disorders and Stroke (NINDS) and the National Institute on Aging (NIA), National Institutes of Health, Department of Health and Human Service. The content is solely the responsibility of the authors and does not necessarily represent the official views of the NINDS or the NIA. Additional funding was from R01 DK084350 from the National Institutes of Health.

Ragama Health Study (RHS) was supported by a grant from the National Center for Global Health and Medicine (NCGM).

Rotterdam Study (RS) are grateful to the participants and staff involved in the study, and the participating general practitioners and pharmacists. RS is funded by Erasmus Medical Center and Erasmus University, Rotterdam, Netherlands Organization for the Health Research and Development (ZonMw), the Research Institute for Diseases in the Elderly (RIDE), the Ministry of Education, Culture and Science, the Ministry for Health, Welfare and Sports, the European Commission (DG XII), and the Municipality of Rotterdam.

Shanghai Breast Cancer Study and Shanghai Women's Health Study (SBCS/SWHS) was supported in part by US National Institutes of Health grants R01CA64277 and R01CA124558, as well as Ingram Professorship and Research Reward funds from the Vanderbilt University School of Medicine. We want to thank participants and research staff of the study, Regina Courtney for plasma and DNA sample preparation, and Hui Cai, Ben Zhang and Jing He for data processing and analyses.

Singapore Chinese Eye Study (SCES) is supported by the National Medical Research Council (NMRC), Singapore (grants 0796/2003, 1176/2008, 1149/2008, STaR/0003/2008, 1249/2010, CG/SERI/2010, CIRG/1371/2013, and CIRG/1417/2015), and Biomedical Research Council (BMRC), Singapore (08/1/35/19/550 and 09/1/35/19/616).

Starr County Health (SCH) was supported by grants from the National Institutes of Health (DK073541, DK085501, HL102830 and DK116378) and funds from the State of Texas. SCH thank the field staff in Starr County for their careful collection of these data and are especially grateful to the participants who so graciously cooperated and gave of their time. Starr County Health

Singapore Chinese Health Study (SCHS) was supported by the US National Institutes of Health grants R01DK08072, R01CA144034 and UM1CA182876.

Slim Initiative for Genomic Medicine in the Americas (SIGMA) was partially supported by a joint US-Mexico project funded by the Carlos Slim Health Institute. The UNAM/INCMNSZ Diabetes Study was supported by Consejo Nacional de Ciencia y Tecnología grants 138826, 128877, SALUD 2009-01-115250, and a grant from Dirección General de Asuntos del Personal Académico, UNAM, IT 214711. The Mexico City Diabetes Study was supported by the National Heart, Lung and Blood Institute (ROHL24799), the Consejo Nacional de Ciencia y Tecnología (grants 2099, M9303, F671-M9407, 251M, 2005-CO1-14502 and SALUD 2010-2-15-1165). SIGMA was also supported by funds from the Fundación Carlos Slim (to J.C.F.).

Singapore Malay Eye Study (SIMES) is supported by the National Medical Research Council (NMRC), Singapore (grants 0796/2003, 1176/2008, 1149/2008, STaR/0003/2008, 1249/2010, CG/SERI/2010, CIRG/1371/2013, and CIRG/1417/2015), and Biomedical Research Council (BMRC), Singapore (08/1/35/19/550 and 09/1/35/19/616).

Singapore Indian Eye Study (SINDI) is supported by the National Medical Research Council (NMRC), Singapore (grants 0796/2003, 1176/2008, 1149/2008, STaR/0003/2008, 1249/2010, CG/SERI/2010, CIRG/1371/2013, and CIRG/1417/2015), and Biomedical Research Council (BMRC), Singapore (08/1/35/19/550 and 09/1/35/19/616).

Samsung Medical Center (SMC) was supported by a grant from Samsung Biomedical Research Institute. Genotyping of the patients and control subjects from SMC was conducted by Duk-Hwan Kim in the Dept. of Molecular Cell Biology, Sungkyunkwan University School of Medicine, and was supported by a grant from Samsung Biomedical Research Institute.

Seoul National University Hospital (SNUH) was supported by a grant from the Korea Health Technology R&D Project through the Korea Health Industry Development Institute, funded by the Ministry of Health & Welfare (grant numbers HI15C1595, HI14C0060, HI15C3131).

Taiwan Metabochip Consortium Zhonghua (TAICHI-G) was supported by grants from: the National Health Research Institutes, Taiwan (PH-099-PP-03, PH-100-PP-03, and PH-101-PP-03); the National Science Council, Taiwan (NSC 101-2314-B-075A-006-MY3, MOST 104-2314-B-075A-006-MY3, MOST 104-2314-B-075A-007, and MOST 105-2314-B-075A-003); and the Taichung Veterans General Hospital, Taiwan (TCVGH-1020101C, TCVGH-1020102D, TCVGH-1023102B, TCVGH-1023107D, TCVGH-1030101C, TCVGH- 1030105D, TCVGH-1033503C, TCVGH-1033102B, TCVGH-1033108D, TCVGH-1040101C, TCVGH-1040102D, TCVGH-1043504C, and TCVGH-1043104B). TAICHI-G was also supported in part by the National Center for Advancing Translational Sciences (CTSI grant UL1TR001881).

Taiwan Type 2 Diabetes (TWT2D) was supported by the GMM Study, Academia Sinica, Taiwan.

Danish T2D Case-Control Study (UCPH) was undertaken by the Novo Nordisk Foundation Center for Basic Metabolic Research, which is an independent Research Center, based at the University of Copenhagen, Denmark and partially funded by an unconditional donation from the Novo Nordisk Foundation (www.cbmr.ku.dk, Grant number NNF18CC0034900). Included study samples were supported by the Danish Research Fund and the National Danish Research Fund (The Vejle Diabetes Biobank), the Velux Foundation, The Danish Medical Research Council and Danish Agency for Science, Technology and Innovation (Health 2006); the Danish Research Council, the Danish Centre for Health Technology Assessment and Novo Nordisk Inc. (Inter99), the Timber Merchant Vilhelm Bang's Foundation and the Danish Heart Foundation (Health 2008), TrygFonden, the Lundbeck Foundation and the Novo Nordisk Foundation (NNF15OC0015896, DanFunD).

UK Biobank (UKBB) analyses were conducted using the UK Biobank resource under application 9161.

Uppsala Longitudinal Study of Adult Men (ULSAM) was supported by Wellcome Trust Grants (WT098017, WT064890, WT090532), Uppsala University, Uppsala University Hospital, the Swedish Research Council and the Swedish Heart-Lung Foundation.

Wake Forest School of Medicine (WFSM) was supported by NIH grants K99 DK081350, R01 DK066358, R01 DK053591, R01 DK087914, U01 DK105556, R01 HL56266, R01 DK070941 and in part by the General Clinical Research Center of the Wake Forest School of Medicine grant M01 RR07122. Genotyping services were provided by the Center for Inherited Disease Research (CIDR), which is fully funded through a federal contract from the National Institutes of Health to The Johns Hopkins University, contract number HHSC268200782096C.

Women's Health Initiative (WHI) is funded by the National Heart, Lung, and Blood Institute, National Institutes of Health, U.S. Department of Health and Human Services through contracts N01-WH-22110, 24152, 32100-2, 32105-6, 32108-9, 32111-13, 32115, 32118-32119, 32122, 42107-26, 42129-32, and 44221. Funding for WHI SHARe genotyping was provided by NHLBI Contract N02-HL-64278. The Molecular Epidemiology of Diabetes in the WHI is supported by R01DK125403 (to S.Liu). The contents of this publication are solely the responsibility of the authors and do not necessarily represent the official view of the National Institutes of Health. The funders had no role in study design, data collection and analysis, decision to publish, or preparation of the manuscript.

Wellcome Trust Case Control Consortium (WTCCC) analysis and genotyping was supported by: Wellcome Trust funding 090367, 098381, 090532, 083948, 085475, 101630 and 203141; MRC (G0601261); EU (Framework 7) HEALTH-F4-2007-201413; and NIDDK DK098032 and U01-DK105535.

FinnGen is funded by two grants from Business Finland (HUS 4685/31/2016 and UH 4386/31/2016) and eleven industry partners (AbbVie Inc, AstraZeneca UK Ltd, Biogen MA Inc, Celgene Corporation, Celgene International II Sàrl, Genentech Inc, Merck Sharp & Dohme Corp, Pfizer Inc., GlaxoSmithKline, Sanofi, Maze Therapeutics Inc., Janssen Biotech Inc). Following biobanks are acknowledged for collecting the FinnGen project samples: Auria Biobank (www.auria.fi/biopankki), THL Biobank (www.thl.fi/biobank), Helsinki Biobank (www.helsinginbiopankki.fi), Biobank Borealis of Northern Finland (www.oulu.fi/university/node/38474), Finnish Clinical Biobank Tampere (www.tays.fi/en-US/Research_and_development/Finnish_Clinical_Biobank_Tampere), Biobank of Eastern Finland (www.ita-suomenbiopankki.fi/en), Central Finland Biobank (www.ksshp.fi/fi-FI/Potilaalle/Biopankki), Finnish Red Cross Blood Service Biobank (www.veripalvelu.fi/verenluovutus/biopankkitoiminta) and Terveystalo Biobank (www.terveystalo.com/fi/Yritystietoa/Terveystalo-Biopankki/Biopankki/). All Finnish Biobanks are members of BBMRI.fi infrastructure (www.bbmri.fi).

Individual author acknowledgements. L.S.A. acknowledges support from the National Institute for Health (NIH), the Eunice Kennedy Shriver National Institute of Child Health and Human Development (NICHD) for R01 HD30880, National Institute on Aging (NIA) for R01 AG065357, National Institute of Diabetes and Digestive and Kidney Diseases (NIDDK) for R01DK104371 and R01HL108427. J.E.B. acknowledges support from the US National Institutes of Health R01DK127084, R01GM133169, R01HL142302, and U01DK105554. M.B. acknowledges funding from US National Institutes of Health grant DK062370. D.W.B. acknowledges support from the US National Institutes of Health U01DK105556 and R01DK66358. F.B. acknowledges support from the BHF Centre of Research Excellence, Oxford (RE/13/1/30181). J.C.C. acknowledges support from the Singapore Ministry of Health's National Medical Research Council under its Singapore Translational Research Investigator (STaR) Award (NMRC/STaR/0028/2017); iHealth-T2D, 643774; and the National Institute for Health Research/Wellcome Trust Imperial Clinical Research Facility. J.Chen acknowledges Inês Barroso for supervision and support (Wellcome WT098051 and WT206194). Y.S.C. acknowledges support from the National Research Foundation of Korea (NRF) Grant funded by the Ministry of Education (NRF-2020R1I1A2075302). C.-Y.C. acknowledges funding from the National Medical Research Council (NMRC), Singapore (CSA-SI/0012/2017). S.K.D. acknowledges support from the NIH/NIDDK grant R01 DK090111. S.D. acknowledges funding from the US National Institutes of Health Fogarty grant D43 TW009077, the National Institute for Health (NIH), the Eunice Kennedy Shriver National Institute of Child Health and Human Development (NICHD) for R01 HD30880, National Institute on Aging (NIA) for R01 AG065357, National Institute of Diabetes and Digestive and Kidney Diseases (NIDDK) for R01DK104371 and R01HL108427. J.D. is supported by R01 DK078616 and U01 DK078616. D.S.E. acknowledges support from the US National Institutes of Health U24AG051129. J.Ferrer acknowledges funding from Ministerio de Ciencia e Innovación (RTI2018-095666-B-I00), Medical Research Council (MR/L02036X/1), Wellcome Trust (WT101033), European Research Council Advanced Grant (789055), and National Institute for Health Research Imperial Biomedical Research Centre. J.C.F. is a Massachusetts General Hospital Research Scholar and was supported by NIDDK U01 DK105554 and NIDDK K24 DK110550. K.J.G. is supported by NIH grants DK105554 and DK114650. A.L.G. is a Wellcome Senior Fellow in Basic Biomedical Science, and was supported by the Wellcome Trust (095101, 200837, 106130, 203141), NIDDK U01DK105535 and NIDDK UM1 DK126185, and the Oxford NIHR Biomedical Research Centre. M.O.G. acknowledges support from the US National Institutes of Health grants P30DK063491 and UL1TR001881, as well as the Eris M. Field Chair in Diabetes Research. P.G.-L. acknowledges support from the National Institute for Health (NIH), the Eunice Kennedy Shriver National Institute of Child Health and Human Development (NICHD) for R01 HD30880, National Institute on Aging (NIA) for R01 AG065357, National Institute of Diabetes and Digestive and Kidney Diseases (NIDDK) for R01DK104371 and R01HL108427. A.T.H. is supported by a Wellcome Trust Senior Investigator award (grant number 098395/Z/12/Z). A.H. acknowledges support from the American Diabetes Association grant 1-19-ICTS-068. E.Ingelsson was supported by NIH/NIDDK 1R01DK106236-01A1. H.K. was funded by Manpei Suzuki Diabetes Foundation Grant-in-Aid for young scientists working abroad. S.-H.K. acknowledges funding from Korea Health Technology R&D Project through the Korea Health Industry Development Institute (grant number HI15C3131). A.Köttgen was supported by the by the Deutsche Forschungsgemeinschaft (DFG, German Research Foundation) KO 3598/5-1 and CRC 1453 Project-ID 431984000. C.Langenberg acknowledge support from the Medical Research

Council Epidemiology Unit (MC_UU_12015/1). A.Leong is supported by grant 2020096 from the Doris Duke Charitable Foundation. N.R.L. acknowledges funding from the US National Institutes of Health TW008288. C.M.L is supported by: the Li Ka Shing Foundation; WT-SSI/John Fell funds, Oxford; NIHR Oxford Biomedical Research Centre, Oxford; Widenlife; and NIH (5P50HD028138-27). A.E.L. acknowledges funding from US National Institutes of Health grant DK062370. R.J.F.L. acknowledges funding from the US National Institutes of Health grants R01DK110113, R01DK107786, R01HL142302 and R56HG010297. J.Luan acknowledges support from the Medical Research Council Epidemiology Unit (MC_UU_12015/1). R.C.W.M acknowledges funding from the Research Grants Council Theme-based Research Scheme (T12-402/13-N), the RGC Research Impact Fund (R4012-18), and a Croucher Foundation Senior Medical Research Fellowship. M.I.M. acknowledges funding from: The European Commission (ENGAGE: HEALTH-F4-2007-201413); MRC (G0601261, L020149); National Institutes of Health (RC2-DK088389, DK085545, R01-DK098032, U01-DK105535); Wellcome (083948, 085475, 090367, 090532, 098381, 101630, 203141, 212259). R.M.-C. acknowledges support from grants NIH U10 EY 11753 and NIH U10 EY 11753. J.B.M acknowledges funding through NIH grants R01DK078616, U01DK078616 and K24DK080140. J.M.M. is funded by American Diabetes Association Innovative and Clinical Translational Award 1-19-ICTS-068. K.L.M. acknowledges funding from the US National Institutes of Health R01DK072193, R01DK093757, U01DK105561. A.P.M. acknowledges support from US National Institutes of Health U01DK105535; Versus Arthritis (grant reference 21754); the Estonian Research Council grant PRG687; Wellcome Trust Core Award Grant Number 203141/Z/16/Z with additional support from the NIHR Oxford BRC; NIHR Manchester Biomedical Research Centre. S.R.M acknowledges funding from the Wellcome Trust [200186/Z/15/Z] and is supported by a Wellcome Trust Investigator Award [212284/Z/18/Z]. G.N.N. is supported by NIH grant R01DK127139. M.A.N. was supported in part by the Intramural Research Program of the NIH, National Institute on Aging (NIA), National Institutes of Health, Department of Health and Human Services; project number ZO1 AG000535, as well as the National Institute of Neurological Disorders and Stroke (NINDS); participation in this project was part of a competitive contract awarded to Data Tecnica International LLC by the National Institutes of Health to support open science research. M.C.Y.N. acknowledges support from the US National Institutes of Health U01DK105556, R01DK66358, and a supplement to R01DK78616-06S1. K.E.N. acknowledges support by R01HD057194, R01DK122503, R01HG010297, R01HL142302, R01HL143885, R01HG009974, and R01DK101855. D.N. acknowledges support from NIEHS grant T32ES013678. Y.O. was supported by JSPS KAKENHI (19H01021, 20K21834), and AMED (JP21km0405211, JP21ek0109413, JP21ek0410075, JP21gm4010006, and JP21km0405217), JST Moonshot R&D (JPMJMS2021, JPMJMS2024), Takeda Science Foundation. K.-S.P. acknowledges funding from Korea Health Technology R&D Project through the Korea Health Industry Development Institute (grant numbers HI15C1595, HI14C0060). E.J.P. was supported by the Canadian Institutes of Health Research (CIHR) and the Banting and Best Diabetes Center, University of Toronto. L.E.P. acknowledges support from the US National Institutes of Health R01DK127084, R01GM133169, R01HL142302, and U01DK105554. D.Saleheen has received funding from NHLBI, NINDS, the British Heart Foundation, Pfizer, Regeneron, Genentech, and Eli Lilly pharmaceuticals. M.Sander acknowledges support from the US National Institutes of Health 5U01DK105554. N.S. is supported by British Heart Foundation Centre of Excellence Grant RE/18/6/34217. R.A.S. acknowledges support from the Medical Research Council Epidemiology Unit

(MC_UU_12015/1). L.S. acknowledges support provided by a Sir Henry Wellcome Fellowship [220457/Z/20/Z] and funding from the Wellcome Trust [200186/Z/15/Z]. C.N.S. was supported by American Heart Association Postdoctoral Fellowship 15POST24470131 and 17POST33650016. D.T. acknowledges funding from US National Institutes of Health grant DK062370. M.S.U. acknowledges funding from NIH-NIDDK grant K23DK114551. N.J.W. acknowledges support from the Medical Research Council Epidemiology Unit (MC_UU_12015/1). E.W. acknowledges Inês Barroso for supervision and support (Wellcome WT098051 and WT206194), and acknowledges support from the Medical Research Council Epidemiology Unit (MC_UU_12015/1). J.-Y.W. was supported by Academia Sinica GMM Study. M.W. was supported by the Deutsche Forschungsgemeinschaft (DFG, German Research Foundation) – CRC 1453 Project-ID 431984000. W.Zhang acknowledges support from iHealth-T2D, 643774 and the National Institute for Health Research/Wellcome Trust Imperial Clinical Research Facility.

<u>Contributors to FinnGen</u>

Steering Committee

Aarno Palotie, Institute for Molecular Medicine Finland, HiLIFE, University of Helsinki, Helsinki, Finland; Mark Daly, Institute for Molecular Medicine Finland, HiLIFE, University of Helsinki, Helsinki, Finland.

Pharmaceutical companies: Howard Jacob, Abbvie, Chicago, IL, United States; Athena Matakidou, Astra Zeneca, Cambridge, United Kingdom; Heiko Runz, Biogen, Cambridge, MA, United States; Sally John, Biogen, Cambridge, MA, United States; Robert Plenge, Celgene, Summit, NJ, United States; Mark McCarthy, Genentech, San Francisco, CA, United States; Julie Hunkapiller, Genentech, San Francisco, CA, United States; Meg Ehm, GlaxoSmithKline, Brentford, United Kingdom; Dawn Waterworth, GlaxoSmithKline, Brentford, United Kingdom; Caroline Fox, Merck, Kenilworth, NJ, United States; Anders Malarstig, Pfizer, New York, NY, United States; Kathy Klinger, Sanofi, Paris, France; Kathy Call, Sanofi, Paris, France.

University of Helsinki and Biobanks: Tomi Mäkelä, HiLIFE, University of Helsinki, Helsinki, Finland; Jaakko Kaprio, Institute for Molecular Medicine Finland, HiLIFE, University of Helsinki, Helsinki, Finland; Petri Virolainen, Auria Biobank / University of Turku / Hospital District of Southwest Finland, Turku, Finland; Kari Pulkki, Auria Biobank / University of Turku / Hospital District of Southwest Finland, Turku, Finland; Terhi Kilpi, THL Biobank / The National Institute of Health and Welfare, Helsinki, Finland; Markus Perola, THL Biobank / The National Institute of Health and Welfare, Helsinki, Finland; Jukka Partanen, Finnish Red Cross Blood Service / Finnish Hematology Registry and Clinical Biobank, Helsinki, Finland; Anne Pitkäranta, Hospital District of Helsinki and Uusimaa, Helsinki, Finland; Riitta Kaarteenaho, Northern Finland Biobank Borealis / University of Oulu / Northern Ostrobothnia Hospital District, Oulu, Finland; Seppo Vainio, Northern Finland Biobank Borealis / University of Oulu / Northern Ostrobothnia Hospital District, Oulu, Finland; Kimmo Savinainen, Finnish Clinical Biobank Tampere / University of Tampere / Pirkanmaa Hospital District, Tampere, Finland; Veli-Matti Kosma, Biobank of Eastern Finland / University of Eastern Finland / Northern Savo Hospital District, Kuopio, Finland; Urho Kujala, Central Finland Biobank / University of Jyväskylä / Central Finland Health Care District, Jyväskylä, Finland.

Other Experts and Non-Voting Members: Outi Tuovila, Business Finland, Helsinki, Finland; Minna Hendolin, Business Finland, Helsinki, Finland; Raimo Pakkanen, Business Finland, Helsinki, Finland.

Scientific Committee

Pharmaceutical companies: Jeff Waring, Abbvie, Chicago, IL, United States; Bridget Riley-Gillis, Abbvie, Chicago, IL, United States; Athena Matakidou, Astra Zeneca, Cambridge, United Kingdom; Heiko Runz, Biogen, Cambridge, MA, United States; Jimmy Liu, Biogen, Cambridge, MA, United States; Shameek Biswas, Celgene, Summit, NJ, United States; Julie Hunkapiller, Genentech, San Francisco, CA, United States; Dawn Waterworth, GlaxoSmithKline, Brentford, United Kingdom; Meg Ehm, GlaxoSmithKline, Brentford, United

Kingdom; Dorothee Diogo, Merck, Kenilworth, NJ, United States; Caroline Fox, Merck, Kenilworth, NJ, United States; Anders Malarstig, Pfizer, New York, NY, United States; Catherine Marshall, Pfizer, New York, NY, United States; Xinli Hu, Pfizer, New York, NY, United States; Kathy Call, Sanofi, Paris, France; Kathy Klinger, Sanofi, Paris, France; Matthias Gossel, Sanofi, Paris, France.

University of Helsinki and Biobanks: Samuli Ripatti, Institute for Molecular Medicine Finland, HiLIFE, University of Helsinki, Helsinki, Finland; Johanna Schleutker, Auria Biobank / Univeristy of Turku / Hospital District of Southwest Finland, Turku, Finland; Markus Perola, THL Biobank / The National Institute of Health and Welfare, Helsinki, Finland; Mikko Arvas, Finnish Red Cross Blood Service / Finnish Hematology Registry and Clinical Biobank, Helsinki, Finland; Olli Carpén, Hospital District of Helsinki and Uusimaa, Helsinki, Finland; Reetta Hinttala, Northern Finland Biobank Borealis / University of Oulu / Northern Ostrobothnia Hospital District, Oulu, Finland; Johannes Kettunen, Northern Finland Biobank Borealis / University of Oulu / Northern Ostrobothnia Hospital District, Oulu, Finland; Reijo Laaksonen, Finnish Clinical Biobank Tampere / University of Tampere / Pirkanmaa Hospital District, Tampere, Finland; Arto Mannermaa, Biobank of Eastern Finland / University of Eastern Finland / Northern Savo Hospital District, Kuopio, Finland; Urho Kujala, Central Finland Biobank / University of Jyväskylä / Central Finland Health Care District, Jyväskylä, Finland.

Other Experts and Non-Voting Members: Outi Tuovila, Business Finland, Helsinki, Finland; Minna Hendolin, Business Finland, Helsinki, Finland; Raimo Pakkanen, Business Finland, Helsinki, Finland.

Clinical Groups

Neurology Group: Hilkka Soininen, Northern Savo Hospital District, Kuopio, Finland; Valtteri Julkunen, Northern Savo Hospital District, Kuopio, Finland; Anne Remes, Northern Ostrobothnia Hospital District, Oulu, Finland; Reetta Kälviäinen, Northern Savo Hospital District, Kuopio, Finland; Mikko Hiltunen, Northern Savo Hospital District, Kuopio, Finland; Jukka Peltola, Pirkanmaa Hospital District, Tampere, Finland; Pentti Tienari, Hospital District of Helsinki and Uusimaa, Helsinki, Finland; Juha Rinne, Hospital District of Southwest Finland, Turku, Finland; Adam Ziemann, Abbvie, Chicago, IL, United States; Jeffrey Waring, Abbvie, Chicago, IL, United States; Sahar Esmaeeli, Abbvie, Chicago, IL, United States; Nizar Smaoui, Abbvie, Chicago, IL, United States; Anne Lehtonen, Abbvie, Chicago, IL, United States; Susan Eaton, Biogen, Cambridge, MA, United States; Heiko Runz, Biogen, Cambridge, MA, United States; Sanni Lahdenperä, Biogen, Cambridge, MA, United States; Janet van Adelsberg, Celgene, Summit, NJ, United States; Shameek Biswas, Celgene, Summit, NJ, United States; John Michon, Genentech, San Francisco, CA, United States; Geoff Kerchner, Genentech, San Francisco, CA, United States; Julie Hunkapiller, Genentech, San Francisco, CA, United States; Natalie Bowers, Genentech, San Francisco, CA, United States; Edmond Teng, Genentech, San Francisco, CA, United States; John Eicher, Merck, Kenilworth, NJ, United States; Vinay Mehta, Merck, Kenilworth, NJ, United States; Padhraig Gormley, Merck, Kenilworth, NJ, United States; Kari Linden, Pfizer, New York, NY, United States; Christopher Whelan, Pfizer, New York, NY, United States; Fanli Xu, GlaxoSmithKline, Brentford, United Kingdom; David Pulford, GlaxoSmithKline, Brentford, United Kingdom.

Gastroenterology Group: Martti Färkkilä, Hospital District of Helsinki and Uusimaa, Helsinki, Finland; Sampsa Pikkarainen, Hospital District of Helsinki and Uusimaa, Helsinki, Finland; Airi Jussila, Pirkanmaa Hospital District, Tampere, Finland; Timo Blomster, Northern Ostrobothnia Hospital District, Oulu, Finland; Mikko Kiviniemi, Northern Savo Hospital District, Kuopio, Finland; Markku Voutilainen, Hospital District of Southwest Finland, Turku, Finland; Bob Georgantas, Abbvie, Chicago, IL, United States; Graham Heap, Abbvie, Chicago, IL, United States; Jeffrey Waring, Abbvie, Chicago, IL, United States; Nizar Smaoui, Abbvie, Chicago, IL, United States; Fedik Rahimov, Abbvie, Chicago, IL, United States; Anne Lehtonen, Abbvie, Chicago, IL, United States; Keith Usiskin, Celgene, Summit, NJ, United States; Joseph Maranville, Celgene, Summit, NJ, United States; Tim Lu, Genentech, San Francisco, CA, United States; Natalie Bowers, Genentech, San Francisco, CA, United States; Danny Oh, Genentech, San Francisco, CA, United States; John Michon, Genentech, San Francisco, CA, United States; Vinay Mehta, Merck, Kenilworth, NJ, United States; Kirsi Kalpala, Pfizer, New York, NY, United States; Melissa Miller, Pfizer, New York, NY, United States; Xinli Hu, Pfizer, New York, NY, United States; Linda McCarthy, GlaxoSmithKline, Brentford, United Kingdom.

Rheumatology Group: Kari Eklund, Hospital District of Helsinki and Uusimaa, Helsinki, Finland; Antti Palomäki, Hospital District of Southwest Finland, Turku, Finland; Pia Isomäki, Pirkanmaa Hospital District, Tampere, Finland; Laura Pirilä, Hospital District of Southwest Finland, Turku, Finland; Oili Kaipiainen-Seppänen, Northern Savo Hospital District, Kuopio, Finland; Johanna Huhtakangas, Northern Ostrobothnia Hospital District, Oulu, Finland; Bob Georgantas, Abbvie, Chicago, IL, United States; Jeffrey Waring, Abbvie, Chicago, IL, United States; Fedik Rahimov, Abbvie, Chicago, IL, United States; Apinya Lertratanakul, Abbvie, Chicago, IL, United States; Nizar Smaoui, Abbvie, Chicago, IL, United States; Anne Lehtonen, Abbvie, Chicago, IL, United States; David Close, Astra Zeneca, Cambridge, United Kingdom; Marla Hochfeld, Celgene, Summit, NJ, United States; Natalie Bowers, Genentech, San Francisco, CA, United States; John Michon, Genentech, San Francisco, CA, United States; Dorothee Diogo, Merck, Kenilworth, NJ, United States; Vinay Mehta, Merck, Kenilworth, NJ, United States; Kirsi Kalpala, Pfizer, New York, NY, United States; Nan Bing, Pfizer, New York, NY, United States; Xinli Hu, Pfizer, New York, NY, United States; Jorge Esparza Gordillo, GlaxoSmithKline, Brentford, United Kingdom; Nina Mars, Institute for Molecular Medicine Finland, HiLIFE, University of Helsinki, Helsinki, Finland.

Pulmonology Group: Tarja Laitinen, Pirkanmaa Hospital District, Tampere, Finland; Margit Pelkonen, Northern Savo Hospital District, Kuopio, Finland; Paula Kauppi, Hospital District of Helsinki and Uusimaa, Helsinki, Finland; Hannu Kankaanranta, Pirkanmaa Hospital District, Tampere, Finland; Terttu Harju, Northern Ostrobothnia Hospital District, Oulu, Finland; Nizar Smaoui, Abbvie, Chicago, IL, United States; David Close, Astra Zeneca, Cambridge, United Kingdom; Steven Greenberg, Celgene, Summit, NJ, United States; Hubert Chen, Genentech, San Francisco, CA, United States; Natalie Bowers, Genentech, San Francisco, CA, United States; John Michon, Genentech, San Francisco, CA, United States; Vinay Mehta, Merck, Kenilworth, NJ, United States; Jo Betts, GlaxoSmithKline, Brentford, United Kingdom; Soumitra Ghosh, GlaxoSmithKline, Brentford, United Kingdom.

Cardiometabolic Diseases Group: Veikko Salomaa, The National Institute of Health and Welfare, Helsinki, Finland; Teemu Niiranen, The National Institute of Health and Welfare,

Helsinki, Finland; Markus Juonala, Hospital District of Southwest Finland, Turku, Finland; Kaj Metsärinne, Hospital District of Southwest Finland, Turku, Finland; Mika Kähönen, Pirkanmaa Hospital District, Tampere, Finland; Juhani Junttila, Northern Ostrobothnia Hospital District, Oulu, Finland; Markku Laakso, Northern Savo Hospital District, Kuopio, Finland; Jussi Pihlajamäki, Northern Savo Hospital District, Kuopio, Finland; Juha Sinisalo, Hospital District of Helsinki and Uusimaa, Helsinki, Finland; Marja-Riitta Taskinen, Hospital District of Helsinki and Uusimaa, Helsinki, Finland; Tiinamaija Tuomi, Hospital District of Helsinki and Uusimaa, Helsinki, Finland; Jari Laukkanen, Central Finland Health Care District, Jyväskylä, Finland; Ben Challis, Astra Zeneca, Cambridge, United Kingdom; Andrew Peterson, Genentech, San Francisco, CA, United States; Julie Hunkapiller, Genentech, San Francisco, CA, United States; Natalie Bowers, Genentech, San Francisco, CA, United States; John Michon, Genentech, San Francisco, CA, United States; Dorothee Diogo, Merck, Kenilworth, NJ, United States; Audrey Chu, Merck, Kenilworth, NJ, United States; Vinay Mehta, Merck, Kenilworth, NJ, United States; Jaakko Parkkinen, Pfizer, New York, NY, United States; Melissa Miller, Pfizer, New York, NY, United States; Anthony Muslin, Sanofi, Paris, France; Dawn Waterworth, GlaxoSmithKline, Brentford, United Kingdom.

Oncology Group: Heikki Joensuu, Hospital District of Helsinki and Uusimaa, Helsinki, Finland; Tuomo Meretoja, Hospital District of Helsinki and Uusimaa, Helsinki, Finland; Olli Carpén, Hospital District of Helsinki and Uusimaa, Helsinki, Finland; Lauri Aaltonen, Hospital District of Helsinki and Uusimaa, Helsinki, Finland; Annika Auranen, Pirkanmaa Hospital District , Tampere, Finland; Peeter Karihtala, Northern Ostrobothnia Hospital District, Oulu, Finland; Saila Kauppila, Northern Ostrobothnia Hospital District, Oulu, Finland; Päivi Auvinen, Northern Savo Hospital District, Kuopio, Finland; Klaus Elenius, Hospital District of Southwest Finland, Turku, Finland; Relja Popovic, Abbvie, Chicago, IL, United States; Jeffrey Waring, Abbvie, Chicago, IL, United States; Bridget Riley-Gillis, Abbvie, Chicago, IL, United States; Anne Lehtonen, Abbvie, Chicago, IL, United States; Athena Matakidou, Astra Zeneca, Cambridge, United Kingdom; Jennifer Schutzman, Genentech, San Francisco, CA, United States; Julie Hunkapiller, Genentech, San Francisco, CA, United States; Natalie Bowers, Genentech, San Francisco, CA, United States; John Michon, Genentech, San Francisco, CA, United States; Vinay Mehta, Merck, Kenilworth, NJ, United States; Andrey Loboda, Merck, Kenilworth, NJ, United States; Aparna Chhibber, Merck, Kenilworth, NJ, United States; Heli Lehtonen, Pfizer, New York, NY, United States; Stefan McDonough, Pfizer, New York, NY, United States; Marika Crohns, Sanofi, Paris, France; Diptee Kulkarni, GlaxoSmithKline, Brentford, United Kingdom.

Opthalmology Group: Kai Kaarniranta, Northern Savo Hospital District, Kuopio, Finland; Joni Turunen, Hospital District of Helsinki and Uusimaa, Helsinki, Finland; Terhi Ollila, Hospital District of Helsinki and Uusimaa, Helsinki, Finland; Sanna Seitsonen, Hospital District of Helsinki and Uusimaa, Helsinki, Finland; Hannu Uusitalo, Pirkanmaa Hospital District, Tampere, Finland; Vesa Aaltonen, Hospital District of Southwest Finland, Turku, Finland; Hannele Uusitalo-Järvinen, Pirkanmaa Hospital District, Tampere, Finland; Marja Luodonpää, Northern Ostrobothnia Hospital District, Oulu, Finland; Nina Hautala, Northern Ostrobothnia Hospital District, Oulu, Finland; Heiko Runz,Biogen, Cambridge, MA, United States; Erich Strauss, Genentech, San Francisco, CA, United States; Natalie Bowers, Genentech, San Francisco, CA, United States; Hao Chen, Genentech, San Francisco, CA, United States; John Michon, Genentech, San Francisco, CA, United States; Anna Podgornaia, Merck, Kenilworth,

NJ, United States; Vinay Mehta, Merck, Kenilworth, NJ, United States; Dorothee Diogo, Merck, Kenilworth, NJ, United States; Joshua Hoffman, GlaxoSmithKline, Brentford, United Kingdom.

Dermatology Group: Kaisa Tasanen, Northern Ostrobothnia Hospital District, Oulu, Finland; Laura Huilaja, Northern Ostrobothnia Hospital District, Oulu, Finland; Katariina Hannula-Jouppi, Hospital District of Helsinki and Uusimaa, Helsinki, Finland; Teea Salmi, Pirkanmaa Hospital District, Tampere, Finland; Sirkku Peltonen, Hospital District of Southwest Finland, Turku, Finland; Leena Koulu, Hospital District of Southwest Finland, Turku, Finland; Ilkka Harvima, Northern Savo Hospital District, Kuopio, Finland; Kirsi Kalpala, Pfizer, New York, NY, United States; Ying Wu, Pfizer, New York, NY, United States; David Choy, Genentech, San Francisco, CA, United States; John Michon, Genentech, San Francisco, CA, United States; Nizar Smaoui, Abbvie, Chicago, IL, United States; Fedik Rahimov, Abbvie, Chicago, IL, United States; Anne Lehtonen, Abbvie, Chicago, IL, United States; Dawn Waterworth, GlaxoSmithKline, Brentford, United Kingdom.

FinnGen Analysis Working Group

Justin Wade Davis, Abbvie, Chicago, IL, United States; Bridget Riley-Gillis, Abbvie, Chicago, IL, United States; Danjuma Quarless, Abbvie, Chicago, IL, United States; Slavé Petrovski, Astra Zeneca, Cambridge, United Kingdom; Jimmy Liu, Biogen, Cambridge, MA, United States; Chia-Yen Chen, Biogen, Cambridge, MA, United States; Paola Bronson, Biogen, Cambridge, MA, United States; Robert Yang, Celgene, Summit, NJ, United States; Joseph Maranville, Celgene, Summit, NJ, United States; Shameek Biswas, Celgene, Summit, NJ, United States; Diana Chang, Genentech, San Francisco, CA, United States; Julie Hunkapiller, Genentech, San Francisco, CA, United States; Tushar Bhangale, Genentech, San Francisco, CA, United States; Natalie Bowers, Genentech, San Francisco, CA, United States; Dorothee Diogo, Merck, Kenilworth, NJ, United States; Emily Holzinger, Merck, Kenilworth, NJ, United States; Padhraig Gormley, Merck, Kenilworth, NJ, United States; Xulong Wang, Merck, Kenilworth, NJ, United States; Xing Chen, Pfizer, New York, NY, United States; Åsa Hedman, Pfizer, New York, NY, United States; Kirsi Auro, GlaxoSmithKline, Brentford, United Kingdom; Clarence Wang, Sanofi, Paris, France; Ethan Xu, Sanofi, Paris, France; Franck Auge, Sanofi, Paris, France; Clement Chatelain, Sanofi, Paris, France; Mitja Kurki, Institute for Molecular Medicine Finland, HiLIFE, University of Helsinki, Helsinki, Finland / Broad Institute, Cambridge, MA, United States; Samuli Ripatti, Institute for Molecular Medicine Finland, HiLIFE, University of Helsinki, Helsinki, Finland; Mark Daly, Institute for Molecular Medicine Finland, HiLIFE, University of Helsinki, Helsinki, Finland; Juha Karjalainen, Institute for Molecular Medicine Finland, HiLIFE, University of Helsinki, Helsinki, Finland / Broad Institute, Cambridge, MA, United States; Aki Havulinna, Institute for Molecular Medicine Finland, HiLIFE, University of Helsinki, Helsinki, Finland; Anu Jalanko, Institute for Molecular Medicine Finland, HiLIFE, University of Helsinki, Helsinki, Finland; Kimmo Palin, University of Helsinki, Helsinki, Finland; Priit Palta, Institute for Molecular Medicine Finland, HiLIFE, University of Helsinki, Helsinki, Finland; Pietro della Briotta Parolo, Institute for Molecular Medicine Finland, HiLIFE, University of Helsinki, Helsinki, Finland; Wei Zhou, Broad Institute, Cambridge, MA, United States; Susanna Lemmelä, Institute for Molecular Medicine Finland, HiLIFE, University of Helsinki, Helsinki, Finland; Manuel Rivas, University of Stanford, Stanford, CA, United States; Jarmo Harju, Institute for Molecular Medicine Finland, HiLIFE,

University of Helsinki, Helsinki, Finland; Aarno Palotie, Institute for Molecular Medicine Finland, HiLIFE, University of Helsinki, Helsinki, Finland; Arto Lehisto, Institute for Molecular Medicine Finland, HiLIFE, University of Helsinki, Helsinki, Finland; Andrea Ganna, Institute for Molecular Medicine Finland, HiLIFE, University of Helsinki, Helsinki, Finland; Vincent Llorens, Institute for Molecular Medicine Finland, HiLIFE, University of Helsinki, Helsinki, Finland; Antti Karlsson, Auria Biobank / University of Turku / Hospital District of Southwest Finland, Turku, Finland; Kati Kristiansson, THL Biobank / The National Institute of Health and Welfare, Helsinki, Finland; Mikko Arvas, Finnish Red Cross Blood Service / Finnish Hematology Registry and Clinical Biobank, Helsinki, Finland; Kati Hyvärinen, Finnish Red Cross Blood Service / Finnish Hematology Registry and Clinical Biobank, Helsinki, Finland; Jarmo Ritari, Finnish Red Cross Blood Service / Finnish Hematology Registry and Clinical Biobank, Helsinki, Finland; Tiina Wahlfors, Finnish Red Cross Blood Service / Finnish Hematology Registry and Clinical Biobank, Helsinki, Finland; Miika Koskinen, Helsinki Biobank / Helsinki University and Hospital District of Helsinki and Uusimaa, Helsinki, Finland; Olli Carpén, Helsinki Biobank / Helsinki University and Hospital District of Helsinki and Uusimaa, Helsinki, Finland; Johannes Kettunen, Northern Finland Biobank Borealis / University of Oulu / Northern Ostrobothnia Hospital District, Oulu, Finland; Katri Pylkäs, Northern Finland Biobank Borealis / University of Oulu / Northern Ostrobothnia Hospital District, Oulu, Finland; Marita Kalaoja, Northern Finland Biobank Borealis / University of Oulu / Northern Ostrobothnia Hospital District, Oulu, Finland; Minna Karjalainen, Northern Finland Biobank Borealis / University of Oulu / Northern Ostrobothnia Hospital District, Oulu, Finland; Tuomo Mantere, Northern Finland Biobank Borealis / University of Oulu / Northern Ostrobothnia Hospital District, Oulu, Finland; Eeva Kangasniemi, Finnish Clinical Biobank Tampere / University of Tampere / Pirkanmaa Hospital District, Tampere, Finland; Sami Heikkinen, Biobank of Eastern Finland / University of Eastern Finland / Northern Savo Hospital District, Kuopio, Finland; Arto Mannermaa, Biobank of Eastern Finland / University of Eastern Finland / Northern Savo Hospital District, Kuopio, Finland; Eija Laakkonen, Central Finland Biobank / University of Jyväskylä / Central Finland Health Care District, Jyväskylä, Finland; Juha Kononen, Central Finland Biobank / University of Jyväskylä / Central Finland Health Care District, Jyväskylä, Finland.

Biobank Directors

Lila Kallio, Auria Biobank / University of Turku / Hospital District of Southwest Finland, Turku, Finland; Sirpa Soini, THL Biobank / The National Institute of Health and Welfare Helsinki, Finland; Jukka Partanen, Finnish Red Cross Blood Service / Finnish Hematology Registry and Clinical Biobank, Helsinki, Finland; Kimmo Pitkänen, Helsinki Biobank / Helsinki University and Hospital District of Helsinki and Uusimaa, Helsinki; Seppo Vainio, Northern Finland Biobank Borealis / University of Oulu / Northern Ostrobothnia Hospital District, Oulu, Finland; Kimmo Savinainen, Finnish Clinical Biobank Tampere / University of Tampere / Pirkanmaa Hospital District, Tampere, Finland; Veli-Matti Kosma, Biobank of Eastern Finland / University of Eastern Finland / Northern Savo Hospital District, Kuopio, Finland; Teijo Kuopio, Central Finland Biobank / University of Jyväskylä / Central Finland Health Care District, Jyväskylä, Finland.

FinnGen Teams

Administration: Anu Jalanko, Institute for Molecular Medicine Finland, HiLIFE, University of Helsinki, Helsinki, Finland; Risto Kajanne, Institute for Molecular Medicine Finland, HiLIFE, University of Helsinki, Helsinki, Finland; Ulrike Lyhs, Institute for Molecular Medicine Finland, HiLIFE, University of Helsinki, Helsinki, Finland.

Analysis: Mitja Kurki, Institute for Molecular Medicine Finland, HiLIFE, University of Helsinki, Helsinki, Finland / Broad Institute, Cambridge, MA, United States; Juha Karjalainen, Institute for Molecular Medicine Finland, HiLIFE, University of Helsinki, Helsinki, Finland / Broad Institute, Cambridge, MA, United States; Pietro della Briotta Parola, Institute for Molecular Medicine Finland, HiLIFE, University of Helsinki, Helsinki, Finland; Sina Rüeger, Institute for Molecular Medicine Finland, HiLIFE, University of Helsinki, Helsinki, Finland; Arto Lehistö, Institute for Molecular Medicine Finland, HiLIFE, University of Helsinki, Helsinki, Finland; Wei Zhou, Broad Institute, Cambridge, MA, United States; Masahiro Kanai, Broad Institute, Cambridge, MA, United States

Clinical Endpoint Development: Hannele Laivuori, Institute for Molecular Medicine Finland, HiLIFE, University of Helsinki, Helsinki, Finland; Aki Havulinna, Institute for Molecular Medicine Finland, HiLIFE, University of Helsinki, Helsinki, Finland; Susanna Lemmelä, Institute for Molecular Medicine Finland, HiLIFE, University of Helsinki, Helsinki, Finland; Tuomo Kiiskinen, Institute for Molecular Medicine Finland, HiLIFE, University of Helsinki, Helsinki, Finland.

Communication: Mari Kaunisto, Institute for Molecular Medicine Finland, HiLIFE, University of Helsinki, Helsinki, Finland.

Data Management and IT Infrastructure: Jarmo Harju, Institute for Molecular Medicine Finland, HiLIFE, University of Helsinki, Helsinki, Finland; Elina Kilpeläinen, Institute for Molecular Medicine Finland, HiLIFE, University of Helsinki, Helsinki, Finland; Timo P. Sipilä, Institute for Molecular Medicine Finland, HiLIFE, University of Helsinki, Helsinki, Finland; Georg Brein, Institute for Molecular Medicine Finland, HiLIFE, University of Helsinki, Helsinki, Finland; Oluwaseun A. Dada, Institute for Molecular Medicine Finland, HiLIFE, University of Helsinki, Helsinki, Finland; Ghazal Awaisa, Institute for Molecular Medicine Finland, HiLIFE, University of Helsinki, Helsinki, Finland; Anastasia Shcherban, Institute for Molecular Medicine Finland, HiLIFE, University of Helsinki, Helsinki, Finland; Tuomas Sipilä, Institute for Molecular Medicine Finland, HiLIFE, University of Helsinki, Helsinki, Finland.

Genotyping: Kati Donner, Institute for Molecular Medicine Finland, HiLIFE, University of Helsinki, Helsinki, Finland.

Sample Collection Coordination: Anu Loukola, Helsinki Biobank / Helsinki University and Hospital District of Helsinki and Uusimaa, Helsinki, Finland.

Sample Logistics: Päivi Laiho, THL Biobank / The National Institute of Health and Welfare, Helsinki, Finland; Tuuli Sistonen, THL Biobank / The National Institute of Health and Welfare, Helsinki, Finland; Essi Kaiharju, THL Biobank / The National Institute of Health and

Welfare, Helsinki, Finland; Markku Laukkanen, THL Biobank / The National Institute of Health and Welfare, Helsinki, Finland; Elina Järvensivu, THL Biobank / The National Institute of Health and Welfare, Helsinki, Finland; Sini Lähteenmäki, THL Biobank / The National Institute of Health and Welfare, Helsinki, Finland; Lotta Männikkö, THL Biobank / The National Institute of Health and Welfare, Helsinki, Finland; Regis Wong, THL Biobank / The National Institute of Health and Welfare, Helsinki, Finland.

Registry Data Operations: Hannele Mattsson, THL Biobank / The National Institute of Health and Welfare, Helsinki, Finland; Kati Kristiansson, THL Biobank / The National Institute of Health and Welfare, Helsinki, Finland; Susanna Lemmelä, Institute for Molecular Medicine Finland, HiLIFE, University of Helsinki, Helsinki, Finland; Tero Hiekkalinna, THL Biobank / The National Institute of Health and Welfare, Helsinki, Finland; Manuel González Jiménez, THL Biobank / The National Institute of Health and Welfare, Helsinki, Finland.

Sequencing Informatics: Priit Palta, Institute for Molecular Medicine Finland, HiLIFE, University of Helsinki, Helsinki, Finland; Kalle Pärn, Institute for Molecular Medicine Finland, HiLIFE, University of Helsinki, Helsinki, Finland; Javier Nunez-Fontarnau, Institute for Molecular Medicine Finland, HiLIFE, University of Helsinki, Helsinki, Finland.

Trajectory Team: Tarja Laitinen, Pirkanmaa Hospital District, Tampere, Finland. Harri Siirtola, University of Tampere, Tampere, Finland. Javier Gracia Tabuenca, University of Tampere, Tampere, Finland.

Contributors to eMERGE Consortium

Debra Abrams[3], Samuel E Adunyah[4], Ladia Albertson-Junkans[5], Berta Almoguera[6], Darren C Ames[7], Paul Appelbaum[8], Samuel Aronson[9], Sharon Aufox[10], Lawrence J Babb[11], Adithya Balasubramanian[1,12], Hana Bangash[13], Melissa Basford[14], Lisa Bastarache[15], Samantha Baxter[11], Meckenzie Behr[3], Barbara Benoit[16], Elizabeth Bhoj[3], Suzette J Bielinski[17], Sarah T Bland[15], Carrie Blout[18], Kenneth Borthwick[19], Erwin P Bottinger[20], Mark Bowser[21], Harrison Brand[22], Murray Brilliant[23], Wendy Brodeur[24], Pedro Caraballo[25], David Carrell[5], Andrew Carroll[26], Lisa Castillo[27], Victor Castro[28], Gauthami Chandanavelli[1], Theodore Chiang[29], Rex L Chisholm[30], Kurt D Christensen[31], Wendy Chung[32], Christopher G Chute[33], Brittany City[14], Beth L Cobb[34], John J Connolly[3], Paul Crane[35], Katherine Crew[36], David R Crosslin[37], Jyoti Dayal[38], Mariza De Andrade[17], Jessica De la Cruz[1,12], Josh C Denny[39], Shawn Denson[1,2], Tim DeSmet[11], Ozan Dikilitas[13], Michael J Dinsmore[11], Sheila Dodge[11], Phil Dunlea[11], Todd L Edwards[40], Christine M Eng[12], David Fasel[41], Alex Fedotov[42], Qiping Feng[43], Mark Fleharty[11], Andrea Foster[1,2], Robert Freimuth[44], Christopher Friedrich[11], Stephanie M Fullerton[45], Birgit Funke[46], Stacey Gabriel[24], Vivian Gainer[47], Ali Gharavi[48], Richard A Gibbs[1,12], Andrew M Glazer[49], Joseph T Glessner[50], Jessica Goehringer[51], Adam S Gordon[52,53], Chet Graham[54], Robert C Green[55], Justin H Gundelach[13], Heather S Hain[56], Hakon Hakonarson[57], Maegan V Harden[24], John Harley[58], Margaret Harr[59], Andrea Hartzler[60], M Geoffrey Hayes[61], Scott Hebbring[62], Nora Henrikson[63], Andrew Hershey[64], Christin Hoell[30], Ingrid Holm[65], Kayla M Howell[14], George Hripcsak[41,66], Jianhong Hu[1], Elizabeth Duffy Hynes[21], Gail P Jarvik[52,67], Joy C Jayaseelan[1], Yunyun Jiang[1,12], Yoonjung Yoonie Joo[68], Sheethal Jose[38], Navya Shilpa Josyula[69], Anne E Justice[70], Sara E Kalla[1], Divya Kalra[1], Elizabeth W Karlson[71], Brendan J Keating[72], Melissa A Kelly[73], Eimear E Kenny[74], Dustin Key[5], Krzysztof Kiryluk[75], Terrie Kitchner[23], Barbara Klanderman[76], Eric Klee[77], David C Kochan[78], Viktoriya Korchina[1], Leah Kottyan[79], Christie Kovar[1], Emily Kudalkar[54], Alanna Kulchak Rahm[80], Iftikhar J Kullo[81], Philip Lammers[82], Eric B Larson[83], Matthew S Lebo[84], Magalie Leduc[85], Ming Ta Lee[86], Niall J Lennon[24], Kathleen A Leppig[87], Nancy D Leslie[88], Rongling Li[89], Wayne H Liang[90], Chiao-Feng Lin[91], Jodell E Linder[14], Noralane M Lindor[92], Todd Lingren[93], James G Linneman[23], Cong Liu[94], Wen Liu[1], Xiuping Liu[1], John Lynch[95], Hayley Lyon[96], Alyssa Macbeth[97], Harshad Mahadeshwar[1], Lisa Mahanta[98], Bradley Malin[99], Teri Manolio[38], Maddalena Marasa[100], Keith Marsolo[101], Michelle L McGowan[102], Elizabeth McNally[53], Jim Meldrim[24], Frank Mentch[3], Hila Milo Rasouly[103], Jonathan Mosley[104], Shubhabrata Mukherjee[35], Thomas E Mullen[24], Jesse Muniz[1], David R Murdock[1,12], Shawn Murphy[105], Mullai Murugan[106], Donna Muzny[107], Melanie F Myers[108], Bahram Namjou[34,109], Yizhao Ni[110], Robert C Onofrio[24], Aniwaa Owusu Obeng[111,112], Thomas N Person[113], Josh F Peterson[114], Lynn Petukhova[115], Cassandra J Pisieczko[116], Siddharth Pratap[117], Cynthia A Prows[118], Megan J Puckelwartz[119], Ritika Raj[1], James D Ralston[120], Arvind Ramaprasan[5], Andrea Ramirez[121], Luke Rasmussen[122], Laura Rasmussen-Torvik[123], Soumya Raychaudhuri[124], Heidi L Rehm[125], Marylyn D Ritchie[126], Catherine Rives[127], Beenish Riza[128], Dan M Roden[129], Elisabeth A Rosenthal[130], Avni Santani[131], Dan Schaid[17], Steven Scherer[1,12], Stuart Scott[132], Aaron Scrol[133], Soumitra Sengupta[134], Ning Shang[41], Himanshu Sharma[135], Richard R Sharp[136], Rajbir Singh[137], Patrick M A Sleiman[138], Kara Slowik[139], Joshua C Smith[140], Maureen E Smith[141], Duane T Smoot[142], Jordan W Smoller[143], Sunghwan Sohn[144], Ian B Stanaway[37], Justin Starren[145], Mary Stroud[15], Jessica Su[146], Casey Overby Taylor[147], Kasia Tolwinski[148], Sara L Van Driest[149,150], Sean M Vargas[151], Matthew Varugheese[152], David Veenstra[153], Eric Venner[1,12], Miguel Verbitsky[154], Gina Vicente[155], Michael Wagner[156], Kimberly Walker[157], Theresa Walunas[158], Liwen

Wang[159], Qiaoyan Wang[160], Wei-Qi Wei[15], Scott T Weiss[161], Quinn S Wells[162], Chunhua Weng[163], Peter S White[164], Georgia L Wiesner[165], Ken L Wiley Jr[38], Janet L Williams[166], Marc S Williams[167], Michael W Wilson[24], Leora Witkowski[168], Laura Allison Woods[14], Betty Woolf[24], Tsung-Jung Wu[1], Julia Wynn[169], Yaping Yang[170], Victoria Yi[1], Ge Zhang[171,172], Lan Zhang[1], Hana Zouk[173].

[1]Human Genome Sequencing Center, Baylor College of Medicine, Houston, TX, USA. [2]Department of Molecular and Human Genetics, Baylor College of Medicine, Houston, TX, USA. [3]Center for Applied Genomics, Children's Hospital of Philadelphia, Philadelphia, PA, USA. [4]Department of Biochemistry and Cancer Biology, Meharry Medical College, Nashville, TN, USA. [5]Kaiser Permanente of WA Health Research Institute, Seattle, WA, USA. [6]Center for Applied Genomics, Children's Hospital of Philadelphia, Philadelphia, PA, USA. [7]DNAnexus Inc, Mountain View, CA, USA. [8]Department of Psychiatry, Columbia University, New York State Psychiatric Institute, NYSPI, New York, NY, USA. [9]Partners HealthCare, Cambridge, MA, USA. [10]Center for Genetic Medicine, Northwestern University, Chicago, IL, USA. [11]Broad Institute, Massachusetts, MA, USA. [12]Department of Molecular and Human Genetics, Baylor College of Medicine, One Baylor Plaza, Houston, TX, USA. [13]Department of Cardiovascular Medicine, Mayo Clinic, Rochester, MN, USA. [14]Vanderbilt Institute for Clinical & Translational Research, Vanderbilt University Medical Center, Nashville, TN, USA. [15]Department of Biomedical Informatics, Vanderbilt University Medical Center, Nashville, TN, USA. [16]Research Information Science and Computing, Partners Healthcare, Somerville, MA, USA. [17]Department of Health Sciences Research, Mayo Clinic, Rochester, MN, USA. [18]Brigham and Women's Hospital, Boston, MA, USA. [19]Geisinger, Hood Center for Health Research, Danville, PA, USA. [20]Hasso Plattner Institute for Digital Health at Mount Sinai, Icahn School of Medicine at Mount Sinai, New York, NY, USA. [21]Partners HealthCare Personalized Medicine, Cambridge, MA, USA. [22]Massachusetts General Hospital, Boston, MA, USA. [23]Marshfield Clinic Research Institute, Marshfield, WI, USA. [24]Broad Institute of MIT and Harvard, Massachusetts, MA, USA. [25]Mayo Clinic, Rochester, MN, USA. [26]Google Inc, Mountain View, CA, USA. [27]Center for Genetic Medicine, Feinberg School of Medicine, Northwestern University, Department of Cardiology, The Louis A Simpson and Kimberly K Querrey Biomedical Research Center Room 5-408, Chicago, IL, USA. [28]Research Information Science and Computing (RISC), Partners Healthcare, Somerville, MA, USA. [29]Baylor College of Medicine, One Baylor Plaza, Houston, USA. [30]Center for Genetic Medicine, Feinberg School of Medicine, Northwestern University, Chicago, IL, USA. [31]Division of Genetics, Department of Medicine, Brigham and Women's Hospital, Department of Medicine, Harvard Medical School, Boston, MA, USA. [32]Departments of Pediatrics and Medicine, Columbia University, New York, NY, USA. [33]Schools of Medicine, Public Health, and Nursing, Johns Hopkins University, Baltimore, MD, USA. [34]Center for Autoimmune Genomics and Etiology, Cincinnati Children's Hospital Medical Center (CCHMC), Cincinnati, OH, USA. [35]Department of Medicine, University of Washington, Seattle, WA, USA. [36]Columbia University Irving Medical Center, New York, NY, USA. [37]Department of Biomedical Informatics and Medical Education, University of Washington, Seattle, WA, USA. [38]National Human Genome Research Institute, Maryland, MD, USA. [39]Departments of Biomedical Informatics and Medicine, Vanderbilt University, Nashville, TN, USA. [40]Division of Epidemiology, Department of Medicine, Vanderbilt Genetics Institute, Vanderbilt University Medical Center, Nashville, TN, USA. [41]Department of Biomedical Informatics, Columbia University, New York, NY, USA. [42]Irving Institute for Clinical and Translational Research, Columbia University, New York, NY, USA. [43]Department of Medicine, Division of Clinical Pharmacology, Vanderbilt University Medical Center, Nashville, TN, USA. [44]Department of Health Sciences Research, Mayo Clinic, Center for Individualized Medicine, Mayo Clinic, Rochester, MN, USA. [45]Department of Bioethics & Humanties, University of Washington, Seattle, WA, USA. [46]Harvard Medical School, Boston, MA, USA. [47]Partners HealthCare, Somerville, MA, USA. [48]Department of Medicine, Division of Nephrology, Columbia University Vagelos College of Physicians and Surgeons, New York, NY, USA. [49]Vanderbilt University Medical Center, Department of Medicine, Nashville, TN, USA. [50]Center for Applied Genomics Children's Hospital of Philadelphia, Division of Human Genetics Children's Hospital of Philadelphia, Department of Pediatrics Perelman School of Medicine University of Pennsylvania, Philadelphia, PA, USA. [51]Geisinger Medical Center, Danville, PA, USA. [52]Department of Medicine (Medical Genetics), University of Washington School of Medicine, Seattle, WA, USA. [53]Center for Genetic Medicine, Northwestern University Feinberg School of Medicine, Chicago, IL, USA. [54]Laboratory for Molecular Medicine, Partners Healthcare Personalized Medicine, Cambridge, MA, USA. [55]Brigham and Women's Hospital, Broad Institute, Harvard Medical School, EC Alumnae Building, Boston, MA, USA. [56]Center for Applied Genomics Children's Hospital of Philadelphia, Division of Human Genetics Children's Hospital of Philadelphia, Philadelphia, PA, USA. [57]Center for Applied Genomics Children's Hospital of Philadelphia, Divisions of Human Genetics and Pulmonary

Medicine Children's Hospital of Philadelphia, Department of Pediatrics Perelman School of Medicine University of Pennsylvania, Philadelphia, PA, USA. [58]Cincinnati Children's Hospital Medical Center, University of Cincinnati College of Medicine, US Department of Veterans Affairs Medical Center, Cincinnati, Cincinnati, OH, USA. [59]Center for Applied Genomics Children's Hospital of Philadelphia, Philadelphia, PA, USA. [60]Department of Biomedical Informatics and Medical Education, University of Washignton School of Medicine, KP Washington Health Research Institute, Seattle, WA, USA. [61]Division of Endocrinology, Metabolism, and Molecular Medicine, Department of Medicine, Northwestern University Feinberg School of Medicine, Center for Genetic Medicine, Northwestern University Feinberg School of Medicine, Department of Anthropology, Northwestern University, Chicago, IL, USA. [62]Center for Precision Medicine Research, Marshfield Clinic Research Institute, Marshfield, WI, USA. [63]KP Washington Health Research Institute, Univ of Washington School of Public Health, Dept of Health Services, Seattle, WA, USA. [64]Cincinnati Children's Hospital Medical Center (CCHMC), University of Cincinnati College of Medicine, Cincinnati, OH, USA. [65]Division of Genetics and Genomics, Boston Children's Hospital, Department of Pediatrics, Harvard Medical School, Boston, MA, USA. [66]Medical Informatics Services, NewYork-Presbyterian Hospital, New York, NY, USA. [67]Department of Genome Sciences, University of Washington School of Medicine, Seattle, WA, USA. [68]Department of Medicine, Northwestern University Feinberg School of Medicine, Chicago, IL, USA. [69]Biomedical and Translational Informatics, Geisinger, Fremont, CA, USA. [70]Biomedical and Translational Informatics, Geisinger, Danville, PA, USA. [71]Brigham & Women's Hospital, Harvard Medical School, Boston, MA, USA. [72]Children's Hospital of Philadelphia, Department of Surgery, University of Pennsylvania, Department of Surgery, University of Pennsylvania, Philadelphia, PA, USA. [73]Geisinger, Danville, PA, USA. [74]Center for Genomic Health, Icahn School of Medicine at Mount Sinai, The Charles Bronfman Institute of Personalized Medicine, Icahn School of Medicine at Mount Sinai, Departments of Genetics and Medicine, Icahn School of Medicine at Mount Sinai, New York, NY, USA. [75]Columbia University, New York, NY, USA. [76]Laboratory for Molecular Medicine, Partners Healthcare Personalized Medicine, Brigham and Women's Hospital, Cambridge, MA, USA. [77]Department of Health Sciences Research, Mayo Clinic, Rochester, MN, USA. [78]Department of Cardiovascular Medicine, Mayo Clinic, Rochester, MN, USA. [79]Department of Pediatrics, University of Cincinnati college of Medicine, University of Cincinnati, Center of Autoimmune Genomics and Etiology, Division of Allergy & Immunology, Cincinnati Children's Hospital Medical Center, Cincinnati, OH, USA. [80]Geisinger Genomic Medicine Institute, Danville, PA, USA. [81]Department of Cardiovascular Medicine, Mayo Clinic, Rochester, MN, USA. [82]Meharry Medical College, Baptist Cancer Center, Memphis, TN, USA. [83]Kaiser Permanente Washington Health Research Institute, Seattle, WA, USA. [84]Partners Healthcare Personalized Medicine, Brigham and Women's Hospital, Harvard Medical School, Cambridge, MA, USA. [85]Baylor College of Medicine, One Baylor Plaza, Houston, TX, USA. [86]Geisinger, Danville, PA, USA. [87]Genetic Services Kaiser Permanente of Washington, Seattle, WA, USA. [88]Cincinnati Children's Hospital Medical Center, Cincinnati, OH, USA. [89]National Human Genome Research Institute, National Institutes of Health, Bethesda, MD, USA. [90]University of Alabama at Birmingham, Birmingham, AL, USA. [91]Partners Healthcare Personalized Medicine, Harvard Medical School, Mountain View, CA, USA. [92]Mayo Clinic, Scottsdale, AZ, USA. [93]Cincinnati Children's Hospital Medical Center, Cincinnati, OH, USA. [94]Department of Biomedical Informatics, Columbia University Medical Center, Columbia University, New York, NY, USA. [95]Department of Communication, University of Cincinnati, Cincinnati, OH, USA. [96]Broad Institute of MIT & Harvard, Cambridge, MA, USA. [97]Broad Institute of MIT & Harvard, Cambridge, MA, USA. [98]Partners Healthcare Personalized Medicine, Cambridge, MA, USA. [99]Department of Biomedical Informatics, Vanderbilt University, Nashville, TN, USA. [100]Department of Medicine, Division of Nephrology, Columbia University, New York, NY, USA. [101]Department of Population Health Sciences, Duke University School of Medicine, Durham, NC, USA. [102]Ethics Center, Cincinnati Children's Hospital Medical Center, Department of Pediatrics, University of Cincinnati, Cincinnati, OH, USA. [103]Department of Medicine, Division of Nephrology, Columbia University, New York, NY, USA. [104]Department of Internal Medicine, Vanderbilt University Medical Center, Nashville, TN, USA. [105]Massachusetts General Hospital, Partners Healthcare, Harvard Medical School, Somerville, MA, USA. [106]Human Genome Sequencing Center at the Baylor College of Medicine, One Baylor Plaza, Houston, TX, USA. [107]Human Genome Sequencing Center at the Baylor College of Medicine, One Baylor Plaza, Houston, TX, USA. [108]Division of Human Genetics, Cincinnati Children's Hospital Medical Center, College of Medicine, University of Cincinnati, Cincinnati, OH, USA. [109]Department of Pediatrics, University of Cincinnati, Cincinnati, OH, USA. [110]Biomedical Informatics, Cincinnati Children's Hospital Medical Center, Cincinnati, OH, USA. [111]The Charles Bronfman Institute for Personalized Medicine, Icahn School of Medicine at Mount Sinai, New York, NY, USA. [112]Pharmacy Department, Mount Sinai Hospital, New York, NY, USA. [113]Geisinger, Danville, PA, USA. [114]Department of Biomedical Informatics, Vanderbilt University Medical Center, Nashville, TN, USA. [115]Department of Dermatology, Columbia University, New York, NY, USA. [116]Geisinger, Danville, PA, USA. [117]School of Graduate Studies and Research, Meharry Medical College, Nashville, TN, USA. [118]Division of

Human Genetics, Division of Patient Services, Cincinnati Children's Hospital, Cincinnati, OH, USA. [119]Department of Pharmacology, Northwestern University Feinberg School of Medicine, Center for Genetic Medicine, Northwestern University, Chicago, IL, USA. [120]Kaiser Permanente Washington Health Research Institute, University of Washington Department of Biomedical Informatics and Medical Education, Seattle, WA, USA. [121]Vanderbilt University Medical Center Department of Medicine, Nashville, TN, USA. [122]Department of Preventive Medicine Northwestern University Feinberg School of Medicine, Chicago, IL, USA. [123]Department of Preventive Medicine Northwestern University Feinberg School of Medicine, Chicago, IL, USA. [124]Medical and Population Genetics, Broad Institute or MIT and Harvard, Center for Genomic Medicine, Massachusetts General Hospital, Boston, MA, USA. [125]Center for Genomic Medicine, Massachusetts General Hospital, Department of Pathology, Massachusetts General Hospital/Harvard Medical School, Broad Institue Clinical Research Sequencing Platform (CRSP), Simches Research Building, Boston, MA, USA. [126]University of Pennsylvania, Perelman School of Medicine, Philadelphia, PA, USA. [127]Human Genome Sequencing Center Baylor College of Medicine, Houston, TX, USA. [128]University of Texas at Arlington, Human Genome Sequencing Center Baylor College of Medicine, Houston, TX, USA. [129]Vanderbilt University Medical Center, Nashville, TN, USA. [130]Division of Medical Genetics, School of Medicine, University of Washington, Seattle, WA, USA. [131]Center for Applied Genomics, Children's Hospital of Philadelphia, Department of Pathology and Laboratory Medicine, University of Pennsylvania, Philadelphia, PA, USA. [132]Icahn School of Medicine at Mount Sinai, New York, NY, USA. [133]KP Washington Health Research Institute, Seattle, WA, USA. [134]Columbia University, New York, NY, USA. [135]Partners Healthcare, Cambridge, MA, USA. [136]Biomedical Ethics Program, Mayo Clinic, Department of Health Sciences Research, Mayo Clinic, Rochester, MN, USA. [137]Clinical and Translational Research Center, Meharry Medical College, Nashville, TN, USA. [138]Center for Applied Genomics, Children's Hospital of Philadelphia, Department of Pediatrics, Perelman School of Medicine, University of Pennsylvania, Philadelphia, PA, USA. [139]Broad Institute of MIT & Harvard, Cambridge, MA, USA. [140]Department of Biomedical Informatics, Vanderbilt University Medical Center, Center for Patient and Professional Advocacy, Vanderbilt University, Nashville, TN, USA. [141]Northwestern University, Chicago, IL, USA. [142]Department of Internal Medicine, Meharry Medical College, Nashville, TN, USA. [143]Department of Psychiatry and Center for Genomic Medicine, Massachusetts General Hospital, Stanley Center for Psychiatric Research, Simches Research Building, Boston, MA, USA. [144]Mayo Clinic, Rochester, MN, USA. [145]Feinberg School of Medicine, Northwestern University, Chicago, IL, USA. [146]Channing Division of Network Medicine, Brigham and Women's Hospital, Boston, MA, USA. [147]Johns Hopkins University, Geisinger, Baltimore, MD, USA. [148]Biomedical Ethics Unit, Social Studies of Medicine, Faculty of Medicine, McGill University, Montreal, QC, Canada. [149]Department of Pediatrics, Vanderbilt University Medical Center, Nashville, TN, USA. [150]Department of Medicine, Vanderbilt University Medical Center, Nashville, TN, USA. [151]The University of Texas at San Antonio, San Antonio, TX, USA. [152]Massachusetts General Hospital, Partners HealthCare, Cambridge, MA, USA. [153]Comparative Health Outcomes, Policy & Economics (CHOICE) Institute, Department of Pharmacy, University of Washington, Seattle, WA, USA. [154]Division of Nephrology Department of Medicine, Columbia University, New York, NY, USA. [155]Broad Institute, Cambridge, MA, USA. [156]Division of Biomedical Informatics, Cincinnati Children's Hospital Medical Center, Cincinnati, OH, USA. [157]Human Genome Sequencing Center, Baylor College of Medicine, Baylor College of Medicine, One Baylor Plaza, Houston, TX, USA. [158]Northwestern University, Chicago, IL, USA. [159]Human Genome Sequencing Center at the Baylor College of Medicine, One Baylor Plaza, Houston, TX, USA. [160]Human Genome Sequencing Center, Baylor College of Medicine, One Baylor Plaza, Houston, TX, USA. [161]Channing Division of Network Medicine, Brigham and Women's Hospital, Department of Medicine, Harvard Medical School, Boston, MA, USA. [162]Department of Medicine, Division of Cardiovascular Medicine, Vanderbilt University Medical Center, Nashville, TN, USA. [163]Columbia University, New York, NY, USA. [164]Department of Pediatrics, Cincinnati Children's Hospital Medical Center, Department of Biomedical Informatics, University of Cincinnati College of Medicine, Cincinnati, OH, USA. [165]Department of Medicine, Vanderbilt Ingram Cancer Center, Vanderbilt University Medical Center, Nashville, TN, USA. [166]Geisinger, Danville, PA, USA. [167]Geisinger, Danville, PA, USA. [168]Laboratory for Molecular Medicine, Partners Healthcare Personalized Medicine, Department of Pathology, Massachusetts General Hospital/Harvard Medical School, Cambridge, MA, USA. [169]Departments of Pediatrics, Columbia University, New York, NY, USA. [170]Department of Molecular and Genetics, Baylor College of Medicine, Houston, TX, USA. [171]Division of Human Genetics, Center for Prevention of Preterm Birth, Perinatal Institute and March of Dimes Prematurity Research Center Ohio Collaborative, Cincinnati Children's Hospital Medical Center, Cincinnati, Cincinnati, OH, USA. [172]Department of Pediatrics, University of Cincinnati College of Medicine, Cincinnati, OH, USA. [173]Laboratory for Molecular Medicine, Partners Healthcare Personalized Medicine, Department of Pathology, Massachusetts General Hospital/Harvard Medical School, Cambridge, MA, USA.

Ethics statements

Anti-aging study cohort (AASC). The ethics committees of Ehime University Graduate School of Medicine approved all study procedures. Written informed consent was obtained from all participants.

Atherosclerosis Risk in Communities (ARIC). Institutional Review Board approvals were obtained at all study sites: National Heart, Lung, and Blood Institute, University of North Carolina at Chapel Hill, Wake Forest Baptist Medical Center, University of Mississippi Medical Center, University of Minnesota and Johns Hopkins University. All participants provided written informed consent.

Biobank Japan (BBJ). All participants provided written informed consent as approved by the ethical committees of the RIKEN Yokohama Institute and the Institute of Medical Science, University of Tokyo.

Beijing Eye Study (BES). Approval was obtained from the Medical Ethics Committee of the Beijing Tongren Hospital. All participants gave written informed consent.

BioMe Biobank (BIOME). Approval was obtained from the Institutional Review Board at the Icahn School of Medicine at Mount Sinai. All participants provided written informed consent for genomic data sharing.

Bangladesh Population Cohort (BPC). The conduct of the BPC was reviewed and approved by Ethical Committees of the Bangladesh Medical Research Council and Institutional Review Boards of the University of Chicago.

Cardiometabolic Genome Epidemiology (CAGE-AMAGASKI and CAKE-GWAS). Approval was obtained from the Institutional Review Boards at the National Center for Global Health and Medicine. All participants provided written informed consent.

Cardiometabolic Genome Epidemiology (CAGE-KING). Approval was obtained from the ethics committees of Aichi Gakuin University, Jichi Medical University, Nagoya University and Kyushu University. All participants provided written informed consent.

Coronary Artery Risk Development in Young Adults (CARDIA). Participating centers (Northwestern University, University of Alabama Birmingham, University of Minnesota, and Kaiser Foundation Research Institute) provided ethics approval for the CARDIA study, and all participants provided written informed consent to participate.

Cleveland Family Study (CFS). Approval was obtained from the Institutional Review Board of Mass General Brigham (formerly Partners HealthCare). Written informed consent was obtained from all participants.

China Health and Nutrition Survey (CHNS). Approval was obtained from the Institutional review Boards at the University of North Carolina at Chapel Hill, the Chinese National

Human Genome Center at Shanghai, and the Institute of Nutrition and Food Safety at the China Centers for Disease Control. All participants provided written informed consent.

Cardiovascular Health Study (CHS). Approval was obtained from the Institutional Review Boards at Wake Forest University, University of California, Davis, Johns Hopkins, University of Pittsburgh, and the University of Washington, Seattle. All participants provided written informed consent.

China Kadoorie Biobank (CKB). All participants provided written informed consent. Ethical approval was obtained from Oxford Tropical Research Ethics Committee (OxTREC) and from the Ethical Review Committees of the Chinese Centre for Disease Control and Prevention and the Chinese Academy of Medical Sciences/Peking Union Medical College.

Cebu Longitudinal Health and Nutrition Survey (CLHNS). Written informed consent was obtained from all participants. Study protocols were approved by the University of North Carolina Institutional review Board for the Protection of Human Subjects.

Diabetic Cohort and Singapore Prospective Study Program (DC/SP2). Study protocols were approved by the Singapore General Hospital Ethics Committee, and National University of Singapore Institutional Review Board. All participants provided written informed consent.

Durban Diabetes Study and Durban Diabetes Case Control (DDS/DCC). Approvals were granted by the Biomedical Research Ethics Committee at the University of KwaZulu-Natal and the UK National Research Ethics Service. All participants provided written informed consent.

deCODE genetics (DECODE). The study was approved by the Icelandic National Bioethics Committee (approval no. VSN-16-112) after evaluation by the Icelandic Data Protection Authority. We obtained written informed consent for all participants in this study who donated samples. All data processing complies with the Icelandic Data Protection Authority (no. PV_2017060950ÞS).

Diabetes Gene Discovery Group (DGDG). All participants signed informed consent, and the protocol was approved by the French ethics committee.

Diabetes Genetics Initiative (DGI). The study was approved by the Ethics Committees of the Helsinki University Hospital, Helsinki, Finland, and Lund University, Sweden.

Estonian Genome Center of the University of Tartu (EGCUT). All analyses were approved by the Ethics Review Committee of the University of Tartu. All participants provided written informed consent.

Electronic Medical Records and Genomics Network (EMERGE). Approval was obtained from the Institutional Review Boards at Boston Children's Hospital, Children's Hospital of Philadelphia, Cincinnati Children's Hospital Medical Center, Essentia Institute of Rural Health, Geisinger Clinic, Group Health Cooperative, Marshfield Clinic Research Foundation, Mayo Clinic, Icahn School of Medicine at Mount Sinai, Northwestern University, Pennsylvania State University, Vanderbilt University Medical Center, and University of Washington. All participants provided written informed consent.

European Prospective Investigation into Cancer and Nutrition (EPIC-INTERACT). The EPIC-InterAct study was approved by the local ethics committee in the participating countries and the Internal Review Board of the International Agency for Research on Cancer. All participants gave written informed consent. The study was coordinated by the Medical Research Council Epidemiology Unit at the University of Cambridge.

Epidemiologic Study of the Screenees for Diabetes Reduction Assessment with Ramipril and Rosiglitazone Medication (EPIDREAM). All study participants consented to analysis of blood samples. Approval was granted by the Hamilton Integrated Research Ethics Board, at McMaster University, Hamilton, Canada.

Family Heart Study (FAMHS). Approval was obtained from the Institutional Review Board at Washington University, St. Louis. Written informed consent, including consent to participate in genetic studies, was obtained from all participants.

Framingham Heart Study (FHS). Approval was obtained from the Institutional review Board of Boston University Medical Campus. All study participants provided written informed consent.

Finland-United States Investigation of NIDDM Genetics (FUSION). Approval was obtained from the coordinating Ethics Committee of the Hospital District of Helsinki and Uusimaa. All participants provided written informed consent.

German Chronic Kidney Disease (GCKD). All participants provided written informed consent. The study was registered in the national registry for clinical studies (DRKS 00003971) and was approved by local ethics committees.

Genetic Study of Atherosclerosis Risk (GENESTAR). Approval was obtained from the Johns Hopkins Medicine Institutional Review Board. All participants gave written informed consent.

Genetic Epidemiology Network of Arteriosclerosis (GENOA). Approval was granted by Institutional Review Boards of the University of Michigan, University of Mississippi Medical Center and Mayo Clinic. Written informed consent was obtained from all participants.

Resource for Genetic Epidemiology on Adult Heath and Aging (GERA). The Institutional Review Boards for Human Subjects Research of both Kaiser Permanente Medical Care Plan (Northern California Region) and the University of California at San Francisco approved the project.

Genetics of Diabetes and Audit Research in Tayside Scotland (GODARTS). Approval was obtained from the Tayside Medical Ethics Committee. Informed consent was obtained for all participants.

Genetics of Latinos Diabetic Retinopathy (GOLDR). Approval was granted by the Institutional Review Board of the Lundquist Institute for Biomedical Innovation at Harbor-UCLA Medical Center.

Genetic Overlap Between Metabolic and Psychiatric Traits and Teens of Attica: Genes and Environment (GOMAP-TEENAGE). Ethical permission for TEENAGE was obtained from the Bioethics Committee of Harokopio University, Athens. Ethical permission for GOMAP was obtained from the Dromokaiteio Scientific Committee, Dromokaiteio Management Committee, Dafni Scientific Committee, Eginitio Scientific Committee and Harokopio Ethics Committee. All participants of GOMAP-TEENAGE gave written informed consent.

Genomic Research Cohort for CCMB Diabetes Study (GRCCDS). Ethics committees of CSIR-Centre for Cellular and Molecular Biology and KEM Hospital and Research Centre approved the project.

Health, Aging and Body Composition Study (HABC). The Institutional Review Boards at the University of Memphis and the University of Pittsburgh granted approval to conduct the Health ABC Study, and all participants provided written informed consent.

Healthy Aging in Neighborhoods of Diversity Across the Life Span Study (HANDLS). Approval was granted by the National Institutes of Health Institutional Review Board (study number 09AGN248). All participants provided written informed consent.

Hispanic Community Health Study/Study of Latinos (HCHS/SOL). Approval was obtained from Institutional Review Boards at the University of North Carolina at Chapel Hill, Albert Einstein College of Medicine, University of Illinois at Chicago, University of Miami, and San Diego State University. All participants provided written informed consent.

Hong Kong Diabetes Registry (HKDR). Approval was obtained from the Chinese University of Hong Kong Clinical Research Ethics Committee.

Health Professionals' Follow-Up Study (HPFS). Approval was obtained from the Human Research Committee at the Brigham and Women's Hospital. All participants provided written informed consent.

Mexican American Hypertension and Insulin Resistance (HTNIR). Approval was granted by Human Subjects Protection Institutional Review Boards at the University of California at Los Angeles, University of Southern California, Lundquist/LABioMed/Harbor-UCLA and Cedars-Sinai Medical Center.

Howard University Family Study (HUFS). All human participants from the HUFS included in the analyses of this manuscript provided written informed consent prior to enrollment. The HUFS study was approved by the Institutional Review Board at Howard University.

Indian Diabetes Consortium (INDICO). Approval was obtained by the Human Ethics Committees of All India Institute of Medical Sciences, New Delhi and CSIR-Institute of Genomics and Integrative Biology, New Delhi, India, and was conducted in accordance with the principles of Helsinki Declarations. Informed written consent was obtained from all of participants.

INTERHEART (INTERHEART). All study participants consented to analysis of blood samples. Approval was granted by the Hamilton Integrated Research Ethics Board, at McMaster University, Hamilton, Canada.

Jackson Heart Study (JHS). Approval was obtained from Institutional Review Boards at Jackson State University, Tougaloo College and the University of Mississippi Medical Center. All participants provided written informed consent.

Korean Association Resource (KARE). Approval was granted by the Institutional review Board at the Korean National Institute of Health. All participants provided written informed consent.

Korean Biobank Array from the Korean Genome and Epidemiology (KoGES) Consortium (KBA). Approval was granted by the Institutional Review Board of the Korean National Institute of Health. All participants provided written informed consent.

Collaborative Health Research in the Region of Augsburg (KORA). Approval was granted by the Ethics Committee of the Medical Association of Bavaria (number 06068). All participants provided informed consent.

Los Angeles Latino Eye Study (LALES). Approval was obtained from the Los Angeles County/University of Southern California Institutional Review Board, and Western Institutional Review Board at Southern California Eye Institute. All participants provided written informed consent.

London Life Sciences Prospective Population (LOLIPOP). Approval was obtained from the London-Fulham Research Ethics Committee (ref 07/H0712/150). All participants gave an written informed consent.

Mexican American Study of Coronary Artery Disease (MACAD). Approval was granted by Human Subjects Protection Institutional Review Boards at the University of California at Los Angeles, University of Southern California, Lundquist/LABioMed/Harbor-UCLA and Cedars-Sinai Medical Center.

Mexico City (MC). Approval was obtained from Institutional Review Boards at the Ethics and Scientific Commission members and the AUTHORIZATION is issued with registration number R-2011-785-018 and the Conacyt SALUD-2010-02-150352. In Canada, approval was obtained from the Research Ethics Board from the University of Toronto (Protocol 15770).

Multi-Ethnic Study of Atherosclerosis (MESA). Approval was obtained from Institutional Review Boards at the University of Washington, Wake Forest School of Medicine, Northwestern University, University of Minnesota, Columbia University, Johns Hopkins University, Cedars-Sinai Medical Center, and the University of California at Los Angeles.

Metabolic Syndrome in Men (METSIM). Approval was granted by the Ethics Committee of the University of Kuopio and the Kuopio University Hospital. All participants gave written informed consent.

Mass General Brigham Biobank (MGB). The MGB Biobank protocol and informed consent documents are reviewed annually by the Partners-MGB Institutional Review Board (#2009P002312). All patients who participate in the MGB Biobank are consented for their samples to be linked to their identified clinical information. They have also consented for their information to be used for a broad range of research and for their deidentified information to be shared outside of MGB.

Michigan Genomics Initiative (MGI). Approval was granted by the IRBMED Institutional Review Board of the University of Michigan. All participants gave written informed consent.

Nagahama Study (NAGAHAMA). Approval was granted by the ethics committees of Kyoto University Graduate School of Medicine. Written informed consent was obtained from all participants.

Netherlands Epidemiology of Obesity (NEO). Approval was obtained from the Medical Ethics Committee of Leiden University Medical Center. All participants gave written informed consent.

Nurses Health Study (NHS). Approval was obtained from the Human Research Committee at the Brigham and Women's Hospital. All participants provided written informed consent**.**

NIDDM-Atherosclerosis Study Hispanic Cohorts (NIDDM). Approval was granted by Human Subjects Protection Institutional Review Boards at the University of California at Los Angeles, University of Southern California, City of Hope, Lundquist/LABioMed/Harbor-UCLA and Cedars-Sinai Medical Center.

Northewestern University Genetics (NUGENE). Approval was obtained from Institutional Review Boards at Northwestern University and Vanderbilt University.

Prospective Investigation of the Vasculature in Uppsala Seniors (PIVUS). Approval was granted by the Ethics Committee of Uppsala University. All participants provided written informed consent.

Pakistan Risk of Myocardial Infarction Study (PROMIS). The study was approved by the Institutional Review Board of the Center for Non-Communicable Diseases Pakistan and by regional Ethical Review Committees in the different centres across Pakistan involved in the study. Institutional Review Boards at the National Institute of Cardiovascular Disorders, Karachi, Punjab Institute of Cardiology, Lahore, and Tabba Heart Institute, Karachi approved the study. All participants provided written informed consent.

Prospective Study of Pravastatin in the Elderly at Risk (PROSPER). Approval was obtained from the Institutional Ethics Review Boards of Cork University (Ireland), Glasgow University

(UK) and Leiden University Medical Center (The Netherlands). All participants gave written informed consent.

Sea Islands Genetic Network Reasons for Geographic and Racial Differences in Stroke (REGARDS). The REGARDS study protocol was approved by the institutional review boards of each participating institution, and written informed consents were obtained from all participants.

Ragama Health Study (RHS). Approval was obtained from Institutional Review Boards at the National Center for Global Health and the University of Kelaniya (P38/09/2006). All participants provided written informed consent.

Rotterdam Study (RS). Approval was granted by the Institutional review Board at Erasmus University Medical Center. All participants provided written informed consent.

Shanghai Breast Cancer Study and Shanghai Women's Health Study (SBCS/SWHS). Approval was obtained from Institutional review Boards at Vanderbilt University Medical Center and Shanghai Cancer Institute. A written informed consent form was obtained from all study participants.

Singapore Chinese Eye Study (SCES). The study adhered to the Declaration of Helsinki. Ethical approval was obtained from the SingHealth Institutional Review Board and National University of Singapore Institutional Review Board. Written informed consent was obtained from all participants.

Starr County Health (SCH). All protocols were reviewed and approved by the Institutional Committee for the Protection of Human Subjects (HSC-SPH-02-042). All participants provided written informed consent permitting the collection and sharing of data.

Singapore Chinese Health Study (SCHS). Approval was obtained from the Institutional Review Board at the National University of Singapore. All participants provided written informed consent.

Slim Initiative for Genomic Medicine in the Americas (SIGMA). Approval was obtained from the Institutional Review Board of the Instituto Nacional de Ciencas Medicas y Nutricion Salvador Zubiran. All participants provided written informed consent.

Singapore Malay Eye Study (SIMES). The study adhered to the Declaration of Helsinki. Ethical approval was obtained from the SingHealth Institutional Review Board and National University of Singapore Institutional Review Board. Written informed consent was obtained from all participants.

Singapore Indian Eye Study (SINDI). The study adhered to the Declaration of Helsinki. Ethical approval was obtained from the SingHealth Institutional Review Board and National University of Singapore Institutional Review Board. Written informed consent was obtained from all participants.

Samsung Medical Center (SMC). Approval was obtained from the Institutional Review Board of the Samsung Medical Center (No. 2004-12-005). All participants provided written informed consent.

Seoul National University Hospital (SNUH). The Institutional Review Board of the Biomedical Research Institute at Seoul National University Hospital approved the study protocol (1205–130–411). Written informed consent was obtained from each participant.

Taiwan Metabochip Consortium Zhonghua (TAICHI-G). Approval was granted by Institutional Review Boards at Stanford University School of Medicine, Hudson-Alpha Biotechnology Institute, Lundquist/LABioMed/Harbor-UCLA, Cedars-Sinai Medical Center, Taichung Veterans General Hospital, Taipei Veterans General Hospital, National Health Research Institute, Tri-Service General Hospital, and National Taiwan University Hospital.

Taiwan Type 2 Diabetes (TWT2D). Approval was obtained from Institutional Review Boards at China Medical University Hospital, Chia-Yi Christian Hospital, and National Taiwan University Hospital.

Danish T2D Case-Control Study (UCPH). The studies included in the Danish T2D Case-Control Study (UCPH) were conducted in accordance with the Declaration of Helsinki II and were approved by the local Ethical Committees of Copenhagen County, the Capital Region of Denmark, or the Region of Southern Denmark.

UK Biobank (UKBB). Approval was obtained from the North West Centre for Research Ethics Committee (11/NW/0382).

Uppsala Longitudinal Study of Adult Men (ULSAM). Approval was granted by the Ethics Committee of Uppsala University. All participants provided written informed consent.

Wake Forest School of Medicine (WFSM). Approval was granted by the Institutional Review Board at Wake Forest School of Medicine. All participants provided written informed consent.

Women's Health Initiative (WHI). Approval was granted by the Institutional review Board at the Fred Hutchinson Cancer Research Centre in accordance with the US Department of Health and Human Services regulations at 45 CFR 46 (approval number IR# 3467-EXT). All participants provided written informed consent. Additional written consent to review medical records was obtained. The Fred Hutchinson Cancer Research Centre has an approved FWA on file with the Office for Human Research Protections under assurance number 0001920.

Wellcome Trust Case Control Consortium (WTCCC). Approval for the study was obtained from Peterborough & Fenland Local Research Ethics Committee, National Research Ethics Service, Leeds (East) Research Ethics Committee, South West Multicentre Research Ethics Committee, Tayside Committee on Medical Research Ethics and Oxford Tropical Research Ethics Committee.

FinnGen. Patients and control subjects in FinnGen provided informed consent for biobank research, based on the Finnish Biobank Act. Alternatively, separate research cohorts, collected prior the start of FinnGen (August 2017), were collected based on study-specific consents and later transferred to the Finnish biobanks after approval by Fimea, the National Supervisory Authority for Welfare and Health. Recruitment protocols followed the biobank protocols approved by Fimea. The Coordinating Ethics Committee of the Hospital District of Helsinki and Uusimaa (HUS) approved the FinnGen study protocol Nr HUS/990/2017. The FinnGen project is approved by Finnish Institute for Health and Welfare (THL), approval number THL/2031/6.02.00/2017, amendments THL/1101/5.05.00/2017, THL/341/6.02.00/2018, THL/2222/6.02.00/2018, THL/283/6.02.00/2019), Digital and population data service agency VRK43431/2017-3, VRK/6909/2018-3, the Social Insurance Institution (KELA) KELA 58/522/2017, KELA 131/522/2018, KELA 70/522/2019 and Statistics Finland TK-53-1041-17. The Biobank Access Decisions for FinnGen samples and data utilized in FinnGen Data Freeze 4 include: THL Biobank BB2017_55, BB2017_111, BB2018_19, BB_2018_34, BB_2018_67, BB2018_71, BB2019_7 Finnish Red Cross Blood Service Biobank 7.12.2017, Helsinki Biobank HUS/359/2017, Auria Biobank AB17-5154, Biobank Borealis of Northern Finland_2017_1013, Biobank of Eastern Finland 1186/2018, Finnish Clinical Biobank Tampere MH0004, Central Finland Biobank 1-2017, and Terveystalo Biobank STB 2018001.

Supplementary Figure 1. Overlap of samples from the DIAMANTE multi-ancestry meta-analysis with recent investigations incorporating T2D GWAS from the DIAMANTE Consortium. The DIAMANTE multi-ancestry meta-analysis includes 180,834 cases and 1,159,055 controls of diverse ancestry, of which 137,385 cases and 1,061,465 controls (77.8% of total effective sample size) have contributed to previous investigation of the genetic contribution to T2D.

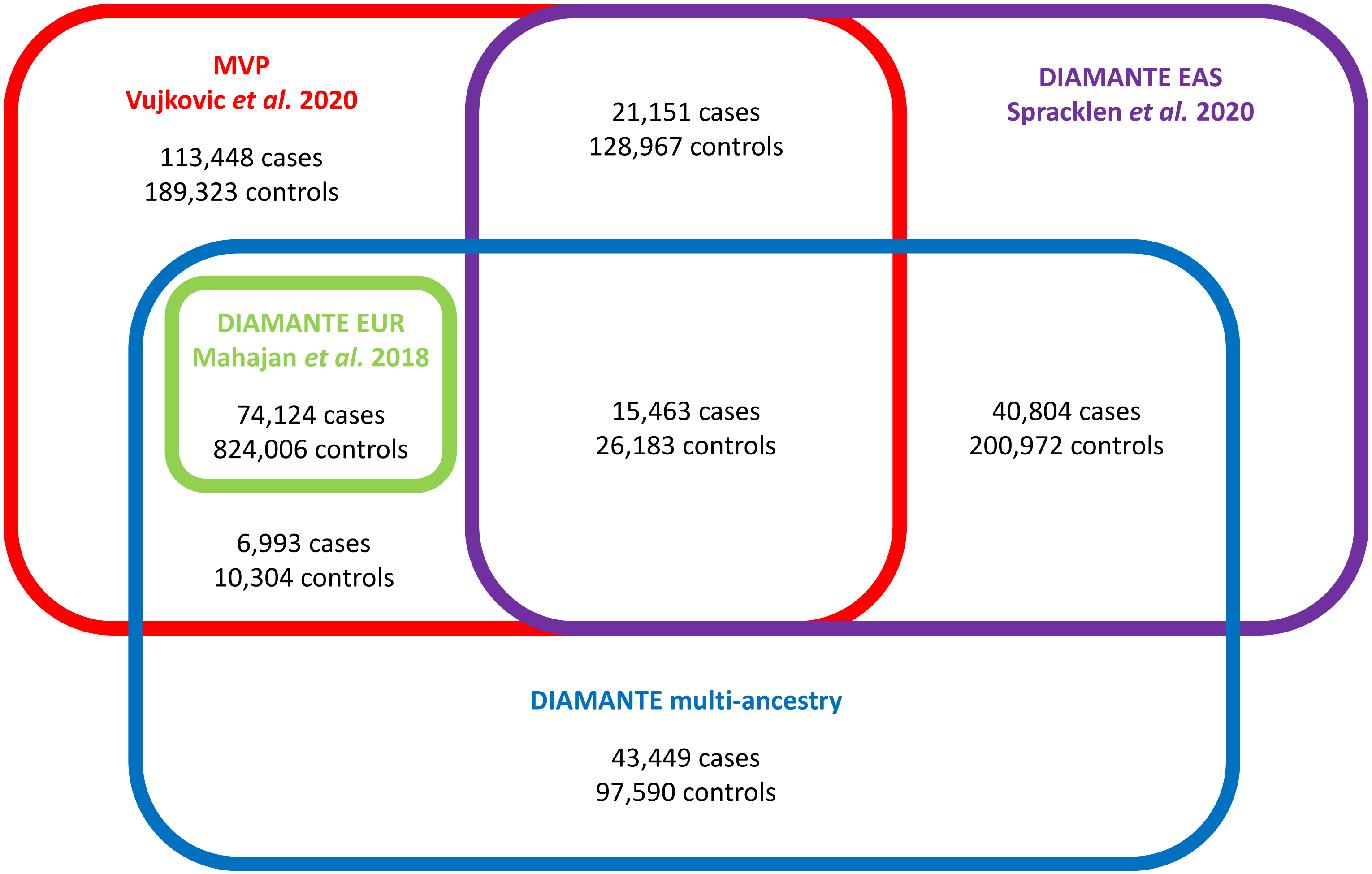

Supplementary Figure 2. Construction of loci across studies incorporating GWAS from the DIAMANTE Consortium. The locus encompassing T2D association signals at *INS-IGF2* and *KCNQ1* was defined by combining overlapping loci across studies and included the region spanning chromosome 11 from 1,697,132bp to 3,358,546bp (build 37).

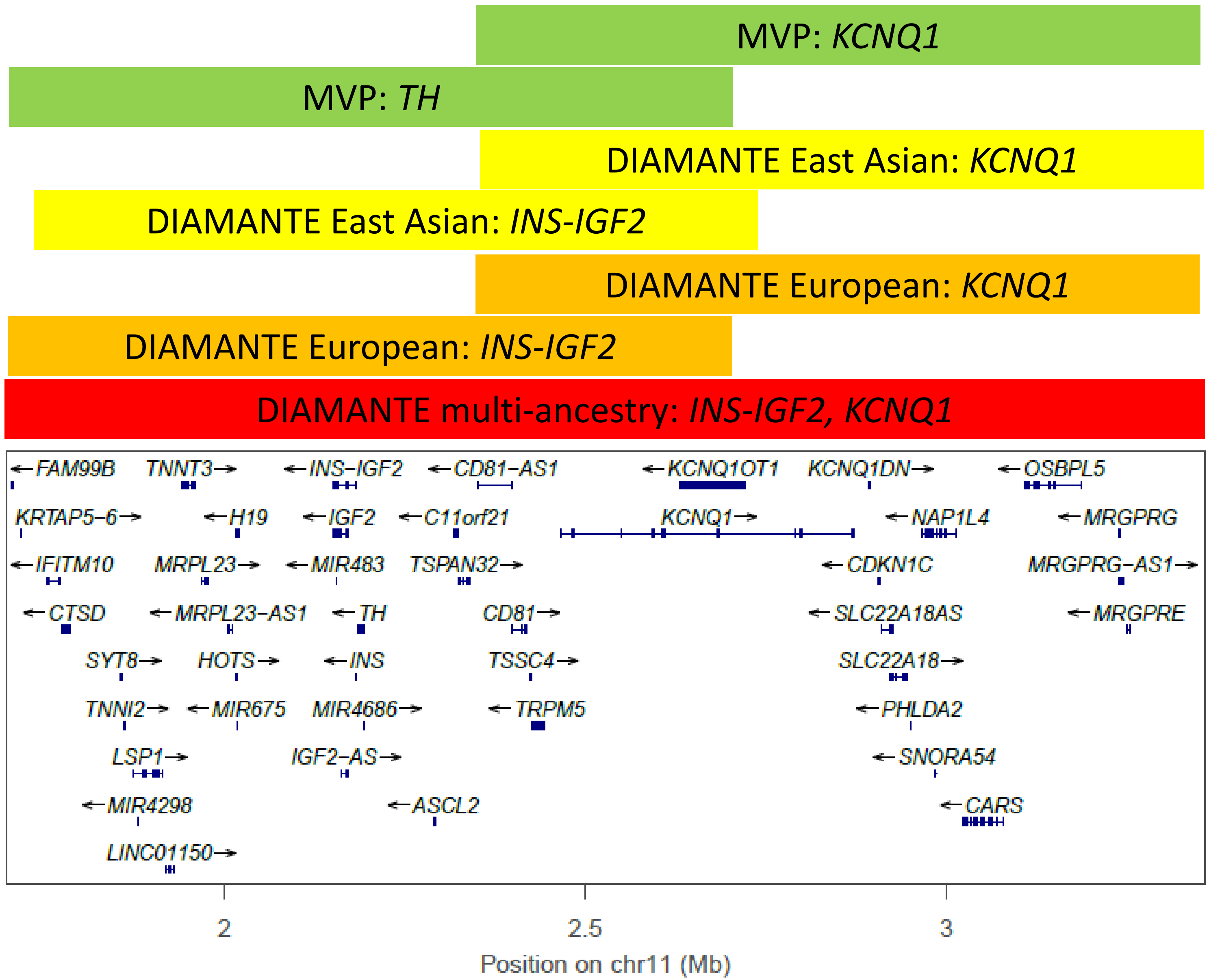

Supplementary Figure 3. Signal plots for distinct T2D association signals at the *TCF7L2* locus from multi-ancestry meta-regression (MR-MEGA) of up to 180,834 cases and 1,159,055 controls. Association summary statistics for each signal are obtained from approximate conditioning after adjusting for all other index SNVs at the locus. Each point represents a SNV passing quality control in the multi-ancestry meta-regression, plotted with their conditional *p*-value (on a -$\log_{10}$ scale) as a function of genomic position (NCBI build 37). In each plot, the index variant is represented by the purple diamond. Gene annotations are taken from the University of California Santa Cruz genome browser. Recombination rates are estimated from the Phase II HapMap.

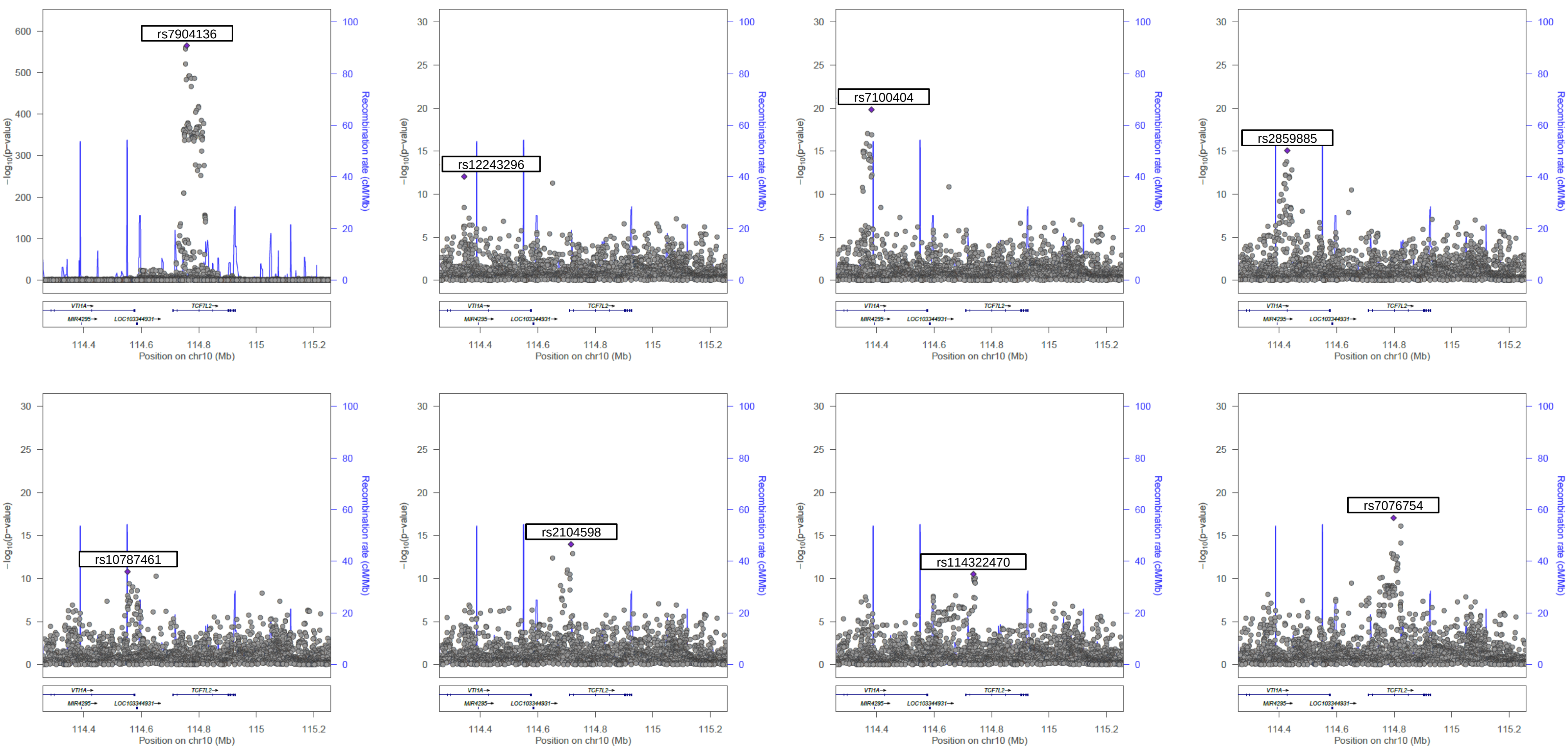

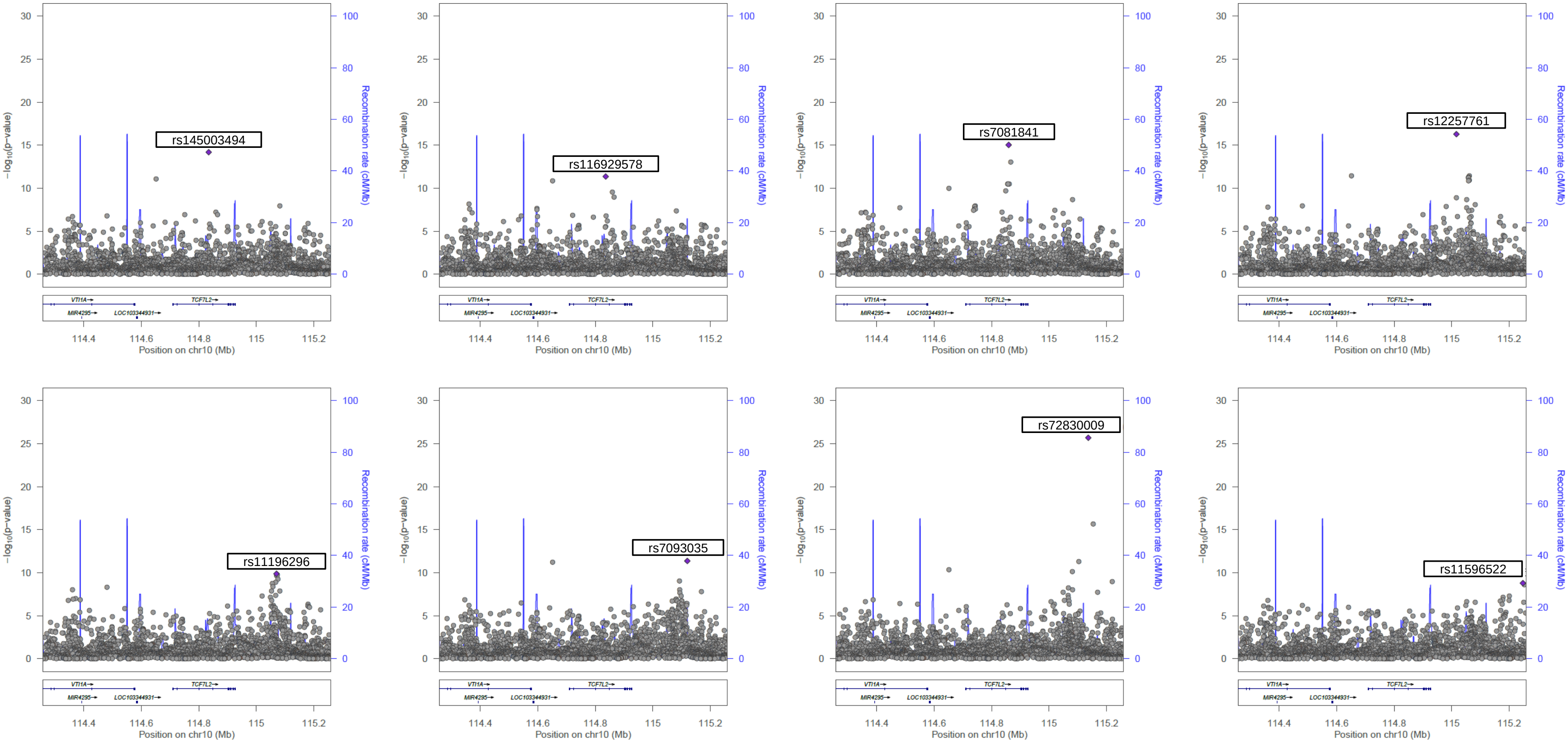
rs145003494
rs116929578
rs7081841
rs12257761
rs11196296
rs7093035
rs72830009
rs11596522
−log10(p−value)
Recombination rate (cM/Mb)
VTI1A
MIR4295
LOC103344931
TCF7L2
114.4
114.6
114.8
115
115.2
Position on chr10 (Mb)

Supplementary Figure 4. Signal plots for distinct T2D association signals at the *INS-IGF2-KCNQ1* locus from multi-ancestry meta-regression (MR-MEGA) of up to 180,834 cases and 1,159,055 controls. Association summary statistics for each signal are obtained from approximate conditioning after adjusting for all other index SNVs at the locus. Each point represents a SNV passing quality control in the multi-ancestry meta-regression, plotted with their conditional *p*-value (on a -$\log_{10}$ scale) as a function of genomic position (NCBI build 37). In each plot, the index variant is represented by the purple diamond. Gene annotations are taken from the University of California Santa Cruz genome browser. Recombination rates are estimated from the Phase II HapMap.

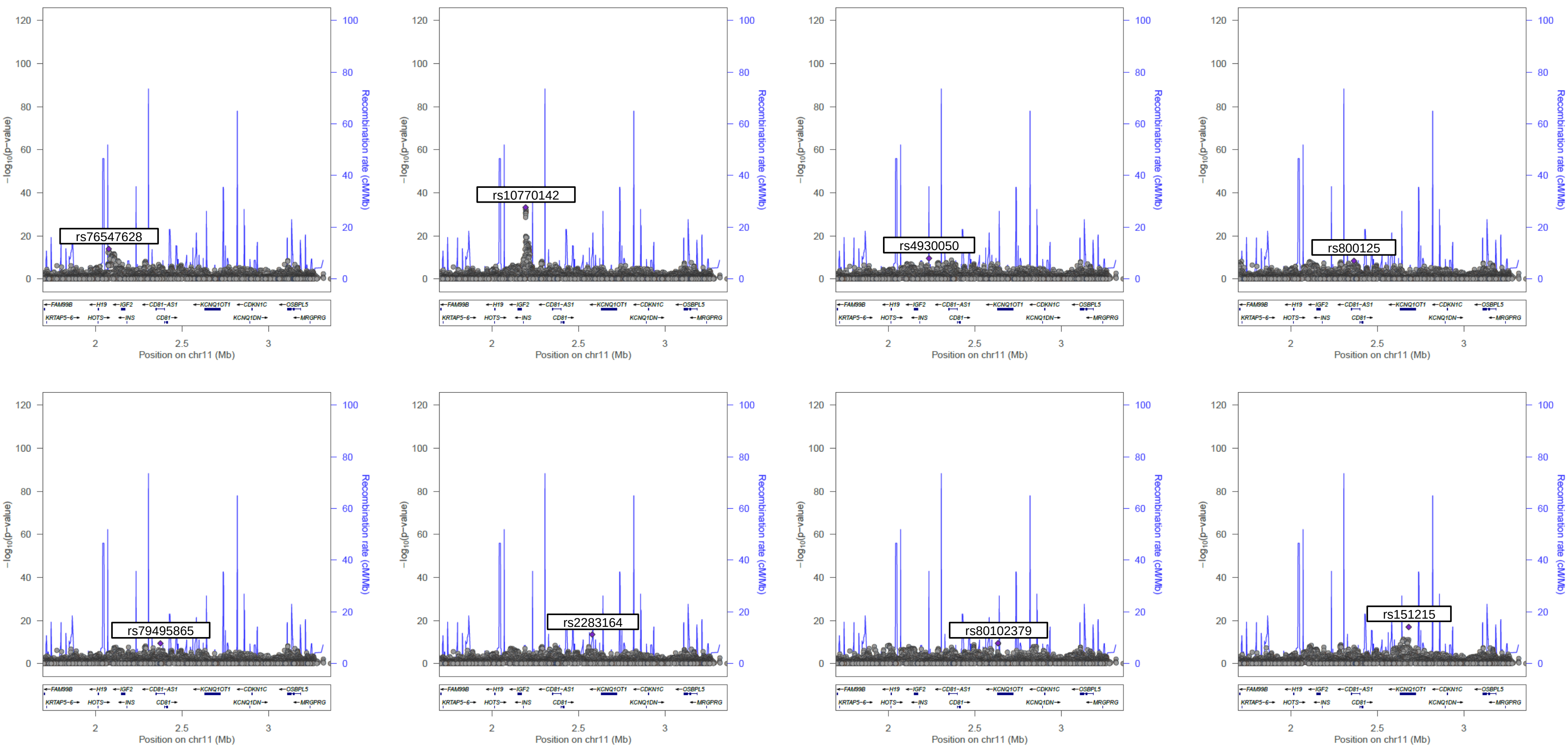

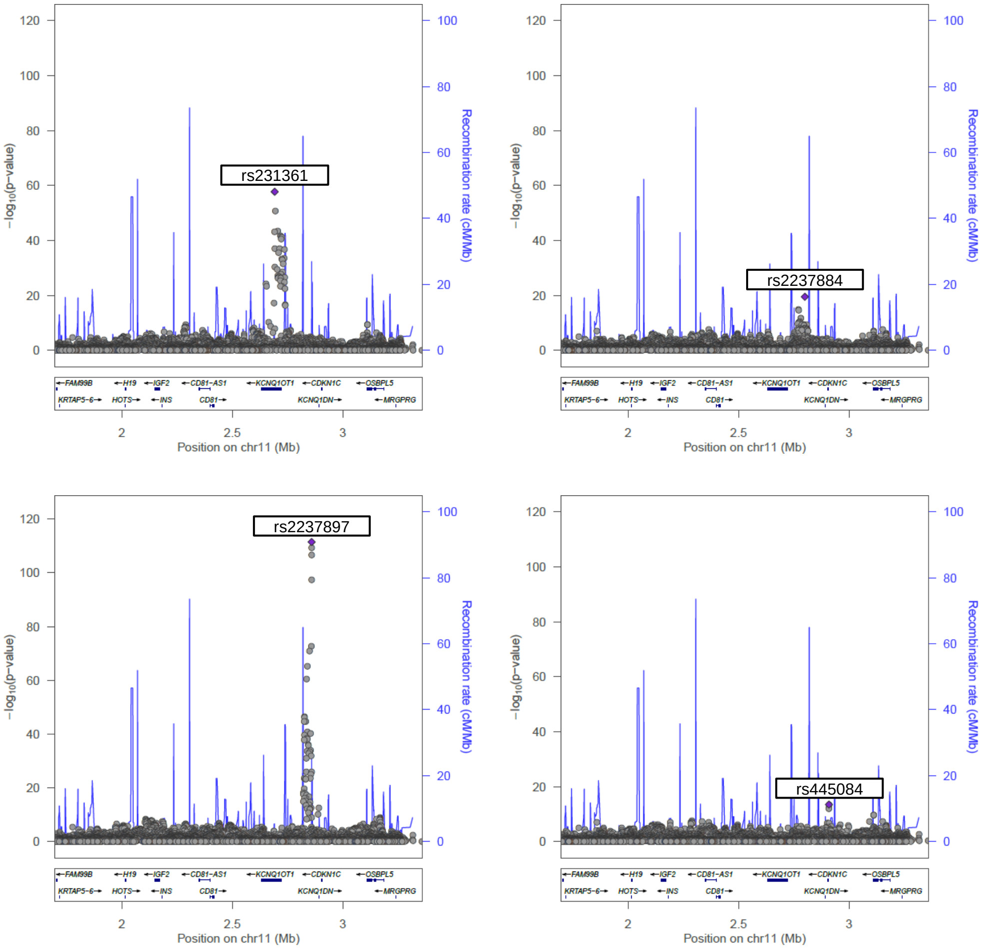
rs231361
rs2237884
rs4930011
rs234866
rs2237897
rs445084
−log10(p−value)
Recombination rate (cM/Mb)
Position on chr11 (Mb)
FAM99B
H19
IGF2
CD81−AS1
KCNQ1OT1
CDKN1C
OSBPL5
KRTAP5−6
HOTS
INS
CD81
KCNQ1DN
MRGPRG

Supplementary Figure 5. Comparison of ancestry-specific association summary statistics obtained from approximate conditional analysis undertaken in loci with multiple distinct signals using LD reference panels from the 1000 Genomes Project and GERA. (a) African ancestry-specific association summary statistics derived from 661 individuals of African ancestry from the 1000 Genomes Project and 1,000 African American individuals from GERA. Association summary statistics were derived from a meta-analysis of 15,487 T2D cases and 23,709 controls. In the left panel, each point represents the log-odds ratio from the approximate conditional analysis and the error bars represent 95% confidence limits. (b) Hispanic ancestry-specific association summary statistics derived from 347 individuals of Hispanic ancestry from the 1000 Genomes Project and 1,000 Hispanic individuals from GERA. Association summary statistics were derived from a meta-analysis of 12,385 T2D cases and 21,423 controls. In the left panel, each point represents the log-odds ratio from the approximate conditional analysis and the error bars represent 95% confidence limits.

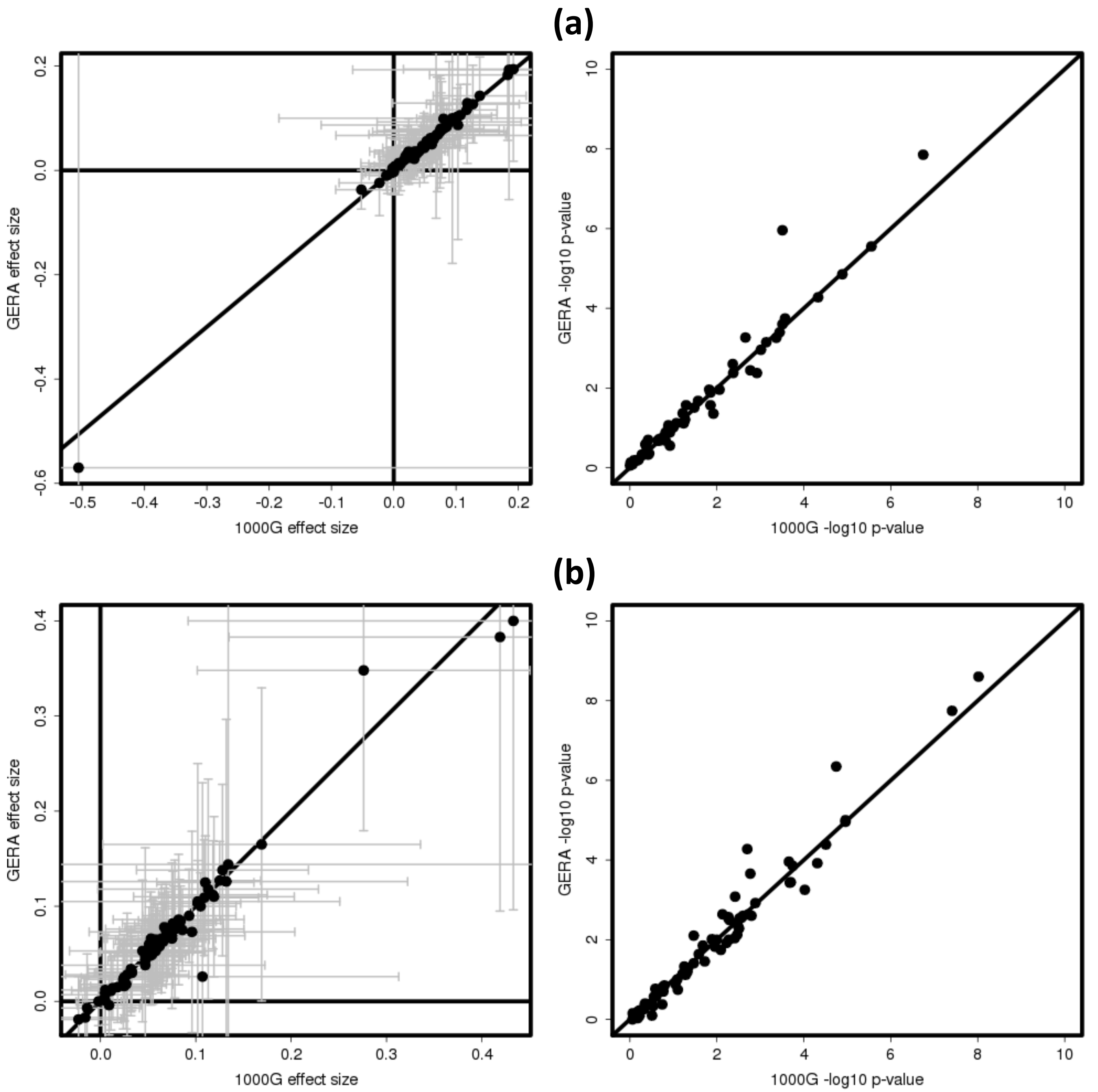

Supplementary Figure 6. Source of heterogeneity in allelic effects on T2D at the *CDKAL1* locus. (a) Forest plot presenting ancestry-specific allelic effects. The plot presents the risk allele frequency (RAF), the point represents the log-OR (BETA) for the risk allele, and the bars represent the corresponding 95% confidence interval (CI), from ancestry-specific fixed-effects meta-analysis. The size of each point represents the relative inverse-variance of the log-OR. The sample size contributing to each ancestry: African 15,043 cases and 22,318 controls; East Asian 56,268 cases and 227,155 controls; European 67,192 cases and 831,463 controls; Hispanic 11,027 cases and 18,885 controls; and South Asian 16,540 cases and 32,952 controls. (b) Correlation between study-level allelic effects and mean BMI. In the plot, each point represents a study contributing to the multi-ancestry meta-regression, plotted according to the mean BMI on the x-axis and the log-OR for the risk allele on the y-axis. The bars represent the 95% confidence interval for the log-OR. The red line is the line of best fit from linear regression of mean BMI on log-OR.

(a)

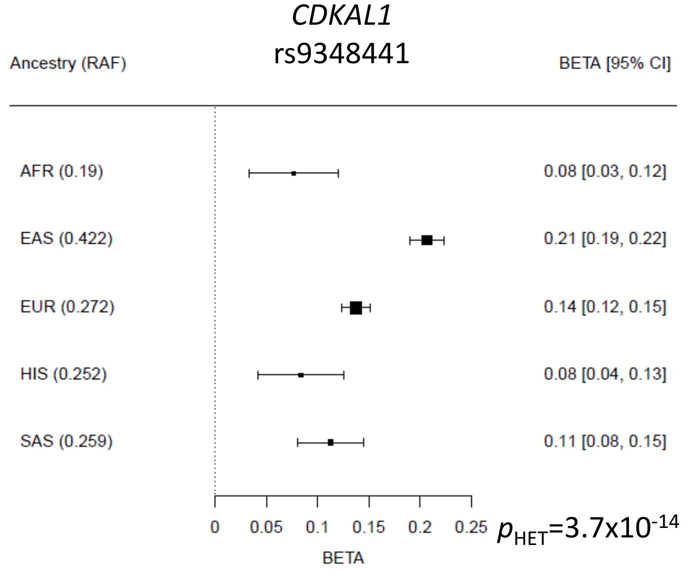

(b)

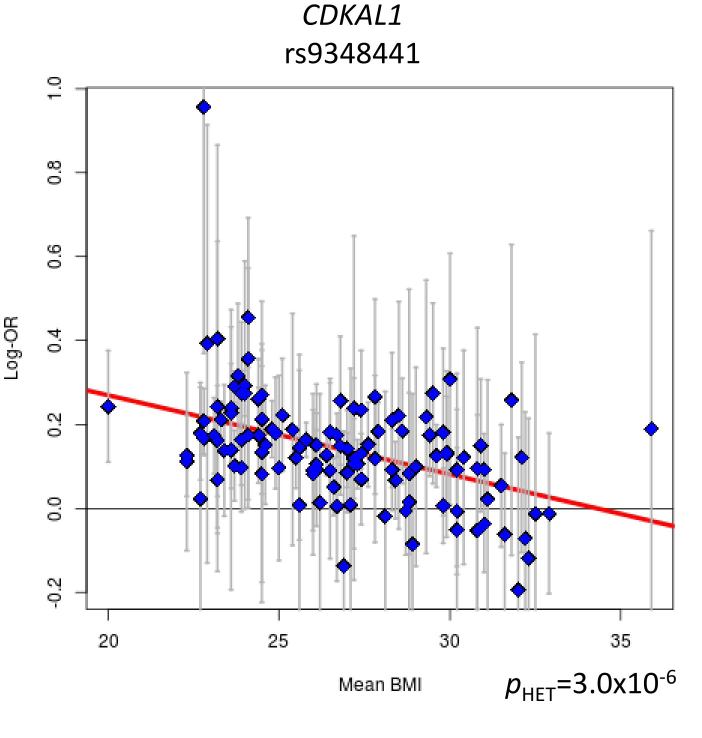

Supplementary Figure 7. Refinement of European ancestry-specific 99% credible set (under uniform prior model of causality) for T2D association at the *FTO* locus after multi-ancestry meta-regression (MR-MEGA) of up to 180,840 cases and 1,159,185 controls. Each point represents a credible set variant, plotted with their posterior probability of association as a function of genomic position (NCBI build 37). The index SNV (rs55872725) is represented by the purple symbol. The colour coding of all other SNVs indicates LD with the index variant in ancestry-specific haplotypes from the 1000 Genomes Project reference panel: red $r^2 \geq 0.8$; gold $0.6 \leq r^2 < 0.8$; green $0.4 \leq r^2 < 0.6$; cyan $0.2 \leq r^2 < 0.4$; blue $r^2 < 0.2$; grey r^2 unknown. Recombination rates are estimated from Phase II HapMap and gene annotations are taken from the University of California Santa Cruz genome browser.

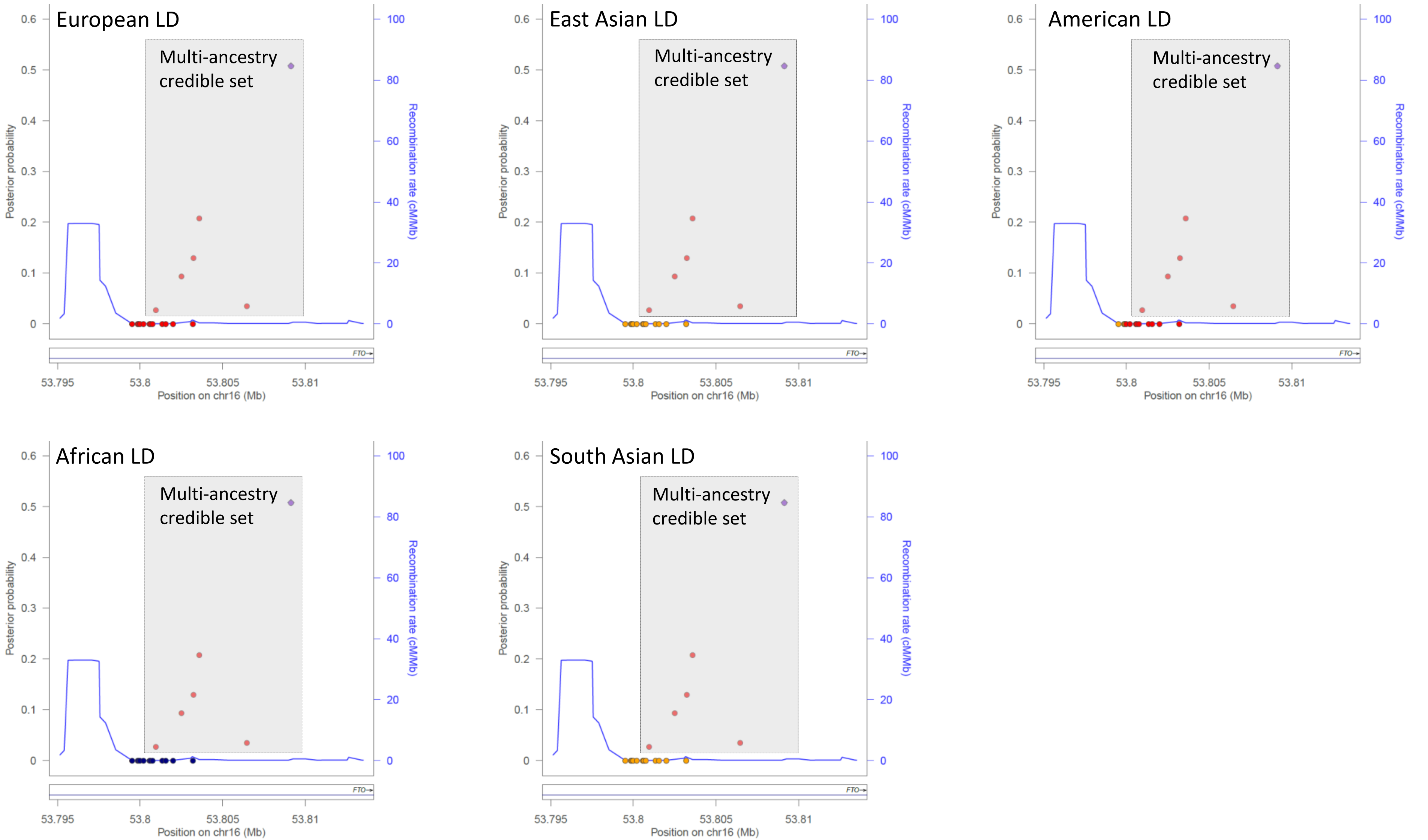

Supplementary Figure 8. Examples of improved fine-mapping of T2D association signals driven by missense variants from multi-ancestry meta-regression (MR-MEGA) of up to 180,834 cases and 1,159,055 controls. Each point represents a SNV passing quality control in the multi-ancestry meta-regression, plotted with their annotation-informed posterior probability of driving T2D association as a function of genomic position (NCBI build 37). In each plot, the index variant is represented by the purple diamond. Gene annotations are taken from the University of California Santa Cruz genome browser. Recombination rates are estimated from the Phase II HapMap.

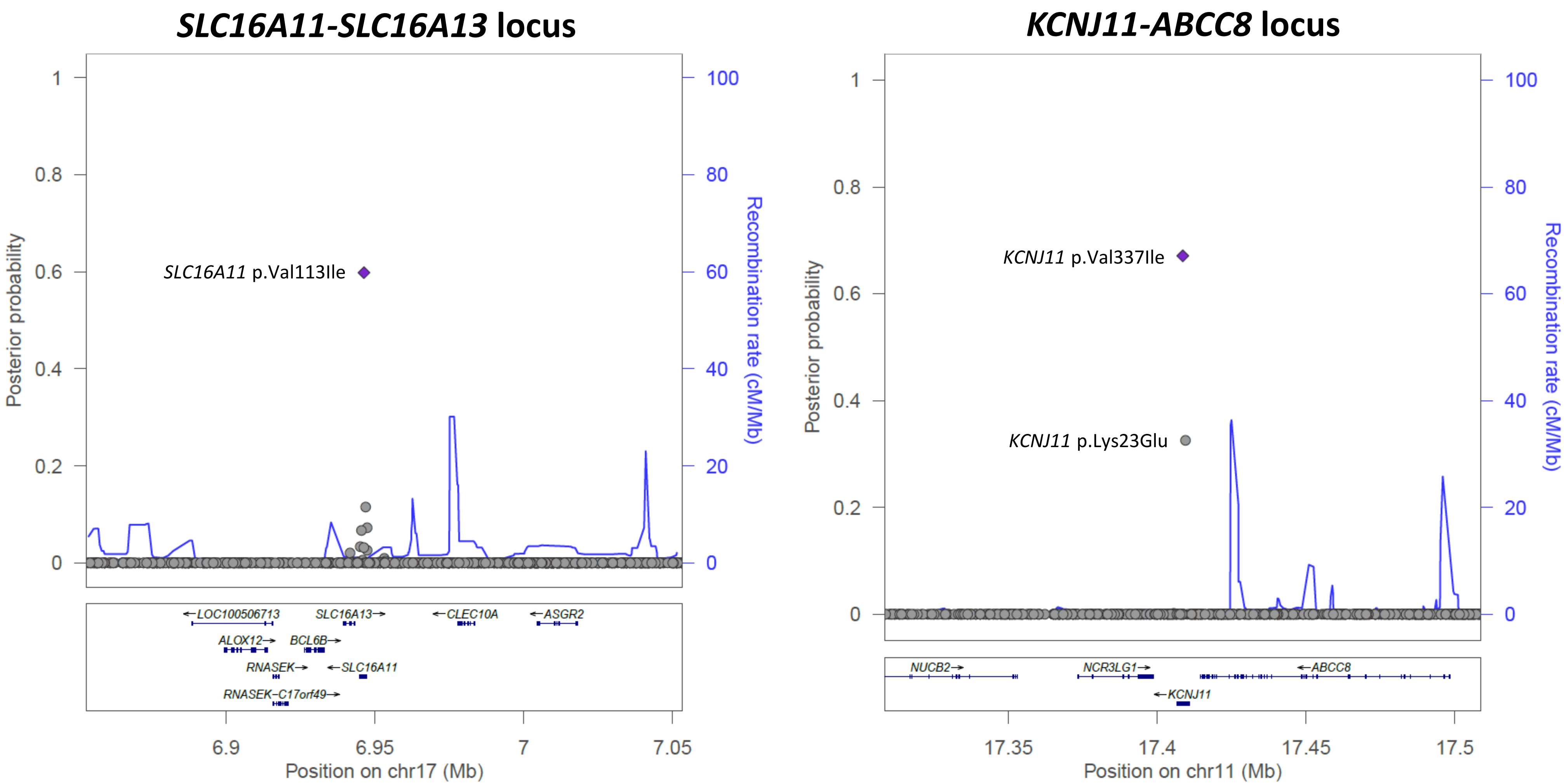

Supplementary Figure 9. The role of coding variation in driving T2D association signals at the *ZFAND3-KCNK16-GLP1R* locus from multi-ancestry meta-regression (MR-MEGA) of up to 180,834 cases and 1,159,055 controls (effective sample size 492,191). Each point represents a SNV passing quality control in the meta-regression, plotted with their annotation-informed posterior probability of driving T2D association as a function of genomic position (NCBI build 37). In each plot, the index variant is represented by the purple diamond. Gene annotations are taken from the University of California Santa Cruz genome browser. Recombination rates are estimated from the Phase II HapMap. (a) Association signal indexed by rs2281342 is driven by novel high-confidence missense variant *GLP1R* p.Pro7Leu (rs10305420). (b) The 99% credible set for the association signal indexed by rs742762, a non-coding SNV, includes *GLP1R* p.Arg131Gln (rs3765467). (c) The 99% credible set for the signal indexed by rs3734618 includes three missense variants that together account for 61.4% of the posterior probability of driving the association: *KCNK17* p.Ser21Gly (rs10947804, π=39.2%); *KCNK16* p.Pro254His (rs11756091, π=14.8%); and *KCNK16* p.Ala277Glu (rs1535500, π=13.7%).

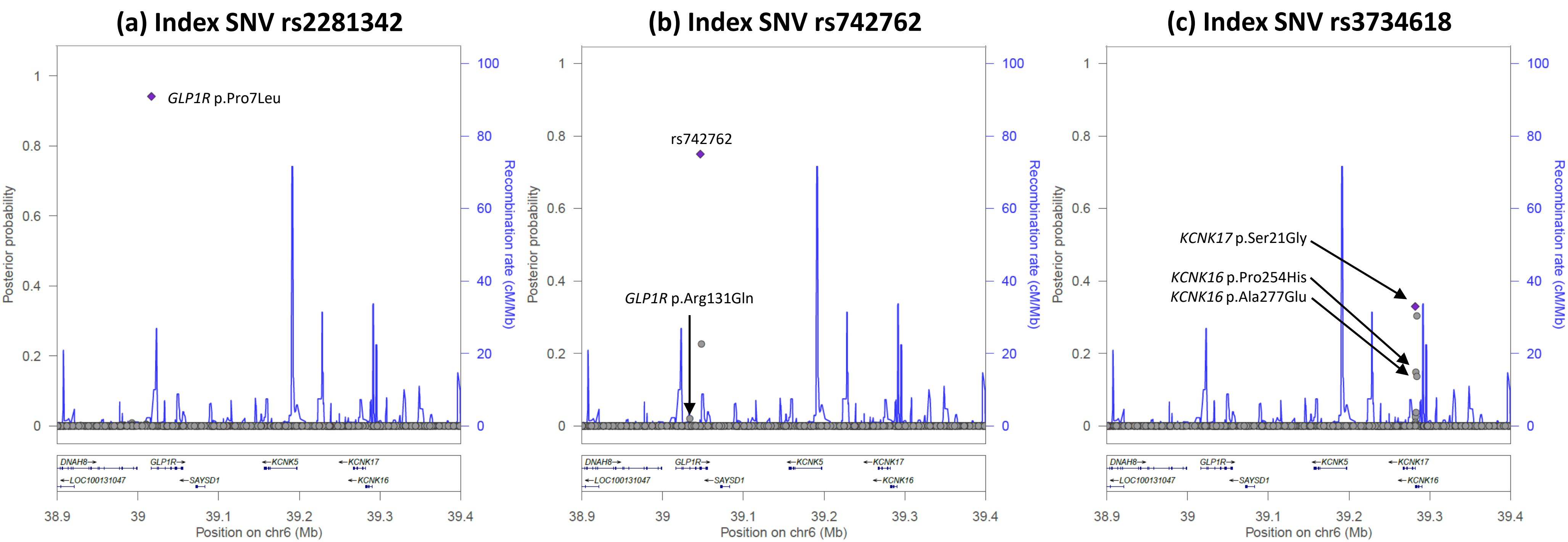

Supplementary Note Table 1. Comparison of sample size, distribution of ancestry groups and analytical strategies utilised by four studies that incorporate GWAS from the DIAMANTE Consortium.

Study	Sample size cases/control	Ancestry-specific sample size: cases/controls (% effective sample size)				Genome-wide significance	Meta-analysis strategy	Correction for residual population structure	Variants interrogated
		AFR	ASN	EUR	HIS				
DIAMANTE European ancestry-specific (Mahajan et al. 2018)	74,124/824,006			74,124/824,006 (100%)		$p<5x10^{-8}$	Fixed-effects (inverse-variance weighted)	Double genomic control	HRC reference panel
DIAMANTE East Asian ancestry-specific (Spracklen et al. 2020)	77,418/356,122		77,418/356,122 (100%)			$p<5x10^{-8}$	Fixed-effects (inverse-variance weighted)	Double genomic control (LDSC intercept after meta-analysis)	1000G reference panel
MVP (Vujkovic et al. 2020)	228,499/1,178,783	24,646/31,446 (7.5%)	46,511/169,776 (19.8%)	148,726/965,732 (70.0%)	8,616/11,829 (2.7%)	$p<5x10^{-8}$	Fixed-effects (inverse-variance weighted)	None	1000G or HRC reference panels, MAF >1% per ancestry group
DIAMANTE multi-ancestry	180,834/1,159,005	15,487/23,709 (6.6%)	72,808/260,107 (36.7%)	80,154/853,816 (51.1%)	12,385/21,423 (5.6%)	$p<5x10^{-9}$	Meta-regression (ancestry correlated heterogeneity)	Double genomic control	Overlap of 1000G and HRC reference panels, MAF >0.5% in at least one ancestry group

AFR: African ancestry. ASN: South and East Asian ancestry. EUR: European ancestry. HIS: Hispanic ancestry. LDSC: LD Score regression. HRC: Haplotype Reference Consortium. 1000G: 1000 Genomes Project.

Supplementary Note Table 2. Overlap of loci reported at genome-wide significance (p<5x10^{-8}) by four studies that incorporate GWAS from the DIAMANTE Consortium: details of sample sizes and analytical approaches summarised in Supplementary Note Table 1.

Locus	Chr	Interval (bp, b37)	DIAMANTE European ancestry			DIAMANTE East Asian ancestry			MVP trans-ancestry/ancestry-specific			DIAMANTE multi-ancestry		
			Lead SNV	Position	*p*-value	Lead SNV	Position	*p*-value	Lead SNV	Position	*p*-value	Lead SNV	Position	*p*-value
PHF13	1	6,172,729-7,172,729							rs11583755	6,672,729	1.3E-19			
MTOR	1	10,817,932-11,817,932							rs7554251	11,317,932	2.9E-11			
PLEKHM2	1	15,550,470-16,550,470							rs12746673	16,050,470	3.3E-10			
VWA5B1, LINC01141	1	20,188,352-21,229,451				rs60573766	20,688,352	4.3E-10	rs10916780	20,707,153	1.6E-13	rs10916784	20,729,451	1.2E-11
C1orf172, TRIM63	1	25,896,065-27,784,913							rs9438610	26,396,065	6.7E-10			
YTHDF2	1	28,560,898-29,560,898							rs3753693	29,060,898	1.1E-10			
	1	32,696,120-33,696,120							rs59020573	33,196,120	1.3E-8			
EVA1B	1	36,289,546-37,289,546							rs12116935	36,789,546	1.5E-8			
MACF1	1	39,355,177-40,535,928	rs3768321	40,035,928	1.3E-26	rs371894931	39,942,242	2.7E-11	rs61779284	39,855,177	1.4E-48	rs3768301	39,870,793	6.2E-31
MAST2	1	45,744,900-46,858,862				rs562138031	46,244,900	4.0E-12				rs34444543	46,358,862	5.5E-13
FAF1	1	50,691,935-51,756,091	rs58432198	51,256,091	1.8E-10	rs11205766	51,191,935	7.5E-15	rs79090772	51,209,148	1.3E-28	rs12073283	51,219,188	6.7E-18
PATJ, INADL	1	62,079,891-63,079,891	rs12140153	62,579,891	1.2E-8				rs12140153	62,579,891	5.0E-8	rs12140153	62,579,891	1.4E-8
PGM1	1	63,607,284-64,614,429				rs2269245	64,107,893	5.4E-10	rs2269247	64,107,284	3.4E-13	rs11576729	64,114,429	2.5E-17
LEPR	1	65,489,878-66,489,878							rs10889560	65,989,878	2.1E-9			
SGIP1	1	66,510,654-67,510,654							rs4655617	67,010,654	1.7E-10			
NEGR1	1	72,251,552-73,251,552							rs2613499	72,751,552	1.0E-11			
	1	91,548,779-92,548,779							rs4658234	92,048,779	9.1E-9			
RP11-147C23.1	1	95,904,462-96,904,462							rs10159026	96,404,462	2.0E-9			
FAM212B-AS1, ST7L	1	111,789,983-113,606,633							rs197374	112,289,983	7.8E-9	rs12137269	113,106,633	6.1E-9
DENND2C	1	114,644,899-115,644,899	rs184660829	115,144,899	2.5E-8									
PTGFRN, FAM46C	1	117,032,790-118,669,463	rs1127215	117,532,790	2.3E-13				rs1127215	117,532,790	1.8E-26	rs1127215	117,532,790	3.9E-17
NOTCH2	1	119,955,586-121,026,982	rs1493694	120,526,982	2.1E-16				rs2453051	120,499,573	1.1E-23	rs835576	120,455,586	2.8E-17
CHD1L	1	146,214,427-147,621,000							rs79489938[a]	147,121,000	4.8E-8	rs11588753	146,714,427	4.8E-8
SV2A	1	149,391,028-150,391,028							rs72692804	149,891,028	2.9E-10			
FAM63A, BNIPL	1	150,517,991-151,517,991	rs145904381	151,017,991	2.2E-8				rs145904381	151,017,991	4.0E-13			
ATP8B2, PKLR	1	153,824,384-155,769,776							rs3020781	155,269,776	7.3E-12			
DNM3	1	171,868,310-172,868,310							rs7546252	172,368,310	2.0E-10			
SEC16B	1	177,378,933-178,389,025	rs539515	177,889,025	1.2E-10	rs532504	177,878,933	7.4E-12	rs539515	177,889,025	5.4E-15	rs539515	177,889,025	4.6E-20
	1	178,748,952-179,748,952							rs2816177	179,248,952	6.8E-9			
LAMC1	1	182,504,334-183,504,334							rs4129858	183,004,334	4.4E-9			
TSEN15	1	183,514,593-184,535,116				rs1327123	184,014,593	7.0E-9	rs1327123	184,014,593	6.8E-10	rs1952256	184,035,116	2.6E-8
ZNF281	1	199,697,538-200,916,099							rs12128213	200,197,538	1.5E-9	rs10919928	200,416,099	4.6E-9
IPO9	1	201,349,926-202,349,926							rs41304257	201,849,926	8.5E-12			
CNTN2, MDM4, DSTYK, SRGAP2	1	203,974,581-207,121,028	rs12048743	205,114,873	4.4E-9	rs201297151	204,474,581	3.4E-8	rs61817176	206,621,028	3.6E-11	rs6689629	204,539,291	2.4E-10
PROX1	1	213,655,398-214,659,256	rs340874	214,159,256	5.6E-26	rs12403994	214,155,398	6.1E-12	rs340874	214,159,256	6.5E-45	rs340874	214,159,256	2.5E-33
LYPLAL1	1	219,248,818-220,248,818	rs2820446	219,748,818	3.7E-16				rs2820446	219,748,818	2.3E-22	rs2820446	219,748,818	2.7E-18
ABCB10, NUP133	1	229,142,499-230,172,955	rs348330	229,672,955	3.9E-14	rs238763	229,642,499	5.0E-11	rs348330	229,672,955	2.8E-20	rs348330	229,672,955	3.7E-18
GNG4, TBCE	1	235,042,023-236,190,800	rs291367	235,690,800	6.1E-10				rs10737818	235,542,023	2.0E-11			
TMEM18	2	0-1,153,874	rs62107261	422,144	1.8E-11	rs10634531	632,789	2.4E-17	rs10188334	653,874	2.5E-24	rs6548240	636,929	2.2E-25
FAM49A, AC142119.1	2	15,738,001-17,074,669	rs11680058	16,574,669	1.3E-8				rs28758542	16,238,001	1.7E-9	rs11680058	16,574,669	1.6E-8
	2	18,207,873-19,207,873							rs11096542	18,707,873	3.0E-9			
DTNB, KIF3C	2	25,033,568-26,692,802	rs17802463	25,643,221	3.5E-8				rs34845373	25,635,771	5.3E-12	rs55928417	25,533,568	4.0E-11

GCKR	2	27,230,940-28,230,940	rs1260326	27,730,940	1.3E-24	rs1260326	27,730,940	1.0E-21	rs1260326	27,730,940	2.2E-57	rs1260326	27,730,940	4.6E-38
HEATR5B	2	36,704,168-37,704,168							rs77424687	37,204,168	2.9E-9			
THADA	2	43,111,883-44,198,028	rs80147536	43,698,028	2.7E-30				rs76675804	43,611,883	1.3E-59	rs13414140	43,671,176	5.2E-31
SIX3, SIX2	2	44,692,080-45,692,080				rs12712928	45,192,080	1.8E-14				rs12712928	45,192,080	2.4E-14
EML6	2	54,657,914-55,657,914							rs5010712	55,157,914	2.9E-9			
BNIPL, LINC01122	2	58,461,136-59,807,725	rs10193538	58,981,064	1.7E-8				rs12986742	58,975,143	5.5E-21	rs17049712	58,961,136	2.3E-9
BCL11A, AC007381.2	2	60,083,665-61,086,707	rs243024	60,583,665	4.4E-20	rs243018	60,586,707	1.5E-15	rs243018	60,586,707	1.2E-39	rs243018	60,586,707	6.7E-35
CEP68	2	64,779,414-66,166,674	rs2249105	65,287,896	1.2E-15				rs2723065	65,279,414	7.2E-28	rs6752053	65,666,674	4.1E-24
ETAA1	2	67,122,243-68,122,243							rs4671799	67,622,243	5.3E-11			
KDM3A	2	86,207,504-87,207,504							rs4832290	86,707,504	3.9E-8			
AFF3	2	100,098,726-101,098,726							rs34506349	100,598,726	1.0E-8			
	2	104,665,674-105,665,674							rs10469860	105,165,674	3.8E-8			
TMEM87B, LOC541471, BCL2L11	2	111,387,754-113,323,114							rs113135335	111,887,754	2.1E-13	rs1345203	112,253,851	2.9E-8
DDX18	2	117,571,061-118,571,061	rs562386202	118,071,061	4.2E-8									
SCTR	2	119,731,070-120,731,070				rs3731600	120,231,070	6.9E-9						
GLI2	2	120,817,747-121,847,612	rs11688682	121,347,612	1.4E-14				rs9308614	121,337,196	4.5E-23	rs11677557	121,317,747	6.5E-15
TEX41	2	145,226,656-146,850,724							rs6716394	146,350,724	1.5E-13			
PABPC1P2	2	147,361,633-148,361,633	rs35999103	147,861,633	8.3E-9									
EPC2	2	148,928,856-150,068,261				rs200576292	149,568,261	1.3E-9	rs66877183	149,428,856	3.0E-8			
	2	151,698,598-152,698,598							rs3845843	152,198,598	2.4E-12			
ACVR1C, CYTIP	2	157,839,550-158,949,081	rs13426680	158,339,550	6.4E-10				rs149447188	158,449,081	2.0E-10	rs7594480	158,390,468	4.0E-12
RBMS1	2	160,635,544-161,833,872	rs3772071	161,135,544	1.6E-11				rs6710938	161,333,872	1.6E-13	rs1020731	161,144,055	1.2E-9
KCNH7	2	163,123,932-164,149,480							rs305686	163,623,932	2.3E-8	rs12614955	163,649,480	8.6E-10
GRB14, COBLL1	2	164,881,518-166,013,091	rs10195252	165,513,091	1.6E-20	rs75536691	165,381,518	1.2E-15	rs10184004	165,508,389	4.4E-54	rs10184004	165,508,389	5.2E-34
GALNT3	2	166,110,827-167,111,006							rs13406280	166,610,827	5.7E-12	rs62174818	166,611,006	3.9E-8
HAT1	2	172,296,774-173,296,774							rs62182438	172,796,774	1.1E-8			
SP9	2	174,697,545-175,697,545							rs12992995	175,197,545	1.1E-8			
TTN	2	179,150,954-180,150,954							rs6715901	179,650,954	1.2E-8			
SCHLAP1	2	181,070,507-182,118,654							rs6741676	181,618,654	6.5E-15	rs12479357	181,570,507	1.8E-8
	2	196,452,010-197,452,010							rs6712905	196,952,010	2.1E-11			
RP11-686O6.2	2	202,735,139-203,735,139							rs6714523	203,235,139	6.3E-11			
AC016903.2	2	204,875,909-205,875,909							rs4482463	205,375,909	1.8E-8			
PLEKHM3	2	208,370,017-209,370,017							rs34329895	208,870,017	1.4E-10			
ERBB4	2	211,774,937-212,774,937							rs3828242	212,274,937	6.5E-9			
AC079610.1, IKZF2	2	213,187,103-214,329,721				rs75179644	213,687,103	5.4E-10	rs4673712	213,829,721	1.7E-9	rs16849467	213,818,731	4.8E-9
PNKD, CRYBA2	2	218,668,432-220,359,171							rs113414093	219,859,171	1.7E-8			
IRS1	2	226,600,490-227,605,921	rs2972144	227,101,411	7.9E-46				rs2943650	227,105,921	1.9E-81	rs2943648	227,100,490	3.6E-52
SPHKAP	2	228,471,884-229,471,884							rs13415288	228,971,884	9.2E-11			
ATG16L1, DGKD	2	233,691,103-234,803,281				rs117809958	234,191,103	2.0E-15	rs838720	234,303,281	4.3E-18	rs117809958	234,191,103	5.6E-12
	3	3,149,850-4,149,850							rs9842137[a]	3,649,850	9.3E-9			
SETD5	3	9,014,016-10,014,016							rs3872707	9,514,016	9.8E-12			
PPARG	3	11,829,783-12,885,357	rs11709077	12,336,507	1.6E-27	rs3963364	12,385,357	3.5E-11	rs17036160	12,329,783	1.5E-53	rs17036160	12,329,783	2.9E-38
ANKRD28	3	15,206,124-16,206,124							rs924753	15,706,124	1.2E-11			
UBE2E2	3	22,758,614-23,957,080	rs35352848	23,455,582	9.5E-20	rs11926494	23,258,614	2.7E-37	rs13094957	23,457,080	2.4E-42	rs13094957	23,457,080	5.2E-48
LINC00693	3	28,231,810-29,231,810							rs9869477	28,731,810	4.1E-9			
	3	35,170,150-36,170,150							rs1470560	35,670,150	1.2E-9			
	3	36,370,230-37,370,230							rs11129735[a]	36,870,230	1.5E-8			
KIF9, SMARCC1	3	46,425,539-48,193,664	rs11926707	46,925,539	1.5E-8				rs62262091	47,693,664	1.5E-10			

RBM6	3	49,480,596-50,674,197	rs4688760	49,980,596	4.5E-10				rs6792892	49,995,518	1.4E-14	rs2624847	50,174,197	6.2E-11
RFT1	3	52,625,429-53,627,677	rs2581787	53,127,677	3.0E-8				rs62255926	53,125,429	4.2E-8	rs2581787	53,127,677	2.0E-8
CACNA2D3	3	54,328,827-55,328,827	rs76263492	54,828,827	6.3E-9				rs76263492	54,828,827	3.2E-9	rs76263492	54,828,827	8.7E-10
PXK	3	57,838,809-58,838,809										rs12629058	58,338,809	3.5E-11
PSMD6, ATXN7, ADAMTS9	3	63,384,800-65,203,394	rs9860730	64,701,146	7.4E-15	rs67114627	63,904,715	9.1E-32	rs13434089	63,948,566	4.5E-31	rs704360	63,884,800	8.0E-33
	3	70,020,917-71,020,917							rs12494424	70,520,917	2.3E-8			
	3	71,148,868-72,148,868							rs853866	71,648,868	2.7E-8			
SHQ1	3	72,303,590-73,365,183	rs13085136	72,865,183	1.4E-8				rs9814945	72,803,590	3.3E-11			
ROBO2	3	77,171,721-78,171,721	rs2272163	77,671,721	1.2E-8				rs2272163	77,671,721	3.6E-9			
	3	86,256,871-87,256,871							rs6549112	86,756,871	1.6E-11			
RP11-159G9.5	3	87,630,136-88,630,136							rs73146095	88,130,136	7.9E-9			
	3	89,486,280-90,486,280							rs11716527[a]	89,986,280	6.7E-9			
	3	93,481,060-94,481,060							rs978444	93,981,060	3.5E-9			
SIDT1	3	112,788,430-113,788,430							rs11929640	113,288,430	8.5E-9			
ZBTB20	3	114,460,798-115,563,672				rs6806156	114,968,018	1.6E-11	rs7645613	115,063,672	1.5E-12	rs1459513	114,960,798	9.6E-15
CASR	3	121,461,461-122,465,199				rs9859381	121,965,199	2.9E-9	rs13059382	121,961,461	1.4E-9			
ADCY5	3	122,565,778-123,674,832	rs11708067	123,065,778	1.3E-31	rs60054445	123,174,832	5.6E-12	rs11708067	123,065,778	1.6E-57	rs11708067	123,065,778	3.4E-46
SLC12A8	3	124,421,457-125,426,637	rs649961	124,926,637	1.3E-9	rs12497133	124,921,920	1.1E-8	rs9873519	124,921,457	2.5E-22	rs9873519	124,921,457	6.5E-14
TMCC1, PLXND1	3	128,079,324-129,833,182	rs9828772	129,333,182	4.2E-8				rs2255703	129,293,256	3.7E-11			
CPNE4	3	131,250,844-132,250,844							rs9857204	131,750,844	2.2E-10			
STAG1	3	135,569,472-136,569,472							rs667920	136,069,472	5.8E-13			
	3	137,555,136-138,555,136							rs6766859	138,055,136	8.1E-12			
ZBTB38	3	140,601,839-141,601,839							rs56243018	141,101,839	8.9E-16			
TSC22D2, TM4SF4	3	148,721,563-150,566,540	rs62271373	150,066,540	1.0E-9				rs28712435	149,221,563	6.1E-11	rs62271373	150,066,540	2.6E-8
MBNL1	3	151,584,243-152,932,042	rs111729685	152,086,533	3.6E-9	rs1850421	152,382,352	1.4E-9	rs7633673	152,084,243	8.2E-16	rs9877505	152,432,042	1.4E-13
LEKR1, CCNL1	3	156,295,525-157,295,525										rs9854955	156,795,525	1.4E-8
TRIM59	3	159,653,305-160,653,305							rs7629	160,153,305	8.2E-14			
EGFEM1P	3	167,718,841-168,726,052	rs7629630	168,218,841	2.2E-8				rs13099581	168,226,052	1.3E-10			
SLC2A2	3	170,143,788-171,233,076	rs9873618	170,733,076	8.5E-21	rs201018682	170,643,788	1.0E-11	rs8192675	170,724,883	3.9E-27	rs8192675	170,724,883	3.5E-28
NLGN1	3	172,607,443-174,210,695							rs247975	173,107,443	2.0E-11			
CCDC39, FXR1	3	180,045,384-181,045,384										rs4854992	180,545,384	9.3E-9
ABCC5	3	183,238,460-184,238,460	rs2872246	183,738,460	1.8E-8				rs2872246	183,738,460	2.6E-11			
IGF2BP2	3	184,382,015-186,034,482	rs6780171	185,503,456	2.5E-58	rs13092876	185,495,320	1.9E-66	rs9859406	185,534,482	2.0E-169	rs7633675	185,510,613	5.8E-131
ST6GAL1	3	186,149,931-187,165,645	rs3887925	186,665,645	1.4E-17	rs11332772	186,649,931	1.1E-10	rs3887925	186,665,645	1.1E-25	rs3887925	186,665,645	3.8E-22
BCL6, LPP	3	187,198,333-188,241,842	rs4686471	187,740,899	3.1E-20	rs13086331	187,698,333	7.3E-9	rs6777684	187,741,842	1.5E-35	rs4686471	187,740,899	2.9E-21
TFRC	3	195,325,077-196,331,237				rs9866168	195,830,310	1.5E-9	rs9872347	195,831,237	5.4E-14	rs74289356	195,825,077	6.8E-12
CTBP1, PCGF3, MAEA	4	220,681-2,284,605	rs56337234	1,784,403	1.4E-17	rs7656416	1,254,535	9.0E-42	rs730831	1,240,299	4.8E-34	rs730831	1,240,299	7.6E-41
HTT	4	2,741,845-3,741,845	rs362307	3,241,845	1.1E-9				rs362307	3,241,845	3.3E-8			
WFS1	4	5,793,237-6,806,763	rs10937721	6,306,763	1.6E-40	rs147834269	6,303,731	9.1E-12	rs10937721	6,306,763	7.2E-70	rs9998835	6,293,237	3.1E-51
LCORL	4	17,292,869-18,547,401	rs12640250	17,792,869	4.5E-8				rs2169033	18,044,357	1.4E-15	rs6855926	18,047,401	8.4E-12
SLIT2	4	19,765,535-20,765,535							rs7664347	20,265,535	9.5E-9			
GNPDA2	4	44,003,503-45,686,139	rs10938398	45,186,139	4.9E-12	rs10938398	45,186,139	3.8E-10	rs10938398	45,186,139	1.5E-30	rs13130484	45,175,691	1.3E-15
CWH43	4	48,567,323-49,567,323							rs2605281	49,067,323	6.9E-12			
USP46	4	52,298,624-53,318,664	rs2102278	52,818,664	4.5E-8				rs1996617	52,798,624	6.5E-13			
MOB1B	4	71,335,822-72,344,118				rs28599782	71,844,118	4.6E-16	rs7674402	71,835,822	4.0E-16	rs7674402	71,835,822	1.2E-13
ART3, SHROOM3	4	75,996,817-78,033,939							rs6835992	76,496,817	5.6E-11			
SCD5	4	83,078,271-84,087,562	rs79920718	83,578,271	5.7E-10				rs993380	83,584,496	3.7E-12	rs10471048	83,587,562	2.3E-11
NKX6-1, CDS1, RP11-42A4.1	4	84,797,954-85,839,618				rs117624659	85,339,618	2.0E-16	rs117233795	85,297,954	1.4E-12	rs117624659	85,339,618	3.1E-14

FAM13A	4	89,213,121-90,240,894	rs1903002	89,740,894	3.0E-8				rs9991328	89,713,121	2.4E-9			
	4	90,743,865-91,743,865							rs7656001[a]	91,243,865	1.2E-8			
UNC5C, RP11-363G15.2, SMARCAD1	4	94,591,911-96,614,385	rs6821438	95,091,911	5.4E-11				rs3755879	96,114,385	5.6E-11	rs6821438	95,091,911	2.5E-9
PPP3CA	4	101,635,363-102,635,363										rs2659518	102,135,363	4.5E-9
SLC9B1	4	102,688,709-104,640,848	rs1580278	104,140,848	2.9E-10				rs7659468	103,895,317	1.4E-14	rs223423	103,725,894	1.6E-9
TET2	4	105,548,291-106,548,291							rs17035289	106,048,291	1.5E-13	rs17035289	106,048,291	1.3E-12
PRDM5	4	121,265,788-122,265,788							rs4833687	121,765,788	2.8E-9			
LARP1B	4	128,524,273-129,524,273							rs4834232	129,024,273	9.4E-9			
RP11-422J15.1	4	130,286,346-131,286,346							rs2952858	130,786,346	1.1E-8			
PABPC4L	4	136,583,193-137,583,193	rs1296328	137,083,193	4.3E-8									
MAML3	4	140,406,390-141,406,390							rs12505942	140,906,390	1.8E-12			
HHIP	4	145,112,552-146,112,552							rs12511407	145,612,552	2.1E-10			
TMEM154	4	153,013,369-154,020,475	rs7669833	153,513,369	1.8E-14	rs10011838	153,520,279	1.4E-27	rs6813195	153,520,475	7.7E-31	rs6813195	153,520,475	3.0E-36
GUCY1B3, PDGFC	4	156,197,784-158,225,916	rs28819812	157,652,753	2.7E-8				rs28819812	157,652,753	2.6E-15	rs1425482	157,725,916	2.3E-11
SORBS2, ACSL1	4	185,214,289-187,080,062	rs58730668	185,717,759	1.0E-13				rs55691245	185,716,100	1.8E-18	rs1996546	185,714,289	1.6E-13
ANKH	5	14,251,305-15,268,092	rs146886108	14,751,305	8.7E-16	rs6885132	14,768,092	2.6E-9	rs146886108	14,751,305	1.7E-31	rs6885132	14,768,092	9.5E-23
RANBP3L	5	35,584,426-36,757,018				rs16902871	36,257,018	3.3E-9	rs114136102	36,084,426	2.8E-8			
MRPS30	5	44,144,006-45,182,589	rs6884702	44,682,589	5.8E-9				rs4479849	44,644,006	2.6E-11	rs6884702	44,682,589	6.0E-12
	5	45,704,748-46,704,748							rs8188241	46,204,748	1.5E-8			
PARP8	5	49,579,603-50,645,266				rs74334916	50,079,603	4.3E-8	rs152839	50,145,266	1.1E-12			
ITGA1	5	51,251,574-52,600,489	rs3811978	52,100,489	4.2E-10	rs12109081	51,751,574	1.1E-8	rs12187734	51,763,665	2.2E-13	rs17261179	51,791,225	6.9E-11
ARL15	5	52,771,420-53,797,591	rs702634	53,271,420	2.1E-13				rs4865796	53,272,664	5.4E-30	rs7736354	53,297,591	1.7E-20
ANKRD55, SLC38A9, AC022431.2	5	54,486,775-56,310,305	rs465002	55,808,475	3.8E-23	rs256904	55,810,305	3.6E-29	rs464605	55,807,370	8.0E-66	rs465002	55,808,475	1.5E-51
RAB3C	5	57,632,702-58,632,702							rs2662390	58,132,702	1.0E-8			
PIK3R1	5	67,214,246-68,216,793							rs4976033	67,714,246	1.0E-10	rs57634870	67,716,793	6.0E-12
POC5, HMGCR, ANKDD1B	5	74,074,984-75,503,678	rs2307111	75,003,678	3.3E-16	rs2126736	74,574,984	1.8E-8	rs34341	74,934,009	4.9E-25	rs2307111	75,003,678	1.3E-18
ZBED3	5	75,924,949-76,935,004	rs4457053	76,424,949	1.4E-17				rs7732130	76,435,004	2.2E-32	rs7732130	76,435,004	6.0E-22
DMGDH, JMY	5	77,930,607-79,046,293	rs1316776	78,430,607	3.5E-12				rs2591392	78,546,293	1.9E-15	rs10052346	78,472,599	5.7E-14
RASA1	5	86,018,243-88,197,533	rs7719891	86,577,352	2.9E-8				rs6870983	87,697,533	6.3E-9	rs11953892	86,518,243	1.9E-8
PCSK1, CTD-2337A12.1	5	95,348,503-96,350,250				rs261982	95,843,763	3.1E-9	rs261967	95,850,250	8.1E-10			
SLCO6A1, PAM, CTC-503K11.2	5	100,732,944-103,473,337	rs115505614	102,422,968	1.7E-29				rs75432112	102,586,407	6.4E-37	rs115505614	102,422,968	5.9E-29
CEP120	5	122,150,885-123,204,342							rs144052331	122,650,885	4.0E-13	rs4267865	122,704,342	9.7E-13
JADE2, PHF15	5	133,361,663-134,364,599	rs329122	133,864,599	9.2E-9	rs329122	133,864,599	2.2E-8	rs329118	133,861,663	2.0E-13	rs329122	133,864,599	6.0E-16
WNT8A	5	136,931,501-137,931,501							rs217256	137,431,501	1.4E-8			
CTB-12O2.1	5	150,824,600-151,824,600							rs302395	151,324,600	1.5E-8			
EBF1	5	157,525,983-158,529,734							rs1650505	158,029,734	1.7E-19	rs748510	158,025,983	3.6E-8
RANBP17	5	170,183,134-171,183,134							rs2913873	170,683,134	1.5E-8			
NSD1, FGFR4	5	176,013,896-177,179,407				rs3135911	176,513,896	1.5E-12	rs4343858	176,679,407	5.4E-11	rs244708	176,589,585	3.8E-9
MGAT1	5	179,726,516-180,726,516							rs6885157	180,226,516	4.7E-8			
SSR1, RREB1	6	6,731,843-7,731,843	rs9379084	7,231,843	2.3E-20	rs9379084	7,231,843	2.2E-14	rs9379084	7,231,843	5.3E-31	rs9379084	7,231,843	6.1E-30
JARID2	6	14,975,051-15,999,419							rs727734	15,475,051	6.7E-11	rs7769291	15,499,419	3.0E-8
CDKAL1	6	19,251,516-21,188,121	rs7756992	20,679,709	3.0E-87	rs9350271	20,683,164	5.0E-183	rs10440833	20,688,121	4.5E-215	rs9348441	20,680,678	6.2E-235
HIST1H4E	6	25,711,146-26,711,146							rs9358912	26,211,146	2.3E-8			
MICF	6	28,426,220-30,316,421				rs6915823	30,073,430	1.8E-10	rs9257408	28,926,220	2.0E-10			
MHC region	6	30,526,236-34,736,973	rs601945	32,573,415	2.7E-21	rs76541615	31,026,236	1.1E-17	rs3130931	31,134,888	2.3E-32	rs879882	31,139,452	5.0E-26
ZNF76	6	34,759,397-35,759,397							rs33959228	35,259,397	3.4E-9			
RP1-90K10.4	6	36,411,274-37,411,274							rs72846863	36,911,274	4.6E-8			
ZFAND3, KCNK16, KCNK17, GLP1R	6	38,546,644-39,782,371				rs742762	39,046,644	1.8E-22	rs34247110	39,282,371	2.1E-15	rs34247110	39,282,371	3.4E-21

USP49, LRFN2	6	39,909,243-42,364,441	rs34298980	40,409,243	1.2E-9				rs34298980	40,409,243	1.2E-10	rs34298980	40,409,243	4.1E-9
VEGFA	6	43,313,711-44,314,190	rs6458354	43,814,190	3.7E-13				rs9472139	43,813,711	1.4E-17	rs6458354	43,814,190	1.3E-13
SUPT3H	6	44,375,762-45,375,762							rs538801	44,875,762	4.7E-8			
TFAP2B	6	50,287,459-51,913,013	rs3798519	50,788,778	1.1E-12	rs62405419	50,787,459	3.8E-9	rs3798519	50,788,778	5.6E-24	rs3798519	50,788,778	2.4E-22
RP3-523E19.2	6	53,289,830-54,289,830							rs9370243	53,789,830	1.0E-10			
	6	63,663,807-64,663,807							rs9449295	64,163,807	4.0E-8			
SLC25A51P1	6	66,887,490-67,887,490	rs555402748	67,387,490	4.6E-8									
BEND3	6	106,931,688-107,945,266	rs4946812	107,431,688	1.0E-8				rs7752666	107,445,266	1.7E-12	rs1665901	107,433,400	6.1E-12
REV3L	6	111,238,793-112,238,793							rs55812705	111,738,793	1.3E-9			
NUS1	6	117,496,631-118,511,723				rs80196932	117,996,631	7.6E-13	rs80196932	117,996,631	9.7E-20	rs72951506	118,011,723	9.9E-11
CENPW, SOGA3, RP11-624M8.1	6	125,561,502-127,916,930	rs11759026	126,792,095	1.3E-18	rs4273712	126,964,510	2.6E-12	rs11759026	126,792,095	1.2E-24	rs11759026	126,792,095	1.0E-36
	6	129,765,266-130,765,266							rs35164294	130,265,266	1.4E-8			
MED23, ENPP3	6	131,426,334-132,454,797				rs7739842	131,954,797	1.6E-11	rs2608953	131,926,334	3.3E-12	rs7739842	131,954,797	1.8E-13
SLC35D3, RPL35AP3	6	136,791,281-137,800,960	rs1573090	137,302,159	8.4E-15	rs35389258	137,294,771	9.5E-14	rs2876354	137,295,352	1.4E-34	rs6937795	137,291,281	5.3E-15
NHSL1, REPS1	6	138,355,975-140,337,128				rs9376382	139,205,386	1.5E-8	rs11155073	139,837,128	1.4E-12	rs9376353	138,855,975	2.7E-10
HIVEP2	6	142,556,556-143,558,692				rs9390022	143,056,556	6.4E-9	rs9390022	143,056,556	5.0E-14	rs6570526	143,058,692	8.2E-10
RGS17	6	152,938,573-153,940,770							rs7758002	153,440,770	4.6E-16	rs6932473	153,438,573	5.5E-13
SLC22A3	6	160,270,312-161,270,918	rs474513	160,770,312	1.0E-9				rs501470	160,770,918	1.6E-17	rs539298	160,770,360	1.4E-15
QKI, RP1-230L10.1	6	163,633,001-164,633,001	rs4709746	164,133,001	5.0E-9				rs4709746	164,133,001	1.5E-21	rs4709746	164,133,001	7.8E-10
	7	1,372,921-3,260,750							rs4721089[a]	1,872,921	7.9E-10			
FOXK1	7	4,183,572-5,191,060							rs62452060	4,683,572	1.7E-9	rs28411900	4,691,060	2.7E-8
TMEM106B	7	11,769,593-12,769,593							rs13237518	12,269,593	2.0E-13			
EUM1	7	13,386,654-14,387,008				rs7787720	13,886,654	2.3E-15	rs7787720	13,886,654	3.8E-13	rs12154701	13,887,008	1.4E-11
DGKB	7	14,398,282-16,426,228	rs10228066	15,063,569	1.9E-25	rs17168486	14,898,282	8.2E-22	rs10228796	15,064,190	2.0E-71	rs2215383	15,062,983	2.1E-44
HDAC9	7	17,831,915-18,831,915							rs583769	18,331,915	7.8E-13			
IGF2BP3	7	23,012,896-24,384,697	rs4279506	23,512,896	5.7E-9				rs2188848	23,884,697	1.2E-11			
LOC646588, NFE2L3	7	25,479,338-26,479,338										rs2391174	25,979,338	1.3E-8
JAZF1	7	27,692,280-28,719,310	rs1708302	28,198,677	4.2E-48	rs3735567	28,219,310	3.1E-12	rs860262	28,194,397	2.9E-82	rs849133	28,192,280	2.3E-69
CRHR2	7	30,228,452-31,228,452	rs917195	30,728,452	5.6E-11				rs917195	30,728,452	1.5E-20	rs917195	30,728,452	3.6E-16
AOAH	7	36,242,886-37,242,886							rs6978327	36,742,886	4.8E-9			
SUGCT	7	40,316,653-41,316,653							rs17439448	40,816,653	3.7E-9			
MYL7, CCM2, GCK	7	43,674,857-45,616,468	rs878521	44,255,643	1.6E-14	rs2908279	44,174,857	8.4E-11	rs730497	44,223,721	9.3E-29	rs878521	44,255,643	2.2E-20
	7	48,339,003-49,339,003							rs12539264	48,839,003	8.6E-11			
DDC, GRB10	7	50,077,968-51,309,085							rs73121277	50,577,968	7.4E-10	rs13236710	50,809,085	2.0E-11
ZNF713, CICP11	7	55,302,063-56,484,953				rs565050730	55,984,953	4.4E-8	rs6972291	55,802,063	2.5E-9	rs9784904	55,835,078	1.4E-8
AUTS2	7	68,555,951-70,196,905				rs12698877	69,696,905	7.0E-22	rs6975279	69,649,683	4.1E-25	rs2533457	69,055,951	3.3E-19
GTF2I	7	73,576,493-74,576,493							rs13238568	74,076,493	1.7E-9			
MAGI2, RP5-899E9.1	7	76,547,102-78,328,991							rs12669521	77,047,102	2.8E-9			
STEAP1, AC004969.1	7	89,252,238-90,303,634				rs62469016	89,752,238	1.5E-15	rs6956980	89,803,634	9.6E-14	rs6978118	89,800,241	2.0E-14
CALCR	7	92,607,093-93,618,736				rs2074120	93,107,093	8.4E-9	rs76369672	93,118,736	1.2E-8			
	7	99,813,420-100,813,420							rs506597	100,313,420	1.5E-10			
RASA4, FBXL13, RELN, DNAJC2	7	101,836,979-103,944,978	rs11496066	102,486,254	1.2E-8	rs75990271	102,336,979	3.2E-11	rs187653072	102,976,385	2.2E-12	rs7781557	102,481,891	8.9E-12
LHFPL3	7	104,016,274-105,016,274							rs73184014	104,516,274	1.2E-8			
CTTNBP2	7	116,995,667-117,995,667	rs6976111	117,495,667	1.5E-8				rs6976111	117,495,667	1.5E-8			
SND1, GCC1, LEP, GRM8, PAX4	7	126,026,991-128,403,272				rs2233580	127,253,550	2.7E-132	rs17866443	127,058,953	8.9E-47	rs12669223	127,250,831	2.4E-39
KLF14	7	129,927,057-130,957,914	rs1562396	130,457,914	7.6E-17				rs3996350	130,427,057	1.2E-18	rs1562396	130,457,914	1.7E-16
AC009518.3	7	131,074,608-132,074,608							rs12667919	131,574,608	3.6E-8			
BRAF	7	140,022,073-141,131,823				rs71170768	140,579,350	2.2E-10	rs60251368	140,522,073	2.2E-12	rs11983228	140,631,823	5.0E-10

TRPV5	7	142,107,301-143,107,301							rs4252505	142,607,301	4.5E-9			
CUL1, CNTNAP2	7	147,158,539-149,738,823							rs1922879	147,658,539	2.1E-8			
AOC1	7	150,037,635-151,037,635	rs62492368	150,537,635	1.5E-10				rs62492368	150,537,635	1.5E-14	rs62492368	150,537,635	1.5E-10
MNX1, UBE3C	7	156,430,550-157,524,510	rs6459733	156,930,550	3.9E-17	rs1182444	157,024,510	1.7E-12	rs6946660	156,948,648	3.3E-33	rs10085650	156,993,413	3.9E-26
	8	3,686,731-4,686,731							rs117173251[a]	4,186,731	2.5E-8			
MFHAS1, RP11-115J16.2, XKR6, MSRA	8	8,221,473-11,569,960	rs17689007	9,974,824	1.7E-13				rs60384372	9,974,584	4.3E-17	rs4240673	10,787,612	1.1E-11
LONRF1, RP11-252C15.1	8	12,118,225-13,143,055							rs12056338	12,643,055	2.2E-10	rs12680692	12,618,225	6.3E-10
SGCZ	8	13,648,990-14,648,990							rs35753840	14,148,990	9.7E-10			
ASAH1	8	17,427,609-18,427,609				rs34642578	17,927,609	1.6E-9						
LPL	8	19,330,921-20,344,415	rs10096633	19,830,921	8.7E-13				rs10096633	19,830,921	8.1E-10	rs7819706	19,844,415	4.3E-13
BIN3	8	21,992,103-22,992,103							rs6558173	22,492,103	7.3E-10			
EBF2	8	25,371,721-26,371,721							rs11998023	25,871,721	9.0E-10			
RP11-380I10.3	8	27,595,939-28,595,939							rs11994255	28,095,939	1.8E-8			
PURG	8	30,352,826-31,363,938	rs10954772	30,863,938	2.3E-9				rs2725370	30,852,826	3.3E-12	rs2725370	30,852,826	2.9E-8
	8	34,002,571-35,002,571							rs4463416	34,502,571	1.1E-8			
ZNF703, RP11-150O12.1, FGFR1, KCNU1	8	36,332,310-38,843,012				rs4739515	37,391,203	1.7E-11	rs13365225	36,858,483	1.6E-12	rs12680217	37,397,803	5.2E-15
ANK1, NKX6-3	8	41,008,577-42,022,991	rs13262861	41,508,577	1.8E-27	rs33981001	41,512,648	5.3E-28	rs13262861	41,508,577	8.2E-79	rs508419	41,522,991	5.7E-47
PENK, RP11-17A4.1	8	56,996,064-57,998,704							rs3887059	57,496,064	5.1E-12	rs6651357	57,498,704	8.4E-9
RP11-1102P16.1	8	71,907,374-72,907,374							rs10101067	72,407,374	1.3E-8			
KCNB2	8	73,003,743-74,003,743				rs349359	73,503,743	3.1E-8						
GDAP1, STAU2	8	74,068,099-75,714,398				rs149265787	75,214,398	5.7E-10	rs28792187	74,568,099	4.1E-8	rs3780012	75,147,209	8.0E-10
TP53INP1, RP11-347C18.3	8	95,460,886-96,467,372	rs10097617	95,961,626	1.1E-15	rs896852	95,960,886	6.4E-9	rs10808671	95,967,372	2.4E-21	rs13257021	95,965,695	3.3E-20
RP11-44N17.2, CPQ	8	96,638,738-98,237,741	rs149364428	97,737,741	1.9E-12				rs546898700	97,724,430	6.0E-12			
AZIN1	8	103,376,325-104,376,325							rs2679745	103,876,325	1.9E-8			
RP11-127H5.1	8	105,162,373-106,162,373							rs112515915	105,662,373	3.2E-11			
TRHR	8	109,623,183-110,623,183	rs12680028	110,123,183	3.1E-8									
TRPS1	8	115,997,173-117,065,365							rs3802219	116,565,365	1.1E-19	rs800909	116,497,173	8.1E-12
SLC30A8	8	117,684,783-118,685,025	rs3802177	118,185,025	6.3E-55	rs13266634	118,184,783	3.7E-67	rs13266634	118,184,783	4.2E-136	rs13266634	118,184,783	3.2E-115
TRIB1	8	125,971,274-126,971,274				rs60089934	126,471,274	3.3E-9						
PVT1, CASC11, RP11-89M16.1	8	128,211,742-130,069,999	rs17772814	128,711,742	5.0E-10				rs1561927	129,568,078	5.0E-13	rs4733612	129,569,999	2.4E-12
EFR3A	8	132,379,795-133,379,795				rs10505581	132,879,777	4.4E-8						
	8	135,275,546-136,275,546							rs4294149	135,775,546	2.3E-8			
BOP1, HSF1	8	145,007,304-146,044,720	rs4977213	145,507,304	4.4E-14				rs13268508	145,525,277	4.1E-20	rs3890400	145,544,720	3.3E-18
DMRT2	9	532,567-1,533,958				rs1016565	1,032,567	2.2E-8	rs1567353	1,033,773	7.1E-12	rs1509195	1,033,958	1.3E-8
RFX3	9	2,749,708-3,749,708							rs75619936	3,249,708	2.4E-8			
GLIS3	9	3,790,085-4,791,928	rs10974438	4,291,928	1.6E-14	rs4237150	4,290,085	4.5E-27	rs4237150	4,290,085	7.0E-31	rs4237150	4,290,085	1.5E-36
	9	7,790,816-8,790,816							rs10758950	8,290,816	7.0E-9			
NFIB	9	13,641,703-14,641,703							rs73642097	14,141,703	2.1E-9			
HAUS6	9	18,567,833-19,574,538	rs7022807	19,067,833	3.6E-10				rs12380322	19,074,538	1.6E-13	rs12380322	19,074,538	4.9E-10
FOCAD	9	19,741,069-21,290,622	rs7867635	20,241,069	4.1E-8				rs2150999	20,790,622	5.5E-10			
CDKN2A, CDKN2B	9	21,632,878-22,634,094	rs10811660	22,134,068	6.6E-79	rs10965248	22,132,878	4.4E-164	rs10811661	22,134,094	9.6E-206	rs10811661	22,134,094	1.1E-201
	9	22,858,495-23,858,495							rs7029718	23,358,495	1.5E-12			
LINGO2	9	27,910,683-29,589,437	rs1412234	28,410,683	2.5E-10				rs1412234	28,410,683	4.4E-21	rs1412234	28,410,683	1.5E-11
UBAP2	9	33,574,476-34,574,476	rs12001437	34,074,476	3.7E-10				rs12001437	34,074,476	4.4E-15	rs12001437	34,074,476	5.6E-11
GBA2	9	35,249,014-36,249,014							rs1570247	35,749,014	2.9E-10			
MTND2P8, TLV4	9	80,844,701-82,417,127	rs17791513	81,905,590	2.9E-14	rs1328412	81,917,111	6.4E-11	rs67269808	81,907,986	1.0E-20	rs13290396	81,914,978	1.4E-26
TLE1, RP11-154D17.1	9	83,808,948-84,808,948	rs2796441	84,308,948	8.5E-24	rs2796441	84,308,948	1.4E-28	rs2796441	84,308,948	2.9E-55	rs2796441	84,308,948	8.0E-42
	9	84,812,075-85,812,075							rs654629	85,312,075	5.2E-12			

C9orf3, ZNF169, PTCH1	9	96,415,002-98,778,413	rs55653563	97,001,682	3.2E-9	rs113154802	98,278,413	3.5E-8	rs10993072	96,915,002	2.9E-14	rs113154802	98,278,413	4.3E-12
ABCA1	9	107,097,527-108,097,527				rs201375651	107,597,527	2.6E-8						
EPB41L4B	9	111,438,268-112,438,268							rs10119430	111,938,268	1.8E-9			
COL27A1	9	116,443,357-117,443,357							rs1431819	116,943,357	2.0E-10			
ASTN2	9	118,752,277-119,752,277							rs1885234	119,252,277	2.7E-10			
STRBP, ZBTB26	9	125,189,694-127,086,563							rs10818763[a]	125,689,694	2.4E-12	rs2416899	126,015,103	3.5E-10
FIBCD1	9	133,286,652-134,286,652							rs6597649	133,786,652	2.3E-9			
MED27	9	134,368,417-135,368,417							rs9411425	134,868,417	4.8E-9			
ABO, LINC00094	9	135,649,229-137,390,704	rs505922	136,149,229	5.4E-12	rs529565	136,149,500	1.7E-10	rs529565	136,149,500	8.0E-27	rs505922	136,149,229	2.0E-21
GPSM1	9	138,741,030-139,748,082	rs28505901	139,241,030	2.6E-21	rs376993806	139,246,588	4.5E-26	rs28642213	139,248,082	5.7E-68	rs28429551	139,243,334	1.4E-39
RN7SL232P, CDC123, CAMK1D	10	11,807,894-12,809,139	rs11257655	12,307,894	3.7E-32	rs11257657	12,309,139	9.8E-62	rs11257655	12,307,894	1.4E-63	rs11257655	12,307,894	1.2E-91
BEND7	10	13,040,869-14,040,869							rs11258422	13,540,869	3.2E-9			
PTF1A	10	22,987,778-23,987,778				rs77065181	23,487,778	1.6E-8						
MYO3A	10	25,997,704-26,997,704										rs7923442	26,497,704	1.2E-9
	10	33,497,227-34,497,227							rs71495046	33,997,227	1.9E-10			
	10	43,527,356-44,527,356							rs3122231	44,027,356	5.8E-10			
ARID5B	10	63,212,602-64,217,113				rs141583966	63,712,602	7.7E-10	rs146716733	63,717,113	1.2E-8			
JMJD1C	10	64,470,928-65,476,133				rs148928116	64,976,133	2.5E-13	rs111765639	64,970,928	5.4E-12	rs41274074	64,974,380	3.1E-11
TFK1, TSPAN15, VPS26A, NEUROG3	10	69,882,179-71,966,578	rs2642588	71,466,578	6.3E-14	rs1955163	71,273,357	1.7E-11	rs177045	71,321,279	2.7E-17	rs177045	71,321,279	5.0E-23
PCBD1	10	72,148,336-73,148,336							rs827237	72,648,336	2.5E-8			
	10	73,335,274-74,335,274							rs12773019[a]	73,835,274	4.8E-8			
CAMK2G	10	75,098,099-76,098,099							rs2633311	75,598,099	3.1E-9			
ZNF503, LRMDA	10	76,744,336-77,823,643				rs7900112	77,314,617	5.4E-12	rs3012060	77,244,336	5.9E-10	rs3012060	77,244,336	1.6E-12
ZMIZ1	10	80,443,841-81,452,826	rs703972	80,952,826	2.5E-28	rs34204798	80,951,130	5.0E-19	rs697239	80,947,438	4.8E-54	rs703980	80,943,841	8.7E-40
GRID1	10	87,617,318-88,628,637							rs11201992	88,117,318	5.8E-11	rs3814613	88,128,637	1.1E-8
PTEN	10	89,184,214-90,266,368				rs1236816	89,684,214	4.3E-10	rs36062478	89,722,731	6.8E-13	rs10887775	89,766,368	8.9E-11
BTAF1, MYOF, HHEX, IDE	10	93,092,703-95,519,524	rs10882101	94,462,427	1.6E-62	rs35906730	94,435,673	1.3E-71	rs1111875	94,462,882	1.4E-128	rs10882101	94,462,427	1.8E-125
RP11-452K12.4, ARHGAP19, SLIT1	10	98,556,190-99,591,369				rs10748694	99,056,190	9.2E-11	rs945187	99,091,369	8.2E-16	rs10748694	99,056,190	5.1E-17
HPSE2	10	99,921,841-100,921,841							rs524903	100,421,841	2.1E-10			
ERLIN1	10	101,412,194-102,412,194							rs1408579	101,912,194	6.1E-11			
RNU2-43P	10	102,565,789-103,565,789							rs620191	103,065,789	1.7E-8			
RNU6-1231P	10	104,063,743-105,063,743							rs2482506	104,563,743	2.3E-12			
BBIP1	10	112,121,837-113,178,657				rs7895872	112,678,657	1.4E-11	rs7895872	112,678,657	1.3E-13	rs7067540	112,621,837	1.1E-14
TCF7L2	10	114,249,734-115,258,349	rs7903146	114,758,349	<E-300	rs7901695	114,754,088	8.2E-62	rs35011184	114,749,734	<E-300	rs7903146	114,758,349	<E-300
	10	115,321,878-116,321,878							rs10787518	115,821,878	8.8E-9			
	10	118,058,736-119,058,736							rs7912336	118,558,736	1.4E-8			
SEC23IP	10	121,160,400-122,160,400							rs11199116	121,660,400	1.0E-9			
WDR11, FGFR2	10	122,415,345-123,430,568				rs10886863	122,929,493	5.3E-17	rs7071036	122,930,568	2.0E-12	rs72631105	122,915,345	1.9E-18
PLEKHA1	10	123,650,342-124,693,181	rs2280141	124,193,181	2.0E-13	rs112820281	124,150,342	1.4E-10	rs2280141	124,193,181	6.0E-21	rs2421016	124,167,512	9.6E-23
RP11-282I1.1	10	124,726,178-125,726,178							rs705145	125,226,178	3.3E-9			
INS, IGF2, KCNQ1, TH	11	1,697,132-3,358,546	rs2237895	2,857,194	3.6E-44	rs2237897	2,858,546	1.9E-245	rs2237897	2,858,546	2.1E-226	rs2237897	2,858,546	5.5E-233
TRIM66	11	8,154,528-9,177,063							rs7941510	8,677,063	1.9E-17	rs10769936	8,654,528	6.9E-11
SBF2	11	9,356,015-10,356,015							rs76789970	9,856,015	9.2E-11			
ARNTL	11	12,840,710-13,840,710							rs10766076	13,340,710	1.3E-9			
PDE3B, COPB1	11	14,018,419-15,263,828	rs141521721	14,763,828	2.8E-8				rs117316450	14,518,419	9.5E-15	rs141521721	14,763,828	2.3E-8
KCNJ11, ABCC8	11	16,908,404-17,918,477	rs5213	17,408,404	1.9E-26	rs4148646	17,415,190	1.7E-26	rs757110	17,418,477	4.6E-52	rs5215	17,408,630	1.3E-54
NELL1	11	20,452,237-21,452,237							rs16907058	20,952,237	4.6E-8			
BDNF	11	27,183,618-28,229,505				rs988748	27,724,745	1.6E-10	rs10767659	27,686,196	4.6E-10	rs4923464	27,683,618	9.4E-10

MPPED2, RP5-1024C24.1	11	30,108,133-31,120,262							rs10835690	30,620,262	2.5E-8	rs11031140	30,608,133	2.8E-8
QSER1	11	32,427,778-33,456,492	rs145678014	32,927,778	1.1E-11				rs62618693	32,956,492	1.4E-13	rs145678014	32,927,778	5.7E-10
SLC1A2, PDHX, APIP	11	34,408,780-35,933,712	rs2767036	34,982,148	2.5E-8				rs2956092	34,908,780	1.7E-10	rs2985149	34,969,534	1.9E-8
HSD17B12	11	43,316,200-44,378,459	rs1061810	43,877,934	8.5E-13				rs35251247	43,878,459	1.7E-13	rs6485462	43,816,200	4.8E-12
CRY2	11	45,358,584-46,412,013	rs7115753	45,912,013	4.8E-9				rs12419690	45,858,584	1.4E-13	rs12419690	45,858,584	4.2E-11
OR4C9P, FOLH1, CELF1, NUP160	11	46,974,146-50,610,597	rs7124681	47,529,947	6.4E-9				rs3816605	47,857,253	8.9E-14	rs6485981	49,477,266	1.5E-9
OR5D18	11	55,088,216-56,088,216							rs116861182	55,588,216	5.4E-9			
OR5B17	11	57,628,015-58,628,015							rs7483027	58,128,015	5.6E-11			
FEN1	11	61,065,908-62,065,908							rs174541	61,565,908	2.4E-11			
AP003774.1	11	63,600,776-64,600,776							rs1662185	64,100,776	3.5E-8			
MAP3K11, LTBP3	11	64,794,799-65,826,154	rs1783541	65,294,799	1.4E-14				rs12789028	65,326,154	3.9E-20	rs12789028	65,326,154	2.1E-17
TPCN2, CCND1	11	68,335,182-69,963,273	rs11820019	69,448,758	1.0E-11	rs602652	69,462,642	5.3E-9	rs3918298	69,463,273	8.0E-25	rs3918298	69,463,273	3.3E-17
CENTD2, ARAP1	11	71,960,398-72,963,435	rs77464186	72,460,398	2.3E-33	rs7109575	72,463,435	5.5E-21	rs11602873	72,460,762	2.0E-62	rs77464186	72,460,398	3.6E-49
C11orf30	11	74,125,997-76,730,357							rs2513505	76,230,357	4.1E-10	rs61894507	76,156,973	2.2E-10
MTNR1B	11	92,208,710-93,208,710	rs10830963	92,708,710	1.5E-43	rs10830963	92,708,710	4.5E-8	rs10830963	92,708,710	1.3E-66	rs10830963	92,708,710	6.1E-66
MAML2	11	95,210,493-96,210,493							rs7130522	95,710,493	4.8E-8			
FXYD6, FXYD2	11	117,193,255-118,193,255							rs529623	117,693,255	4.3E-9	rs529623	117,693,255	1.5E-8
HMBS	11	118,453,202-119,453,202							rs7127212	118,953,202	2.4E-8			
ETS1	11	127,734,144-128,898,938	rs67232546	128,398,938	1.4E-12				rs10750397	128,234,144	1.7E-21	rs11819995	128,389,391	2.5E-14
CCND2	12	3,881,981-4,884,844	rs76895963	4,384,844	5.3E-70	rs7304270	4,381,981	1.0E-12	rs76895963	4,384,844	1.2E-96	rs76895963	4,384,844	3.7E-71
CHD4	12	6,191,452-7,191,452							rs7316626	6,691,452	3.3E-9			
CDKN1B	12	12,371,099-13,371,099	rs2066827	12,871,099	3.5E-8				rs2066827	12,871,099	2.2E-10	rs2066827	12,871,099	7.1E-11
PDE3A	12	20,079,392-21,091,332							rs7134150	20,591,332	2.7E-10	rs7488780	20,579,392	3.1E-8
LDHB, KCNJ8, RP11-59N23.3	12	21,343,576-22,371,751							rs11046164	21,843,576	4.0E-10	rs10841890	21,871,751	4.2E-8
ITPR2, RP11-283G6.4	12	25,953,283-26,974,867	rs718314	26,453,283	1.1E-10				rs11048457	26,463,174	2.2E-19	rs10842708	26,474,867	5.5E-14
KLHDC5, RN7SKP15	12	27,463,402-28,465,150	rs10842994	27,965,150	2.5E-20	rs3751236	27,963,402	6.6E-21	rs3751239	27,963,676	2.0E-47	rs12578595	27,964,996	7.8E-33
FAM60A, SINHCAF, DENND5B	12	30,917,019-31,941,179				rs80234489	31,441,179	4.3E-32	rs80234489	31,441,179	6.1E-18	rs78345706	31,417,019	1.2E-24
PKP2, SYT10	12	32,870,406-33,910,855							rs10844519	33,410,855	1.4E-12	rs6488140	33,370,406	9.1E-12
	12	38,210,523-39,210,523							rs7315028[b]	38,710,523	1.5E-8			
PDZRN4	12	41,363,393-42,363,393							rs2730827	41,863,393	2.1E-13			
RP11-25I15.2	12	42,546,449-43,546,449							rs11181613	43,046,449	2.4E-12			
	12	45,368,623-46,368,623							rs2408252	45,868,623	1.1E-9			
	12	48,212,932-49,212,932							rs2732469	48,712,932	4.8E-14			
FAIM2	12	49,763,148-50,769,863				rs77978149	50,269,863	5.7E-9	rs7132908	50,263,148	7.4E-14	rs7132908	50,263,148	6.5E-10
HOXC6	12	53,929,385-54,929,385							rs12422600	54,429,385	3.1E-9			
PRIM1	12	56,646,069-58,468,738							rs2277339	57,146,069	6.9E-15			
	12	60,750,814-61,750,814							rs11173646	61,250,814	1.5E-9			
HMGA2, RPSAP52	12	65,716,162-66,746,181	rs2258238	66,221,060	2.0E-25	rs2583934	66,232,810	5.0E-16	rs2257883	66,216,162	3.9E-47	rs2583930	66,246,181	5.1E-38
TSPAN8, LGR5	12	70,949,521-72,022,953	rs1796330	71,522,953	3.2E-14	rs7313668	71,449,521	4.9E-11	rs10879261	71,520,761	6.8E-19	rs7313668	71,449,521	2.7E-17
LIN7A	12	80,809,262-81,809,262							rs11114650	81,309,262	3.3E-9			
	12	87,838,461-88,838,461							rs10745460[b]	88,338,461	3.3E-8			
USP44	12	95,428,113-96,428,560	rs2197973	95,928,560	4.4E-8				rs11108094	95,928,113	1.1E-10			
RMST	12	97,348,775-98,351,611	rs77864822	97,848,775	2.2E-8	rs10860209	97,850,215	5.7E-9	rs6538805	97,849,120	1.5E-14	rs7972074	97,851,611	1.1E-10
	12	105,788,445-106,788,445							rs12825669	106,288,445	3.8E-8			
WSCD2	12	108,129,780-109,129,780	rs1426371	108,629,780	1.1E-11	rs1426371	108,629,780	7.8E-12	rs1426371	108,629,780	1.3E-21	rs1426371	108,629,780	9.7E-19
BRAP, SH2B3, ALDH2, PTPN11, HECTD4	12	111,109,727-113,617,897				rs149212747	111,836,771	2.1E-11				rs77753011	113,117,897	4.0E-15
RBM19	12	113,623,722-114,623,722				rs7307263	114,123,722	3.6E-8						
KSR2, NOS1	12	117,223,613-118,912,373	rs34965774	118,412,373	3.5E-9	rs111246699	118,400,856	1.5E-15	rs79310463	118,406,696	7.2E-21	rs34965774	118,412,373	1.5E-21

HNF1A	12	120,863,506-121,932,117	rs56348580	121,432,117	3.8E-19	rs118074491	121,363,506	8.8E-20	rs56348580	121,432,117	1.5E-27	rs1169299	121,429,194	1.9E-21
C12orf65, ZNF664, MPHOSPH9, CCDC92	12	122,950,765-125,045,435	rs4148856	123,450,765	2.2E-10				rs4930726	124,428,331	7.5E-18	rs1790116	123,618,544	2.2E-11
ZNF10, EP400, FBRSL1	12	132,044,643-134,230,500	rs12811407	133,069,698	2.4E-12				rs11614914	133,070,294	2.6E-19	rs12811407	133,069,698	2.0E-15
SGCG, FGF9	13	22,089,883-23,809,382				rs9316706	22,589,883	3.3E-9	rs314879	23,309,382	2.8E-15	rs314879	23,309,382	3.7E-11
RNF6	13	26,276,999-27,281,367	rs34584161	26,776,999	2.9E-10	rs568052023	26,781,367	2.6E-22	rs34584161	26,776,999	1.6E-37	rs34584161	26,776,999	3.5E-19
	13	27,745,127-28,745,127							rs9319382[a]	28,245,127	2.9E-8			
HMGB1	13	30,517,268-31,542,452	rs11842871	31,042,452	1.5E-8				rs12856169	31,017,268	2.7E-9			
KL	13	33,054,302-34,057,644	rs576674	33,554,302	6.8E-10	rs7983505	33,557,173	3.2E-18	rs57286125	33,557,644	1.8E-33	rs2858980	33,554,587	6.2E-22
	13	41,188,401-42,188,401							rs4397977	41,688,401	1.1E-11			
	13	46,014,492-47,014,492							rs6561273	46,514,492	7.5E-9			
DLEU1, RP11-175B12.2	13	49,931,987-51,596,095	rs963740	51,096,095	2.6E-8	rs123378	51,088,809	2.2E-10	rs9316500	51,094,114	1.0E-22	rs963740	51,096,095	3.8E-11
OLFM4	13	53,607,583-54,607,583							rs9568868	54,107,583	5.8E-11	rs9568868	54,107,583	1.5E-12
PCDH17, SRGAP2D	13	57,866,634-59,577,406	rs9563615	59,077,406	3.9E-9				rs7991679	58,691,107	1.1E-8			
	13	65,704,880-66,704,880							rs9564268	66,204,880	7.7E-10			
SPRY2	13	80,205,315-81,217,156	rs1359790	80,717,156	5.7E-31	rs17072370	80,705,730	1.3E-31	rs11616380	80,705,315	1.0E-69	rs1215468	80,707,429	2.4E-56
MIR17HG	13	91,442,919-92,449,562				rs9523295	91,948,047	7.2E-18	rs9515905	91,949,562	2.1E-27	rs34165267	91,942,919	6.7E-21
HS6ST3	13	96,676,585-97,676,585							rs61967710	97,176,585	2.5E-8			
IRS2	13	109,446,882-110,447,213	rs7987740	109,947,213	4.1E-8				rs9587811	109,946,882	4.9E-11			
	13	111,687,882-112,687,882							rs9560114	112,187,882	3.3E-8			
SLC7A7	14	22,788,935-23,788,935	rs17122772	23,288,935	2.0E-8									
NYNRIN	14	24,378,370-25,378,370				rs12437434	24,878,370	1.0E-9						
	14	25,447,436-26,447,436							rs11159347	25,947,436	1.5E-9			
PRKD1	14	29,586,481-30,586,481							rs12433335	30,086,481	1.6E-8			
AKAP6	14	32,802,882-33,803,540	rs17522122	33,302,882	4.0E-9				rs12883788	33,303,540	2.8E-16	rs12883788	33,303,540	1.9E-11
RP11-85K15.2	14	34,909,701-35,909,701							rs712315	35,409,701	3.9E-8			
CLEC14A	14	38,303,756-39,348,419	rs8017808	38,848,419	2.6E-8	rs61975988	38,809,661	2.0E-9	rs7147483	38,804,675	9.4E-18	rs2183237	38,803,756	5.0E-15
MDGA2	14	46,804,091-47,804,091							rs723355	47,304,091	2.0E-9			
RP11-349A22.5, PSMA3	14	58,212,860-59,232,748							rs12892257	58,732,748	1.0E-8	rs61450169	58,712,860	5.4E-9
MNAT1	14	60,729,411-61,729,411							rs4902002	61,229,411	1.4E-9			
	14	68,959,229-69,959,229							rs242105	69,459,229	3.6E-11			
	14	74,432,641-75,432,641							rs12586772	74,932,641	6.4E-9			
LRRC74A, C14orf166B	14	76,800,863-77,882,503				rs58524310	77,382,503	8.4E-11	rs2056857	77,300,863	5.2E-11	rs72627178	77,372,210	2.1E-8
NRXN3	14	79,432,041-80,444,099	rs17836088	79,932,041	9.7E-14				rs7156625	79,942,647	5.4E-27	rs8008910	79,944,099	3.3E-15
FOXN3	14	89,050,378-90,050,378										rs17714667	89,550,378	4.2E-8
SMEK1	14	91,463,722-92,463,722	rs8010382	91,963,722	8.1E-9				rs8010382	91,963,722	3.0E-12	rs8010382	91,963,722	5.3E-9
UNC79	14	93,539,845-94,539,845							rs11848361	94,039,845	2.2E-8			
DLK1, MEG3	14	100,755,172-101,758,584				rs73347525	101,255,172	7.5E-11	rs112324411	101,258,584	1.4E-12	rs73347525	101,255,172	1.8E-15
MARK3, TRAF3	14	102,737,952-104,460,026	rs62007683	103,894,071	3.8E-8	rs55700915	103,237,952	1.5E-8	rs4906272	103,376,031	5.2E-11	rs11160699	103,252,270	5.9E-12
HERC2	15	28,046,173-29,046,173				rs76704029	28,546,173	3.4E-8						
	15	35,892,562-36,892,562							rs11073147[a]	36,392,562	4.3E-8			
C15orf52, INFAM2, RP11-624L4.1, RASGRP1	15	38,328,140-41,134,717	rs34715063	38,873,115	3.3E-14	rs12907887	40,615,872	1.7E-20	rs8043085	38,828,140	9.1E-22	rs12912777	38,852,386	2.7E-16
LTK	15	41,301,512-42,318,917	rs11070332	41,809,205	1.3E-13				rs2289739	41,801,512	4.4E-11	rs1473781	41,818,917	2.1E-11
PPIP5K1, STRC	15	43,350,486-44,395,118							rs2447198	43,895,118	5.0E-10	rs475486	43,850,486	3.2E-8
FAM227B	15	49,294,020-50,294,020							rs7169799	49,794,020	3.2E-8			
ONECUT1, WDR72, MYO5C	15	52,017,714-54,247,228	rs2456530	53,091,553	4.7E-9	rs149336329	52,587,740	1.7E-9	rs149336329	52,587,740	2.9E-18	rs3825801	52,517,714	3.8E-11
TCF12	15	56,869,850-58,090,203	rs117483894	57,456,802	3.9E-8				rs28490139	57,369,850	1.5E-12	rs8024992	57,590,203	6.9E-9
ALDH1A2	15	58,176,821-59,176,821							rs11858759	58,676,821	4.3E-8			
	15	60,438,816-61,438,816							rs8033609[a]	60,938,816	1.1E-8			

C2CD4A, C2CD4B	15	61,891,608-62,894,264	rs8037894	62,394,264	3.7E-13	rs8037894	62,394,264	7.3E-33	rs7163757	62,391,608	6.1E-30	rs7163757	62,391,608	2.4E-37
USP3	15	63,371,292-64,371,292	rs7178762	63,871,292	7.0E-10				rs7178762	63,871,292	1.8E-15	rs7178762	63,871,292	9.2E-12
MAP2K5	15	66,760,238-68,580,886	rs4776970	68,080,886	6.2E-9	rs4776970	68,080,886	3.4E-8	rs4776970	68,080,886	1.1E-12	rs4776970	68,080,886	5.7E-13
PML	15	73,828,576-74,828,576							rs9479	74,328,576	4.0E-13			
PTPN9, SIN3A	15	75,242,095-76,432,129	rs13737	75,932,129	7.3E-10	rs7171507	75,737,287	1.8E-11	rs6495182	75,814,388	2.1E-22	rs11636031	75,815,758	4.9E-19
HMG20A	15	77,276,562-78,318,128	rs1005752	77,818,128	5.7E-29	rs952471	77,776,498	1.6E-26	rs12910361	77,782,335	5.2E-65	rs952472	77,776,562	4.1E-56
FSD2	15	82,961,873-83,961,873							rs36111056	83,461,873	1.4E-8			
ADAMTSL3	15	84,047,222-85,047,222							rs1812707	84,547,222	5.9E-9			
AP3S2	15	89,879,632-90,928,894	rs4932265	90,423,293	7.2E-20	rs10852123	90,428,894	8.4E-13	rs893617	90,381,278	2.1E-38	rs6496609	90,379,632	3.2E-34
PRC1	15	91,011,260-92,022,253	rs12910825	91,511,260	2.4E-15	rs8026714	91,522,253	1.1E-22	rs2290203	91,512,067	2.3E-31	rs2890156	91,513,157	3.8E-34
RP11-266O8.1, RGMA	15	93,325,384-94,425,327				rs61021634	93,825,384	1.4E-11	rs4777857	93,925,327	4.8E-11	rs7167984	93,832,067	3.4E-13
IGF1R	15	98,776,521-99,866,409				rs79826452	99,366,409	3.2E-8	rs59646751	99,276,521	3.4E-9			
LMF1, ITFG3	16	0-1,467,241	rs6600191	295,795	7.0E-13				rs55857387	300,388	1.7E-21	rs6600191	295,795	2.4E-15
CLUAP1, SLX4	16	3,083,173-4,156,482	rs3751837	3,583,173	1.7E-8	rs2240885	3,647,098	2.8E-9	rs8061528	3,656,482	2.6E-14	rs12445430	3,613,126	2.5E-11
NTAN1	16	14,653,717-15,653,717							rs9927842	15,153,717	7.0E-10			
GP2	16	19,823,168-20,834,808				rs117267808	20,323,168	4.9E-17	rs4609857	20,334,808	1.1E-10	rs117267808	20,323,168	3.0E-8
ATP2A1	16	28,397,452-29,415,217	rs8046545	28,915,217	2.3E-8				rs8056890	28,897,452	1.5E-12			
FAM57B, TMEM219	16	29,458,216-30,545,789	rs11642430	30,045,789	1.2E-10				rs8054556	29,958,216	1.9E-16	rs11642430	30,045,789	6.6E-10
FTO	16	53,300,954-54,887,084	rs1421085	53,800,954	2.4E-78	rs1421085	53,800,954	1.6E-48	rs1421085	53,800,954	1.3E-189	rs55872725	53,809,123	4.7E-128
AMFR	16	55,959,589-56,959,589							rs111283203	56,459,589	3.4E-8			
PKD1L3, IL34, NFAT5	16	69,151,866-72,522,534	rs862320	69,651,866	5.1E-11	rs12600132	72,022,534	5.9E-9	rs244415	69,666,683	2.0E-22	rs862320	69,651,866	1.5E-10
RP11-346C20.3, ZFHX3	16	72,598,091-73,600,308				rs6416749	73,100,308	3.4E-12	rs1075855	73,098,091	3.5E-9	rs6416749	73,100,308	1.5E-13
BCAR1, CTRB2	16	74,734,872-75,746,035	rs72802342	75,234,872	1.3E-27				rs72802365	75,246,035	1.1E-40	rs72802358	75,243,657	2.9E-29
CMIP	16	81,033,789-82,034,790	rs2925979	81,534,790	2.1E-14	rs2925979	81,534,790	1.5E-9	rs56823429	81,533,789	3.3E-20	rs2925979	81,534,790	1.6E-21
GINS2	16	85,216,463-86,216,463							rs11646052	85,716,463	2.7E-11			
ZFPM1	16	87,356,424-89,054,480							rs9937296	88,554,480	2.4E-10	rs9937296	88,554,480	5.3E-10
SPG7, RPL13	16	89,064,055-90,130,630	rs12920022	89,564,055	2.9E-9				rs12932337	89,630,630	8.3E-11	rs12920022	89,564,055	9.9E-10
VPS53	17	0-981,604							rs11870735	481,604	7.6E-9			
ENO3, ZZEF1	17	3,488,451-5,354,480	rs1377807	4,045,440	5.7E-17				rs8071043	3,988,451	5.4E-30	rs8071043	3,988,451	4.3E-15
SAT2, SLC16A11, SLC16A13	17	6,453,155-8,031,965				rs186568031	6,953,781	9.0E-24	rs73239895	6,953,558	3.0E-15	rs113748381	6,953,155	2.3E-24
GLP2R	17	9,285,187-10,287,845	rs7222481	9,785,187	1.7E-8				rs17810376	9,787,845	2.8E-9			
RAI1	17	17,161,802-18,251,478	rs4925109	17,661,802	3.9E-12				rs2297508	17,715,317	2.4E-14	rs1108646	17,751,478	2.8E-13
KCNJ12	17	20,784,910-21,784,910							rs117642733	21,284,910	9.5E-9			
CRYBA1	17	27,070,622-28,070,622							rs9913225	27,570,622	5.4E-11			
NF1	17	28,913,019-30,204,002	rs71372253	29,413,019	4.3E-8	rs7502556	29,642,430	3.8E-11	rs2040792	29,628,549	2.0E-15	rs1048317	29,704,002	1.4E-14
MYO19	17	34,362,220-35,362,220							rs1109442	34,862,220	6.1E-9			
HNF1B, TCF2	17	35,599,840-36,601,586	rs10908278	36,099,952	3.1E-30	rs8064454	36,101,586	6.5E-61	rs11651755	36,099,840	8.6E-67	rs10908278	36,099,952	7.4E-74
	17	37,246,307-38,246,307							rs11078916	37,746,307	1.2E-14			
MLX, LINC00910, RP11-400F19.6	17	40,196,915-41,956,413	rs34855406	40,731,411	3.2E-12				rs676387	40,706,273	3.3E-24	rs684214	40,696,915	3.0E-13
GIP, TTLL6, CBX1	17	45,678,674-47,560,322	rs35895680	47,060,322	3.8E-15				rs35895680	47,060,322	8.4E-27	rs35895680	47,060,322	2.3E-14
KIF2B	17	51,640,805-52,640,805	rs569511541	52,140,805	1.5E-8									
ERN1, ACE	17	61,065,025-62,703,304	rs60276348	62,203,304	2.9E-8				rs4335	61,565,025	1.1E-15	rs57676627	62,203,128	1.8E-10
PITPNC1, BPTF	17	65,141,651-66,457,568	rs61676547	65,892,507	1.0E-11	rs2706710	65,641,651	1.7E-8	rs12603589	65,825,248	1.1E-19	rs9899520	65,957,568	1.3E-14
SLC39A11	17	70,145,032-71,145,032							rs61736066	70,645,032	4.9E-11			
SUMO2	17	72,687,031-73,687,031				rs35559984	73,187,031	7.9E-9						
UBE2O	17	73,918,176-75,886,909							rs1656794[a]	75,386,909	3.6E-9			
CYTH1	17	76,272,288-77,292,179							rs7224711	76,772,288	1.2E-15	rs1044486	76,792,179	3.2E-13
RPTOR	17	77,395,311-79,257,626							rs11150745	78,757,626	5.2E-9			

RP11-172F10.1	18	4,345,027-5,345,027							rs9958640	4,845,027	2.3E-8			
LAMA1	18	6,570,642-7,576,836	rs7240767	7,070,642	2.0E-8	rs9948462	7,076,836	8.7E-10	rs7240767	7,070,642	2.1E-11	rs9948462	7,076,836	3.9E-15
	18	12,771,367-13,771,367							rs11662800[a]	13,271,367	2.4E-9			
C18orf8	18	20,583,738-21,583,738							rs303760	21,083,738	2.0E-14			
NOL4	18	31,082,890-32,082,890							rs17747955	31,582,890	1.6E-8			
COMMD9	18	35,778,709-37,246,623	rs62080313	36,278,709	9.1E-9				rs7227272	36,746,623	4.7E-13			
LINC00907	18	39,566,006-40,566,006							rs410150	40,066,006	1.2E-9			
TCF4	18	52,550,646-53,550,646	rs72926932	53,050,646	3.6E-13				rs72926932	53,050,646	4.3E-20	rs72926932	53,050,646	1.2E-9
WDR7	18	54,078,482-55,175,384	rs17684074	54,675,384	3.5E-8				rs10048404	54,578,482	6.1E-9			
RNU4-17P, GRP, MC4R	18	56,376,228-58,352,587	rs523288	57,848,369	7.5E-14	rs476828	57,852,587	4.8E-27	rs6567160	57,829,135	7.5E-34	rs6567160	57,829,135	1.1E-37
BCL2A	18	60,345,884-61,345,884	rs12454712	60,845,884	5.1E-13	rs12454712	60,845,884	1.4E-15	rs12454712	60,845,884	2.4E-27	rs12454712	60,845,884	4.1E-20
CDH7	18	62,916,719-63,926,979							rs2032217	63,426,979	2.7E-11	rs1942267	63,416,719	7.3E-9
ZNF236	18	74,055,593-75,058,999							rs6565922	74,558,999	6.2E-13	rs12457906	74,555,593	6.0E-13
TCF3	19	1,146,712-2,146,712							rs4807125	1,646,712	2.6E-8			
UHRF1, PTPRS, KDM4B	19	4,448,862-5,467,739	rs7249758	4,948,862	1.2E-8				rs12185519	4,967,739	2.5E-11	rs262549	4,951,064	2.5E-9
MAP2K7, INSR, AC010336.1	19	6,740,848-8,486,638	rs4804833	7,970,635	1.1E-12	rs475002	7,986,638	9.8E-10	rs2115107	7,968,168	2.3E-20	rs2115107	7,968,168	1.1E-18
FARSA, ZNF799, GCDH	19	12,005,873-13,538,415	rs3111316	13,038,415	1.6E-12	rs4804181	12,509,536	1.5E-8	rs9384	13,010,643	8.4E-23	rs3111316	13,038,415	1.3E-13
CILP2, CRTC1, TM6SF2	19	18,334,514-19,888,500	rs8107974	19,388,500	6.3E-15				rs58542926	19,379,549	1.6E-23	rs58542926	19,379,549	1.6E-13
ZNF257, ZNF738	19	21,029,576-22,600,706				rs142395395	22,100,706	6.9E-23				rs142395395	22,100,706	1.2E-15
AC007796.1	19	31,365,946-32,365,946							rs2867570	31,865,946	2.1E-11			
PEPD	19	33,390,838-34,396,432	rs10406327	33,890,838	4.6E-8	rs7250869	33,887,405	2.3E-16	rs4805881	33,896,432	8.4E-22	rs10406327	33,890,838	3.5E-20
RN7SL836P, EML2, TOMM40, APOE, GIPR	19	44,911,941-46,658,417	rs10406431	46,157,019	2.5E-19	rs113036890	46,157,928	1.0E-32	rs8107527	46,158,417	4.2E-41	rs10406431	46,157,019	8.7E-44
ZC3H4	19	47,069,003-48,097,102	rs3810291	47,569,003	1.2E-11				rs10408163	47,597,102	1.1E-13	rs3810291	47,569,003	8.6E-19
FCGRT	19	49,516,759-50,516,759							rs142385484	50,016,759	2.0E-8			
STK35	20	1,600,095-2,600,095							rs6137042	2,100,095	2.3E-8			
CFAP61	20	19,568,635-20,568,635										rs7261425	20,068,635	1.2E-8
FOXA2, NKX2-2	20	20,966,795-22,930,241	rs13041756	21,466,795	1.3E-8	rs73085586	22,430,241	1.7E-9	rs7274134	22,428,284	2.3E-9	rs2181063	22,427,370	5.9E-10
RALY, EIF2S2	20	32,096,704-33,175,727	rs2268078	32,596,704	2.9E-10				rs6059662	32,675,727	2.1E-17	rs4911405	32,674,967	4.4E-12
ZHX3	20	39,332,628-40,332,628							rs17265513	39,832,628	3.0E-9			
IFT52, HNF4A	20	41,730,695-43,542,364	rs1800961	43,042,364	3.2E-20	rs12625671	42,994,812	2.3E-21	rs12625671	42,994,812	6.1E-28	rs12625671	42,994,812	9.5E-40
EYA2	20	45,094,711-46,098,564	rs6063048	45,598,564	5.8E-11				rs6066138	45,594,711	6.3E-19	rs6063046	45,596,378	1.5E-10
CEBPB	20	48,330,772-49,332,135	rs11699802	48,832,135	2.5E-11	rs13040225	48,830,772	1.6E-14	rs13040225	48,830,772	1.1E-17	rs6091115	48,832,020	9.3E-23
NFATC2, TSHZ2, RP4-723E3.1	20	49,655,386-52,120,857	rs34454109	51,223,594	8.8E-9	rs6021276	50,155,386	6.7E-10	rs4809906	51,033,681	5.1E-18	rs34454109	51,223,594	8.1E-9
GNAS	20	56,887,352-57,977,177	rs6070625	57,394,628	3.2E-12	rs11477757	57,477,177	1.3E-8	rs4810145	57,396,495	1.1E-15	rs736266	57,387,352	6.6E-10
SLCO4A1	20	60,777,014-61,777,014							rs1815591	61,277,014	3.2E-14			
ZBTB46	20	61,950,664-62,950,664							rs6011155	62,450,664	5.9E-13			
	21	47,267,295-48,267,295							rs75756987[a]	47,767,295	1.6E-9			
ARVCF	22	19,469,696-20,469,696							rs2240716	19,969,696	4.8E-10			
MTMR3, ASCC2, ZNRF3, CTA-85E5.10	22	28,869,398-31,109,554	rs6518681	30,609,554	9.6E-13	rs147413364	29,380,119	3.4E-8	rs56392746	30,451,688	3.5E-14	rs36575	30,205,572	1.9E-13
YWHAH, DEPDC5	22	31,703,334-32,848,841	rs117001013	32,348,841	1.5E-8				rs75307421	32,203,334	2.6E-8	rs75307421	32,203,334	3.1E-11
TOM1	22	35,205,359-36,205,359							rs138771	35,705,359	3.8E-9			
MAFF	22	38,099,767-39,099,767							rs4820323	38,599,767	3.6E-8			
EP300, RP1-85F18.5	22	40,041,838-42,093,581	rs5758223	41,489,920	4.6E-8				rs11913442	41,593,581	8.2E-10	rs738630	41,511,171	5.4E-9
PNPLA3	22	43,824,730-44,824,855	rs738408	44,324,730	1.8E-10				rs3747207	44,324,855	3.7E-21	rs738408	44,324,730	5.5E-10
WNT7B	22	45,813,618-46,813,618				rs28637892	46,313,618	3.7E-9						
PIM3	22	49,856,302-50,856,850	rs1801645	50,356,850	1.5E-10	rs28691713	50,356,302	1.8E-17	rs1801645	50,356,850	4.2E-17	rs28691713	50,356,302	5.9E-22

[a]Reported only in MVP European ancestry-specific meta-analysis. [b]Reported only in MVP African ancestry-specific meta-analysis.

Supplementary Note Table 3. Loci attaining genome-wide significant evidence (p<5x10^{-8}) of association with T2D in European ancestry-specific meta-analysis of up to 80,154 cases and 853,816 controls (effective sample size 251,740) that were not identified at the same threshold in the trans-ancestry meta-regression.

Locus	Lead SNV	Chr	Position (bp, b37)	Alleles		European ancestry-specific meta-analysis				Non-European ancestry meta-analysis		
				Risk	Other	RAF	OR (95% CI)	*p*-value	*Q p*-value	RAF	OR (95% CI)	*p*-value
EGFEM1P	rs7642311	3	168,223,132	A	G	0.872	1.06 (1.04-1.08)	1.5x10^{-8}	0.034	0.823	1.01 (0.98-1.04)	0.67
HTT	rs362307	4	3,241,845	T	C	0.078	1.07 (1.05-1.10)	6.8x10^{-9}	0.47	0.083	1.03 (0.98-1.08)	0.32
FAM13A	rs1903002	4	89,740,894	G	C	0.506	1.04 (1.02-1.05)	1.4x10^{-8}	0.46	0.685	1.01 (0.99-1.02)	0.22
RFX3	rs672271	9	3,273,781	C	T	0.094	1.06 (1.04-1.08)	4.8x10^{-8}	0.38	0.175	0.99 (0.97-1.01)	0.52
USP44	rs61939481	12	95,921,998	C	T	0.068	1.07 (1.05-1.10)	1.7x10^{-8}	0.16	0.043	1.01 (0.96-1.06)	0.72
HMGB1	rs11842871	13	31,042,452	G	T	0.733	1.04 (1.03-1.06)	4.8x10^{-8}	0.097	0.870	1.02 (1.00-1.04)	0.082
PCDH17-SRGAP2D	rs9563615	13	59,077,406	A	T	0.709	1.04 (1.03-1.06)	1.6x10^{-8}	0.12	0.535	1.01 (1.00-1.02)	0.18
LIG4	rs7325671	13	108,797,836	T	C	0.126	1.06 (1.04-1.08)	1.5x10^{-8}	0.74	0.195	1.01 (0.99-1.03)	0.24
SLC7A7	rs17122772	14	23,288,935	G	C	0.226	1.04 (1.03-1.06)	3.3x10^{-8}	0.21	0.145	1.02 (1.00-1.05)	0.044
GLP2R	rs55973554	17	9,793,756	A	G	0.322	1.04 (1.03-1.05)	1.0x10^{-8}	0.57	0.119	1.01 (0.98-1.04)	0.51
PIK3C3-RIT2	rs1431841	18	40,087,098	T	G	0.211	1.04 (1.03-1.06)	3.1x10^{-8}	0.78	0.158	1.02 (1.00-1.03)	0.10

Chr: chromosome. RAF: risk allele frequency. OR: odds-ratio. CI: confidence interval.

Supplementary Note Table 4. Comparison of African ancestry-specific association summary statistics obtained from approximate conditional analysis undertaken in loci with multiple distinct signals using two LD reference panels: 661 individuals of African ancestry from the 1000 Genomes Project; and 1,000 African American individuals from GERA.

Locus	Index SNV	Alleles		RAF	1000 Genomes Project LD reference			GERA African American LD reference		
		Risk	Other		log OR	SE	*p*-value	log OR	SE	*p*-value
TMEM18	rs62107261	T	C	0.985	0.103	0.112	0.36	0.087	0.112	0.44
TMEM18	rs10188334	C	T	0.862	0.107	0.030	0.00036	0.106	0.030	0.00040
CEP68	rs2540949	A	T	0.581	0.026	0.019	0.16	0.025	0.019	0.19
CEP68	rs6752053	T	C	0.417	0.036	0.019	0.054	0.035	0.019	0.062
PPARG	rs17036160	C	T	0.976	0.089	0.059	0.13	0.093	0.059	0.11
PPARG	rs4684855	T	C	0.115	0.102	0.028	0.00031	0.103	0.028	0.00025
UBE2E2	rs13094957	T	C	0.642	0.024	0.019	0.21	0.024	0.019	0.19
UBE2E2	rs76435632	G	C	0.011	0.192	0.090	0.033	0.194	0.090	0.031
PSMD6-ADAMTS9	rs2292662	C	T	0.595	0.016	0.019	0.41	0.019	0.019	0.31
PSMD6-ADAMTS9	rs66815886	G	T	0.448	0.046	0.019	0.014	0.047	0.019	0.013
MBNL1	rs1426385	A	G	0.419	0.053	0.019	0.0043	0.056	0.019	0.0025
MBNL1	rs10935897	A	G	0.560	0.035	0.018	0.061	0.036	0.018	0.043
MBNL1	rs75417759	C	T	0.985	0.068	0.082	0.41	0.067	0.081	0.41
ST6GAL1	rs3887925	T	C	0.213	0.033	0.022	0.14	0.033	0.022	0.13
ST6GAL1	rs9799068	A	C	0.575	0.031	0.018	0.085	0.031	0.018	0.076
ANKH	rs147581833	C	T	0.999	-0.506	0.797	0.53	-0.570	0.796	0.47
ANKH	rs30614	A	G	0.637	0.070	0.056	0.21	0.069	0.056	0.21
ARL15	rs702634	A	G	0.751	0.041	0.021	0.058	0.037	0.021	0.077
ARL15	rs6876198	C	T	0.302	0.071	0.020	0.00043	0.069	0.020	0.00055
ANKRD55	rs256904	T	A	0.573	0.101	0.019	1.8×10^{-7}	0.101	0.018	1.4×10^{-8}
ANKRD55	rs42251	A	G	0.206	0.000	0.023	0.99	-0.003	0.022	0.88
ANKRD55	rs3936510	T	G	0.231	0.019	0.022	0.38	0.027	0.021	0.20
SSR1-RREB1	rs77630070	G	T	0.966	0.074	0.055	0.18	0.074	0.055	0.18
SSR1-RREB1	rs9379084	G	A	0.967	0.183	0.064	0.0042	0.183	0.064	0.0042
ZFAND3-KCNK16-GLP1R	rs2281342	T	C	0.920	0.076	0.035	0.027	0.080	0.035	0.021
ZFAND3-KCNK16-GLP1R	rs742762	A	C	0.870	0.022	0.027	0.41	0.032	0.027	0.24
ZFAND3-KCNK16-GLP1R	rs3734618	G	A	0.876	0.047	0.030	0.12	0.045	0.030	0.13
DGKB	rs17168486	T	C	0.109	0.008	0.031	0.80	0.014	0.031	0.65
DGKB	rs2215383	C	T	0.568	0.081	0.019	1.3×10^{-5}	0.081	0.019	1.4×10^{-5}
JAZF1	rs849133	C	T	0.741	0.080	0.022	0.00031	0.099	0.020	1.1×10^{-6}
JAZF1	rs552707	T	C	0.138	0.037	0.015	0.014	0.032	0.015	0.027
JAZF1	rs10226758	C	A	0.798	0.038	0.014	0.0087	0.035	0.014	0.011

KCNU1	rs10092900	G	T	0.403	0.061	0.019	0.00097	0.060	0.019	0.0011
KCNU1	rs12680217	T	C	0.704	0.085	0.021	$4.7x10^{-5}$	0.084	0.021	$5.3x10^{-5}$
ANK1	rs12550613	C	G	0.715	0.064	0.021	0.0017	0.059	0.020	0.0036
ANK1	rs508419	G	A	0.724	0.033	0.021	0.12	0.022	0.020	0.28
GLIS3	rs4237150	C	G	0.531	0.008	0.020	0.67	0.009	0.020	0.65
GLIS3	rs4258054	T	C	0.561	-0.004	0.021	0.87	-0.005	0.021	0.82
TLE1	rs9332453	C	T	0.883	-0.023	0.033	0.48	-0.024	0.032	0.46
TLE1	rs2796441	G	A	0.827	0.011	0.026	0.68	0.012	0.026	0.65
VPS26A-NEUROG3	rs190925	A	G	0.438	-0.052	0.021	0.012	-0.037	0.019	0.044
VPS26A-NEUROG3	rs41277236	T	C	0.013	0.185	0.128	0.15	0.193	0.127	0.13
VPS26A-NEUROG3	rs2642588	G	T	0.500	-0.010	0.020	0.63	-0.009	0.018	0.63
HHEX-IDE	rs10882099	T	C	0.767	0.032	0.021	0.13	0.031	0.020	0.12
HHEX-IDE	rs139027698	T	C	0.069	0.059	0.036	0.10	0.062	0.037	0.092
HHEX-IDE	rs1112718	A	G	0.560	-0.012	0.014	0.38	-0.010	0.014	0.47
WDR11	rs11199753	G	T	0.973	0.118	0.061	0.051	0.129	0.059	0.027
WDR11	rs2172073	A	C	0.499	0.061	0.019	0.0012	0.050	0.017	0.0042
WDR11	rs11592107	A	G	0.078	0.049	0.034	0.15	0.043	0.034	0.21
MTNR1B	rs10830963	G	C	0.084	0.138	0.038	0.00027	0.143	0.038	0.00018
MTNR1B	rs11020308	A	C	0.114	0.024	0.032	0.44	0.036	0.032	0.26
ETS1	rs10893827	A	G	0.741	0.033	0.022	0.13	0.036	0.021	0.086
ETS1	rs7104712	C	A	0.202	0.028	0.023	0.23	0.028	0.022	0.21
ETS1	rs11819995	T	C	0.266	0.032	0.021	0.13	0.034	0.020	0.096
HMGA2	rs343093	G	C	0.811	0.117	0.025	$2.8x10^{-6}$	0.116	0.025	$2.8x10^{-6}$
HMGA2	rs7970350	T	C	0.377	-0.002	0.018	0.91	0.004	0.018	0.82
RASGRP1	rs28582094	G	A	0.251	0.053	0.022	0.015	0.055	0.022	0.011
RASGRP1	rs34715063	C	T	0.058	0.077	0.047	0.10	0.078	0.047	0.097
GRP-MC4R	rs9957320	G	T	0.866	0.002	0.028	0.96	0.008	0.026	0.74
GRP-MC4R	rs6567160	C	T	0.196	0.075	0.024	0.0022	0.079	0.023	0.00054
GRP-MC4R	rs76227980	C	T	0.956	0.075	0.052	0.15	0.076	0.051	0.14
HNF4A	rs12625671	C	T	0.083	0.127	0.038	0.00073	0.127	0.038	0.00071
HNF4A	rs1800961	T	C	0.008	0.094	0.142	0.51	0.100	0.142	0.48

RAF: risk allele frequency. OR: odds-ratio. SE: standard error.

Supplementary Note Table 5. Comparison of Hispanic ancestry-specific association summary statistics obtained from approximate conditional analysis undertaken in loci with multiple distinct signals using two LD reference panels: 347 individuals of American ancestry from the 1000 Genomes Project; and 1,000 Hispanic individuals from GERA.

Locus	Index SNV	Alleles		RAF	1000 Genomes Project LD reference			GERA Hispanic LD reference		
		Risk	Other		log OR	SE	*p*-value	log OR	SE	*p*-value
DSTYK-MDM4	rs6689629	A	G	0.910	0.028	0.033	0.41	0.028	0.033	0.41
DSTYK-MDM4	rs12039805	A	G	0.341	0.059	0.020	0.0025	0.059	0.020	0.0025
TMEM18	rs62107261	T	C	0.969	0.113	0.059	0.056	0.118	0.059	0.047
TMEM18	rs10188334	C	T	0.877	0.064	0.029	0.026	0.066	0.029	0.023
CEP68	rs2540949	A	T	0.659	0.033	0.020	0.090	0.030	0.020	0.13
CEP68	rs6752053	T	C	0.649	0.050	0.020	0.011	0.048	0.020	0.015
PPARG	rs17036160	C	T	0.890	0.109	0.029	0.00021	0.109	0.031	0.00037
PPARG	rs4684855	T	C	0.378	0.025	0.018	0.18	0.016	0.019	0.42
UBE2E2	rs13094957	T	C	0.857	0.053	0.028	0.061	0.051	0.028	0.071
UBE2E2	rs76435632	G	C	0.076	0.078	0.037	0.034	0.076	0.037	0.039
PSMD6-ADAMTS9	rs2292662	C	T	0.869	0.005	0.030	0.86	0.012	0.030	0.70
PSMD6-ADAMTS9	rs66815886	G	T	0.758	0.032	0.023	0.16	0.034	0.023	0.14
MBNL1	rs1426385	A	G	0.486	0.018	0.018	0.34	0.015	0.019	0.42
MBNL1	rs10935897	A	G	0.312	0.058	0.020	0.0034	0.053	0.020	0.0075
MBNL1	rs75417759	C	T	0.982	0.102	0.076	0.18	0.105	0.074	0.16
ST6GAL1	rs3887925	T	C	0.376	0.047	0.019	0.011	0.047	0.019	0.011
ST6GAL1	rs9799068	A	C	0.208	0.025	0.023	0.28	0.025	0.023	0.27
ARL15	rs702634	A	G	0.813	0.027	0.025	0.29	0.018	0.024	0.46
ARL15	rs6876198	C	T	0.273	0.066	0.021	0.0019	0.063	0.021	0.0023
ANKRD55	rs256904	T	A	0.743	0.067	0.021	0.0017	0.078	0.021	0.00022
ANKRD55	rs42251	A	G	0.292	0.058	0.020	0.0038	0.065	0.019	0.00083
ANKRD55	rs3936510	T	G	0.218	0.125	0.022	9.6×10^{-9}	0.127	0.021	2.5×10^{-9}
SLCO6A1-PAM	rs78408340	G	C	0.005	0.433	0.174	0.013	0.400	0.155	0.0097
SLCO6A1-PAM	rs115505614	T	C	0.014	0.132	0.097	0.17	0.126	0.087	0.15
SLCO6A1-PAM	rs186327337	G	A	0.998	0.134	0.297	0.65	0.144	0.297	0.63
SSR1-RREB1	rs77630070	G	T	0.934	0.044	0.039	0.26	0.053	0.038	0.17
SSR1-RREB1	rs9379084	G	A	0.913	0.082	0.035	0.021	0.086	0.035	0.014
ZFAND3-KCNK16-GLP1R	rs2281342	T	C	0.766	0.083	0.022	0.00018	0.085	0.022	0.00014
ZFAND3-KCNK16-GLP1R	rs742762	A	C	0.868	0.076	0.027	0.0054	0.082	0.028	0.0029
ZFAND3-KCNK16-GLP1R	rs3734618	G	A	0.485	0.051	0.019	0.0074	0.060	0.020	0.0023
DGKB	rs17168486	T	C	0.428	0.047	0.020	0.019	0.043	0.020	0.035
DGKB	rs2215383	C	T	0.456	0.055	0.019	0.0031	0.053	0.019	0.0052

JAZF1	rs849133	C	T	0.642	0.105	0.019	$3.9x10^{-8}$	0.100	0.018	$1.8x10^{-8}$
JAZF1	rs552707	T	C	0.151	0.005	0.012	0.66	0.001	0.013	0.93
JAZF1	rs10226758	C	A	0.812	-0.002	0.012	0.87	0.000	0.013	1.0
MNX1	rs887609	A	G	0.189	0.093	0.025	0.00020	0.090	0.025	0.00036
MNX1	rs2366214	A	G	0.537	0.052	0.019	0.0060	0.048	0.019	0.012
KCNU1	rs10092900	G	T	0.203	0.032	0.023	0.17	0.030	0.023	0.20
KCNU1	rs12680217	T	C	0.760	-0.023	0.023	0.32	-0.019	0.023	0.40
ANK1	rs12550613	C	G	0.598	0.013	0.017	0.45	0.014	0.017	0.43
ANK1	rs508419	G	A	0.776	0.060	0.020	0.0030	0.061	0.021	0.0029
GLIS3	rs4237150	C	G	0.515	0.084	0.019	$1.1x10^{-5}$	0.084	0.019	$1.1x10^{-5}$
GLIS3	rs4258054	T	C	0.503	0.025	0.020	0.22	0.025	0.020	0.21
TLE1	rs9332453	C	T	0.708	0.024	0.021	0.25	0.023	0.021	0.27
TLE1	rs2796441	G	A	0.519	0.058	0.019	0.0027	0.058	0.019	0.0028
VPS26A-NEUROG3	rs190925	A	G	0.393	0.033	0.019	0.082	0.031	0.019	0.10
VPS26A-NEUROG3	rs41277236	T	C	0.036	0.096	0.055	0.079	0.073	0.054	0.18
VPS26A-NEUROG3	rs2642588	G	T	0.695	0.011	0.021	0.59	0.011	0.021	0.59
HHEX-IDE	rs10882099	T	C	0.640	0.075	0.018	$3.1x10^{-5}$	0.066	0.016	$4.1x10^{-5}$
HHEX-IDE	rs139027698	T	C	0.025	0.047	0.064	0.47	0.038	0.063	0.55
HHEX-IDE	rs1112718	A	G	0.475	0.009	0.017	0.60	-0.004	0.016	0.81
WDR11	rs11199753	G	T	0.875	0.055	0.028	0.048	0.052	0.028	0.065
WDR11	rs2172073	A	C	0.827	0.069	0.025	0.0051	0.074	0.025	0.0032
WDR11	rs11592107	A	G	0.172	0.053	0.025	0.034	0.066	0.025	0.0079
MTNR1B	rs10830963	G	C	0.214	0.102	0.023	$1.1x10^{-5}$	0.103	0.023	$1.0x10^{-5}$
MTNR1B	rs11020308	A	C	0.305	-0.016	0.021	0.45	-0.017	0.021	0.40
ETS1	rs10893827	A	G	0.690	0.054	0.020	0.0081	0.049	0.021	0.018
ETS1	rs7104712	C	A	0.392	0.062	0.020	0.0016	0.058	0.019	0.0025
ETS1	rs11819995	T	C	0.205	0.024	0.023	0.31	0.018	0.024	0.45
CCND2	rs10848960	G	C	0.867	-0.014	0.028	0.63	-0.007	0.029	0.81
CCND2	rs3812821	G	C	0.656	0.071	0.022	0.0013	0.072	0.022	0.0012
CCND2	rs3217792	C	T	0.938	0.119	0.043	0.0053	0.110	0.043	0.010
CCND2	rs76895963	T	G	0.991	0.419	0.145	0.0039	0.383	0.147	0.0092
CCND2	rs78470967	T	A	0.985	0.169	0.085	0.046	0.165	0.084	0.051
HNF1A	rs1800574	T	C	0.013	0.276	0.089	0.0020	0.348	0.086	$5.3x10^{-5}$
HNF1A	rs61953351	G	T	0.820	0.110	0.026	$1.8x10^{-5}$	0.125	0.025	$4.5x10^{-7}$
RASGRP1	rs28582094	G	A	0.382	0.056	0.019	0.0033	0.054	0.019	0.0044
RASGRP1	rs34715063	C	T	0.069	0.075	0.039	0.052	0.069	0.039	0.076
INFAM2	rs484943	T	C	0.214	0.005	0.024	0.84	0.007	0.023	0.78
INFAM2	rs3743140	A	G	0.171	0.065	0.025	0.010	0.065	0.025	0.010
GRP-MC4R	rs9957320	G	T	0.751	0.086	0.022	$9.5x10^{-5}$	0.075	0.022	0.00056

GRP-MC4R	rs6567160	C	T	0.131	0.118	0.029	4.9×10^{-5}	0.112	0.029	0.00012
GRP-MC4R	rs76227980	C	T	0.989	0.107	0.105	0.31	0.026	0.104	0.80
HNF4A	rs12625671	C	T	0.446	0.077	0.021	0.00022	0.080	0.021	0.00011
HNF4A	rs1800961	T	C	0.045	0.128	0.046	0.0054	0.138	0.046	0.0027

RAF: risk allele frequency. OR: odds-ratio. SE: standard error.

Supplementary Note Table 6. Assessment of the impact of BMI on heterogeneity in allelic effects at distinct T2D association signals from multi-ancestry meta-regression (MR-MEGA) of up to 166,070 cases and 1,132,773 controls[a].

Locus	Index SNV	Chr	Position (bp, b37)	Alleles		Heterogeneity *p*-value				BMI effect (SE) on log-OR of risk allele
				Risk	Other	Ancestry (unadjusted)	Ancestry (BMI adjusted)	BMI (ancestry adjusted)	Residual	
VWA5B1	rs10916784	1	20,729,451	G	C	0.27	0.25	0.55	0.71	0.00267 (0.00428)
MACF1	rs3768301	1	39,870,793	T	C	0.60	0.70	0.91	0.15	-0.00067 (0.00608)
MAST2	rs34444543	1	46,358,862	G	A	0.0063	0.66	0.39	0.89	-0.00399 (0.00420)
FAF1	rs12073283	1	51,219,188	C	G	0.34	0.94	0.47	0.77	-0.00562 (0.00737)
PGM1	rs11576729	1	64,114,429	G	T	0.042	0.042	0.85	0.83	-0.00099 (0.00497)
PTGFRN	rs1127215	1	117,532,790	C	T	0.088	0.19	0.58	0.41	0.00249 (0.00452)
NOTCH2	rs835576	1	120,455,586	C	T	0.037	0.081	0.85	0.18	-0.00127 (0.00707)
SEC16B	rs539515	1	177,889,025	C	A	0.52	0.50	0.66	0.88	-0.00242 (0.00504)
ZNF281	rs10919928	1	200,416,099	A	G	1.8×10^{-5}	1.8×10^{-5}	0.95	0.047	-0.00039 (0.00744)
DSTYK-MDM4	rs6689629	1	204,539,291	A	G	0.77	0.49	0.25	0.68	0.00601 (0.00503)
DSTYK-MDM4	rs12039805	1	205,107,793	A	G	0.19	0.43	0.29	0.14	0.00484 (0.00486)
SRGAP2	rs9429893	1	206,600,992	A	G	0.54	0.097	0.042	0.053	-0.00937 (0.00509)
PROX1	rs79687284	1	214,150,821	C	G	0.073	0.078	0.79	0.39	-0.00522 (0.01953)
PROX1	rs340874	1	214,159,256	C	T	0.40	0.36	0.62	0.72	0.00286 (0.00547)
LYPLAL1	rs2820446	1	219,748,818	C	G	0.029	0.11	0.71	0.20	-0.00179 (0.00515)
ABCB10-NUP133	rs348330	1	229,672,955	G	A	0.50	0.72	0.50	0.79	-0.00311 (0.00438)
TMEM18	rs62107261	2	422,144	T	C	0.29	0.34	0.79	0.47	0.00432 (0.01625)
TMEM18	rs10188334	2	653,874	C	T	0.12	0.094	0.11	0.56	0.01153 (0.00712)
DTNB	rs55928417	2	25,533,568	G	T	0.14	0.11	0.30	0.41	0.00481 (0.00469)
GCKR	rs1260326	2	27,730,940	C	T	0.91	0.93	0.48	0.0030	0.00321 (0.00543)
THADA	rs13414140	2	43,671,176	C	T	3.9×10^{-6}	4.2×10^{-6}	0.92	0.53	0.00076 (0.00734)
SIX3-SIX2	rs12712928	2	45,192,080	C	G	2.1×10^{-14}	0.0063	0.45	0.66	-0.00394 (0.00501)
BNIPL	rs17049712	2	58,961,136	T	C	0.75	0.63	0.46	0.58	0.00361 (0.00477)
BCL11A	rs243018	2	60,586,707	G	C	0.83	0.87	0.95	0.80	-0.00027 (0.00414)
CEP68	rs2540949	2	65,284,231	A	T	0.26	0.46	0.97	0.45	-0.00014 (0.00437)
CEP68	rs6752053	2	65,666,674	T	C	0.91	0.92	0.70	0.041	0.00177 (0.00518)
GLI2	rs11688682	2	121,347,612	G	C	0.14	0.17	0.17	0.53	0.00883 (0.00633)
GLI2	rs10864859	2	121,440,218	T	G	0.056	0.044	0.43	0.77	0.00587 (0.00696)
CYTIP	rs7594480	2	158,390,468	T	C	0.92	0.51	0.073	0.58	-0.01747 (0.00953)
RBSM1	rs1020731	2	161,144,055	A	G	0.020	0.20	0.99	0.11	-0.00006 (0.00531)
KCNH7	rs12614955	2	163,649,480	T	C	0.64	0.52	0.41	0.19	-0.00378 (0.00481)
GRB14	rs10184004	2	165,508,389	C	T	0.045	0.19	0.93	0.065	-0.00043 (0.00551)
IKZF2	rs16849467	2	213,818,731	T	C	0.58	0.36	0.19	0.31	-0.00693 (0.00549)
IRS1	rs2943648	2	227,100,490	G	A	0.064	0.14	0.97	0.29	0.00020 (0.00528)
ATG16L1-DGKD	rs117809958	2	234,191,103	A	T	0.21	0.24	0.77	0.94	0.00949 (0.02744)
PPARG	rs17036160	3	12,329,783	C	T	0.89	0.82	0.31	0.99	-0.00742 (0.00606)

PPARG	rs4684855	3	12,490,951	T	C	0.32	0.60	0.97	0.28	0.00018 (0.00494)
UBE2E2	rs13094957	3	23,457,080	T	C	0.0023	0.43	0.96	0.053	-0.00026 (0.00577)
UBE2E2	rs76435632	3	23,632,174	G	C	0.92	0.75	0.39	0.29	-0.00790 (0.00947)
RBM6	rs2624847	3	50,174,197	G	T	0.00043	0.00046	0.42	0.48	0.00445 (0.00548)
CACNA2D3	rs76263492	3	54,828,827	T	G	0.40	0.29	0.32	0.39	0.01415 (0.01436)
PXK	rs12629058	3	58,338,809	T	C	0.074	0.024	0.081	0.74	0.00858 (0.00469)
PSMD6-ADAMTS9	rs2292662	3	63,897,215	C	T	0.0087	0.38	0.80	0.28	-0.00132 (0.00545)
PSMD6-ADAMTS9	rs66815886	3	64,703,394	G	T	0.020	0.060	0.40	0.60	-0.00399 (0.00465)
ZBTB20	rs1459513	3	114,960,798	C	A	0.085	0.073	0.35	0.16	-0.00545 (0.00626)
ADCY5	rs11708067	3	123,065,778	A	G	0.16	0.095	0.26	0.96	-0.00704 (0.00541)
SLC12A8	rs9873519	3	124,921,457	T	C	0.55	0.29	0.10	0.99	-0.00723 (0.00372)
MBNL1	rs1426385	3	151,998,053	A	G	0.18	0.043	0.065	0.32	-0.00785 (0.00438)
MBNL1	rs10935897	3	152,399,693	A	G	0.23	0.20	0.067	0.76	0.00793 (0.00410)
MBNL1	rs75417759	3	152,530,027	C	T	$2.7x10^{-7}$	0.0097	0.97	0.56	-0.00035 (0.01079)
SLC2A2	rs8192675	3	170,724,883	T	C	$9.6x10^{-5}$	$4.9x10^{-5}$	0.056	0.87	0.00927 (0.00447)
IGF2BP2	rs7633675	3	185,510,613	G	T	0.16	0.57	0.53	0.89	-0.00285 (0.00417)
ST6GAL1	rs3887925	3	186,665,645	T	C	0.079	0.25	0.95	0.83	-0.00026 (0.00365)
ST6GAL1	rs9799068	3	186,676,455	A	C	0.099	0.32	0.87	0.081	0.00084 (0.00568)
BCL6-LPP	rs4686471	3	187,740,899	C	T	0.061	0.044	0.35	0.87	0.00516 (0.00507)
TFRC	rs74289356	3	195,825,077	T	C	0.50	0.46	0.59	0.71	-0.00304 (0.00548)
CTBP1-PCGF3-MAEA	rs73221123	4	726,202	T	C	0.85	0.88	0.86	0.88	0.00189 (0.00965)
CTBP1-PCGF3-MAEA	rs730831	4	1,240,299	T	G	0.045	0.051	0.27	0.079	-0.00702 (0.00697)
CTBP1-PCGF3-MAEA	rs6831006	4	1,784,605	G	C	0.66	0.86	0.86	0.41	0.00085 (0.00477)
WFS1	rs9998835	4	6,293,237	G	C	$2.5x10^{-6}$	0.00017	0.56	0.14	-0.00293 (0.00542)
LCORL	rs6855926	4	18,047,401	A	G	0.17	0.22	0.78	0.39	-0.00132 (0.00479)
GNPDA2	rs13130484	4	45,175,691	T	C	0.31	0.11	0.086	0.75	-0.00770 (0.00427)
MOB1B	rs7674402	4	71,835,822	A	G	0.67	0.84	0.55	0.29	-0.00412 (0.00708)
SCD5	rs10471048	4	83,587,562	G	C	0.0068	0.017	0.62	0.80	0.00221 (0.00416)
NKX6-1-CDS1	rs117624659	4	85,339,618	T	C	0.89	0.80	0.29	0.74	0.03403 (0.03007)
SMARCAD1	rs6821438	4	95,091,911	A	G	$8.2x10^{-5}$	$1.4x10^{-5}$	0.056	0.36	-0.00843 (0.00450)
PPP3CA	rs2659518	4	102,135,363	A	G	0.24	0.67	0.11	0.72	0.00927 (0.00557)
SLC9B1	rs223423	4	103,725,894	G	A	$3.8x10^{-5}$	0.0028	0.53	0.075	-0.00271 (0.00469)
TET2	rs17035289	4	106,048,291	C	T	0.044	0.0096	0.058	0.48	-0.01003 (0.00528)
TMEM154	rs6813195	4	153,520,475	C	T	0.49	0.36	0.23	0.045	0.00544 (0.00504)
PDGFC	rs1425482	4	157,725,916	T	C	$5.6x10^{-5}$	0.12	0.31	8.8E-01	0.00482 (0.00435)
ACSL1	rs1996546	4	185,714,289	G	T	0.14	0.34	0.026	6.7E-01	-0.01755 (0.00754)
ANKH	rs147581833	5	14,755,919	C	T	0.38	0.39	0.29	2.0E-01	-0.05915 (0.06125)
ANKH	rs30614	5	14,780,521	A	G	0.40	0.27	0.25	6.3E-01	-0.00740 (0.00608)
MRPS30	rs6884702	5	44,682,589	G	A	0.0022	0.0016	0.38	4.2E-02	-0.00389 (0.00491)
ITGA1	rs17261179	5	51,791,225	T	C	0.77	0.66	0.44	8.5E-02	-0.00342 (0.00487)
ARL15	rs702634	5	53,271,420	A	G	0.89	0.90	0.86	5.3E-01	0.00088 (0.00485)
ARL15	rs6876198	5	53,303,595	C	T	0.17	0.61	0.51	5.5E-01	0.00292 (0.00442)
ANKRD55	rs256904	5	55,810,305	T	A	0.78	0.77	0.83	1.3E-01	-0.00095 (0.00479)

ANKRD55	rs42251	5	55,840,633	A	G	0.30	0.33	0.84	8.5E-01	0.00085 (0.00400)
ANKRD55	rs3936510	5	55,860,866	T	G	0.0033	0.00098	0.11	4.4E-01	0.00862 (0.00540)
PIK3R1	rs57634870	5	67,716,793	G	T	0.93	0.93	0.92	8.6E-01	-0.00052 (0.00499)
HMGCR-POC5	rs2307111	5	75,003,678	T	C	9.7×10^{-7}	0.051	0.93	2.1E-01	-0.00038 (0.00464)
ZBED3	rs7732130	5	76,435,004	G	A	0.15	0.073	0.19	1.9E-03	-0.00734 (0.00677)
DMGDH	rs10052346	5	78,472,599	G	T	0.0056	0.36	0.77	5.3E-01	0.00129 (0.00434)
SLCO6A1-PAM	rs78408340	5	102,338,739	G	C	0.28	0.34	0.97	5.9E-01	0.00156 (0.03690)
SLCO6A1-PAM	rs115505614	5	102,422,968	T	C	0.77	0.77	0.92	3.0E-02	-0.00163 (0.02166)
SLCO6A1-PAM	rs186327337	5	103,364,257	G	A	0.012	0.027	0.10	2.8E-01	0.07139 (0.04685)
CEP120	rs4267865	5	122,704,342	G	T	0.18	0.27	0.58	5.0E-01	-0.00475 (0.00865)
PHFI5	rs329122	5	133,864,599	A	G	0.30	0.42	0.71	8.0E-01	0.00164 (0.00410)
NSD1	rs244708	5	176,589,585	G	A	0.22	0.24	0.74	5.2E-01	0.00152 (0.00450)
SSR1-RREB1	rs77630070	6	7,196,323	G	T	0.40	0.62	1.0	9.9E-01	0.00003 (0.00609)
SSR1-RREB1	rs9379084	6	7,231,843	G	A	0.0058	0.65	0.43	4.8E-01	0.00565 (0.00716)
CDKAL1	rs9348441	6	20,680,678	A	T	9.4×10^{-14}	0.22	3.0×10^{-6}	6.7E-04	-0.02157 (0.00563)
MHC region	rs879882	6	31,139,452	C	T	0.032	0.021	0.34	1.5E-01	0.00519 (0.00597)
MHC region	rs3806155	6	32,373,378	T	A	0.085	0.029	0.10	6.5E-01	0.03172 (0.01850)
MHC region	rs7452864	6	32,439,077	C	T	0.00012	0.055	0.88	5.6E-01	-0.00089 (0.00570)
MHC region	rs62405954	6	33,524,820	T	C	0.34	0.46	0.60	6.9E-01	0.00612 (0.01104)
MHC region	rs4711389	6	34,214,670	A	G	0.00039	0.00067	0.42	6.2E-01	0.00914 (0.01100)
ZFAND3-KCNK16-GLP1R	rs2281342	6	38,992,668	T	C	0.073	0.18	0.72	4.6E-01	-0.00183 (0.00510)
ZFAND3-KCNK16-GLP1R	rs742762	6	39,046,644	A	C	1.1×10^{-7}	7.9×10^{-5}	0.39	3.0E-01	-0.00467 (0.00567)
ZFAND3-KCNK16-GLP1R	rs3734618	6	39,284,184	G	A	0.00042	0.019	0.68	9.8E-01	0.00177 (0.00369)
LRFN2	rs34298980	6	40,409,243	T	C	0.27	0.28	0.12	5.0E-01	0.00699 (0.00454)
VEGFA	rs6905288	6	43,758,873	A	G	0.89	0.89	0.70	5.7E-01	-0.00178 (0.00462)
VEGFA	rs6458354	6	43,814,190	C	T	0.13	0.16	0.87	9.4E-01	0.00087 (0.00469)
TFAP2B	rs3798519	6	50,788,778	C	A	0.78	0.70	0.49	2.3E-01	-0.00358 (0.00542)
BEND3	rs1665901	6	107,433,400	A	T	0.18	0.53	0.25	2.0E-01	-0.00600 (0.00545)
NUS1	rs72951506	6	118,011,723	C	T	0.72	0.77	0.69	2.0E-01	-0.00223 (0.00587)
CENPW-SOGA3	rs11759026	6	126,792,095	G	A	0.12	0.12	0.41	7.6E-01	-0.00441 (0.00512)
CENPW-SOGA3	rs2800733	6	127,416,930	A	G	0.79	0.83	0.16	0.40	-0.00799 (0.00581)
MED23-ENPP3	rs7739842	6	131,954,797	G	T	0.0067	0.063	0.47	0.47	0.00344 (0.00483)
SLC35D3	rs6937795	6	137,291,281	A	C	0.065	0.085	0.27	0.81	-0.00472 (0.00405)
REPS1	rs9376353	6	138,855,975	A	T	0.10	0.11	0.66	0.44	0.00195 (0.00446)
HIVEP2	rs6570526	6	143,058,692	G	C	0.59	0.34	0.23	0.14	-0.00520 (0.00463)
RGS17	rs6932473	6	153,438,573	T	A	0.50	0.53	0.67	0.12	0.00190 (0.00482)
SLC22A3	rs539298	6	160,770,360	A	G	0.22	0.37	0.72	0.86	0.00159 (0.00405)
QKI	rs4709746	6	164,133,001	C	T	0.54	0.49	0.60	0.85	-0.00357 (0.00626)
ETV1	rs12154701	7	13,887,008	A	C	0.020	0.084	0.92	0.32	0.00044 (0.00447)
DGKB	rs17168486	7	14,898,282	T	C	0.27	0.29	0.60	0.20	-0.00252 (0.00509)
DGKB	rs2215383	7	15,062,983	C	T	0.92	0.75	0.35	0.017	-0.00409 (0.00502)
JAZF1	rs849133	7	28,192,280	C	T	0.0015	0.0030	0.76	0.76	-0.00155 (0.00467)
JAZF1	rs552707	7	28,205,303	T	C	6.5×10^{-5}	0.00024	0.73	0.78	-0.00106 (0.00285)

JAZF1	rs10226758	7	28,214,614	C	A	4.4×10^{-13}	3.7×10^{-12}	0.82	0.58	-0.00077 (0.00325)
CRHR2	rs917195	7	30,728,452	C	T	0.61	0.24	0.11	0.69	-0.00826 (0.00503)
GCK	rs882019	7	44,178,829	G	A	0.31	0.22	0.33	0.077	-0.00418 (0.00471)
GCK	rs878521	7	44,255,643	A	G	0.046	0.094	0.63	0.0016	-0.00224 (0.00567)
GRB10	rs13236710	7	50,809,085	G	A	0.10	0.10	1.0	0.93	0.00001 (0.00604)
AUTS2	rs2533457	7	69,055,951	G	A	0.00078	0.0032	0.92	0.85	0.00044 (0.00415)
STEAP1	rs6978118	7	89,800,241	A	T	0.00019	0.0053	0.25	0.56	-0.00511 (0.00441)
FBXL13-RELN-RASA4	rs7781557	7	102,481,891	C	T	0.56	0.38	0.31	0.77	-0.00732 (0.00675)
GCC1-PAX4-LEP	rs12669223	7	127,250,831	A	G	0.040	0.16	0.59	0.39	-0.00898 (0.01696)
KLF14	rs1562396	7	130,457,914	G	A	0.0015	0.0022	0.97	0.80	0.00018 (0.00430)
BRAF	rs11983228	7	140,631,823	C	G	0.42	0.56	0.59	0.60	0.00385 (0.00706)
AOC1	rs62492368	7	150,537,635	A	G	0.064	0.059	0.61	0.91	0.00227 (0.00401)
MNX1	rs887609	7	156,794,983	A	G	7.0×10^{-5}	0.00066	0.90	0.91	0.00071 (0.00508)
MNX1	rs2366214	7	156,992,461	A	G	0.18	0.77	0.64	0.10	0.00207 (0.00481)
MSRA-XKR6	rs4240673	8	10,787,612	T	C	0.14	0.051	0.12	0.38	-0.00769 (0.00499)
LONRF1	rs12680692	8	12,618,225	A	T	0.0088	0.13	0.24	0.044	0.00577 (0.00553)
LPL	rs7819706	8	19,844,415	A	G	0.054	0.051	0.17	0.77	-0.00923 (0.00642)
KCNU1	rs10092900	8	36,854,711	G	T	0.29	0.28	0.72	0.47	0.00181 (0.00504)
KCNU1	rs12680217	8	37,397,803	T	C	0.015	0.013	0.38	0.49	-0.00512 (0.00578)
ANK1	rs12550613	8	41,510,260	C	G	0.25	0.33	0.24	0.26	-0.00474 (0.00421)
ANK1	rs508419	8	41,522,991	G	A	0.52	0.93	0.22	0.24	-0.00618 (0.00522)
GDAP1	rs3780012	8	75,147,209	C	G	0.18	0.54	0.32	0.40	-0.02392 (0.02446)
TP53INP1	rs13257021	8	95,965,695	A	G	0.065	0.098	0.91	0.21	-0.00050 (0.00457)
TRPS1	rs800909	8	116,497,173	T	C	0.014	0.15	0.87	0.39	-0.00077 (0.00477)
SLC30A8	rs13266634	8	118,184,783	C	T	0.23	0.93	0.63	0.040	-0.00226 (0.00529)
PVT1	rs4733612	8	129,569,999	G	A	0.083	0.11	0.056	0.61	-0.01044 (0.00534)
BOP1	rs3890400	8	145,544,720	A	G	0.88	0.91	0.74	0.85	-0.00151 (0.00431)
BOP1	rs7014773	8	145,972,670	T	C	0.83	0.72	0.33	0.074	0.00442 (0.00496)
GLIS3	rs4237150	9	4,290,085	C	G	0.23	0.30	0.40	0.39	0.00352 (0.00424)
GLIS3	rs4258054	9	4,297,892	T	C	0.14	0.12	0.52	0.60	0.00299 (0.00454)
HAUS6	rs12380322	9	19,074,538	G	A	0.24	0.36	0.98	0.54	-0.00009 (0.00450)
CDKN2A-CDKN2B	rs7856455	9	21,840,834	G	T	0.0068	0.0073	0.64	0.44	-0.00347 (0.00757)
CDKN2A-CDKN2B	rs10757282	9	22,133,984	C	T	0.0051	0.00042	0.010	0.28	-0.01006 (0.00407)
CDKN2A-CDKN2B	rs10811661	9	22,134,094	T	C	0.0055	0.00013	0.0048	0.0032	-0.01357 (0.00575)
CDKN2A-CDKN2B	rs1575972	9	22,301,092	T	A	0.090	0.45	0.22	0.75	-0.01324 (0.01018)
LINGO2	rs1412234	9	28,410,683	C	T	0.012	0.092	0.34	0.66	0.00479 (0.00491)
UBAP2	rs12001437	9	34,074,476	C	T	0.058	0.031	0.24	0.19	0.00522 (0.00466)
TLE4	rs13290396	9	81,914,978	C	T	0.77	0.76	0.77	0.039	0.00219 (0.00854)
TLE1	rs9332453	9	83,998,346	C	T	0.0068	0.92	0.12	0.25	-0.00756 (0.00504)
TLE1	rs2796441	9	84,308,948	G	A	0.073	0.18	0.067	0.37	-0.00810 (0.00451)
ZNF169	rs12345069	9	96,971,175	C	T	0.35	0.55	0.012	0.52	0.01388 (0.00549)
PTCH1	rs113154802	9	98,278,413	C	T	0.00061	0.00069	0.62	0.41	0.00390 (0.00795)
STRBP	rs2416899	9	126,015,103	T	G	0.0081	0.017	0.35	0.20	-0.00502 (0.00563)

ABO	rs505922	9	136,149,229	C	T	0.12	0.044	0.14	0.77	0.00660 (0.00418)
GPSM1	rs28429551	9	139,243,334	A	T	0.0051	0.18	0.62	0.080	-0.00290 (0.00636)
GPSM1	rs74604683	9	139,247,229	C	T	0.32	0.13	0.083	0.12	-0.01238 (0.00772)
CDC123-CAMK1D	rs11257655	10	12,307,894	T	C	0.016	0.0035	0.040	0.46	0.00987 (0.00482)
MYO3A	rs7923442	10	26,497,704	A	G	0.37	0.11	0.028	0.99	-0.01114 (0.00432)
JMJD1C	rs41274074	10	64,974,380	G	C	0.23	0.32	0.89	0.21	-0.00118 (0.00864)
VPS26A-NEUROG3	rs190925	10	71,320,943	A	G	1.1×10^{-5}	0.0066	0.70	0.65	-0.00199 (0.00502)
VPS26A-NEUROG3	rs41277236	10	71,332,301	T	C	0.41	0.44	0.83	0.64	-0.00319 (0.01459)
VPS26A-NEUROG3	rs2642588	10	71,466,578	G	T	0.0010	0.40	0.22	0.41	-0.00706 (0.00589)
ZNF503-LRMDA	rs3012060	10	77,244,336	T	A	0.020	0.00021	0.0018	0.84	-0.01880 (0.00559)
ZMIZ1	rs703980	10	80,943,841	G	A	0.29	0.10	0.088	0.32	-0.00745 (0.00450)
PTEN	rs10887775	10	89,766,368	A	G	0.23	0.24	0.92	0.68	0.00054 (0.00522)
HHEX-IDE	rs10882099	10	94,460,650	T	C	1.5×10^{-14}	2.2×10^{-11}	0.55	0.64	-0.00160 (0.00261)
HHEX-IDE	rs139027698	10	94,468,247	T	C	5.8×10^{-10}	2.5×10^{-8}	0.20	0.0061	-0.01532 (0.01411)
HHEX-IDE	rs1112718	10	94,479,107	A	G	2.8×10^{-6}	0.00010	0.15	0.17	0.00383 (0.00282)
ARHGAP19-SLIT1	rs10748694	10	99,056,190	A	T	0.0098	0.55	0.11	0.37	-0.00717 (0.00455)
BBIP1	rs7067540	10	112,621,837	C	T	0.097	0.19	0.48	0.15	0.00322 (0.00491)
TCF7L2	rs12243296	10	114,344,288	G	A	0.026	0.35	0.39	0.84	0.00512 (0.00530)
TCF7L2	rs7100404	10	114,381,965	C	T	0.0043	0.054	0.33	0.54	0.00552 (0.00556)
TCF7L2	rs2859885	10	114,428,364	C	T	2.0×10^{-7}	2.4×10^{-7}	0.90	0.38	-0.00096 (0.00748)
TCF7L2	rs10787461	10	114,552,267	G	A	0.0086	0.0088	0.98	0.15	0.00016 (0.00708)
TCF7L2	rs2104598	10	114,715,598	G	A	0.00017	0.00029	0.16	0.071	-0.00843 (0.00701)
TCF7L2	rs114322470	10	114,736,670	T	G	0.80	0.77	0.047	0.50	0.05380 (0.02693)
TCF7L2	rs7903146	10	114,758,349	T	C	0.00043	8.1×10^{-5}	0.053	3.0×10^{-9}	-0.01210 (0.01048)
TCF7L2	rs7076754	10	114,797,893	G	A	0.0048	0.023	0.24	0.13	0.00993 (0.00944)
TCF7L2	rs145003494	10	114,834,411	A	G	0.00018	7.9×10^{-5}	0.044	0.52	-0.06314 (0.03099)
TCF7L2	rs116929578	10	114,836,181	G	A	0.81	0.82	0.84	0.031	-0.00334 (0.02006)
TCF7L2	rs7081841	10	114,859,416	G	C	0.0019	0.0020	0.21	0.41	-0.00817 (0.00667)
TCF7L2	rs12257761	10	115,016,408	T	C	6.2×10^{-5}	0.00018	0.47	0.094	-0.00636 (0.00993)
TCF7L2	rs11196296	10	115,069,951	T	C	1.3×10^{-11}	4.8×10^{-11}	0.83	0.50	0.00394 (0.01872)
TCF7L2	rs7093035	10	115,119,864	G	A	0.98	0.91	0.49	0.87	-0.00831 (0.01058)
TCF7L2	rs72830009	10	115,136,540	G	A	0.025	0.015	0.090	0.55	0.03716 (0.02147)
TCF7L2	rs11596522	10	115,247,447	T	G	0.0052	0.0047	0.64	0.12	0.00511 (0.01229)
WDR11	rs11199753	10	122,834,572	G	T	0.037	0.19	0.16	0.64	-0.00938 (0.00653)
WDR11	rs2172073	10	122,909,625	A	C	0.52	0.79	0.88	0.56	0.00089 (0.00574)
WDR11	rs11592107	10	122,968,964	A	G	0.57	0.71	0.76	0.67	-0.00145 (0.00457)
PLEKHA1	rs2421016	10	124,167,512	C	T	0.00092	0.0031	0.26	0.62	-0.00483 (0.00422)
INS-IGF2-KCNQ1	rs76547628	11	2,077,271	T	C	1.4×10^{-11}	0.00024	0.34	0.14	0.00575 (0.00650)
INS-IGF2-KCNQ1	rs10770142	11	2,194,420	G	C	0.21	0.21	0.61	0.077	-0.00270 (0.00584)
INS-IGF2-KCNQ1	rs4930050	11	2,235,129	G	A	1.9×10^{-8}	0.018	0.82	0.55	0.00257 (0.01104)
INS-IGF2-KCNQ1	rs800125	11	2,364,549	A	C	2.1×10^{-9}	2.2×10^{-9}	0.54	0.13	0.00276 (0.00494)
INS-IGF2-KCNQ1	rs79495865	11	2,375,458	G	A	9.7×10^{-9}	0.0065	0.47	0.54	0.00458 (0.00632)
INS-IGF2-KCNQ1	rs2283164	11	2,579,163	A	G	0.18	0.18	0.35	0.35	0.00981 (0.01077)

INS-IGF2-KCNQ1	rs80102379	11	2,634,177	G	T	0.14	0.23	0.10	0.29	0.02756 (0.01763)
INS-IGF2-KCNQ1	rs151215	11	2,681,072	G	A	$1.8x10^{-11}$	$1.2x10^{-5}$	0.47	0.82	0.00380 (0.00486)
INS-IGF2-KCNQ1	rs231361	11	2,691,500	A	G	$1.8x10^{-5}$	0.17	0.36	0.15	0.00416 (0.00497)
INS-IGF2-KCNQ1	rs2237884	11	2,799,679	T	C	$6.2x10^{-6}$	$9.0x10^{-6}$	0.78	0.24	-0.00136 (0.00515)
INS-IGF2-KCNQ1	rs4930011	11	2,856,658	G	C	$4.5x10^{-5}$	0.081	0.096	0.14	-0.00641 (0.00418)
INS-IGF2-KCNQ1	rs234866	11	2,857,897	G	A	0.019	0.096	0.60	0.047	0.00228 (0.00489)
INS-IGF2-KCNQ1	rs2237897	11	2,858,546	C	T	$7.1x10^{-9}$	0.034	0.66	0.081	0.00264 (0.00673)
INS-IGF2-KCNQ1	rs445084	11	2,908,754	G	A	0.047	0.061	0.41	0.62	-0.00420 (0.00500)
TRIM66	rs10769936	11	8,654,528	C	T	0.066	0.061	0.47	0.036	0.00323 (0.00503)
KCNJ11-ABCC8	rs5215	11	17,408,630	C	T	0.24	0.30	0.35	0.15	0.00418 (0.00480)
BDNF	rs4923464	11	27,683,618	C	T	0.0018	0.012	0.99	0.46	0.00004 (0.00501)
QSER1	rs145678014	11	32,927,778	G	T	0.040	0.077	0.85	0.76	0.00300 (0.01524)
HSD17B12	rs6485462	11	43,816,200	C	T	0.00065	0.0051	0.54	0.25	-0.00280 (0.00473)
CRY2	rs12419690	11	45,858,584	G	A	0.52	0.49	0.72	0.41	-0.00162 (0.00454)
FOLH1	rs6485981	11	49,477,266	T	C	0.0019	0.0014	0.42	0.50	0.00502 (0.00619)
MAP3K11	rs12789028	11	65,326,154	A	G	0.35	0.43	0.80	1.0	-0.00150 (0.00501)
TPCN2-CCND1	rs3918298	11	69,463,273	G	A	0.054	0.41	0.18	0.97	-0.01651 (0.01073)
CENTD2	rs77464186	11	72,460,398	A	C	0.076	0.36	0.094	0.10	-0.01083 (0.00701)
C11orf30	rs61894507	11	76,156,973	G	A	0.057	0.0089	0.018	0.49	0.01220 (0.00514)
MTNR1B	rs10830963	11	92,708,710	G	C	$7.6x10^{-6}$	0.12	0.87	$3.6x10^{-6}$	0.00081 (0.00638)
MTNR1B	rs11020308	11	93,131,667	A	C	0.18	0.074	0.043	0.036	-0.01039 (0.00577)
ETS1	rs10893827	11	128,040,810	A	G	0.079	0.23	0.36	0.87	0.00484 (0.00487)
ETS1	rs7104712	11	128,235,252	C	A	0.13	0.13	0.99	0.96	0.00005 (0.00430)
ETS1	rs11819995	11	128,389,391	T	C	0.66	0.24	0.075	0.36	-0.00930 (0.00533)
CCND2	rs10848960	12	4,033,222	G	C	0.046	0.072	0.75	0.25	0.00250 (0.00822)
CCND2	rs3812821	12	4,382,324	G	C	0.041	0.033	0.45	0.74	0.00519 (0.00647)
CCND2	rs3217792	12	4,384,696	C	T	0.00070	0.0028	0.85	0.79	-0.00214 (0.01066)
CCND2	rs76895963	12	4,384,844	T	G	0.00034	0.00014	0.16	0.31	-0.04356 (0.03247)
CCND2	rs78470967	12	4,521,511	T	A	0.95	0.85	0.40	0.99	-0.01581 (0.01457)
CDKN1B	rs2066827	12	12,871,099	G	T	0.94	0.98	0.58	0.81	0.00338 (0.00576)
ITPR2	rs10842708	12	26,474,867	G	A	0.026	0.065	0.73	0.81	0.00164 (0.00441)
KLHDC5	rs12578595	12	27,964,996	C	T	0.13	0.17	0.86	0.88	0.00095 (0.00480)
FAM60A	rs78345706	12	31,417,019	A	G	0.57	0.43	0.24	0.47	-0.01136 (0.00972)
PKP2-SYT10	rs6488140	12	33,370,406	A	G	0.0015	0.083	0.36	0.46	-0.00466 (0.00510)
FAIM2	rs7132908	12	50,263,148	A	G	0.15	0.23	0.88	0.16	-0.00072 (0.00497)
HMGA2	rs343093	12	66,255,005	G	C	0.059	0.76	0.53	0.68	0.00312 (0.00481)
HMGA2	rs7970350	12	66,360,164	T	C	0.13	0.18	0.81	0.032	0.00108 (0.00507)
TSPAN8	rs7313668	12	71,449,521	T	G	0.052	0.033	0.27	0.57	0.00508 (0.00451)
RMST	rs7972074	12	97,851,611	C	T	0.030	0.031	0.87	0.63	-0.00086 (0.00499)
WSCD2	rs1426371	12	108,629,780	G	A	0.96	0.72	0.29	0.60	-0.00515 (0.00477)
SH2B3-ALDH2-BRAP	rs3782886	12	112,110,489	T	C	$4.0x10^{-8}$	$3.0x10^{-8}$	0.11	$2.9x10^{-6}$	0.01856 (0.01670)
PTPN11-HECTD4	rs77753011	12	113,117,897	G	T	$2.7x10^{-8}$	$2.3x10^{-8}$	0.14	0.00033	0.02023 (0.01862)
KSR2	rs34965774	12	118,412,373	A	G	0.35	0.91	0.20	0.92	-0.00691 (0.00485)

HNF1A	rs1800574	12	121,416,864	T	C	0.00051	0.00087	0.23	0.17	-0.01434 (0.01283)
HNF1A	rs61953351	12	121,456,616	G	T	2.0×10^{-6}	1.7×10^{-6}	0.55	0.00017	0.00342 (0.00758)
MPHOSPH9-ZNF664	rs1790116	12	123,618,544	T	G	0.046	0.10	0.79	0.71	0.00156 (0.00551)
MPHOSPH9-ZNF664	rs2451321	12	124,545,435	C	G	0.28	0.31	0.51	0.48	0.00292 (0.00443)
FBRSL1	rs12811407	12	133,069,698	A	G	0.37	0.39	0.55	0.00010	-0.00304 (0.00648)
SGCG	rs314879	13	23,309,382	C	T	0.32	0.38	0.99	0.63	-0.00009 (0.00539)
RNF6	rs34584161	13	26,776,999	A	G	0.067	0.38	0.22	0.58	-0.00598 (0.00485)
KL	rs2858980	13	33,554,587	G	A	0.12	0.67	0.024	0.20	-0.01224 (0.00570)
DLEU1	rs963740	13	51,096,095	A	T	0.84	0.50	0.20	0.079	0.00603 (0.00514)
OLFM4	rs9568868	13	54,107,583	T	G	0.91	0.99	0.47	0.23	-0.00411 (0.00592)
SPRY2	rs1215468	13	80,707,429	A	G	0.44	0.50	0.27	0.20	-0.00539 (0.00515)
MIR17HG	rs34165267	13	91,942,919	C	T	0.00012	0.012	0.42	0.77	-0.00433 (0.00510)
AKAP6	rs12883788	14	33,303,540	T	C	0.46	0.74	0.69	0.0017	-0.00180 (0.00545)
CLEC14A	rs2183237	14	38,803,756	G	A	0.37	0.27	0.20	0.31	0.00576 (0.00465)
NRXN3	rs8008910	14	79,944,099	A	G	0.62	0.23	0.091	0.34	-0.01089 (0.00662)
DLK1-MEG3	rs12878003	14	101,124,721	G	A	0.022	0.088	0.58	0.030	-0.00287 (0.00586)
DLK1-MEG3	rs73347525	14	101,255,172	A	G	0.66	0.45	0.30	0.58	0.00593 (0.00563)
DLK1-MEG3	rs1053900	14	101,301,866	C	T	0.14	0.064	0.10	0.12	-0.00711 (0.00473)
TRAF3	rs11160699	14	103,252,270	A	G	0.93	0.93	1.0	0.92	0.00001 (0.00482)
RASGRP1	rs28582094	15	38,843,887	G	A	0.20	0.039	0.042	0.054	-0.01042 (0.00576)
RASGRP1	rs34715063	15	38,873,115	C	T	0.86	0.86	0.80	0.11	0.00227 (0.00969)
INFAM2	rs484943	15	40,398,754	T	C	0.26	0.88	0.82	0.033	-0.00114 (0.00549)
INFAM2	rs3743140	15	40,616,742	A	G	0.00015	0.0034	0.66	0.93	0.00251 (0.00520)
LTK	rs1473781	15	41,818,917	A	G	0.0019	0.053	0.63	0.95	-0.00231 (0.00429)
MYO5C	rs3825801	15	52,517,714	C	T	0.058	0.056	0.64	0.30	-0.00299 (0.00661)
C2CD4A-C2CD4B	rs7163757	15	62,391,608	C	T	0.00026	0.18	0.0016	0.11	-0.01378 (0.00472)
USP3	rs7178762	15	63,871,292	C	T	0.63	0.48	0.36	0.45	0.00439 (0.00484)
MAP2K5	rs4776970	15	68,080,886	A	T	0.040	0.19	0.55	0.33	-0.00275 (0.00468)
PTPN9-SIN3A	rs11636031	15	75,815,758	T	C	0.47	0.51	0.90	0.044	0.00060 (0.00524)
HMG20A	rs952472	15	77,776,562	C	A	0.79	0.81	0.97	0.0090	-0.00015 (0.00517)
AP3S2	rs6496609	15	90,379,632	C	A	0.057	0.13	0.62	0.22	-0.00244 (0.00510)
PRC1	rs2890156	15	91,513,157	A	T	0.39	0.41	0.45	0.91	0.00385 (0.00460)
RGMA	rs7167984	15	93,832,067	G	A	0.25	0.51	0.54	0.11	-0.00335 (0.00586)
ITFG3	rs6600191	16	295,795	T	C	0.22	0.33	0.75	0.23	0.00156 (0.00521)
CLUAP1-SLX4	rs12445430	16	3,613,126	T	C	0.89	0.57	0.20	0.38	-0.00665 (0.00529)
FAM57B	rs11642430	16	30,045,789	G	C	0.023	0.040	0.44	0.88	-0.00340 (0.00406)
FTO	rs55872725	16	53,809,123	T	C	0.042	0.055	0.91	0.020	-0.00053 (0.00545)
NFAT5	rs862320	16	69,651,866	C	T	0.11	0.12	0.34	0.28	0.00455 (0.00495)
ZFHX3	rs6416749	16	73,100,308	C	T	0.010	0.13	0.99	0.11	0.00004 (0.00553)
BCAR1	rs72802358	16	75,243,657	G	C	1.8×10^{-6}	0.0038	0.047	0.54	-0.01511 (0.00752)
CMIP	rs2925979	16	81,534,790	T	C	0.43	0.37	0.35	0.24	-0.00438 (0.00491)
ZFPM1	rs9937296	16	88,554,480	C	T	0.13	0.058	0.13	0.63	-0.00883 (0.00568)
SPG7	rs12920022	16	89,564,055	A	T	0.044	0.023	0.20	0.22	0.00802 (0.00664)

ZZEF1	rs1043246	17	3,828,086	G	C	0.65	0.67	0.89	0.22	-0.00093 (0.00705)
ZZEF1	rs8071043	17	3,988,451	C	T	0.0021	0.029	0.45	0.90	-0.00407 (0.00481)
SLC16A11-SLC16A13	rs113748381	17	6,953,155	A	G	0.0020	0.00013	0.0024	0.074	-0.03054 (0.01103)
RAI1	rs1108646	17	17,751,478	A	G	0.068	0.0024	0.0065	0.15	0.01319 (0.00519)
NF1	rs1048317	17	29,704,002	T	C	0.41	0.15	0.11	0.43	0.00704 (0.00443)
HNF1B	rs3094515	17	36,043,653	C	T	0.33	0.15	0.13	0.57	-0.00742 (0.00476)
HNF1B	rs12449654	17	36,056,076	C	G	$8.7x10^{-6}$	$1.2x10^{-5}$	0.50	0.31	0.00334 (0.00513)
HNF1B	rs10908278	17	36,099,952	T	A	$3.1x10^{-8}$	0.0083	0.87	0.12	0.00075 (0.00493)
MLX	rs684214	17	40,696,915	T	C	0.18	0.28	0.33	0.52	-0.00476 (0.00490)
GIP-TTLL6	rs35895680	17	47,060,322	C	A	0.46	0.46	0.98	0.96	0.00016 (0.00507)
ACE	rs57676627	17	62,203,128	T	C	0.15	0.44	0.63	0.80	-0.00408 (0.00792)
BPTF-PITPNC1	rs80320393	17	65,643,646	T	C	0.0064	0.48	0.72	0.32	-0.00328 (0.00954)
BPTF-PITPNC1	rs9899520	17	65,957,568	A	G	0.0028	0.0099	0.48	0.56	0.00349 (0.00482)
CYTH1	rs1044486	17	76,792,179	G	A	0.32	0.32	0.85	0.50	0.00082 (0.00438)
LAMA1	rs9948462	18	7,076,836	T	C	0.0096	0.21	0.64	0.33	0.00209 (0.00459)
TCF4	rs72926932	18	53,050,646	C	A	0.75	0.65	0.52	0.91	0.00706 (0.00981)
GRP-MC4R	rs9957320	18	56,876,430	G	T	0.0098	0.0087	0.17	0.24	-0.00755 (0.00582)
GRP-MC4R	rs6567160	18	57,829,135	C	T	0.16	0.15	0.49	0.39	0.00354 (0.00517)
GRP-MC4R	rs76227980	18	58,036,384	C	T	0.38	0.45	0.99	0.47	-0.00024 (0.01495)
BCL2A	rs12454712	18	60,845,884	T	C	0.27	0.32	0.76	0.44	-0.00146 (0.00486)
ZNF236	rs12457906	18	74,555,593	G	A	0.82	0.61	0.22	0.38	0.00528 (0.00439)
UHRF1-PTPRS	rs262549	19	4,951,064	G	C	0.78	0.59	0.36	0.48	0.00573 (0.00625)
MAP2K7	rs2115107	19	7,968,168	A	G	0.50	0.78	0.43	1.0	0.00348 (0.00356)
FARSA-ZNF799	rs4804181	19	12,509,536	A	C	0.55	0.72	0.59	0.84	-0.00272 (0.00472)
FARSA-ZNF799	rs3111316	19	13,038,415	A	G	0.34	0.17	0.14	0.29	-0.00688 (0.00480)
CILP2-TM6SF2	rs58542926	19	19,379,549	T	C	0.013	0.030	0.20	0.47	-0.01056 (0.00833)
ZNF257	rs142395395	19	22,100,706	A	G	0.45	0.38	0.38	0.95	0.02193 (0.02071)
PEPD	rs10406327	19	33,890,838	C	G	0.028	0.79	0.59	0.28	-0.00236 (0.00454)
TOMM40-APOE-GIPR	rs1871045	19	45,326,768	T	C	0.70	0.79	0.90	0.62	0.00056 (0.00425)
TOMM40-APOE-GIPR	rs429358	19	45,411,941	T	C	0.071	0.13	0.85	0.67	0.00122 (0.00642)
TOMM40-APOE-GIPR	rs10406431	19	46,157,019	A	G	0.057	0.37	0.69	0.58	0.00168 (0.00419)
TOMM40-APOE-GIPR	rs2238689	19	46,178,661	C	T	0.47	0.52	0.13	0.37	-0.00655 (0.00436)
ZC3H4	rs3810291	19	47,569,003	A	G	0.23	0.26	0.58	0.59	-0.00260 (0.00455)
FOXA2	rs2181063	20	22,427,370	C	G	0.10	0.25	0.029	0.88	-0.01091 (0.00459)
RALY	rs4911405	20	32,674,967	T	C	0.0061	0.22	0.67	0.61	-0.00225 (0.00509)
HNF4A	rs12625671	20	42,994,812	C	T	0.61	0.84	0.70	0.065	0.00201 (0.00585)
HNF4A	rs1800961	20	43,042,364	T	C	0.21	0.27	0.45	0.43	0.01021 (0.01364)
EYA2	rs6063046	20	45,596,378	A	G	0.80	0.16	0.026	0.75	-0.01319 (0.00560)
CEBPB	rs6091115	20	48,832,020	T	C	0.73	0.80	0.64	0.47	-0.00205 (0.00438)
GNAS	rs736266	20	57,387,352	T	A	0.18	0.22	0.55	0.39	-0.00261 (0.00444)
MTMR3-ZNRF3	rs36575	22	30,205,572	C	T	0.67	0.57	0.45	0.98	0.00787 (0.00865)
YWHAH	rs75307421	22	32,203,334	A	G	0.0093	0.014	0.45	0.25	-0.01016 (0.01398)
PNPLA3	rs738408	22	44,324,730	T	C	0.0046	0.23	0.22	0.22	0.00591 (0.00504)

PIM3	rs28691713	22	50,356,302	C	T	0.037	0.44	0.15	0.88	-0.00687 (0.00437)

Chr: chromosome. SE: standard error. OR: odds-ratio.

[a]The sample size contributing to each ancestry: African 15,043 cases and 22,318 controls; East Asian 56,268 cases and 227,155 controls; European 67,192 cases and 831,463 controls; Hispanic 11,027 cases and 18,885 controls; and South Asian 16,540 cases and 32,952 controls.

Supplementary Note Table 7. Candidate causal genes at T2D loci identified from functional annotation and colocalization with molecular QTLs in the DIAMANTE multi-ancestry study, and support from complementary analyses undertaken by recent T2D GWAS efforts overlapping with DIAMANTE.

Candidate causal gene[a]	Locus	DIAMANTE multi-ancestry			MVP (Vujkovic et al. 2020)		DIAMANTE European (Mahajan et al. 2018)	DIAMANTE East Asian (Spracklen et al. 2020)
		Missense variant	**pQTL**	**eQTL[b]**	**Missense variant**	**TWAS[b]**	**Missense variant**	**eQTL[b]**
ABO	*ABO*		cis	SM,VAT				
AC012354.6	*SIX3-SIX2*			I				I
AC122129.1	*RAI1*			SM		SM,SAT,VAT		
ACVR1C	*CYTIP*	p.Ile482Val						
ADCY5	*ADCY5*			I		SM		
ANK1	*ANK1*			SM,SAT		SM,SAT		SM,SAT
AP3S2	*AP3S2*			I,SM		L,P,SM,SAT,VAT		
APOE	*TOMM40-APOE-GIPR*	p.Cys130Arg	cis		p.Cys130Arg		p.Cys130Arg	
ARAP1	*CENTD2*			I				
ARHGAP19	*ARHGAP19-SLIT1*			SAT,VAT		SM,SAT,VAT		SAT
ATP2A3	*ZZEF1*	p.Gly216Arg				SM		
ATP5G1	*GIP-TTLL6*			SM		SM		
C12orf65	*MPHOSPH9-ZNF664*			SAT		SAT,VAT		
CALR	*FARSA-ZNF799*			SAT		SAT		
CAMK1D	*CDC123-CAMK1D*			I				
CARD9	*GPSM1*			I				
CCDC67	*MTNR1B*			I				
CCNE2	*TP53INP1*			VAT		VAT		
CD101	*PTGFRN*			I				
CDK8	*RNF6*			I				
CDKN1B	*CDKN1B*	p.Val109Gly					p.Val109Gly	
CEP68	*CEP68*			I,L,SM,SAT,VAT		L,P,SM,SAT,VAT		
CLUAP1	*CLUAP1-SLX4*			H		H,SM,SAT,VAT		
CPB1	*BCAR1*		trans					
CPLX1	*CTBP1-PCGF3-MAEA*			I				
CRHR2	*CRHR2*			I				
CTA-85E5.10	*MTMR3-ZNRF3*			SAT				
CTD-2021H9.3	*TSPAN8*			SM		SM		
CTRB1	*BCAR1*		cis					
DCAF16	*LCORL*			SAT		P,VAT		
DGKB	*DGKB*			I				
DLK1	*DLK1-MEG3*		cis	I				
DNLZ	*GPSM1*			I				
FAM134C	*MLX*			SM		SM		
FAM85B	*MSRA-XKR6*			SAT				
FBXL22	*USP3*			SM		SM		

GCKR	*GCKR*	p.Leu446Pro			p.Leu446Pro		p.Leu446Pro	
GLP1R	*ZFAND3-KCNK16-GLP1R*	p.Pro7Leu			p.Pro7Leu			
GPSM1	*GPSM1*			I	p.Leu391Ser			
HAUS6	*HAUS6*			I		SAT,VAT		
HERC1	*USP3*			VAT		SAT,VAT		
HMG20A	*HMG20A*			I		VAT		
HNF1A	*HNF1A*	p.Ala98Val					p.Ala98Val, p.Gly226Ala	
HNF4A	*HNF4A*	p.Thr139Ile					p.Thr139Ile	
HSD17B12	*HSD17B12*			H,I,L	p.Leu280Ser	H,L,P,SM,SAT,VAT		
IGF2BP2	*IGF2BP2*			I				
INHBB	*GLI2*			VAT				
IRS1	*IRS1*			SAT,VAT		SAT,VAT		
ITFG3	*ITFG3*			SAT		SAT,VAT		
ITGB6	*RBSM1*			H,SAT,VAT		SAT,VAT		
JAZF1	*JAZF1*			L,SM,SAT,VAT		L,P,SM,SAT,VAT		
KCNJ11	*KCNJ11-ABCC8*	p.Val337Ile			p.Lys23Glu	SM		
KLF14	*KLF14*			SAT		SAT		
KLHL42	*KLHDC5*			I		SM		
MAN2C1	*PTPN9-SIN3A*			L,SM,SAT		H,P,SM,SAT,VAT		
MED23	*MED23-ENPP3*			SM		SM		SM
MTNR1B	*MTNR1B*			I				
MYO5C	*MYO5C*	p.Glu1075Lys				P		SM
NDUFAF6	*TP53INP1*			SAT,VAT		SM,SAT,VAT		
NEUROG3	*VPS26A-NEUROG3*	p.Gly167Arg					p.Gly167Arg	
NKX6-3	*ANK1*			I				I
NOTCH2	*NOTCH2*			L		L,P		
NUS1	*NUS1*			I		P		I,P,SM
PAM	*SLCO6A1-PAM*	p.Ser539Trp	cis				p.Ser539Trp	
PCGF3	*CTBP1-PCGF3-MAEA*			SM,SAT,VAT				
PGM1	*PGM1*		cis					
PLA2G4B	*LTK*			SM,SAT,VAT		SAT,VAT		
PLEKHA1	*PLEKHA1*			I,SAT		SM,SAT		
PLRP1	*BCAR1*		trans					
POC5	*HMGCR-POC5*	p.His36Arg				SAT,VAT	p.His36Arg	
PRC1-AS1	*PRC1*			SAT				
PRSS2	*BCAR1*		trans					
PTGFRN	*PTGFRN*			I	p.Ile837Val			
PXK	*PXK*			I				
QSER1	*QSER1*	p.Arg1101Cys			p.Arg1101Cys		p.Arg1101Cys	
RBM6	*RBM6*			I,SM,SAT,VAT		H,L,P,SM,SAT,VAT		
RCCD1	*PRC1*			I,SM,SAT,VAT		H,SM,SAT,VAT		
RNF6	*RNF6*			I				
RP11-107F6.3	*LTK*			SAT		SM,SAT		

RP11-282O18.3	*MPHOSPH9-ZNF664*			SM,VAT				
RP11-395N3.2	*IRS1*			SAT,VAT		SAT,VAT		
RP11-419C23.1	*KCNU1*			SAT				SAT
RP11-463M16.4	*GIP-TTLL6*			SM		SM		
RP11-53O19.3	*MRPS30*			SAT		H,SAT		
RP11-613D13.5	*HSD17B12*			SAT				
RP11-817O13.8	*PTPN9-SIN3A*			SAT,VAT		P,SAT,VAT		
RP11-89K21.1	*SIX3-SIX2*			I				I
RP1-239B22.5	*KCNJ11-ABCC8*			SAT				
RP5-1042I8.7	*NOTCH2*			VAT				
RPL39L	*ST6GAL1*			I				
RREB1	*SSR1-RREB1*	p.Asp1171Asn			p.Asp1171Asn		p.Asp1171Asn	
SCD5	*SCD5*	p.Glu197Gln					p.Glu197Gln	
SETD8	*MPHOSPH9-ZNF664*			SM		SM		
SIX2	*SIX3-SIX2*			I				I
SIX3	*SIX3-SIX2*			I				I,P
SKOR1	*MAP2K5*			SM				
SLC12A8	*SLC12A8*			I				
SLC16A11	*SLC16A11-SLC16A13*	p.Val113Ile						
SLC22A3	*SLC22A3*			L		L		
SLC30A8	*SLC30A8*	p.Arg325Trp			p.Arg325Trp		p.Arg325Trp	
SMCO4	*MTNR1B*			I		P,SM		
ST6GAL1	*ST6GAL1*			I		P		
STARD10	*CENTD2*			I				
STEAP2	*STEAP1*			SAT				
SYCE2	*FARSA-ZNF799*			L		L		
TCF7L2	*TCF7L2*			I				
TH	*INS-IGF2-KCNQ1*			I		P		
TOM1L2	*RAI1*			SM		SM,SAT,VAT		
TSPAN8	*TSPAN8*			L		L		
TUBG2	*MLX*			SM		SM		
UBE2E2	*UBE2E2*			I				
UBE2Z	*GIP-TTLL6*			SM		SM		
WFS1	*WFS1*			SAT		SM,SAT		
WSCD2	*WSCD2*	p.Thr266Ile			p.Thr266Ile		p.Thr113Ile	
ZBTB20	*ZBTB20*			VAT		SAT		SAT
ZNF236	*ZNF236*			SAT				
ZNF703	*KCNU1*			SAT				SAT

pQTL: protein quantitative trait locus. eQTL: expression quantitative trait locus. TWAS: transcriptome-wide association study.
[a]Genes highlighted in bold not reported in complementary analyses conducted by DIAMANTE European, DIAMANTE East Asian or MVP.
[b]Tissues: hypothalamus (H); islet (I); liver (L); skeletal muscle (SM); subcutaneous adipose (SAT); visceral adipose (VAT).